The distribution and physiological roles of nitric oxide in the locomotor circuitry of the mammalian spinal cord

Thesis submitted to the University of St Andrews
for the degree of Doctor of Philosophy

By Catherine Dunford

Declarations

Candidate's declarations:

I, Catherine Dunford hereby certify that this thesis, which is approximately 40000 words in length, has been written by me, that it is the record of work carried out by me and that it has not been submitted in any previous application for a higher degree.

I was admitted as a research student in October 2007 and as a candidate for the degree of Doctor of Philosophy in September 2008; the higher study for which this is a record was carried out in the University of St Andrews between 2007 and 2011.

Date ……..… signature of candidate ……

Supervisor's declaration:

I hereby certify that the candidate has fulfilled the conditions of the Resolution and Regulations appropriate for the degree of Doctor of Philosophy in the University of St Andrews and that the candidate is qualified to submit this thesis in application for that degree.

Date …… ……..signature of supervisor ……..

Permission for electronic publication:

In submitting this thesis to the University of St Andrews I understand that I am giving permission for it to be made available for use in accordance with the regulations of the University Library for the time being in force, subject to any copyright vested in the work not being affected thereby. I also understand that the title and the abstract will be published, and that a copy of the work may be made and supplied to any bona fide library or research worker, that my thesis will be electronically accessible for personal or research use unless exempt by award of an embargo as requested below, and that the library has the right to migrate my thesis into new electronic forms as required to ensure continued access to the thesis. I have obtained any third-party copyright permissions that may be required in order to allow such access and migration, or have requested the appropriate embargo below.

The following is an agreed request by candidate and supervisor regarding the electronic publication of this thesis:

Embargo on both all of printed copy and electronic copy for the same fixed period of 2 years on the ground that publication would preclude future publication.

Date ……..……..signature of candidate ……..……..

Date ……..……..signature of supervisor…….....

Acknowledgements

I would like to thank my supervisor Dr Gareth Miles. Professor Keith Sillar, Professor Pat Willmer, Dr Roger Griffiths, and Ian Grieve, along with the entirety of the support staff in the School and the SMAU. For funding my studentship, I am grateful to the University of St Andrews and the Biotechnology and Biological Sciences Research Council (BBSRC). I would also like to thank Jill McVee for helping me with the histology. Dr Neil Symington, thank you for 'Python support' in the early days.

To avoid the risk of offending by omission, I would just like to say thank you to all my friends and family for their love, support and encouragement. Most importantly, thank you to my husband Hugh Martin, for completely supporting me and without whom the last 4 years would have been impossible.

Dedication

For my mother, who was chosen and who chose me.

Abstract

The mammalian spinal cord contains the neuronal circuitry necessary to generate rhythmic locomotor activity in the absence of inputs from the higher brain centre or sensory system. This circuitry is regulated by local neuromodulatory inputs, which can adjust the strength and timing of locomotor output. The free radical gas nitric oxide has been shown to act as an important neuromodulator of spinal circuits, which control locomotion in other vertebrate models such as the tadpole and lamprey. Despite this, the involvement of the NO-mediated soluble guanylate cyclase/cyclic guanosine monophosphate secondary messenger-signalling pathway (NO/sGC/cGMP) in mammalian locomotion has largely been under-investigated.

The NADPH diaphorase histochemical reaction was used to identify sources of NO in the lumbar spinal cord. The largest population NADPH diaphorase reactive neurons were located in the dorsal horn, followed by the laminae of the ventral horn, particularly around the central canal (lamina X) and lamina VII. NADPH diaphorase reactive neurons were found along a rostrocaudal gradient between lumbar segments L1 to L5. These results show that that discrete neuronal sources of NO are present in the developing mouse spinal cord, and that these cells increase in number during the developmental period postnatal day P1 – P12. NADPH diaphorase was subsequently used to identify NADPH diaphorase reactive neurons at P12 in the mouse model of ALS using the SOD^{G93A} transgenic mouse.

Physiological recordings of ventral root output were made to assess the contribution of NO to the regulation induced rhythmic fictive locomotion in the *in vitro* isolated spinal cord preparation. Exogenous NO inhibits central pattern generator (CPG) output while facilitating and inhibiting motor neuron output at low and high concentrations respectively. Removal of endogenous NO increases CPG output while decreasing motor neuron output and these effects are mediated by cGMP. These data suggest that an endogenous tone of NO is involved in the regulation of fictive locomotion and that this involves the NO/sGC/cGMP pathway.

Intracellular recordings from presumed motor neurons and a heterogeneous, unidentified sample of interneurons shows that NO modulates the intrinsic properties of spinal neurons. These data suggest that the net effect of NO appears to be a reduction in motor neuron excitability.

List of figures

Abbreviations

5HT	5-hyroxytryptamine, serotonin
aCSF	artificial cerebral spinal fluid
AHP	after hyperpolarisation
ALS	amyotrophic lateral sclerosis
AP	action potential
Ca^{2+}	calcium ion
cGMP	cyclic guanosine mono-phosphate
CNGC	cyclic nucleotide gated ion channels
CNS	central nervous system
CPG	central pattern generator
cPTIO	2-(4-carboxyphenyl)-4, 4, 5, 5-tetramethylimidazoline-1-oxyl-3-oxide
DA	dopamine
DAPI	4, 6-diamidino-2-phenylindole
DEA NO	2-(N, N-diethyl amino)-diazenolate-2-oxide diethyl ammonium salt
EDRF	endothelial derived relaxing factor
FALS	familial amyotrophic lateral sclerosis
GTP	guanosine tri-phosphate
GABA	γ-Aminobutyric acid
IML	intermediolateral layer
K^+	potassium ion
L-NAME	N5-[imino (nitro amino) methyl] -L-ornithine,methyl ester
L-NNA	N5-[imino (nitro amino) methyl] -L-ornithine
L/R	left/right
LHS	left hand-side
MFF	maximum firing frequency
MRR	maximum rate of rise
NA	noradrenaline
Na^+	sodium ion
NADPH	nicotinamide adenine dinucleotide phosphate
NMDA	N-Methyl-D-aspartate

NMDAR	N-Methyl-D-aspartate receptor
NO	nitric oxide
NOS	nitric oxide synthase
ODQ	1H-[1,2,4] oxadiazolo [4,3-a] quinoxalin-1-one
ONOO	peroxynitrite
PBS	phosphate buffered saline
PKC	Protein kinase C
PKG	Protein kinase G
PTIO	2-phenyl-4, 4, 5, 5-tetramethylimidazoline-1-oxyl 3-oxide
RHS	right hand-side
SALS	sporadic amyotrophic lateral sclerosis
sGC	soluble guanylate cyclase
SOD	superoxide dismutase
SPN	sympathetic preganglionic neuron
VDCC	voltage dependent calcium channels

Contents

Chapter 1: General introduction

1.1 Introduction

Nitric oxide (NO) is a free radical, diatomic gas with a plethora of physiological and pathophysiological effects. While the role of NO in vasculature is well known and it has been described as a neuromodulator of non-mammalian locomotion, little is known about the role of NO in relation to mammalian locomotion. This general introduction will provide a brief background of the study of locomotion, detail the structure and function of the mammalian locomotor network and cover the modulatory mechanisms involved in locomotor activity. I will then describe NO signalling and outline the aims of this thesis.

The isolated spinal cord has the capacity to generate a variety of spontaneous and coordinated locomotor behaviours, such as swimming, scratching, and walking. These movements are modulated in a variety of natural environmental circumstances, for example, during the transition from a walk to a gallop or to generate escape swimming in response to stress. In 1911, Thomas Graham Brown showed that the spinal cord contains sufficient circuitry to generate and maintain locomotion in the absence of supraspinal and sensory inputs. Brown postulated that proprioceptive inputs have a regulatory and not an intrinsic role in movement, that movement produced in the absence of afferents shared great similarity with movement when afferents remained intact, and that "The rhythmic sequence of the act of progression is consequently determined by phasic changes innate in the local centre" (Brown, 1911). In 1914, Brown went on to develop further the half-centre model, which he first postulated in his 1911 study, to describe the spinal circuitry, which controls rhythmic locomotor activity. He hypothesized that an individual central pattern generator or CPG, which takes the form of a half-centre, controls each limb (though the term CPG was coined much later (Brown, 1914, Brownstone and Stuart, 2011). The half-centre CPG comprises two sets of excitatory interneurons that control the activity of flexor and extensor motor neurons. These two sets of excitatory interneurons are usually prevented from simultaneous activation by mutual inhibitory inputs during locomotion. Inhibition of one set of

excitatory interneurons is therefore tightly coupled to the activity of the other set of excitatory interneurons (termed reciprocal inhibition). Additionally, and by an undetermined mechanism, fatigue in one set of inhibitory interneurons causes a phase switch as inhibition is released from the antagonist set of excitatory interneurons.

A contemporary of Brown, Charles Sherrington (who had published a detailed account of reflex control of hind limb muscles), preferred the reflex driven model for locomotor organisation, but conceded that the origins of the control of locomotion were most likely located in the spinal cord. The study of locomotion has been historically chronicled in detail in numerous reviews (Brownstone, 2006, Clarac, 2008, McCrea and Rybak, 2008, Brownstone and Stuart, 2011), so is not rehearsed further here. Partly as a consequence of Sherrington's influence, the half-centre model remained unpopular for the subsequent sixty years as researchers investigated the reflex control of stepping. However there was a resurgence in interest in Brown's approach during the late 1960s, notably because of the revival of the half-centre model by Anders Lundberg, and the subsequent body of research has re-established the half-centre model as a basis for understanding the function of the locomotor network in both vertebrates and invertebrates (Burke et al., 2001, Jankowska, 2001, Marder et al., 2005, Jankowska, 2008).

The nervous system is a complex network of neurons and, over the last century, delineating the precise cellular components of this complex network has proved difficult. Elucidating the connectivity of the locomotor networks has relied on the classical techniques of relating electrical properties and physiology to anatomical studies and descriptions of cell types. With the advent of genetic manipulation, involving recombinase technology and gene expression studies, our understanding of the spinal cord network has been greatly enhanced.

1.2 Spinal cord structure

Understanding the anatomical arrangement of the spinal cord network is integral to our understanding of the function of the spinal cord in both health and disease. Spinal cord

anatomy has therefore been studied at all levels in great detail using the rodent, rat and mouse.

The cells of the mammalian spinal cord have been classified into numerical laminae, from dorsal to ventral, according to the cytoarchitectonic description first devised from transverse sections of cat spinal cord (Rexed, 1954). The dorsal horn of the rodent lumbar spinal cord accounts for laminae I to VI. Neurons in the dorsal laminae receive inputs from cutaneous sensory and proprioceptive afferents. Laminae VII to IX comprise the ventral horn and these neurons receive inputs from descending, ascending, propriospinal, and sensory neurons. Neurons in the lumbar spinal cord integrate sensory and motor commands. The surfaces of the laminae are located parallel to the dorsal (posterior) and ventral (anterior) surfaces of the spinal cord. The spinal vasculature consists of a single ventral spinal artery and two dorsal spinal arteries that branch into vertebral arteries.

Investigation of spinal cord network function is aided by the understanding of the individual cell types and their spatial arrangement within the spinal segments. In order to help interpret the potential function of nitrergic neurons located in specific regions of the spinal cord – one of the main aims of the present study – a brief spatial and functional description of the ten laminae follows:

Lamina I, also known as the marginal layer, is a thin layer often appearing continuous with the white matter, covering the top of the dorsal horn. The layer contains small, fusiform neurons that project to the lateral and dorsal funiculi and are involved in processing of reflex input.

Lamina II corresponds to substantia gelatinosa Rolandi, and is divided into an inner (medial) and outer (lateral) zone. Lamina II contains neurons expressing opioid receptors involved in sensory processing, particularly pain.

Lamina III, also referred to as the superficial nucleus proprius, contains small cells involved in sensory processing.

Laminae I to III are located parallel to the dorsal surface and extend over the edge of the dorsal surface.

Lamina IV was formerly referred to as the base of the nucleus proprius and comprises small, medium and large cells involved in sensory reflex pathways. In the lower thoracic and upper lumbar cord, the medial zone is interrupted by Clarke's column.

Lamina V was formerly referred to as the neck of the dorsal horn and is the thickest layer of the dorsal horn. Neurons located in this lamina receive primary afferent input from the dorsal roots of lower spinal cord and project to the dorsolateral funiculus. The lateral zone corresponds to the formation reticularis, while the medial aspect is interrupted by Clarke's column.

Lamina VI is only visible in the intumescences or enlargements (cervical and lumbar), with indistinct borders. It is thickest in the medial zone, narrowing towards the midline and again towards the lateral edge. Lamina VI forms the curved base of the dorsal horn. Relative to the medial section, neurons in the lateral zone are large but scarce, while in the medial zone, neurons are small and tightly packed.

Lamina VII is the largest lamina located in the centre of the grey matter, also referred to as the zona intermedia. Neurons in lamina VII are regular in size and distribution. In the enlargements, the lateral motor nuclei (IX) are accommodated more laterally and dorsally than in the rest of the cord with lamina VII cells medial to the lamina IX pools. Autonomic neurons of the sympathetic system are located in the intermediolateral layer (IML) and intercalated nucleus (ICN), located within lamina VII.

Neurons in laminae V to VII project predominantly to the ventral and lateral funiculi on the ipsilateral side of the cord. Mechanoreceptive, nociceptive and Ia spindle afferents project to the neurons in these laminae. The lamina VII interneurons project to the inter- and intra-segmental homolateral motor nuclei. The neurons in the IML and ICN integrate and relay sympathetic preganglionic reflexes.

Lamina VIII is restricted to the medial half of the ventral horn. Neurons are heterogeneous in appearance and size and project into the contralateral grey and contralateral ventral funiculi. Lamina VIII propriospinal interneurons are involved in the inter- and intra-segmental control of contralateral motor reflexes.

Lamina IX contains the medial and large lateral motor neuron groups. Both α- and γ-motor neurons are located in IX.

Lamina X, also referred to as the substantia grisea centralis or substantia gelatinosa centralis, is the area around the central canal and marks the midline of the cord. The central canal is a remnant of the embryonic ventricular system and is continuous with the fourth cranial ventricle. Lamina X neurons are typically small and irregularly distributed and receive visceral and somatic afferents.

1.3 Identification of spinal locomotor-related neurons

The final lamina location and phenotype of developing neurons is determined by both the expression of morphogens and activity-dependent mechanisms (Jessell, 2000, Ben-Ari and Spitzer, 2010). During embryonic development, neurons develop and differentiate from the ventricular zone of the neural tube epithelium. Expressed along an opposing concentration gradient, the signalling proteins (morphogens), Sonic hedgehog (Shh), bone morphogenic proteins (BMP 4,6,7), and growth differentiation factor 7 (GDF7), are secreted from the notochord floor plate ventral to the neural tube (Shh) and the roof plate (BMP4, 6, 7 and GDF7), respectively (Jessell, 2000). Combinatorial expression patterns of transcription factors, induced by varying morphogen concentrations, determine the phenotypic fate of neurons differentiating along Shh/BMP morphogenic gradients. At embryonic day 11 (E11), eleven progenitor domains have developed and will go on to generate different classes of neurons.

Progenitor domains pd1 to pd6 give rise to the sensory neurons of the dorsal horn, dI1-dI6 interneurons, the four progenitor domains p0 to p3 give rise to the ventral interneurons V0 to V3, and the pMN progenitor domain differentiates into the lateral, medial and visceral motor neurons (Jessell, 2000, Goulding, 2009). Identification of the ventral neuron classes by transcription factor expression, alongside traditional physiological techniques, has accelerated the functional delineation of neurons involved in locomotor output. However, the spinal circuitry is complex and interneuron classes are themselves heterogeneous, further increasing the complexity of relating transcription factor phenotype to physiological function.

Nevertheless, progress continues to be made in assigning functions to the transcription factor-led identification of neuronal classes and subclasses during development. Recent advances in genetic manipulation, such as Cre-Lox recombination to conditionally influence gene expression, have added high-resolution information about the identity and contribution to network function at the cellular component level (Lobe and Nagy, 1998). Selective ablation of transcription factor specific neuron classes has provided an unprecedented acceleration in understanding the functional components of the locomotor network and their interconnectivity.

The V0 class of interneurons is defined by expression of the transcription factor developing brain homoebox1 (Dbx1; p0). The V0 class of neurons comprises two identified subclasses. The largest subclass is the $V0_D$ neurons, which account for 70% of all V0 neurons; they are GABA/glycinergic and project to contralateral motor neurons (Lanuza et al., 2004). V0 interneurons are critically linked with the maintenance of L/R alternation, in a speed dependent manner. Dbx1 mutant mice do not have the capacity to produce normal L/R alternating output and instead exhibit L/R synchronous locomotor output (Lanuza et al., 2004). The remaining 30% are $V0_V$ (even-skipped homeobox gene, Evx1/2$^+$) neurons, to which the cholinergic and glutamatergic Pitx2 (pituitary homeobox2-expressing) $V0_C$ and $V0_G$ subclasses belong. The cholinergic Pitx2 neurons, which represent just 5% of the total V0 population, originate from a small population of neurons located adjacent to the central canal and have been described as the source of the modulatory C-bouton inputs onto motor

neurons (Zagoraiou et al., 2009). These neurons are particularly interesting as they are intimately involved in the modulation of motor neuron and therefore locomotor output. C-boutons increase the excitability of motor neurons by reducing the action potential after hyperpolarization (AHP), possibly via direct actions on calcium dependent potassium channels (I_{KCa}), and they are synaptically opposed to muscarinic receptors (m2) and voltage-dependent delayed rectifier K+ channels (K_{dr}; Kv2.1), (Wilson et al., 2005, Miles et al., 2007, Zagoraiou et al., 2009).

The V1 interneurons are the major ipsilateral inhibitory input to motor neurons in the lumbar spinal cord (Mentis et al., 2005). Originating from the V1 class of interneurons, the Ia inhibitory interneurons and Renshaw Cells are defined by the EN1 (engrailed-1; p1) transcription factor. These neurons represent just 25-30% of the total neuronal complement that constitute the V1 interneurons (Gosgnach et al., 2006). Silencing of V1 interneurons leads to increases in the step-cycle period during fictive locomotion, suggesting these neurons play an important role in coordinating locomotor output (Gosgnach et al., 2006, Wilson et al., 2010). However, they are not the sole source of inhibition to motor neurons during locomotion.

These two distinct subclasses of neurons, the Ia inhibitory neurons and Renshaw Cells, originate from the same progenitor domain and yet have very distinct projection targets and receptive fields. Activity-dependent maturation of the network synergistic with genetic programming has been postulated to be the mechanism by which these two classes develop differential projection patterns (Siembab et al., 2010).

V2 interneurons are marked by Lhx2 (LIM homeobox2; p2) expression during development. Two subclasses of V2 interneurons have been identified. V2a – glutamatergic neurons expressing the post-mitotic transcription factors Sox14 and Chx10 (SRY-related HMG-box 14 and ceh-10 homeo domain containing homolog) and the V2b inhibitory interneurons (GABA/glycinergic) expressing the post-mitotic GATA2/3 transcription factors (GATA binding protein) (Butt et al., 2005). The contribution of V2b neurons to locomotor output has not yet been explored. However, the V2a interneurons have been shown to have a role in maintenance of L/R alternation

and project to contralateral $V0_V$ interneurons and motor neurons (Lanuza et al., 2004). Ablation of V2a interneurons in the mouse results in a speed-dependent gait change. Locomotion is not affected under normal conditions, but does result in a change of gait from walking to hopping at high treadmill speeds (Crone et al., 2009, Zhong et al., 2010). Ablation of the excitatory V2a-expressing Chx10 subclass of interneurons does not affect locomotion at normal speeds but does result in an abnormal gait change to hopping at high treadmill speeds. These neurons therefore appear to form an integral part of the locomotor network (Crone et al., 2008, Crone et al., 2009, Zhong et al., 2010).

Less progress has been made in deciphering the distinct role of V3 interneurons, which express single-minded homolog 1 (Sim1) during development and appear to be exclusively excitatory interneurons. V3 Sim1-expressing interneurons are excitatory and mostly commissural, involved in the precise timing of L/R alternation, and their selective removal increases the variability in L/R alternation (Zhang et al., 2008).

The neurons that express Hb9 (homeobox9; pMN) during development give rise to the excitatory interneurons ($Hb9^+$/$VGLUT2^+$) located in lamina VIII that are potentially involved in rhythm generation (Wilson et al., 2005). Selective ablation of the glutamatergic Hb9 expressing neurons has not been attempted, as Hb9 is expressed in both motor neurons and interneurons. However, characterisation of the Hb9 neurons continues, as they exhibit properties that suggest they may form an integral part of the rhythm generator (Wilson et al., 2005, Kwan et al., 2009).

Spinal motor neurons (pMN, Islet1, Islet2, Hb9) develop into either visceral or somatic neurons projecting via the spinal nerves to visceral targets and skeletal muscle fibres (αMN, extrafusal and γ, intrafusal respectively). Descending and sensory inputs, as well as commands from the CPG, are transmitted by the motor neurons to the relevant effector muscles (Figure 1.2). Thus, motor neurons have been termed the final common pathway for integrated information from the central nervous system (CNS) to target muscles. Figure 1.1 provides a schematic overview of the last order interneurons and their inputs to motor neurons.

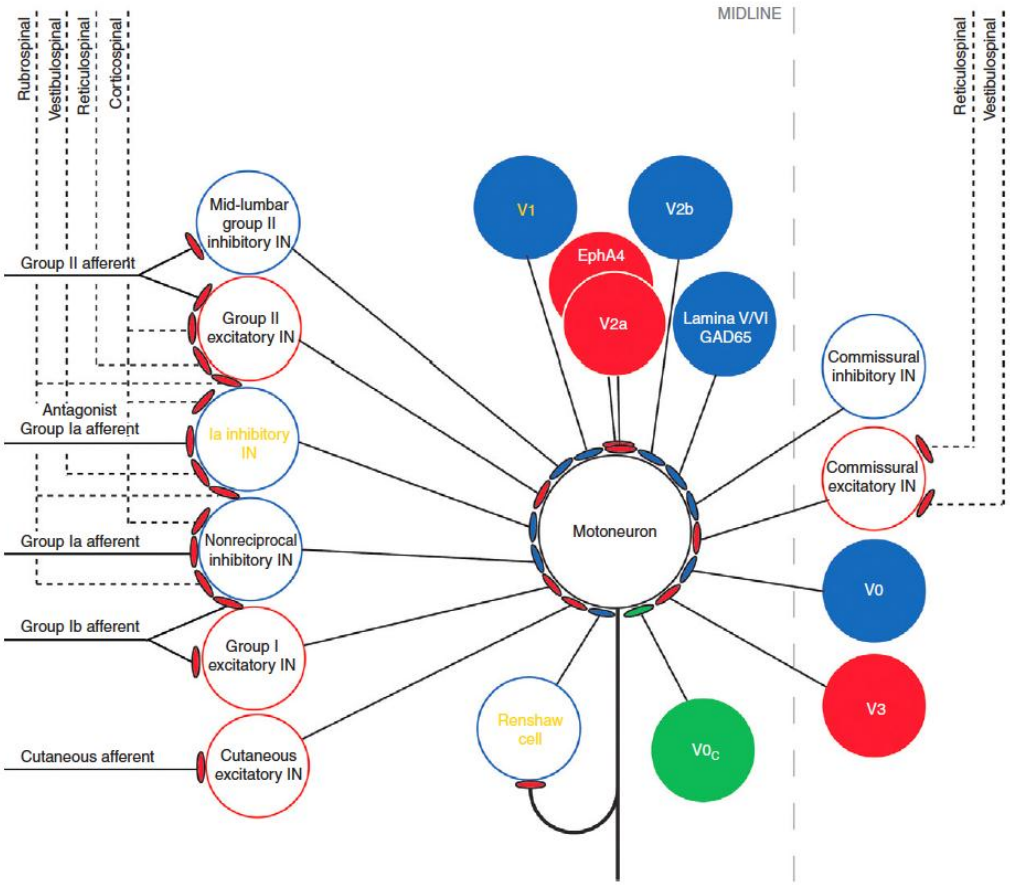

Figure 1.1. Simplified schematic of last order interneuron inputs to a single motor neuron. Motor neurons are the final common pathway for information from the CNS to target muscles. Motor neurons receive descending and sensory inputs represented by dashed black lines. The colour scheme is as follow; red indicates excitatory neurons, blue indicates inhibitory neurons and neuromodulatory neurons are depicted as green. The solid lines monosynaptic inputs and the dashed vertical line represents the midline. Diagram taken from (Brownstone and Bui, 2010), with permission © Elsevier Science BV.

1.4 The spinal locomotor network

As stated previously, the spinal cord is capable of generating locomotor output in the absence of supraspinal inputs. In the rodent, forelimb and hind limb locomotor networks are located in the cervical and lumbar spinal cord. The spinal cord generates spontaneous and coordinated locomotor output and motor function in mice begins before birth during embryonic development.

At embryonic day 12 (E12) in the rodent, 5HT receptors can be activated, before descending serotonergic inputs have reached the lumbar spinal cord, and simple synchronous rhythmic output can be induced. A more complicated pattern of output can be induced by 5HT at E14 and this may mark a key point in development, since by E15 the activity develops an element of left-right alternation. By E18, left-right alternating rhythmic output is established and this pattern is maintained after birth (Branchereau et al., 2000, Yvert et al., 2004).

Prenatal spontaneous activity in rodents has been attributed to the fact that during embryonic development, the neurotransmitter GABA produces excitatory, giant depolarising potentials mediated by the NKCC1 transporter. This was first shown in hippocampal cells and has since been described in numerous studies of the developing spinal cord network (Ben-Ari et al., 1989, O'Donovan et al., 1998, Vinay and Jean-Xavier, 2008, Gonzalez-Islas et al., 2009, Gonzalez-Islas et al., 2010, Spitzer, 2010). Highly rhythmic, spontaneous activity occurs in the developing spinal cord at E11.5 – E14.5 and is mediated by nicotinic acetylcholine receptors (nAChR) and electrical coupling. It is likely that this activity is a result of excitatory, cholinergic inputs from motor neurons onto each other and onto GABAergic interneurons (Hanson and Landmesser, 2003).

The isolated neonatal rodent spinal cord provides a functional and scalable network for the study of locomotor activity generated by the brainstem-spinal cord and spinal cord (Smith and Feldman, 1987, Kudo and Yamada, 1987). By birth, propriospinal networks have reached functional maturity; for instance, coupling of locomotor activity in the

fore and hind limb circuits has been described (Gordon and Whelan, 2006a, Gordon and Whelan, 2006b) but has been postulated to be less complex than in the mature network (Whelan et al., 2000).

In the neonatal mouse, forelimb locomotor-like activity can be initiated by electrical stimulation in the cervical spinal cord (Gordon et al., 2008), and, in separate brainstem-spinal cord studies in both the mouse and the rat, pharmacologically-activated cervical and lumbar networks interact to produce coordinated locomotor-like activity (Ballion et al., 2001, Juvin et al., 2005). This interaction in concert with bulbospinal descending excitatory drive contributes to activation and maintenance of locomotor activity (Zaporozhets et al., 2006, Zaporozhets et al., 2011).

Locomotor output can be evoked by a number of mechanisms in the isolated lumbar spinal cord of the neonatal mouse. As previously mentioned, some spontaneous rhythmic motor output has been noted at P0-2 (Bonnot et al., 1998). Electrical stimulation of the cauda equina, sural or other afferent nerves produces locomotor output sufficient for study, whilst electrical stimulation of ventral roots initiates glutamatergic-mediated synchronous activity (Whelan et al., 2000, Bonnot et al., 2002a, Bonnot et al., 2009). The isolated spinal cord with hind limbs attached validates the isolated spinal cord preparation but illustrates that the induced innervation of hind limb muscles produces functionally relevant locomotor output. The hind limb attached preparation provides corroborative evidence that the upper segments (L1-3) and lower segments (L5- L6) predominantly innervate the hind limb flexor and extensor muscles, respectively (Whelan et al., 2000, Hayes et al., 2009).

Systematic reduction of the rodent spinal cord involving the separation of the symmetrical halves or hemi-segments (sagittal separation, down the midline), segmental lesions and removals (transverse sectioning, from rostral to caudal ends), and removal of laminae (such as the dorsal horn) to gain access to specific areas in the ventral horn (coronal or horizontal sectioning), have provided anatomical evidence of the location of regions crucial to locomotor rhythmogenesis.

Lesion studies have shown the location of regions of rhythmogenic importance in the neonatal rat. These studies show that the ability to generate hind limb locomotor-related activity is distributed throughout the lumbar spinal cord segments, but with greater rhythmogenic potential in the rostral lumbar segments (Kiehn and Kjaerulff, 1996). In the same study, it was shown that CPG elements are located medially, ventral to the central canal and in all lumbar segments (L1-L6). Indeed, the rostral segments of the thoracolumbar spinal cord appear to be more rhythmogenic during pharmacological activation of fictive locomotion than caudal segments, and L2/L3 appear to be especially critical for rhythm generation in the neonatal rat (Bertrand and Cazalets, 2002).

Each hemi-segment contains sufficient circuitry to generate spontaneous rhythmic locomotor output while an intact segment is necessary for the generation of left-right alternating output. Combining lesions with the pharmacological block of glycinergic and GABAergic inhibition, it has been shown that, between P5 – 10 in the neonatal rat, a single ventral horn is sufficient to produce the excitatory drive responsible for ipsilateral burst output, and that commissural input from contralateral half-centres of at least two segments are required to maintain left-right alternation (Bracci et al., 1996). In fact, complete removal of endogenous glutamatergic signalling within the spinal cord, using a VGLUT2 knock-out mouse, shows that, in the absence of endogenous glutamatergic excitation, the locomotor network can still generate locomotor-like output (Talpalar et al., 2011). In a recent study, inhibitory driven locomotor output was initiated and maintained by excitatory neurotransmitters and was completely ablated by picrotoxin and strychnine, inhibitors of $GABA_A$ and glycine receptors (Talpalar et al., 2011).

Understanding of the mammalian locomotor network has been and continues to be influenced by the significant contribution of research conducted in other vertebrate systems, such as the *Xenopus laevis* tadpole, the adult lamprey *Lampetra fluviatilis/Petromyzon marinus* and the zebra fish *Danio rerio*, which all share similar locomotor network connectivity. The tadpole has a complement of about ten identified neuron classes in the pre-metamorphic stages of development, and with a relatively

small network of well-characterised neurons it provides an ideal system for understanding the organisation of simple neural networks (Li et al., 2001, Roberts et al., 2010). Fictive locomotion at between 10-20Hz can be induced by electrical stimulation or sensory stimuli, such as light dimming, to produce bouts of swimming for manipulation and study.

The half-centre model can be explained particularly clearly in the tadpole and lamprey locomotor networks where descending inputs originating from reticulospinal neurons activate the locomotor CPG and the motor neurons are segmentally organized and innervate axial muscles to produce undulatory swimming. Following the transcription factor-led identification of rodent neuronal phenotypes, homologs have been identified in the tadpole. Descending interneurons in the tadpole are equivalent to the rodent V2a, V3 and Hb9 neuron classes, while the ascending GABAergic interneurons of the tadpole integrate mechanosensory inputs (equivalent to the V1 En1 and V2b interneurons) (Kiehn, 2011). Excitatory glutamatergic interneurons project to commissural glycinergic interneurons. Commissural glycinergic inhibitory interneurons (the equivalent to dl6 and $V0_V$ Dbx1, Evx1/2$^-$ in the rodent) provide reciprocal inhibition to motor neurons on the contralateral side and also project to ipsilaterally projecting inhibitory neurons (Goulding, 2009, Roberts et al., 2010, Kiehn, 2011).

1.5 Initiation, maintenance and modulation of locomotion

As the neuronal components of the locomotor CPG and their interconnectivity are elucidated, it is also vital to understand how ‘neuromodulation’ of intrinsic neuronal properties and synaptic connectivity within the CPG can affect network output.

The descending pathway that initiates locomotion in the intact brain-spinal cord is supraspinal in origin. Locomotor drive potentials (LDP) caused by stimulation of the mesencephalic locomotor region (MLR) in the dorsal midbrain can induce locomotion in the spinal locomotor network (Noga et al., 2003). Fictive locomotion in the present study is described as the generation of rhythmic motor output from the isolated spinal

cord in the absence of the effector muscles and actual movement, and can be induced by pharmacological or electrical stimulation.

Fibres projecting to the spinal cord from the forebrain, cerebellum, raphe nuclei, and locus coeruleus innervate the locomotor network, though other descending projections are also involved in the modulation of this network. Descending excitatory fibres contribute to both the initiation and modulation of spinal locomotor output, for example, the glutamatergic reticulospinal neurons (located in the brainstem), which project to the spinal cord (Rekling et al., 2000). The block of glutamatergic descending input to the spinal cord by NMDA antagonists during electrical stimulation of the MLR inhibits fictive locomotion (Douglas et al., 1993). In addition to supraspinal glutamatergic inputs, noradrenergic (NA) fibres also project to the spinal cord from the locus coeruleus (Gabbay and Lev-Tov, 2004) and descending serotonergic fibers from the raphe nuclei are involved in the development and maturation of the spinal locomotor network (Vinay et al., 2000, Garraway and Hochman, 2001, Pearlstein et al., 2005). Descending dopaminergic inputs contribute to locomotor output but are not reticular in origin and originate from the A11 area of the hypothalamus (Clemens et al., 2006).

Exogenous neuroactive compounds can initiate and maintain fictive locomotor output in the rodent spinal cord in the absence of descending inputs. Neuroactive compounds, particularly monoamines, are thought to mimic the natural excitatory descending inputs from the brainstem that regulate network activity in the spinal locomotor network. The pharmacological activation of the CPG has been studied extensively; of particular interest has been the initiation of fictive locomotion by serotonin (5HT). Descending raphe inputs are generally severed in the isolated preparation, requiring the addition of serotonin by bath application to activate the locomotor network. 5HT7 and 5HT2 receptors have been identified as critical for eliciting alternating locomotor activity (Branchereau et al., 2000, Nishimaru et al., 2000, Madriaga et al., 2004, Liu and Jordan, 2005, Liu et al., 2009, Dunbar et al., 2010). The locomotor activity evoked by 5HT7 and 5HT2 agonists has also been shown to interact with dopaminergic receptors D1/2 (Madriaga et al., 2004), and rostrocaudal excitability gradients have been uncovered in the neonatal mouse using combinations of monoamines including 5HT/DA (Christie

and Whelan, 2005) and combinations of N-Methyl-D-aspartic acid (NMDA), 5HT and dopamine (DA) (Cazalets et al., 1992, Beato et al., 1997, Jiang et al., 1999, Whelan et al., 2000, Bonnot et al., 2002a). NMDA alone can also induce locomotor activity (Kudo and Yamada, 1987), although it is not clear whether NMDA receptor activation is an absolute requirement during fictive locomotion (Beato et al., 1997, Nishimaru et al., 2000, Cowley et al., 2005).

Other neuropeptides generate or regulate locomotor networks; for example, noradrenaline (NA) has been shown to be involved in maintenance of 5HT/NMDA-induced locomotor activity (Kiehn et al., 1999, Gabbay and Lev-Tov, 2004). In a study to investigate eleven neuroactive peptides, four were shown to elicit uncoordinated output whilst all eleven were shown either to induce or modulate NMDA-induced locomotion in the neonatal rat (Barriere et al., 2005).

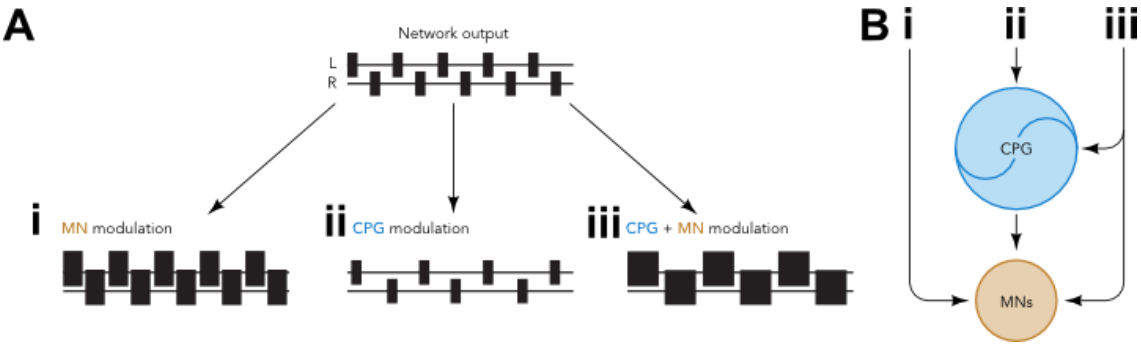

Figure 1.2. Schematic representation of rhythmic, alternating motor output generated by antagonistic motor pools. Schematic showing how rhythmic, alternating motor output generated by antagonistic motor pools (A) can be altered in amplitude (i), frequency (ii), or both (iii), depending on whether a given modulator acts at the level of the motoneurons (Bi), the CPG (Bii), or a combination of the two (Biii). Diagram adapted from the original, with kind permission of the authors (Miles and Sillar, 2011).

1.5.1 Modulation of locomotion

Neurotransmitters from the descending sources already described or local sources (local neuronal network and glia) are involved in the ionotropic transmission that directly facilitates neural communication between higher centres, CPG interneurons and motor neurons to drive locomotor activity (Figure 1.2). Neuromodulation, on the other hand, is defined as the modulatory changes as a result of metabotropic actions of

neurotransmitters that influence the response of neurons to ionotropic transmission. Neuromodulation has become an increasingly important aspect of the study of locomotor networks; particularly as the actions of metabotropic processes are continually revealed to play a role in the homeostatic function of locomotor-related neurons and influencing behavioural states. As such, these pathways are also of significant interest in pathophysiological conditions, where homeostasis appears to be disrupted, for instance, in ALS where motor neurons receive an elevated level of excitatory inputs which are thought to subsequently contribute to cell death (Heckman et al., 2009, Quinlan et al., 2011).

Ion channels located in the neuronal membrane determine the intrinsic properties of neurons at rest and during activity. Thus intrinsic properties can vary from cell to cell according to specific expression patterns and ion channel densities, in concert with modulation of ion channel properties by neurotransmitters. The intrinsic properties of individual neurons are a complex orchestration of interactions between cation channel conductance (i.e. $I_{Na+,}$ I_{K+} and I_{Ca2+}). Categorical and functional studies of ion channels provide important information about the nature of cell communication. A large body of work exists detailing individual ion channel families and their role in cellular communication, a comprehensive summary of which is outside the scope of this thesis. There are many books and review articles collating and detailing this information (Takahashi and Berger, 1990, Takahashi, 1990, Catterall, 2000, Goldin et al., 2000, Rekling et al., 2000, Hille, 2001, Jentsch et al., 2002, Gutman et al., 2005, Ulbricht, 2005).

Neuromodulation specifically refers to the metabotropic pathways that modulate neuronal output. Most neurotransmitters can have both ionotropic and metabotropic effects. For instance, glutamate, already discussed as a fast-acting neurotransmitter via NMDA/Kainate/AMPA receptors, can also modulate the excitability of neurons via metabotropic receptor linked secondary messenger cascades. Metabotropic glutamate receptors (mGluR) are G-protein coupled receptors and modulate the intrinsic excitability of motor neurons (Rekling et al., 2000). There are three groups (Group I to III), with a total of eight types (mGluR1–8). Directly involved in modulating motor

neurons are the Group I mGluRs (mGluR1 and mGluR5) which activate Protein kinase C (PKC) directly and indirectly by increasing cytosolic Ca^{2+}. Additionally they activate Protein kinase A (PKA) by increasing cAMP (Kim et al., 2008). This mGluR activity is not necessary for maintenance of rhythmic locomotion, but is involved in setting the rhythm (Taccola et al., 2003). mGluR1 activation initiates second messenger cascades that modulate locomotor output notably by decreasing motor neuron excitability by both presynaptic and postsynaptic mechanisms while increasing the frequency of locomotor output (Iwagaki and Miles, 2011). In the lamprey, the activation of mGluR1 also increases both the short and long term frequency of locomotor output (Kyriakatos and El Manira, 2007).

The 5HT (serotonin) receptor family consists of fifteen receptor subtypes: $5HT_3$ is a ligand-gated ion channel and the remainder are G-protein coupled receptors. 5HT enhances, amongst other things, the low voltage Ca^{2+} (LVA) and high voltage L-type Ca^{2+} channels (HVA) that underlie plateau potentials and the hyperpolarization-activated inward current, I_h (Li and Bennett, 2007). Serotonergic modulation of spinal neurons occurs principally via 5HT1, 5HT2 and 5HT7 receptors; the latter two facilitate excitation and the first appears to mediate inhibition, possibly at the action potential initiation site (Dunbar et al., 2010). Serotonin depolarises the resting membrane potential and increases the input resistance of spinal motor neurons. It has also been shown to induce oscillations in locomotor-related interneurons (Carlin et al., 2006), to modulate bi-stability (plateau potentials) in motor neurons (Kiehn and Eken, 1998) and to co-localise with Substance P and Thyrotropin releasing hormone (TRH)
(Rekling et al., 2000).

Another neuromodulatory pathway involves dopamine. Coupled to Adenylyl cyclase, D1 dopamine receptors activate, and D2 inhibit, this second messenger cascade in locomotor-related neurons. Dopamine receptors are also expressed in the membranes of Renshaw cells where their activation leads to an increase in excitability (Rekling et al., 2000). Spinal Hb9 interneurons and motor neurons express dopamine receptors but their role and the full extent to which they modulate the spinal locomotor circuitry are not yet fully understood (Han et al., 2007).

The main neurotransmitters involved in rhythm generating networks are conserved across the species most actively studied in relation to motor control, particularly in rodents – the focus of this study – and in the lamprey, zebrafish, and tadpole. In the hatchling tadpole, swimming at stage 37 is modulated by descending aminergic fibers from the raphe (serotonin) and locus coeruleus (noradrenaline). Serotonin released from raphe projections to the spinal cord facilitates maturation of the swimming pattern between stage 37, when motor neurons fire once per cycle, and stage 42, when the motor neurons are able to fire repetitively during locomotor activity (Sillar et al., 1995). Activation of NMDA receptors in the presence of 5HT causes membrane oscillations in commissural interneurons suggesting an activity-dependent modulation of locomotor output (Sillar et al., 1998, McLean and Sillar, 2002). Evidence from the tadpole has shown that non-NMDA excitatory amino acids activate the locomotor network as a result of descending input from the brainstem (Sillar et al., 1992). NA has been shown to inhibit locomotor output slowing the motor pattern and facilitating glycinergic inhibition and NO has been shown to modulate this NA-mediated effect (McLean and Sillar, 2004).

Similarities between the basic components of the mammalian and non-mammalian vertebrates and the description of a NO-mediated modulation during fictive locomotion warrant this brief mention of tadpole swimming here. For an excellent discussion of the generation and modulation of tadpole swimming, the following review is recommended (Roberts et al., 2010).

1.5.2 NO-mediated modulation of locomotor networks

NO is an important modulator in both invertebrate and non-mammalian vertebrate species but the likely role of NO in mammalian locomotion has yet to be described. However, suggestion of the likely role of NO in the mammalian spinal cord network may be drawn from the established roles of NO in the locomotor networks of other species.

NO has been shown to modulate locomotor circuits in a broad range of marine invertebrates including *Clione limacina* and *Lymnaea stagnalis* (Palumbo, 2005). *Clione limacina* (winged, gelatinous pelagic molluscs also known as sea angels) are opportunistic predators that feed on shelled molluscs. On detecting suitable prey, they accelerate swimming, produce rhythmic buccal movements, and the feeding orifice displays an "explosive extrusion of buccal cones", leading to the marine equivalent of eating a fine meal (Moroz et al., 2000). NO modulates the neural networks that activate motor neurons and interneurons that coordinate these behaviours via cGMP, and reduces their excitability, by cGMP-independent hyperpolarization of the interneurons involved in lip closure. Similarly, NO is involved in regulating the speed circuits involved in feeding in the pond snail *Lymnaea stagnalis*, and a modulatory relationship between NO and 5HT at motor neuron synapses has been established (Elofsson et al., 1993, Moroz et al., 1993, Straub et al., 2007). The simplicity and ease of use of the invertebrate nervous system makes it an attractive model for locomotor studies, though, unfortunately, direct translational capacity between invertebrate and higher mammals is difficult, due to the differences in the fundamental design of the CNS of higher mammals. However, findings in invertebrate systems provide clues for potential mechanisms in vertebrate models.

NO has been established as a neuromodulator in non-mammalian vertebrate models of locomotion. In the tadpole and lamprey, nitric oxide synthase (NOS) positive reticulospinal neurons in the caudal hindbrain are thought to be the source of NO-mediated modulation of swim circuits. In the tadpole, NO slows swimming frequency and reduces swimming episode duration, by facilitating both glycinergic and GABAergic transmission via presynaptic mechanisms (McLean and Sillar, 2001, McLean and Sillar, 2000). The GABAergic effects of NO are a result of direct NO effects, whilst glycinergic-mediated increases in cycle period are a result of metamodulation, where NO modulates the activity of another downstream modulator, NA. This meta-modulatory hierarchy is evidence that neuromodulation can result from potentially complex interactions between neurotransmitters as well as from direct modulation of intrinsic cellular properties. NO also modulates the intrinsic properties of

postsynaptic neurons by depolarising the membrane potential and increasing membrane input resistance in the tadpole but not in the lamprey (McLean and Sillar, 2004, Kyriakatos et al., 2009). In contrast to NO effects in the tadpole, NO increases lamprey swim frequency by reducing mid-cycle inhibition and facilitating on-cycle excitation (Kyriakatos et al., 2009). Interestingly, NO is also involved in spinal mGluR1-mediated long-term plasticity, though a mechanism for this action is not currently known. Altogether, this convincing evidence from the non-mammalian vertebrates suggests that a role for NO in the mammalian locomotor network is highly probable.

We do know that in the rodent respiratory circuit, NO inhibits inspiratory drive received by hypoglossal motor neurons, by cGMP-dependent mechanisms (Montero et al., 2008, Saywell et al., 2010). Furthermore, NO enhances excitatory transmission during inspiratory phase transition controlled by neurons in the brainstem (Pierrefiche et al., 2007)and long-term facilitation of XII motor neuron output, in concert with NA (Saywell et al., 2010). During hypoxia, NO also inhibits inspiratory drive by modulation of K_{ATP} channels (Mironov and Langohr, 2007).

Another example of a role for NO in motor systems of mammals is provided by studies of the trigeminal nucleus, which coordinates complex oral motor tasks. NO produced by pre-trigeminal and pre-hypoglossal motor neurons in the cat has been shown to decrease glutamatergic signalling to trigeminal motor neurons (Pose et al., 2011, Pose et al., 2005).

However, there is an absence of research into the effects of NO in mammalian spinal locomotor networks. Research currently being undertaken in our laboratory has used immunohistochemistry and fluorescence labelling to locate neurons that produce NO in the spinal cord ventral horn (Fig. 1.2). This thesis is an investigation into the likelihood that NO is involved in the regulation of mouse hind limb locomotion.

1.6 Nitric oxide signalling

Research into the identity, causes and effects of NO has been the focus of numerous groups over the last thirty years. Whilst effectors and consequences of NO production were identified from the early 1960s onwards, NO was identified as an endogenous modulator of vascular smooth muscle in the late 1980s. NO was identified as the endothelial derived relaxing factor by four independent research groups (Murad, 1986, Palmer et al., 1987, Ignarro et al., 1987, Palmer et al., 1988). The Nobel Prize was awarded for "for their discovery concerning NO as a signalling molecule in the cardiovascular system" to Robert Furchgott, Louis Ignarro and Ferid Murad in 1998. NO continues to be studied in a variety of model organisms with at least one clear role for NO defined in the periphery and emerging roles in the CNS. However, the actions of NO have been relatively understudied in the networks that generate and maintain locomotion. In order to understand the possible roles of NO in mammalian locomotor networks the production of NO must be considered. A simplified summary of NO signalling accompanies the following detailed text (Fig. 1.1).

1.6.1 Nitric oxide synthase structure and function

NO is produced biologically by the enzyme NOS of the oxidoreductase enzyme family (EC 1.14.13.39). The mammalian NOS family constitutes three isozymes with molecular weights of between 125-155kDa and with more than 60% homology (Moncada et al., 1991, Dawson et al., 1991, Knowles and Moncada, 1994). The neuronal (nNOS or NOS-1) and endothelial (eNOS or NOS-3) NOS are constitutively expressed and require calcium for normal function whilst the inducible form (iNOS or NOS-2) is calcium independent and expressed by activated macrophages, neutrophils and microglia in response to immune stimulation. While the inducible form is expressed specifically at times of inflammation and immune challenge, the constitutively expressed isoforms are distributed throughout the body, particularly in the vasculature (eNOS) and the CNS (nNOS).

The NOS enzyme is a homodimer and requires several cofactors to produce NO: calmodulin (CaM) nNOS/eNOS; flavin adenine dinucleotide (FAD); flavin mononucleotide (FMN); haem; NADPH (Nicotinamide adenine dinucleotide phosphate); and tetrahydrobiopterin (BH_4). All three isozymes have a reductase domain consisting of a NADPH binding site, flavin cofactors FAD and FMN, and an oxygenase domain consisting of a haem and BH_4 binding site. The constitutive forms contain an autoinhibitory sequence between the FMN and CaM binding site that acts as a hinge, separating the reductase and oxygenase domains until the enzyme is activated by CaM.

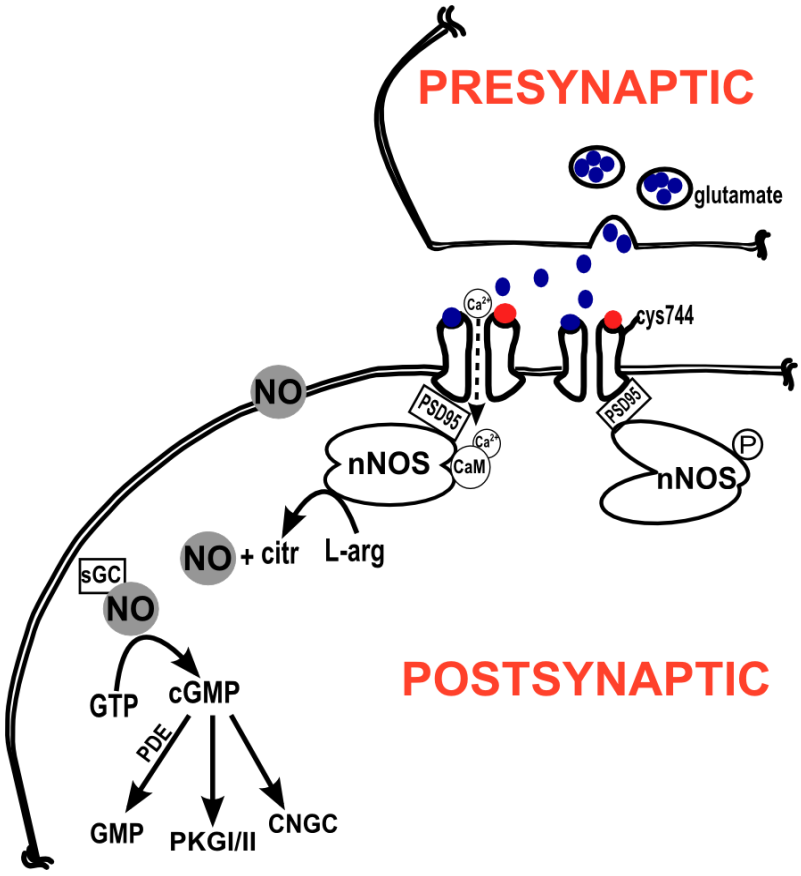

Figure 1.3. Simplified schematic of NO production and signalling via sGC/cGMP. NOS is activated by calcium influx through NMDA receptors. NOS catalyses the reaction between l-arginine and O_2 to produce citrulline and NO. NO binds to soluble guanylate cyclase (sGC) initiating cGMP production and with subsequent downstream effects. NO is free to diffuse in a retrograde manner to the presynaptic cell and participate in the same range of reactions.

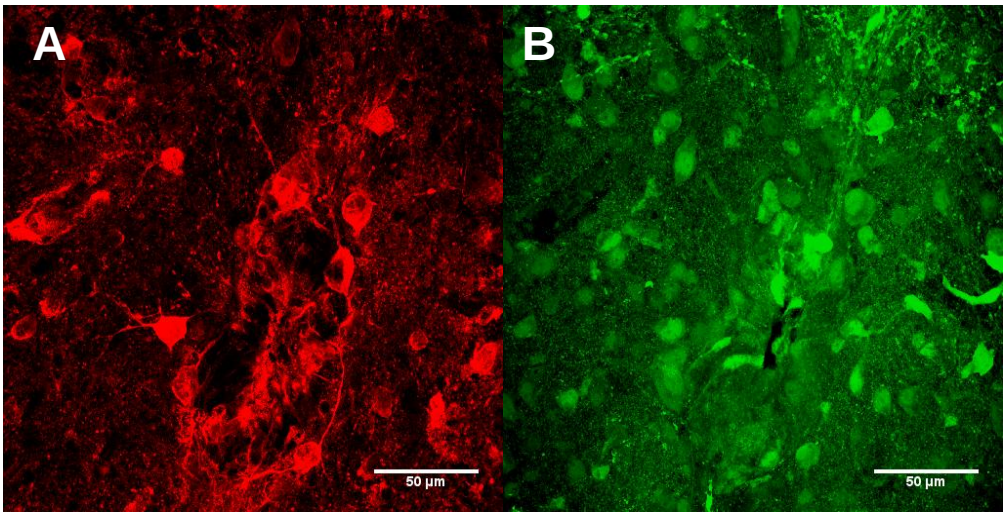

Figure 1.4. Representative images of nitrergic neurons located in lamina X of the mouse spinal cord. Representative images from the postnatal mouse spinal cord reveal nNOS immunostaining **A** and DAF 2DA fluorescence (indicating the presence of NO) **B** in the mouse lumbar spinal cord. (Images courtesy of Dr Lissa Herron).

Adjacent to the N-terminal haem, nNOS is linked to membrane ion channels via the molecular adaptor molecule, PDZ (**P**SD95 **D**lg1 **z**o-1), that interacts with postsynaptic density-95 (PSD95). The discovery that nNOS is an NADPH-diaphorase enzyme (Hope et al., 1991) resulted in a large number of studies, mapping the localization of NO producing cells. The distribution of NO producing cells in the spinal cord is discussed in Chapter 2. All three isoforms generate NO and citrulline by the NADPH dependent oxygenation of l-arginine.

1.6.2 Nitric oxide synthesis

The biological production of NO was the first biochemical pathway discovered to synthesize a gas. The calcium dependent forms of the enzyme are activated by an increase in intracellular Ca^{2+} levels, via glutamate binding to NMDA receptors or voltage dependent calcium channels with the subsequent formation of the Ca^{2+}/calmodulin complex (Moncada et al., 1991). Each Ca^{2+}/calmodulin complex recruits tetrahydrobiopterin, forming a stable tetramer and activating the enzyme complex. The NOS reductase domain transfers a hydride to FAD from NADPH forming NADP+ and $FADH_2$ followed by a sequence of 1e- transfers from FADH2 to FMN. CaM removes the spatial inhibition imposed by the autoinhibitory site, bringing

together the $FMNH_2$ and the oxygenase domain haem allowing the transfer of electrons. CaM activates O_2 resulting in the oxygenation of l-arginine; this N-hydroxy-l-arginine binds to the haem at the active site. BH_4 accepts an electron from the Fe-NO complex, liberating NO and citrulline (Feng and Tollin, 2009, Daff, 2010). Cellular signaling cascades regulate NO production. Protein kinase C (PKC) phosphorylates the enzyme, modestly increasing activity, whilst CaM kinase II phosphorylation results in a decrease in activity (Nakane et al., 1991).

L-citrulline is the by-product of NO production and is recycled by argininosuccinate synthetase (AS) and argininosuccinate lyase (AL) to arginine. This recycling has been studied in glial cells in the context of inducible NO production but not in the context of the constitutively expressed isoforms or in the locomotor network (Wiesinger, 2001, Mori and Gotoh, 2000). A recent study carried out using the rat phrenic nerve, hemi-diaphragm preparation, suggests that citrulline may also cause inhibition of [3H] acetylcholine release by activating adenosine receptors (Barroso et al., 2007, Timoteo et al., 2008).

NO is free to diffuse, unrestricted, through the cytoplasm and across cell membranes to a target receptor, in an autocrine, paracrine or retrograde manner. L- arginine is the only physiological substrate involved in NO synthesis and analogues of the amino acid are potent inhibitors of the NOS enzyme.

1.6.3 The NO/sGC/cGMP signalling pathway in the CNS

NO is a free radical, diatomic gas with a plethora of physiological and pathophysiological effects. NO has been described as both a direct modulator of cellular function and a retrograde transmitter; that is, a molecule that is released from the postsynaptic neuron diffuses to the presynaptic bouton where it activates a specific receptor and alters synaptic transmission (Regehr et al., 2009). As a direct modulatory agent and a retrograde messenger, NO is able to modulate synaptic function through coupling to enzymes, direct modification of proteins by s-nitrosation, and initiation of signalling cascades.

The receptor for NO is soluble guanylate cyclase (sGC; EC 4.6.1.2), which produces cyclic guanosine 3', 5'- monophosphate (cGMP) from guanosine 5' triphosphate (GTP) (Bredt and Snyder, 1989, Bredt and Snyder, 1992, Snyder and Bredt, 1992). Soluble guanylate cyclase is a heterodimeric haemoprotein comprising two subunits, α1/α2 and β1/β2, and is a member of the nucleotide cyclase family exhibiting a degree of similarity in structure to adenylyl cyclase. The α and β protein subunits are between 70 to 82 kDa in size and are highly related (Koesling et al., 1988, Nakane et al., 1988). The β subunit N-terminus contains the haem/NO/oxygen-binding (H-NOX) domain, and the catalytic domain, consisting of both α and β subunit components, is located at the C-terminus. The N-terminus haem selectively combines with NO, inducing a conformational change that activates the catalytic domain, which converts GTP to cGMP. The mechanism of sGC activation and action is the subject of numerous studies and has yet to be described definitively (Winger et al., 2007, Fernhoff et al., 2009, Garthwaite, 2010).

The predominant isoform of the NO sensitive soluble guanylate cyclase molecule in the vasculature is $\alpha_1\beta_1$ in the CNS $\alpha_2\beta_1$ (Russwurm et al., 2001, Friebe and Koesling, 2003). Much of the research into the location of NOS and cGMP has been in relation to pain processing and immune stimulation (Murphy, 2000, Friebe et al., 2007, Baltrons et al., 2008). Indeed, a significant amount of research into the distribution of sGC and cGMP in the ventral lumbar spinal cord is needed to understand fully the role of NO-mediated processes in mammalian locomotion.

In the absence of detailed information on the role of NO in the lumbar spinal cord specifically, interesting suggestions for the role of NO/sGC/cGMP-mediated signalling can be gleaned from the involvement of NO in nociception. Immunohistochemical studies have confirmed that the sGC β_1 subunit is present specifically in spinal cord tissue though expression patterns in L4 and L5 of the ventral horn were not reported (Ding and Weinberg, 2006). In this study, it was postulated that NO acts as a paracrine agent during nociceptive processing as nNOS and sGC did not co-localize in the same neurons. Validating a paracrine role for NO, nNOS positive neurons were found to

appose neurons containing sGC. sGC β_1 immunohistochemistry indicates that sGC is primarily located in neurons in the dorsal horn and around the central canal (Schmidtko et al., 2008). Knock-out of the sGC β_1 subunit in the mouse has revealed that NO/cGMP signalling is essential for life. The sGC β_1 knock-out was lethal for 60% of mice within the first 2 days of birth. Knock-outs were 40% smaller than wild types, hypertensive, absolutely unable to prevent platelet aggregation and were found to have severe dysfunctional gut peristalsis. The inability to coordinate relaxation and contraction of the gut leads to death at weaning when fibre becomes a major component of the diet (Friebe et al., 2007).

In the cervical spinal cord, large cholinergic, cGMP-reactive boutons have been visualised near ventral motor neurons (Vles et al., 2000). Another investigation by the same authors has shown, using NO donors and an sGC agonist, that NO-mediated increases in cGMP are predominantly found in the dorsal horn and the ventral laminae (VII - X) (de Vente et al., 2006). Though the motor neurons were devoid of cGMP reactivity in this study, cGMP co-localised with a population of vesicular glutamate transporter (VGLUT2) and some vesicular acetylcholine transporter (vACHT) reactive neurons in laminae (VII- X), and isolated cGMP-positive boutons in lamina VIII and IX, regions that contain the locomotor-related neuronal circuits. Furthermore, in situ hybridization showed that ventral motor neurons and interneurons express phosphodiesterase (PDE) 2, 5 and 9, all involved in the breakdown of cGMP. A similar study in the lumbar ventral horn would help to address the lack of knowledge relating to NO/sGC/cGMP involvement in mammalian locomotion, though findings in the dorsal horn are again encouraging of a putative role for NO in the lumbar hind limb locomotor network.

The level of sGC activity is dependent on the concentration of NO and the active site haem. A haem-independent binding site is also thought to be involved in full activation of the enzyme. In the absence of NO, sGC exhibits a basal level of activity. When NO binds to the haem moiety, cGMP production is increased, and in the presence of non-haem modification, sGC enters a highly activated, but reversible state that persists in the presence of excess NO (Winger et al., 2007, Fernhoff et al., 2009). Adenosine

triphosphate (ATP) reduces sGC sensitivity to NO whilst still allowing it to bind to the enzyme, possibly to act as a barrier to serendipitous activation of the enzyme or to provide a cellular sink of NO (Garthwaite, 2010, Roy et al., 2008).

NO potency in activation of cerebellar and vascular sGC ($\alpha_1\beta_1$) is greater than that observed in tissue homogenates (Bellamy et al., 2000), suggesting that NO activation of sGC may be tissue- and thus subunit-specific. The NO activation of sGC is responsible for activating cGMP-mediated pathways such as cGMP-dependent protein kinase and cGMP-regulated phosphodiesterase, and cyclic-nucleotide gated ion channels (Dawson et al., 1998, Denninger and Marletta, 1999, Francis et al., 2010).

NO-mediated effects have been alluded to in the preceding sections detailing the structure and function of the locomotor network and NO metabolism. With no clear role ascribed to NO in the rodent locomotor network, suggestions of the possible effects exerted by NO in the spinal network can be drawn from the range of NO-mediated effects in the CNS. In the rat cerebellum, hyperpolarization-activated cyclic nucleotide-gated ion channels (HCN) are modulated by NO-mediated cGMP production (Wilson and Garthwaite, 2010). In the ventral spinal cord, HCN channels have been identified in areas associated with the locomotor network (Milligan et al., 2006), though a definitive role for NO-mediated modulation of cyclic nucleotide-gated ion channels in spinal cord locomotor networks, and in particular motor neurons, is still to be fully elucidated (Sirois et al., 2002, Biel et al., 2009).

NO has been described as a retrograde transmitter in long term potentiation (LTP) in the hippocampus (Boulton et al., 1995, Ko and Kelly, 1999) and involved in long term depression (LTD) of adaptive motor learning coordinated by the cerebellum (Yanagihara and Kondo, 1996). NO also facilitates GABAergic transmission in the hypothalamic paraventricular nucleus of the rat by a cGMP-dependent mechanism (Li et al., 2004).

NO has also been shown to inhibit cytochrome c in the mitochondrial respiratory chain (Brown and Cooper, 1994, Brown and Borutaite, 2007). In the CNS, NO has been

shown to disrupt synaptic transmission in hippocampal cells, by inhibition of mitochondria and the subsequent release of adenosine (Bon and Garthwaite, 2001).

NO activates Ba^{2+} sensitive leak K^{+} channels causing hyperpolarisation in cholinergic basal forebrain neurons. This effect can be mimicked by the PKG agonist 8BrcGMP (Kang et al., 2007, Toyoda et al., 2008). At the Calyx of Held, a giant synapse in the mammalian auditory complex NO is produced after glutamate receptor stimulation and inhibits the actions of K_V3 ion channels. Further investigation of the NO activity dependent effects at this synapse has shown that NO mediates the suppression of K_V3 and the simultaneous switch to K_V2 ion channels to control action potential firing at high frequencies (Steinert et al., 2008, Steinert et al., 2011).

Interestingly, in the pond snail *Helisoma trivolvis*, NO depolarises the membrane potential and increases firing rates of B5 neurons in the buccal ganglion before eventually causing the same neurons to fall silent. These effects are mediated by NO inhibition of calcium-activated and apamin-sensitive potassium channels (Artinian et al., 2010).

These studies indicate that NO has a wide range of roles in both vertebrates and invertebrates CNS, increasing the likelihood of a role for NO in the mammalian spinal cord locomotor network.

1.6.4 cGMP-dependent protein kinases

PKGI α/β and II are NO/cGMP signal transducers. In addition to involvement in PKG stimulation, cGMP is also thought to regulate cAMP-dependent protein kinases (Hofmann et al., 2009). NO stimulation of sGC facilitates the production of cGMP, which binds to PKGI at two allosteric sites resulting in increasing phosphotransferase activity. PKGI α is located predominantly in the cerebellum and medulla while the PKG1β isoform is located predominantly in the hypothalamus, cortex, hippocampus and olfactory bulb. PKG1 mediates a wide variety of reactions including the facilitation of

vascular smooth muscle relaxation, platelet disaggregation and the neuronal voltage-gated K+ channels Kv3.1 and Kv3.2 via serine-threonine phosphatase (Moreno et al., 2001, Schmidt et al., 1992).

PKGII is found throughout the mammalian brain, but its expression in the spinal cord, and therefore relationship to locomotion, has been less well studied (Hofmann et al., 2009). PKGII null mice exhibit reduced bone development and increased behavioural disorder phenotype defined by increased anxiety and excessive ethanol consumption (Pfeifer et al., 1996, Werner et al., 2004). More recently, the NO/sGC/cGMP/PKGII pathway has been reported to modulate mouse HCN2 channel activity(Hammelmann et al., 2011).

1.6.5 cGMP metabolism

cGMP levels will also be affected primarily by phosphodiesterase (PDE) breakdown and to a lesser extent trafficking out of the cell by ATP-dependent multidrug resistant proteins (Jedlitschky et al., 2000). cGMP is broken down by cyclic nucleotide PDEs. Prolonging the life of cGMP and increasing the duration and magnitude of its related downstream effects make PDEs ideal therapeutic targets (Boswell-Smith et al., 2006). The pharmacological success stories of PDE5 inhibitors sildenafil and tadalafil (Viagra and Cialis), and PDE3 inhibitor cilostazol, used to treat hypertension, erectile dysfunction, and acute heart failure respectively, are well documented. The role of these and other PDEs have been studied extensively in the neuronal and peripheral vascular system and to some extent in the immune system. In the CNS, PDE5 ameliorates autoimmune encephalomyelitis in the mouse model of Multiple Sclerosis (Pifarre et al., 2011) and inhibition of cGMP metabolism by PDE9 leads to enhancement of learning and memory in the rat hippocampus (van Zundert et al., 2008, Wunder et al., 2005).

1.7 NO forms reactive nitrogen species

1.7.1 Nitrosative stress

NO can participate in a number of thermodynamically favourable, chemical reactions that modify cellular activity independent of the NO/sGC/cGMP pathway. These reactions are classified as occurring under either oxidative or nitrosative stress and result from an increased level of NO in the cellular environment, with nitrosative stress the predicted result at the highest concentrations of NO. Whilst it may seem extraneous to consider the chemistry of NO under physiological conditions, the confirmation that these reactions can occur during normal cellular function, and the added complication that manipulation of the NO system routinely involves other reactive pharmacological agents, give validation to their consideration.

The auto-oxidation of NO in the reaction with oxygen forms nitrogen dioxide according to the reaction:

$$2{\cdot}NO + O_2 \rightleftharpoons 2NO_2 \qquad [1]$$

In an environment where an excess of NO persists, nitrogen dioxide reacts with dinitrogen trioxide as follows:

$${\cdot}NO + {\cdot}NO_2^- \rightleftharpoons {\cdot}N_2O_3 \qquad [2]$$

Dinitrogen trioxide reacts with water to produce nitrite as follows:

$$H_2O + N_2O_3 \rightleftharpoons 2{\cdot}NO_2^- + 2H^+ \qquad [3]$$

Though oxidative reactions can occur, at high levels of NO the balance is predicted to shift towards nitrosative stress. In conditions of nitrosative stress, NO can react with superoxide to produce peroxynitrite:

$$\cdot NO + O_2^- \rightleftharpoons ONOO^- \quad [4]$$

Peroxynitrite can react with NO to produce both dinitrogen trioxide and nitrite:

$$ONOO^- + 2\cdot NO \rightleftharpoons N_2O_3 + \cdot NO_2^- \quad [5]$$

And in the presence of carbon dioxide peroxynitrite reacts with NO to produce dinitrogen trioxide and nitrogen dioxide:

$$ONOO^- + 2\cdot NO \rightleftharpoons N_2O_3 + NO_2 \quad [6]$$

In the absence of L-arginine, NO synthase will produce superoxide. Superoxide dismutase has a lower affinity for NO than the superoxide radical and as a consequence, traces of NO can produce peroxynitrite. Peroxynitrite participates in lipid peroxidation and thiol modification with potentially mutagenic consequences. It has been shown that nitrate glutathione (GSH) and phenolic compounds such as tyrosine and peroxynitrite can uncouple NO synthase by oxidizing BH4. Dinitrogen trioxide (equations 2, 5 and 6) is also a potent nitrating agent, and nitrite, like NO, is endogenously produced and a potent free radical (Kuzkaya et al., 2005, Radi, 2004). This reactive radical chemistry is a facet of NO metabolism and is normally counteracted by antioxidant levels. Haemoglobin is a potent scavenger of NO, nitrite and peroxynitrite, whilst physiological plasma levels of urate and ascorbic acid scavenge peroxynitrite (Griffiths et al., 2003, Kuzkaya et al., 2005).

The diverse range of reactions, leading to both protective and apoptotic states, can be accounted for by the signalling pathways and direct stimulation of cellular targets by NO and the indirect, chemical reactions that involve nitrosation. Typically, S-nitrosation requires higher concentrations (≈1μM) of NO than does activation of sGC (≈1-30nM) and it has been suggested that thiol modification takes place more readily in pathophysiological states (Thomas et al., 2008). However, evidence of a wide range of physiologically relevant nitrosation modifications has been described.

Cysteine has been identified as the amino acid residue that is most often the target of s-modification (Lipton et al., 1993). S-nitrosation has been shown to modify the activity of ion channels, in particular the NMDA receptor, suggesting an activity dependent role for NO synthase activity. The NMDA receptor is intimately linked with NOS through the PDZ domain of PSD95. Cys399 of the NMDA receptor NR2 subunit is s-nitrosated and NO dependent activity is reduced (Stamler et al., 1992, Choi et al., 2000). NO dependent s-nitrosation and subsequent activation of nociceptive, acid-sensing ion channels (ASIC) increases the open probability, but not the maximum conductance, of these channels (Cadiou et al., 2007). Similarly, ryanodine receptors (RyR3) can be s-nitrosated (Sun et al., 2001), and in isolated aortic smooth muscle, s- nitrosation (also referred to as s-nitrosylation) has been shown to desensitise sGC, leading to a negative feedback loop in which NO inactivates sGC and desensitises the receptor to further stimulation by NO (Sayed et al., 2007). Nitrosation of proteins is the second main pathway by which NO can exert its effects and the breadth of these studies involving endogenous and pathophysiological s-nitrosation indicates that this mechanism is important in both normal and abnormal function.

1.7.2 Nitrosative stress in ALS

It has been postulated that NO in involved in the progression of a number of neurodegenerative diseases such as Multiple Sclerosis (MS), Alzheimers' disease (AD) and ALS (Smith et al., 2001, Raoul et al., 2006).

ALS in particular is relevant to the present study, which seeks to investigate the distribution and function of NO in the mammalian spinal locomotor networks. NO has been implicated in ALS, an adult-onset disease characterised by the progressive loss of somatic motor neurons, leading to rapid muscle wasting, paralysis and death typically within 3-4 years of diagnosis (Chapter 2, Section 2.1.4). NO may facilitate disease progression, through mechanisms that involve nitrosative stress

However, NO has a variety of physiological effects in the CNS, and the role of NO in ALS is not clear. For instance, as a modulator of neural output, NO on the one hand maintains vascular tension and reduces the impact of oxidative stress (Wingler et al., 2011) while on the other hand contributes to programmed cell death by nitrosative stress (Boillee et al., 2006). In ALS, NO dependent production of peroxynitrite leads to caspase-mediated cell death (Martin et al., 2005, Raoul et al., 2006, Locatelli et al., 2007, Martin et al., 2007) and is also thought to be involved in axon retraction and synaptic stripping (Sunico et al., 2005, Sunico et al., 2010, Moreno-López et al., 2011, Sunico et al., 2011).

However, the distribution of NO producing neurons and the chronological contribution of NO to ALS remain unclear and are likely a product of the neuronal environment. It is also likely that NO signalling acts in concert with other mechanisms in the progression of ALS. Most studies investigating the causes and progression of ALS have not considered a change in NOS expression as part of the disease mechanism and a study of the distribution of NOS in the spinal cord of the mouse model of ALS has yet to be carried out.

1.8 Scope of this investigation

It is clear that NO is a modulator of neuronal function in the locomotor networks of both invertebrate and vertebrate species. NO is an important modulator in the vertebrate locomotor network, illustrated by its role in tadpole and lamprey swimming. NO also has a wide range of effect in other networks of the CNS but a role for NO-mediated transmission or modulation in the mammalian locomotor network has yet to be described. In order to better understand the role of NO in the mammalian spinal locomotor network, the present study aims to identify the sources of NO in the lumbar spinal cord, assess the effect of NO on whole network locomotor-related output and investigate the potential modulation of neuronal properties by NO that contribute to the regulation of locomotor output.

In Chapter 2, I will describe the spatial and temporal distribution of NOS positive neurons in the lumbar spinal cord over a developmentally relevant period, using the NADPH diaphorase histochemical reaction in wild type CD1 mice. Additionally I will describe the distribution of NOS positive neurons in the lumbar spinal cord of the SOD^{G93A} transgenic mouse. The contribution of NO to the regulation of rhythmic fictive locomotion recorded from *in vitro* isolated spinal cord preparations and the pathways involved in any effects will be described in Chapter 3. Finally, in Chapter 4, using quiescent slice preparations, the effects of NO on the intrinsic properties of lumbar spinal neurons will be assessed.

Together these chapters aim to investigate the role of NO-mediated modulation in the mammalian hind limb spinal locomotor network.

Chapter 2: Spatiotemporal distribution of NADPH Diaphorase containing neurons in the lumbar spinal cord of the neonatal mouse.

2.1 Introduction

2.1.1 Background

While the brain and spinal cord constitute a single organ, historically, delineation of the structure and function of the CNS has centred on the cortices. From the mid-eighteenth century, efforts to understand the structure and function of the spinal cord were largely at the level of gross structure, akin to the studies of the cortices of the brain. At the turn of the twentieth century, studies investigating the structure of the spinal cord were heavily influenced by the revolutionary histological work and theories of Golgi and Ramon y Cajal, neuroanatomists for whom synaptological studies and their findings were the best strategy for the study of the spinal cord.

By the middle of the twentieth century, research into the structure of the spinal cord found a middle ground between the studies at the gross and synaptic level, when Bror Rexed, incorporating newly available knowledge of prominent cell columns, published his research investigating the structure of the cat spinal cord. His hypothesis that the spinal cord, like the brain is "generally…built up of a number of cell layers, regions or nuclei, which are adequately characterized by the shape, arrangement and connections of their constituent cells" marked a turning point in the study of spinal cord neurons in specific, anatomically characterised areas (Rexed, 1954). His canonical delineation and methodical categorisation of the cells of the spinal cord has been shown to be broadly consistent across species and remains a reference for anatomical studies sixty years after its first publication (Watson, 2009).

The spinal cord matter can be described at the gross level as consisting of two distinct substances, white and grey matter. White matter consists of myelinated axon tracts, while the grey matter consists of soma, dendrites and both myelinated and unmyelinated

axons. The grey matter is composed of nine cell layers (laminae I to IX) and the area around the central canal (lamina X). The ventral horn, comprising laminae VII – IX, is associated with motor control. Locomotor-related interneurons are located in laminae VII, VIII, IX and X while the motor nuclei are found in lamina IX. The projection patterns and transcription factor identity of the neurons were detailed in Chapter 1 (Section 1.2).

Conventionally described as segmented, the spinal cord consists of two halves or hemi-segments and each half has a dorsal or afferent nerve and a complimentary ventral nerve, through which axons respectively return from and project to the periphery. The rodent spinal cord comprises thirty-eight segments: cervical, C1 – C8; thoracic, Th1 – Th13; lumbar, L1 – L6; sacral, S1 – S4; and coccygeal, Co1 – Co3. The present study is concerned specifically with the spinal hind limb locomotor-related ventral interneurons (laminae VII, VIII, IX and X) and the motor neurons in the medial and lateral motor pools (lamina IX) located in the lumbar spinal cord.

Determining the location of nitrergic neurons in the mammalian spinal cord is integral to our understanding of the role of NO during development and disease. The following section details what is known of the distribution of nitrergic neurons in the spinal cord and the roles of NO in spinal cord development together with the putative role of NO in the fatal neurodegenerative disease, ALS.

2.1.2 Expression of nitric oxide synthase in the spinal cord

Since NOS was identified as an NADPH-dependent enzyme in the brain, the NADPH diaphorase histochemical reaction has become a selective marker for NOS reactivity throughout the CNS (Dawson et al., 1991, Hope et al., 1991). Tetrazolium salts can act as substrates for the NADPH-dependent reaction catalysed by NOS, producing an insoluble visible, blue/purple formazan. The reaction is particularly useful as the NADPH diaphorase reactivity of the NOS enzyme is resistant to formaldehyde fixation.

The terms NOS positive and NADPH diaphorase reactive are used here interchangeably.

NADPH diaphorase activity has been described in the spinal cord of a large number of vertebrates and invertebrates. Extensive spatiotemporal studies have been conducted in the brain and spinal cord of the anuran amphibian, *Xenopus laevis.* In the spinal cord, NADPH diaphorase reactivity increases between developmental stages 29, at the onset of early locomotor activity, and stage 47, when limb buds appear (McLean and Sillar, 2001). A subsequent study during the early stages of metamorphosis (stages 47 to 66) showed that NADPH diaphorase reactivity peaks at the time of emergence of the limbs (although it is not co-localised with motor pools in developing limb circuits), before declining (Ramanathan et al., 2006).

In the adult rat, the greatest NADPH diaphorase reactivity is observed in the dorsal horn, specifically the superficial layer (I and II), consistent with the large body of research detailing the role of NO in sensory processing (Cury et al., 2011, Murphy, 2000, Schmidtko et al., 2009). Reactivity in the intermediolateral layer (IML) is closely related to the vasculature, and in the ventral horn some scattered weak reactivity is seen amongst the motor neurons. Neurons exhibiting reactivity around the central canal are uniformly distributed with axons extending across the midline of the grey matter (Dun et al., 1993, Spike et al., 1993, Valtschanoff et al., 1992).

A comparative study of the rat, mouse, cat, and squirrel monkey showed that, across species, the distribution of NADPH diaphorase reactivity in the spinal cord is broadly similar (Dun et al., 1993). All species showed reactivity in the superficial dorsal horn, IML, ventral horn, and central canal. However, fewer reactive neurons were recorded around the central canal in the cat and squirrel monkey, with the squirrel monkey recording the least reactivity in lamina X of all the species tested. NADPH diaphorase reactivity was notably absent from the motor neuron population in all of the species examined. However, in the rabbit, upregulation of NOS expression in ventral horn motor neurons has been observed after induced ischemia in the rabbit (Schreiberová et al., 2006). This highlights the possibility that NOS expression can be state specific.

Transient expression of NOS in populations devoid of NOS at certain stages of development or pathophysiology is possible. Similarities to the non-human expression patterns described were recorded in a small study of the developing human spinal cord; between 42 to 98 days post conception, NADPH diaphorase neurons appear in the dorsal and ventral horns and migrate to the deeper dorsal horn, IML and Lamina X (Foster and Phelps, 2000).

NO production has been linked to NMDA receptor signalling in nociception and therefore it is thought that NO production is activity-dependent (Maihofner et al., 2000, Xu et al., 2007)**.** An increase in NO production during development in the rat spinal cord has been supported by the observation that the molecular scaffolding molecule PSD95 and nNOS co-localise in rat lumbar neurons. Neurons showing co-localisation increase in number from birth to P14, followed by a decline, suggesting that NO may have a predominant role in spinal cord development and a lesser role in normal network function (Gao et al., 2008). However, the exact developmental and network interactions of NO are not known.

NADPH diaphorase reactivity in the mouse lumbar spinal cord has been examined in relation to neurons involved in nociception (de Vente et al., 2006, Schmidtko et al., 2009, Todd, 2010). Over the developmental period P5-P30, the NADPH diaphorase reactivity pattern was described in the superficial dorsal horn neurons of lumbar sections L3-L6 to investigate the potential mediation of nociception by NO. NADPH reactive neurons increased in number over the period, peaking at P20 before declining, and the number of reactive neurons increased in response to NMDA, confirming activity-dependent activation of NOS, as would be expected after nerve injury (Xu et al., 2006).

Immunohistochemistry has revealed the neurotransmitter phenotype of neurons possessing NADPH diaphorase reactivity, providing insight into the excitatory or inhibitory characteristics of these neurons. In the rat, mouse, cat, and squirrel monkey, there is some co-localisation of NADPH diaphorase reactivity with choline acetyltransferase (ChAT) in the IML of lamina VII and lamina X (Dun et al., 1993).

Motor neurons of the ventral horn are cholinergic but not NOS positive (Dun et al., 1993). Furthermore, NADPH diaphorase reactive neurons can be GABAergic/glycinergic, in addition to showing cholinergic immunoreactivity. In the superficial dorsal horn (laminae I and II), NADPH diaphorase reactivity was restricted to neurons that are either glycinergic or GABAergic. In the deeper dorsal horn neurons (lamina III), NADPH diaphorase reactivity was found in neurons with either GABA- and glycinergic or GABAergic and cholinergic neurotransmitter phenotypes (Spike et al., 1993). Higher resolution studies using confocal microscopy have revealed that, in fact, nNOS is also expressed by a significant proportion of excitatory interneurons in the same laminae I and II populations that also express protein kinase C (PKC) (Sardella et al., 2011).

Cholinergic transmission, mediated by C-bouton synapses on motor neurons, is an important modulator of motor neuron excitability; however, 99% of C-boutons have been shown to be devoid of NOS immunoreactivity (Miles et al., 2007, Zagoraiou et al., 2009), precluding a role for direct involvement of NO in this motor neuron gain control system. However, ChAT reactive terminals that are NOS positive have been described in close proximity to motor neurons (Miles et al., 2007). Furthermore, the C-boutons that excite motor neurons originate from $V0_C$ interneurons that are located around the central canal (lamina VII) and the medial zone of lamina VII (Zagoraiou et al., 2009) and therefore by the close proximity of NOS expressing neurons to the $V0_C$ population, NO may directly (autocrine) or indirectly (paracrine) influence locomotor behaviour.

The spatiotemporal distribution of NOS-producing neurons has been previously described in the tadpole brainstem and spinal cord (McLean and Sillar, 2000, Lopez and Gonzalez, 2002). The endogenous production and exogenous application of NO modulates locomotor activity in the tadpole by facilitating glycinergic transmission (McLean and Sillar, 2000, McLean and Sillar, 2002). This evidence from a non-mammalian model organism not only shows that NO is located in neurons that regulate locomotor output but that NO explicitly modulates locomotor activity. Given the similarities between core spinal locomotor mechanisms in the non-mammalian

vertebrate and in mammals, these studies strongly suggest that NO may modulate mammalian locomotor output.

Despite the evidence that NO is produced by neurons in the mammalian ventral horn, the expression and function of NO in the locomotor network have not been studied in great detail. In particular, little is known about the expression pattern and role of NO during postnatal development of the spinal locomotor networks as they mature.
A preliminary study of NADPH diaphorase reactivity was performed in the lumbar spinal cord of the neonatal mouse (Collett, 2007). A comparison of lumbar segments L2 and L3 at P1, P5, and P14 showed an increase in the total number of NADPH diaphorase reactive neurons. The present study aims to advance these preliminary findings by investigating NOS expression, at greater detail by examining expression within individual laminae, during postnatal development in the wider L1-L5 neonatal lumbar mouse spinal cord. Detailed knowledge of the expression patterns of NOS in the developing spinal cord is critical in progressing our current understanding of the role of NO in the development of spinal motor systems and the potential physiological roles of NO in the control of movement.

2.1.3 Roles of nitric oxide in spinal cord development

NO has been shown to have both morphogenic and axonogenic properties. The main receptor for NO is soluble guanylate cyclase, which catalyses the production of cGMP from GTP, initiating changes to cellular properties through PKG. NO signalling through cGMP-dependent mechanisms potentiates the Sonic hedgehog protein (Shh) -mediated induction of ventral cell-types in chick neural explants (Robertson et al., 2001). The physiological radical/antioxidant balance between NO and folic acid controls cell proliferation and cell death in chick neural tube development; high levels of NO promote pre-mitotic proliferative effects and increase neural tube closure defects. In contrast, in the absence of NO, mitosis is potentiated. Inhibition of the morphogen, bone morphogenic protein 4 (BMP4), induces NO mediated apoptosis leading to neural tube defects (Plachta et al., 2003, Weil et al., 2003, Traister et al., 2004).

A variety of studies suggest that NO has diverse roles later on in development. In the chick embryo, NO causes a reduction in motor neuron dendritic tree arborisation via the cGMP/PKG pathway (Xiong et al., 2007). Similar results were observed in the zebra fish embryo where inhibition of NO production causes an increase in axon collaterals (Bradley et al., 2010). In the chick embryo, symmetrical ryanodine receptor calcium induced calcium (RCIC) release is involved in directional polarity of growth cones. Through cGMP-dependent mechanisms, NO reverses the attraction or repulsion of the growth cone towards or against cell adhesion molecule substrates (Murray et al., 2009, Tojima et al., 2009).

However, in contrast to studies in the chick, NO production in the rat causes growth cone collapse and axon retraction by thiol modification of microtubule associated protein 1B determining primary dendrite length (Stroissnigg et al., 2007). Similarly, NO reversibly inhibits neurite growth in dorsal root ganglion nerves by thiol-modification (Hess et al., 1993). In contrast, NO promotes 2^{nd}, 3^{rd} and 4^{th} order dendrite arborisation but appears to have no effect on primary dendrite length in the mouse (Inglis et al., 1998).

These contrasting developmental effects of NO are evidence that much work remains to be done in elucidating the tissue-specific, species-specific and mechanistic roles of NO during development. An integral part of understanding the role of NO in the mammalian locomotor network will involve describing the expression of NOS in the developing lumbar spinal cord.

2.1.4 Nitric oxide in Amyotrophic lateral sclerosis (ALS)

NO has been implicated in neurodegenerative diseases such as Multiple Sclerosis (MS), Alzheimers' disease (AD) and ALS (Smith et al., 1997, Smith et al., 2001, Raoul et al., 2006). Of these, ALS is most relevant to the present study as NO has previously been implicated in the progression of ALS. ALS is an adult-onset disease characterised by

the progressive loss of somatic motor neurons, which consequently leads to rapid muscle wasting, paralysis and death, predominantly from respiratory failure (typically within 3-4 years of diagnosis). The majority of ALS cases are sporadic (SALS), while ~10% of all cases are familial (FALS) with 20% of FALS cases a result of mutations in the superoxide dismutase 1 (SOD1) gene. The most studied murine models of ALS express mutant human Cu/Zn superoxide dismutase 1 transgenes, particularly the SOD^{G93A} mutation (Boillee et al., 2006, Van Den Bosch, 2011).

The mechanisms involved in the onset and progression of ALS are poorly understood though motor neuron death has been linked to glutamate-mediated excitotoxicity. Riluzole is the only current treatment for ALS; a persistent sodium and calcium channel blocker, known to inhibit presynaptic release of glutamate, and thereby it is presumed to act by reducing putative aberrant excitatory input to motor neurons (Wang et al., 2004, Lamanauskas and Nistri, 2008). Riluzole has been used to treat the disease since 1994, with limited success, increasing life expectancy by just 3-4 months; thus, the study of the mechanisms involved in disease cause and progression are the subject of intense research (Bensimon et al., 1994, Aggarwal and Cudkowicz, 2008).

Though oxidative and nitrosative stress are not the sole cause of ALS progression, wild-type motor neurons in culture are less susceptible than cultured SOD^{G93A} mice motor neurons to NO-mediated programmed cell death (Raoul et al., 2006). In SOD^{G93A} mice, upregulation of nNOS and subsequent peroxynitrite production leads to FAS activation and cell death mediated by caspase-8 (Martin et al., 2005, Raoul et al., 2006, Locatelli et al., 2007, Martin et al., 2007). There is also evidence that NOS is upregulated in motor neurons in adult $SOD1^{mutant}$ mice at early pre-symptomatic (<24 weeks) and during symptomatic (>32 weeks) stages of the disease (Sasaki et al., 2002). A role for NO in ALS has also been postulated due to the observation that the NO/sGC/cGMP pathway and subsequent activation of RhoA/Rho kinase (ROCK) leads to axon retraction from their target muscles (Moreno-López et al., 2011). NO has also been implicated in synaptic stripping, which involves the elimination of synapses with motor neurons, by cGMP dependent and cGMP-independent mechanisms (Sunico et al., 2005, Sunico et al., 2010, Sunico et al., 2011).

An increase in the excitability of motor neurons has been shown in cultured motor neurons and during development in SOD1^{mutant} mice, over the period P1 to P12 (Kuo et al., 2004, Kuo et al., 2005, Heckman et al., 2009). Changes in motor neuron excitability during this period of development provide the impetus to investigate whether NO production may be upregulated during the same period in SOD1^{mutant} compared to wild type mice. Investigating NOS expression during the period when the changes in excitability occur will provide an indication of whether NO signalling is involved in these changes.

Despite the significant interest in the potential contribution of NO to ALS, little is known about the expression of NOS in postnatal SOD1^{mutant} mice. Though the majority of research is focussed on the development of the ALS phenotype from pre-symptomatic stages onwards, information regarding the changes that occur during development is relatively scarce.

2.1.5 Scope of this study

This chapter aims to describe the spatiotemporal distribution of neurons in the lumbar spinal cord of the mouse that exhibit NADPH diaphorase, and thus NO, reactivity over the first twelve postnatal days of development, when mice develop the ability to bear weight and walk.

NO is an important mediator of developmental processes and function of the spinal cord circuitry. In the mouse lumbar spinal cord, the expression of NOS, which is a NADPH diaphorase enzyme, has been studied in relation to sensory processing with little attention given to the potential role of NO in the locomotor network. At birth, the neonatal locomotor network continues to develop and locomotion consists of gradually improving attempts to coordinate limbs. Maturity of the locomotor network occurs at P10 in BALB/c mice and rats, indicated by the ability to move with the ventral surface supported on all four limbs (Clarac et al., 1998, Jiang et al., 1999). It is well known that

the lumbar spinal cord contains the CPG that coordinates hind limb locomotion. This provides the impetus for the investigation of NADPH diaphorase reactivity in the neonatal mouse spinal cord during this period, which is developmentally relevant to the study of locomotor networks.

It is not known whether NOS expression differs during postnatal development in $SOD1^{mutant}$ compared to $SOD1^{WT}$animals. Thus, a preliminary investigation was made to assess NADPH diaphorase reactivity in a small group of $SOD1^{G93A}$mice, as changes in NOS expression and therefore NO signalling may contribute to the pathogenesis of ALS.

2.2 Materials and Methods

2.2.1 Tissue collection and preparation

All experiments were performed in accordance with the United Kingdom Animals (Scientific Procedures) Act 1986. CD-1 wild-type (CD-1WT) mice were obtained from Charles River Laboratories (Scotland, UK). The mice were bred under conditions of a 12-h light/dark cycle in individual ventilated cages at a constant temperature of 22°C and 56% humidity with free unrestricted access to food and water. Following cervical dislocation, decapitation, evisceration and vertebrectomy, spinal cord sections from mid cervical to upper sacral region were isolated in a chamber containing gassed artificial cerebral spinal fluid (aCSF; equilibrated with 95% oxygen, 5% carbon dioxide, ~4ºC). Spinal cord tissue was removed from mice between the ages of postnatal day (P)1-12 and placed in 4% paraformaldehyde overnight. Following fixation, the lumbar segments L1-L5 were cryoprotected in 30% sucrose overnight. Each lumbar segment was then cut using a cryostat (Bright lnstrument Co Ltd, Cambs., UK) at -21^{o}C, into 10-15μm transverse sections. The sections were placed on SuperFrost poly-L-lysine coated slides and left to dry at room temperature for between 60 and 90 minutes. The sections were washed with 0.1M phosphate buffered saline (PBS, pH7.4) in preparation for the nicotinamide adenine dinucleotide phosphate diaphorase staining procedure. At P12,

SOD1^{G93A} and wild-type (SOD1 WT) littermate control animals were dissected and fixed as per CD-1WT protocol. The litter analysed comprised SOD1^{G93A} (n = 4) and wild-type (SOD1 WT) littermate control animals (L1, L3, L4 and L5, n = 3 and L2, n = 2). The notation SOD1 WT is used to describe wild type littermates.

Transgenic mice expressing the G93A mutation in the human SOD1 gene were utilised in a subset of experiments. Expression of the *SOD1*^{G93A} *t*ransgene was detected using polymerase chain reaction of DNA from tail clippings. DNA was extracted and polymerase chain reaction (PCR) was performed using the RED Extract-N-Amp Tissue PCR Kit (Sigma-Aldrich) as per the manufacturer's instructions.

The following primers were used:
SOD1 forward primer 5'-CAT CAG CCC TAA TCC ATC TGA-3'
SOD1 reverse primer 5'-CGC GAC TAA CAA TCA AAG TGA-3'
Internal control forward primer 5'-CTA GGC CAC AGA ATT GAA AGA TCT-3'
Internal control reverse primer 5'-GTA GGT GGA AAT TCT AGC ATC ATC C-3'

Thermal cycling was performed on a PCR machine (PCR sprint thermal cycler, Thermo Fisher Scientific, Massachusetts, USA). PCR products were run on a 1.5% agarose gel alongside a 1kb DNA ladder for analysis. Tail clipping, PCR and gel-analysis were performed by Noboru Iwagaki (Iwagaki, 2011).

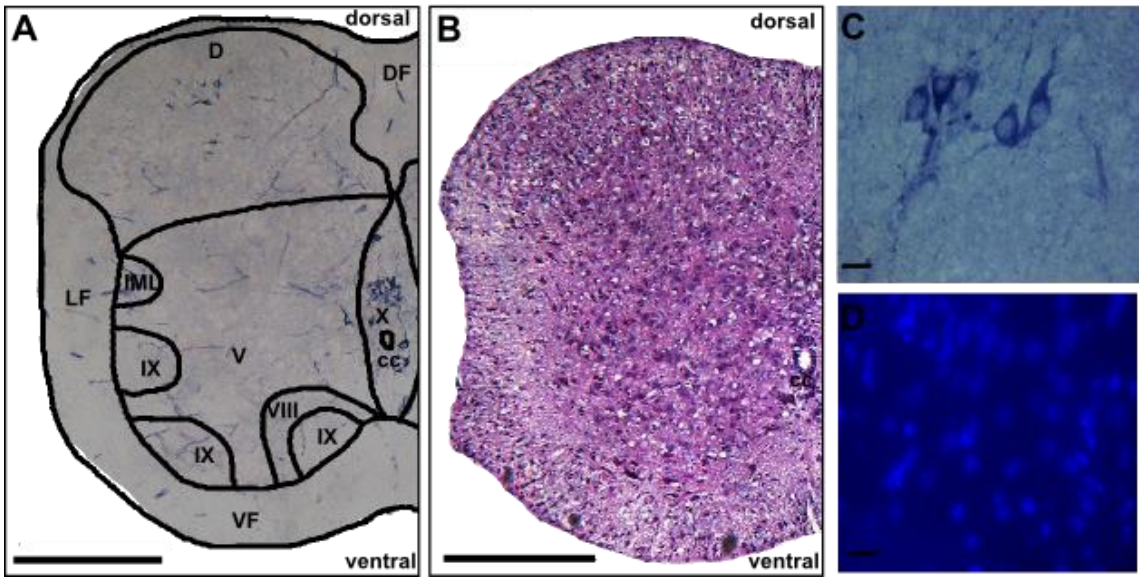

Figure 2.1. NADPH diaphorase reactivity in the neonatal spinal cord of the mouse. A. Derivation of Rexed's laminae used to assign location to reactive neurons during cell count (P5L1, NADPH stain). B, Haematoxylin and Eosin and D, DAPI nuclear stain confirm that the discrete number of reactive neurons were not a consequence of fixing protocol and staining procedures. DAPI histomount was used to coverslip NADPH tissue, C, and images were taken simultaneously comfirming the integrity of the tissue and staining prodecure. Annotations: cc – central canal, D – dorsal, DF – dorsal funiculus, LF – lateral funiculus, V – ventral, VF – ventral funiculus, IML – intermediolateral layer, VII – lamina VII, VIII – lamina VIII, IX – lamina IX, X – lamina X. Scale bars = 200µm, A and B; 20µm, C and D. (Haematoxylin and Eosin, courtesy of Jill McVee).

2.2.2 Nicotinamide adenine dinucleotide phosphate diaphorase (NADPH) staining procedure

The NADPH diaphorase histochemical staining procedure was based on the method previously described (Xu et al., 2006). The slide-mounted sections were incubated for 110 minutes at 37^{o}C in 0.1M PBS (pH 7.4) containing 1mg/ml β-NADPH, 0.13 mg/ml NBT and 0.3% Triton-X100. The reaction was terminated by washing the slides with PBS and distilled water, and slides were then left to dry overnight at room temperature. The dry sections were cleared in xylene and coverslipped using dibutyl phthalate in xylene (DPX). Hemotoxylin and Eosin staining and NADPH diaphorase with fluorescent DAPI (histomount) were used in a small sample group of sections to confirm tissue viability (Fig 2.1).

2.2.3 Image collection and analysis

The animals were divided into four age groups: Group 1 – P1 to 3; Group 2 – P4 to 6; Group 3 – P7 to 9; and Group 4 – P10 to 12. Whole section digital images were captured using a 7.1 Megapixel camera (Canon A620) mounted on a Zeiss Axiolab optical microscope. High power images at specific laminar locations were collected under brightfield and fluorescent illumination using a Hamamatsu ORCA ER camera (Hamamatsu Corp., GmbH) mounted on a Zeiss Axioplan 2 microscope (Carl Zeiss Ltd., UK) with x40 and x63 objectives, collected and optimised using Zeiss Axiovision software (Axiovision Release 4.8.1., Carl Zeiss Ltd., UK). All images were imported into GNU Image Manipulation Program for contrast/colour manipulation and figure assembly was performed in the Inkscape graphics package (Inkscape and GIMP; Free Software Foundation, MA, USA).

Section outlines were made using the grey matter boundary and cell plots created with reference to Rexed's laminae (Rexed, 1954) (Fig. 2.1). Cells in the dorsal horn are predominantly involved in sensory processing and thus were not assigned to individual lamina, instead, laminae I-VI were pooled. Cells were counted in five separate sections of the same spinal segment in each animal and assigned a laminar position. In each age group, the mean number of cells in each lamina for six separate animals was recorded using Excel (version 2010, Microsoft Corp.).

The NADPH diaphorase technique is non-specific for NOS isoforms and therefore labels blood vessels which express endothelial NOS as well as neurons which express nNOS. Positive staining of neurons was defined as staining intensity equal to or greater than that of the blood vessels and distinct from background stain. Neurons exhibited staining of the soma with an absence of staining in what is presumed to be the nucleus. Some light reactivity was observed around cells in the ventral horn; this was not included in the cell counts.

2.2.4 Statistics

Data are presented as mean ± SEM. Segmental and age group data were analysed by two-way ANOVA with Bonferroni multiple comparisons post-hoc test unless stated otherwise. $P < 0.05$ was considered statistically significant (see Table 2.3, 2.6). All statistical data were calculated using GraphPad Prism software (Graphpad, La Jolla, CA).

2.3 Results

2.3.1 NADPH diaphorase reactivity in CD-1 wild-type mice

NADPH Diaphorase reactivity was recorded in several areas within the grey matter of the lumbar spinal cord, including: the superficial and deeper laminae of the dorsal horn; the intermediolateral column (IML), intercalated nucleus (ICN) and lumbar dorsal commissural nucleus of lamina VII (regions in the upper lumbar spinal cord containing sympathetic preganglionic neurons); the remainder of lamina VII; and lamina X, the area encompassing the central canal. Fewer reactive neurons were found scattered in lamina VIII and the medial and lateral motor columns (lamina IX). NADPH diaphorase reactivity was measured in four groups by age: Group 1 – P1 to 3; Group 2 – P4 to 6; Group 3 – P7 to 9; and Group 4 – P10 to 12. NADPH diaphorase reactivity was recorded in the lumbar spinal cord of six animals in each age group.

As mentioned previously, the NADPH diaphorase reaction is non-specific for NOS isoforms and consequently, vascular staining was visible at all levels of the lumbar spinal cord in both white and grey matter. Typically, NADPH diaphorase reactivity was confined to the cytoplasm of neurons containing the enzyme. In the superficial dorsal horn, reactivity appeared continuous throughout the soma, likely due to the combination of small cell size and limited imaging resolution.

Dorsal Horn (Lamina I – VI)

The laminae of the dorsal horn contained the largest population of NADPH diaphorase reactive neurons, which accounted for between 19±3 and 68±5% of all reactive neurons across segments L1-L5 of Groups 1-4 (Table 2.2). A representative selection of dorsal horn neurons was measured and varied in size from approximately 10 to 15µm (Fig. 2.2B and Fig. 2.8B). Along the rostral-caudal axis this dorsal population of NADPH diaphorase reactive neurons was greatest at the caudal levels. (Figs. 2.3, 2.5, 2.7, 2.9 A-E, 2.10B provide a schematic summary of the group and lamina distribution.)

Over the developmental period studied, NADPH diaphorase reactive neurons in the dorsal horn increased in number (1.5-fold increase between Group 1 and 2, 1.3-fold increase between Group 2 and 3; Table 2.1), with the greatest increase in number at Group 4 (3-fold increase between Group 3 and 4; Table 2.1). The greatest mean increase at all levels of the lumbar spinal cord occurred in the L1 segment between Group 1 and Group 4 (10-fold increase; Table 2.1; Fig. 2.10A).

Lamina VII

Neurons in lamina VII form the third largest population of NADPH diaphorase reactive neurons in spinal grey matter across the age groups and spinal segments analysed. Reactivity in the intercalated nucleus (ICN), where visible, was predominantly restricted to fibre tracts and, therefore, was not treated as distinct *per se* from the wider lamina VII area. If neurons showed reactivity and appeared to be in the approximate region of the ICN, they were included in the wider lamina VII count. NADPH diaphorase reactive neurons in lamina VII were irregularly distributed throughout the lamina, and did not appear to form specific nuclei. A mixture of neurons was observed in all segments, with approximate sizes of between 10-30 µm in diameter (Figs. 2.6E, 2.8E). The largest populations of stained neurons within lamina VII were located in the rostral segments (L1-L3) with lower levels in L4 and L5 (Fig. 2.10C).

The proportion of NADPH diaphorase reactive neurons which were found within lamina VII increases from as low as 12±1% up to a maximum of 27±3% (P3L2 and P12L3 respectively; Fig.2.3 and Fig.2.9; Table 2.2) over the period P3 to P12. NADPH

diaphorase reactivity increased in lamina VII throughout the developmental period studied in all segments (Figs. 2.10C, 2.3, 2.5, 2.7 and 2.9, A-E). The total number of NADPH diaphorase reactive neurons in lamina VII increased from Group 1 to Group 4 by approximately 70% (Tables 2.1).

The sympathetic preganglionic neurons of the intermediolateral layer (IML) exhibited NADPH diaphorase reactivity. These neurons formed clusters in the upper lumbar segments (L1 – L3) and were often observed in dense plexuses of neurons closely associated with what appeared to be blood vessels (Fig. 2.6A and C). The level of NADPH diaphorase activity in the IML remained relatively consistent during development, with a peak at L2 in Group 3 (Fig. 2.2; Table 2.1).

Lamina VIII

Light NADPH diaphorase staining was noted infrequently in lamina VIII with less than one neuron recorded per group. The few neurons that were positively stained tended to be located in the rostral segments, with approximate sizes of between 10-20 μm in diameter (Tables 2.1 and 2.2).

Lamina IX

A small number of neurons were NADPH diaphorase reactive in lamina IX (approximately one per segment). These neurons were found mostly in the rostral segments and the largest proportion of these neurons was noted in Group 1 (Tables 2.1 and 2.2). Light punctate staining in the areas around the approximate location of the motor pools, which appeared different in texture and intensity from staining seen in the other laminae, was noted across all segments and age groups (compare Fig. 2.11B, C, and D). Typically, this staining occurred in regions associated with both the medial and lateral motor pools (Fig. 2.11 A; x63, Fig. 2.11B).

Lamina X

Neurons in lamina X form the second largest population of NADPH diaphorase reactive neurons in spinal grey matter. Labelled neurons were approximately 15 to 30μm in diameter (Fig. 2.6D and Fig. 2.8D), with the largest neurons appearing in Group 4. The

projections from labelled neurons appeared to extend along both the dorsolateral and medioventral axes. The proportion of NADPH diaphorase reactive neurons in lamina X in each segment remained relatively constant across the developmental period analysed, except in Group 4 where dorsal horn neurons dominate and lamina X neurons contribute 15±2 to 25±2% of the total Group 4 population, as opposed to 35±2 to 42±4% in Group 1 (Table 2.2). It was not always possible to separate the neurons of the lumbar dorsal commissural nucleus from those recorded in lamina X on the basis of NADPH reactivity alone and therefore, no distinction was made between the two groups.

Across all age groups, there are more NADPH diaphorase reactive neurons within lamina X of the rostral segments (L1, L2 and L3) than the caudal segments (L4 and L5). In each age group, the lamina X population peaks at L2/L3, with the least neurons recorded in L4 segments (Figs. 2.10A, 2.3, 2.5, 2.7 and 2.9, A-E).

2.3.2 NADPH diaphorase reactivity in SOD1 wild-type and SOD1^{G93A} mouse

NO has been implicated in a number of neurodegenerative diseases including ALS. There is evidence that NOS is upregulated in motor neurons in adult SOD1^{mutant} mice at early presymptomatic (<24 weeks) and during symptomatic (>32 weeks) stages of the disease (Sasaki et al., 2002). However, little is known about the expression of NOS in the postnatal SOD1^{mutant,} thus, a preliminary investigation was made to assess NADPH diaphorase reactivity in the SOD1 ^{G93A} mouse model of ALS.

NADPH diaphorase reactivity was recorded in the grey matter of the lumbar spinal cord of both SOD1^{G93A} mice and wild type littermates at P12. The pattern of reactivity in both SOD1 WT and SOD1 G93A mice was consistent with that observed in CD-1WT mice. No difference in the total number of NADPH diaphorase reactive neurons was noted between SOD1 WT and CD-1WT mice (two-way ANOVA with Bonferroni multiple comparison post-hoc test). However, the total number of NADPH diaphorase reactive neurons was significantly lower in the P12 SOD1^{G93A} when compared to the SOD1 WT mice (Student's t-test, $P<0.05$).

Dorsal Horn (Lamina I – VI)

The laminae of the dorsal horn contain the largest population of NADPH diaphorase reactive neurons (Table 2.6). Reactive neurons in both SOD1 WT and SOD1^{G93A} sections did not appear to differ in size from CD-1WT neurons. NADPH diaphorase reactive neurons constitute a similar percentage of the total population of reactive neurons in the dorsal horn of both SOD1 WT and SOD1^{G93A} mice (approximately 60% of the total segmental population; Table 2.6). However, there were less reactive neurons overall in the rostral segments L1 and L2 of SOD1^{G93A}, when compared to SOD1 WT mice. The total number of reactive neurons in SOD1 WT mice was 68±1 in L1 and 79±2 in L2 compared to 53±1 in L1 and 49±1 in L2 of SOD1^{G93A} mice (Table 2.5).

The number of reactive neurons increased in the cord along the rostral-caudal axis with the largest population recorded in the caudal levels of both SOD1 WT and SOD1^{G93A} mice (Fig. 2.12A; Table 2.5.).

Lamina VII

NADPH diaphorase reactive neurons were again distributed throughout lamina VII with a trend towards the largest population being located within the first three rostral segments of the spinal cord. NADPH diaphorase reactive neurons comprised a similar percentage of the total population of reactive neurons in lamina VII of both SOD1 WT and SOD1^{G93A} mice, except in L2 where a higher proportion of the total reactive population were found in lamina VII of SOD1^{G93A} mice compared to SOD1 WT mice (approximately 25% of the total segmental population in the SOD1^{G93A} and approximately 17% in the wild type; Table 2.6). However, there were less reactive neurons in L1 and L2 of the SOD1^{G93A}, when compared to the SOD1 WT. The total number of reactive neurons in the SOD1^{G93A} mouse was 23±1 in L1 compared to 30±1 in L1 of the wild type littermates (Table 2.5; Fig. 2.13C).

The sympathetic preganglionic neurons were again observed as clusters in the IML of upper lumbar segments (L1-L2 only) (Fig. 2.11A). Interestingly, the level of NADPH diaphorase reactivity in the IML was approximately 16-fold lower in SOD1^{G93A} than in

SOD1 WT, particularly at L2 ($P<0.05$, Mann-Whitney test, $SOD1^{G93A}$, n=4 and WT, n=2; Fig. 2.12A and B, Fig. 2.12D; Table 2.5).

Lamina VIII and IX

Very few neurons were NADPH diaphorase reactive in laminae VIII and IX (less than one per segment). The lamina VIII neurons were found mostly in the rostral segments of the SOD1 WT. In lamina X, only one reactive neuron was recorded in the SOD1 WT while none were recorded in the SOD^{G93A} (Tables 2.5). Light punctate staining in the areas around the approximate location of the motor pools was noted occasionally in both SOD1 WT and SOD^{G93A} sections.

Lamina X

The population of NADPH diaphorase reactive neurons in lamina X remained relatively constant along the rostral-caudal axis and no difference was noted between the SOD1 WT and $SOD1^{G93A}$ groups (Table 2.5 and 2.6). The neurons of the lumbar dorsal commissural nucleus were recorded in the cell count for lamina X as described in the CD-1WT. NADPH diaphorase reactive neurons constitute a similar percentage of the total population of reactive neurons in lamina X of both SOD1 WT and $SOD1^{G93A}$, with the exception of L5. In L5 the $SOD1^{G93A}$ had a lower proportion of the total reactive population compared to the SOD1 WT (approximately 16% of the total segmental population in the SOD1G93A and approximately 21% in the wild type; Table 2.6). The total number of reactive neurons in the $SOD1^{G93A}$ mouse was 17±1 in L5 compared to 23±1 in L5 of the wild type littermates (Table 2.5; Fig. 2.13B). NADPH diaphorase reactive neurons comprised a similar percentage of the total population of reactive neurons in L2 of both SOD1 WT and SOD1G93A but the total number of reactive neurons in the $SOD1^{G93A}$ mouse was lower in L2 compared to the wild type littermates (17±1 and 27±1, respectively; Table 2.5).

In both SOD1 WT and SOD1G93A, the pattern of NADPH diaphorase reactive neurons closely resembled that of the CD1 WT mouse. There were overall less NADPH diaphorase reactive neurons in the SOD1G93A compared to the SOD1 WT mouse, in all the laminae described and particularly in the rostral regions (L1 and L2).

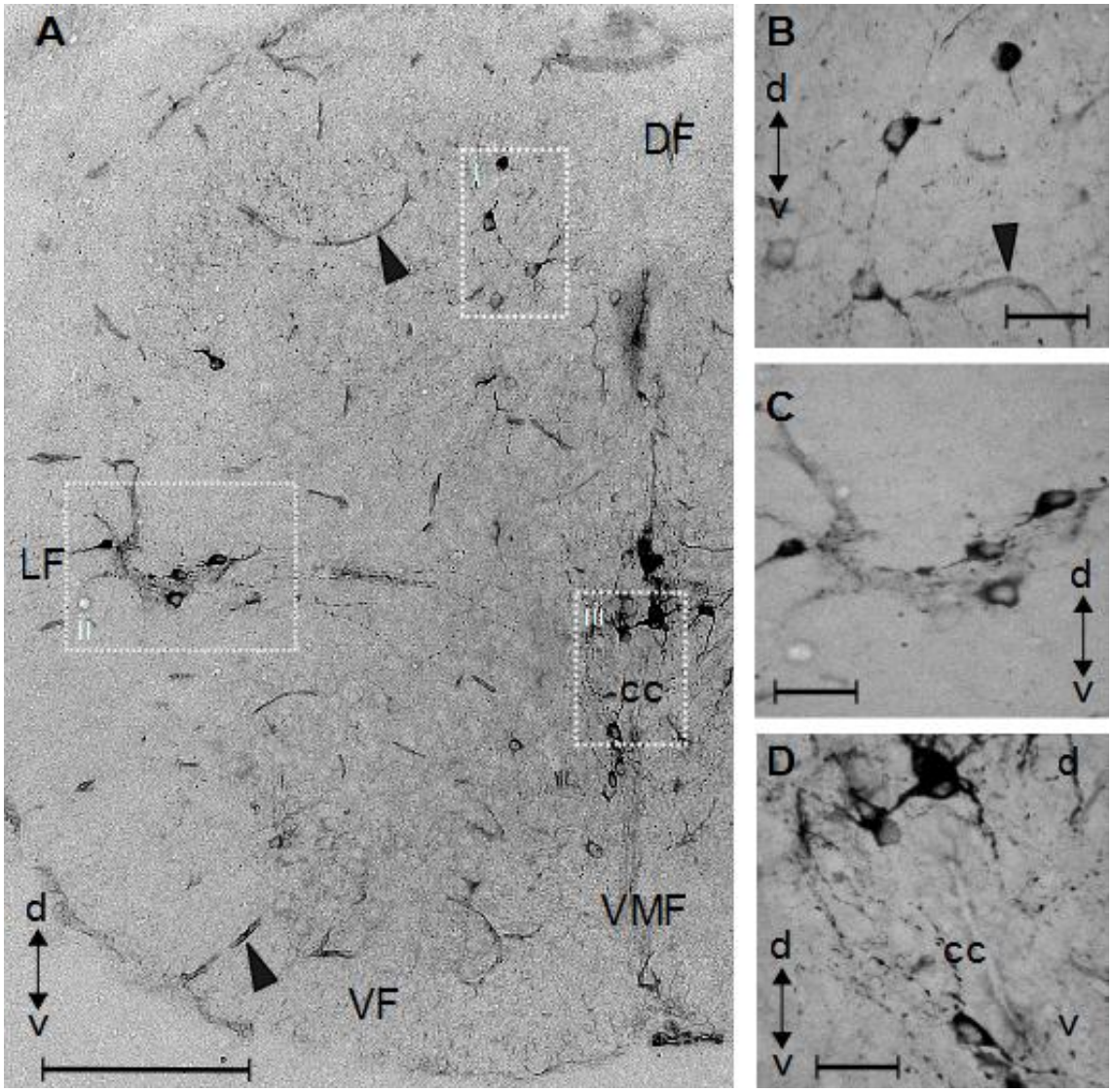

Figure 2.2. Transverse section taken at P3L1 demonstrates NADPH diaphorase reactivity in lumbar spinal cord. **A.** Discrete populations of neurons stain throughout the spinal cord section, stained neurons are visible in the dorsal **Ai,** intermediolateral layer **Aii** and lamina X (LX) **Aiii.** High magnification (x40) brightfield images of typical neurons in the dorsal horn with dorsoventral projections **B, Ai**., sympathetic preganglionic neurons in the intermediolateral layer project laterally and are closely associated with the vasculature **C, Aii** and neurons in LX with both dorsoventral and lateral projections. Staining appears to be restricted to the cytoplasm in all lamina expect those of the superficial dorsal horn which appear to stain in both nucleus and cytoplasm. **D, Aiii**. Vascular staining is visible, throughout the section (black arrowheads). Annotations: cc – central canal, d – dorsal, DF – dorsal funiculus, LF – lateral funiculus, v – ventral, VF – ventral funiculus, VMF – ventral median fissure. Scale bars = 200µm, A; 50µm, B, C and D.

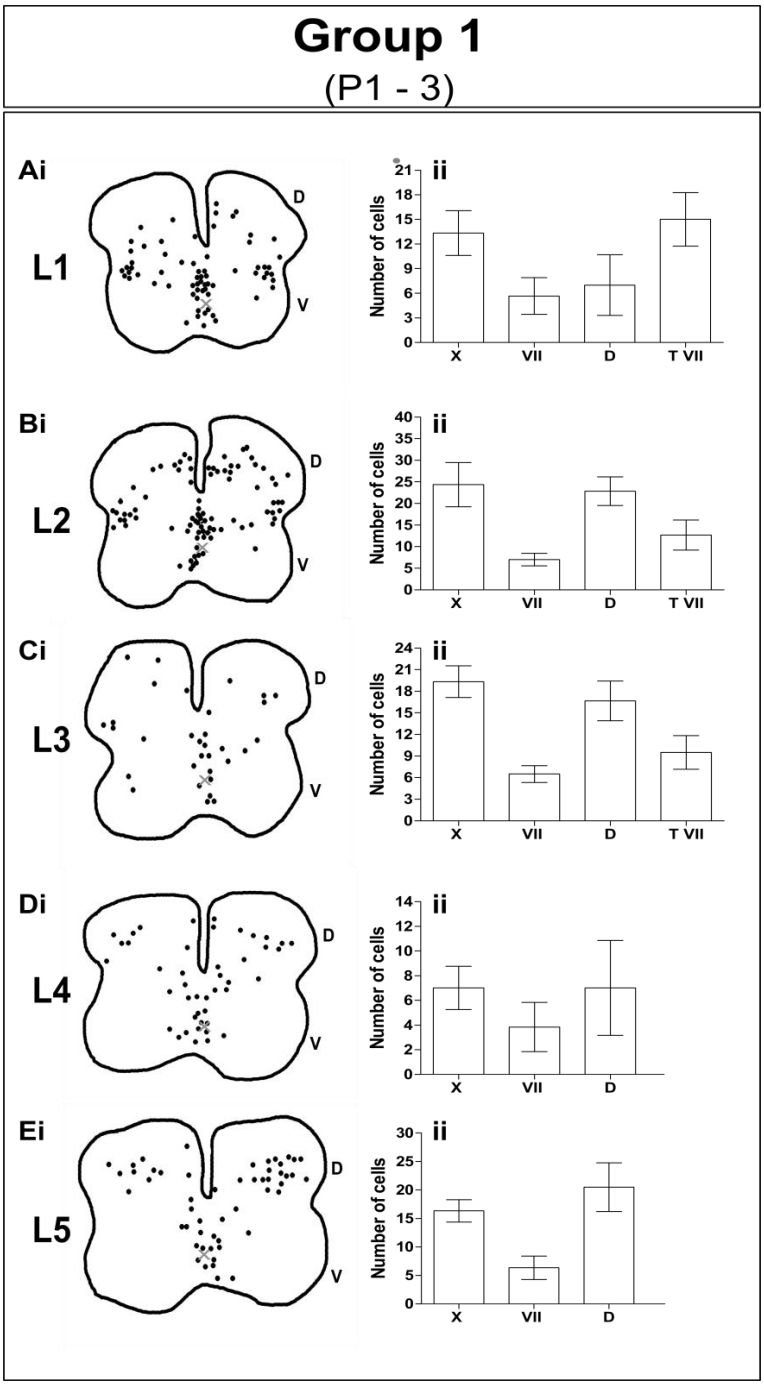

Figure 2.3. Schematic diagram of NADPH diaphorase activity in the mouse spinal cord at P1-3 taken from spinal segments lumbar (L)1-5. **Ai-Ei.** Approximate positions of positively stained neurons are indicated by black filled circles. Each lumbar segment represents 5 transverse segments from 1 mouse and each filled circle represents one neuron. d and v indicate dorsal and ventral orientation. Diagrams are not to scale. **Aii-Eii**. Graphs showing the total number of positively stained neurons in LX, LVII, D and the total in LVII which include the SPN cells of the IML (TVII for L1-3 only). Data are mean ±SEM, n=6.

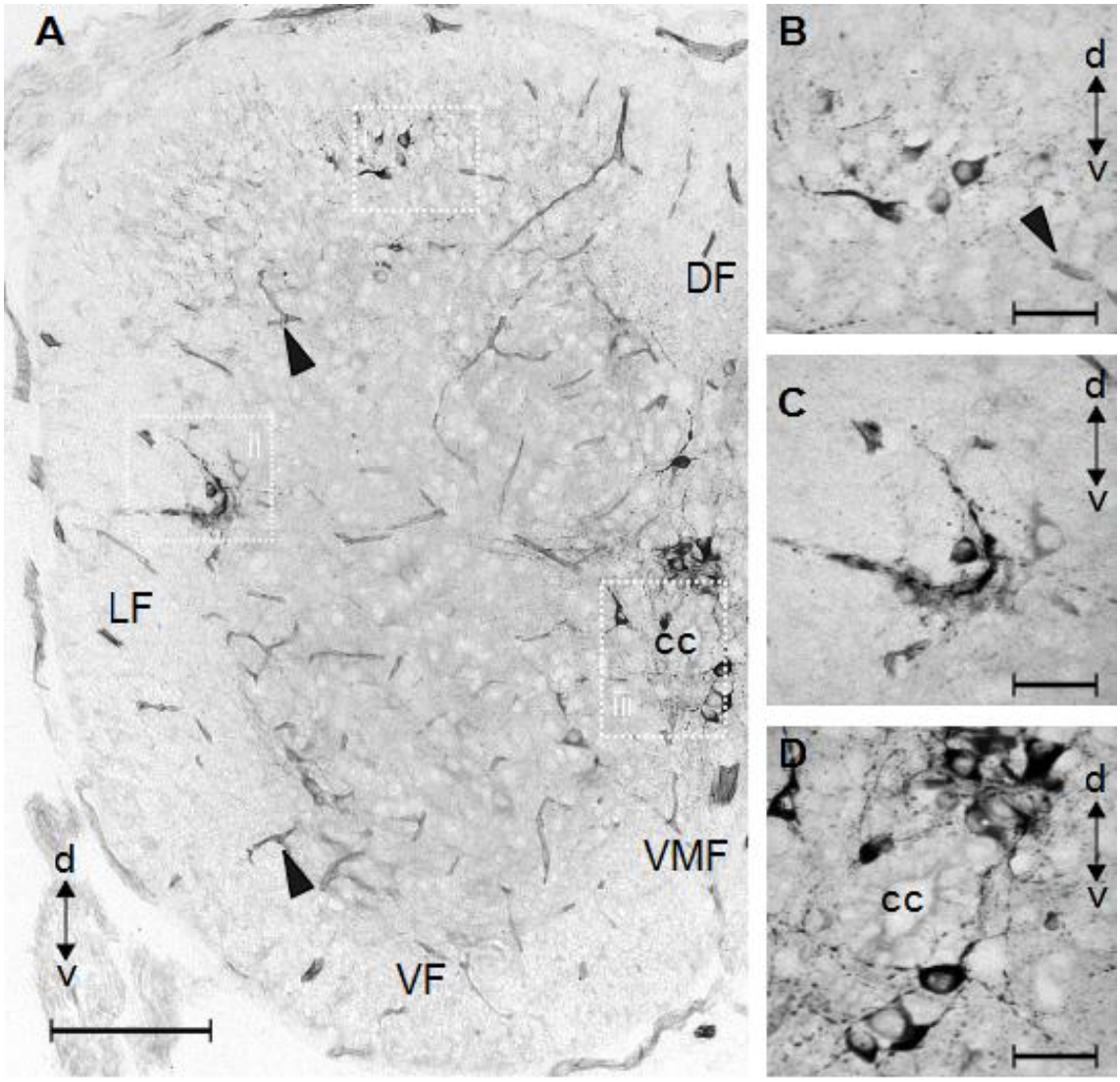

Figure 2.4. Transverse section taken at P5L1 demonstrates NADPH diaphorase reactivity in lumbar spinal cord. **A.** Discrete populations of neurons stain throughout the spinal cord section, stained neurons are visible in the dorsal **Ai,** intermediolateral layer **Aii** and lamina X (LX) **Aiii.** High magnification (x40) brightfield images of typical neurons in the dorsal horn with dorsoventral projections **B, Ai**., sympathetic preganglionic neurons in the intermediolateral layer project laterally and are closely associated with the vasculature **C, Aii** and neurons in LX with both dorsoventral and lateral projections. Staining appears to be restricted to the cytoplasm in all lamina expect those of the superficial dorsal horn which appear to stain in both nucleus and cytoplasm. **D, Aiii**. Vascular staining is visible, throughout the section (black arrowheads). Annotations: cc – central canal, d – dorsal, DF – dorsal funiculus, LF – lateral funiculus, v – ventral, VF – ventral funiculus, VMF – ventral median fissure. Scale bars = 200µm, A; 50µm, B, C and D.

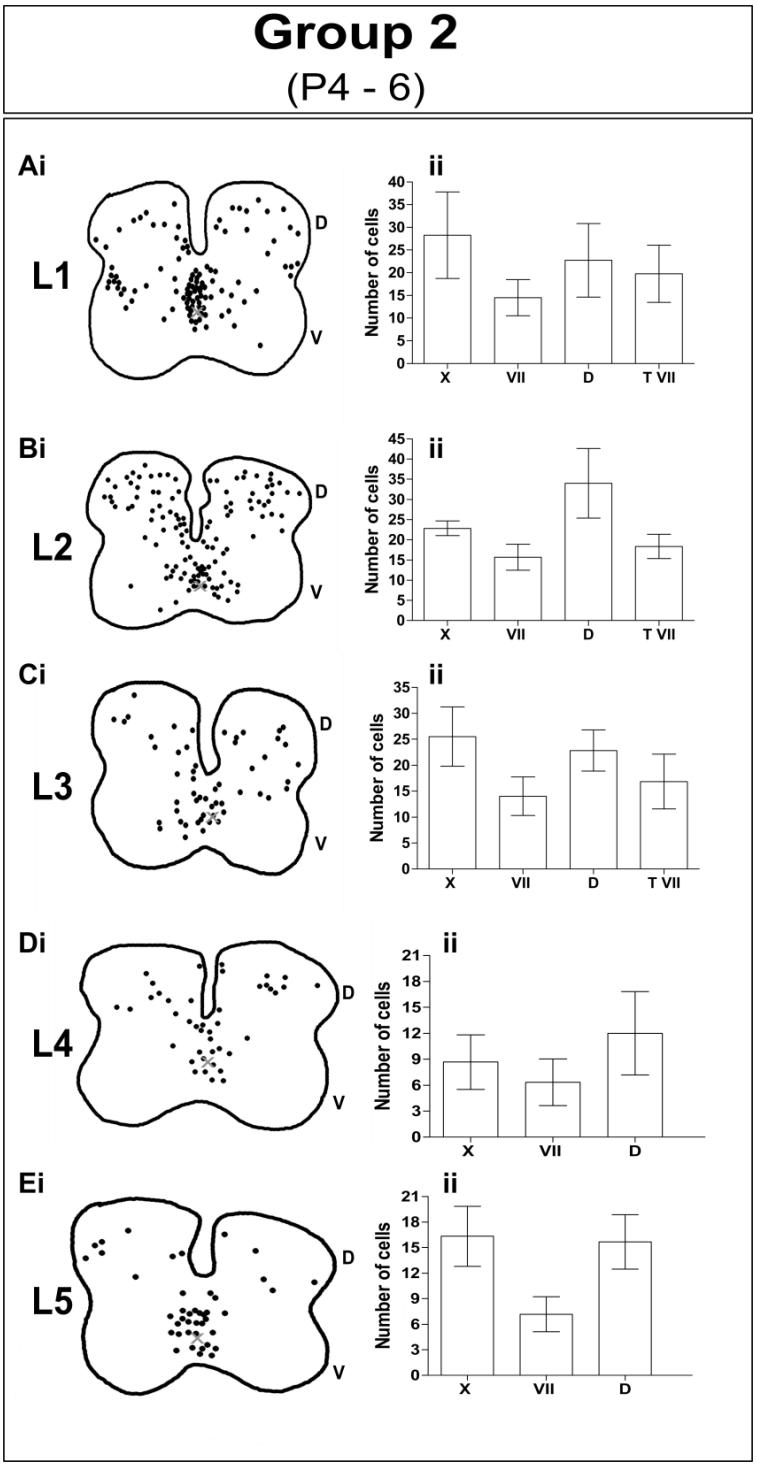

Figure 2.5. Schematic diagram of NADPH diaphorase activity in the mouse spinal cord at P4-6 taken from spinal segments lumbar (L)1-5. **Ai-Ei.** Approximate positions of positively stained neurons are indicated by black filled circles. Each lumbar segment represents 5 transverse segments from 1 mouse and each filled circle represents one neuron. d and v indicate dorsal and ventral orientation. Diagrams are not to scale. **Aii-Eii.** Graphs showing the total number of positively stained neurons in LX, LVII, D and the total in LVII which include the SPN cells of the IML (TVII for L1-3 only). Data are mean ±SEM, n=6.

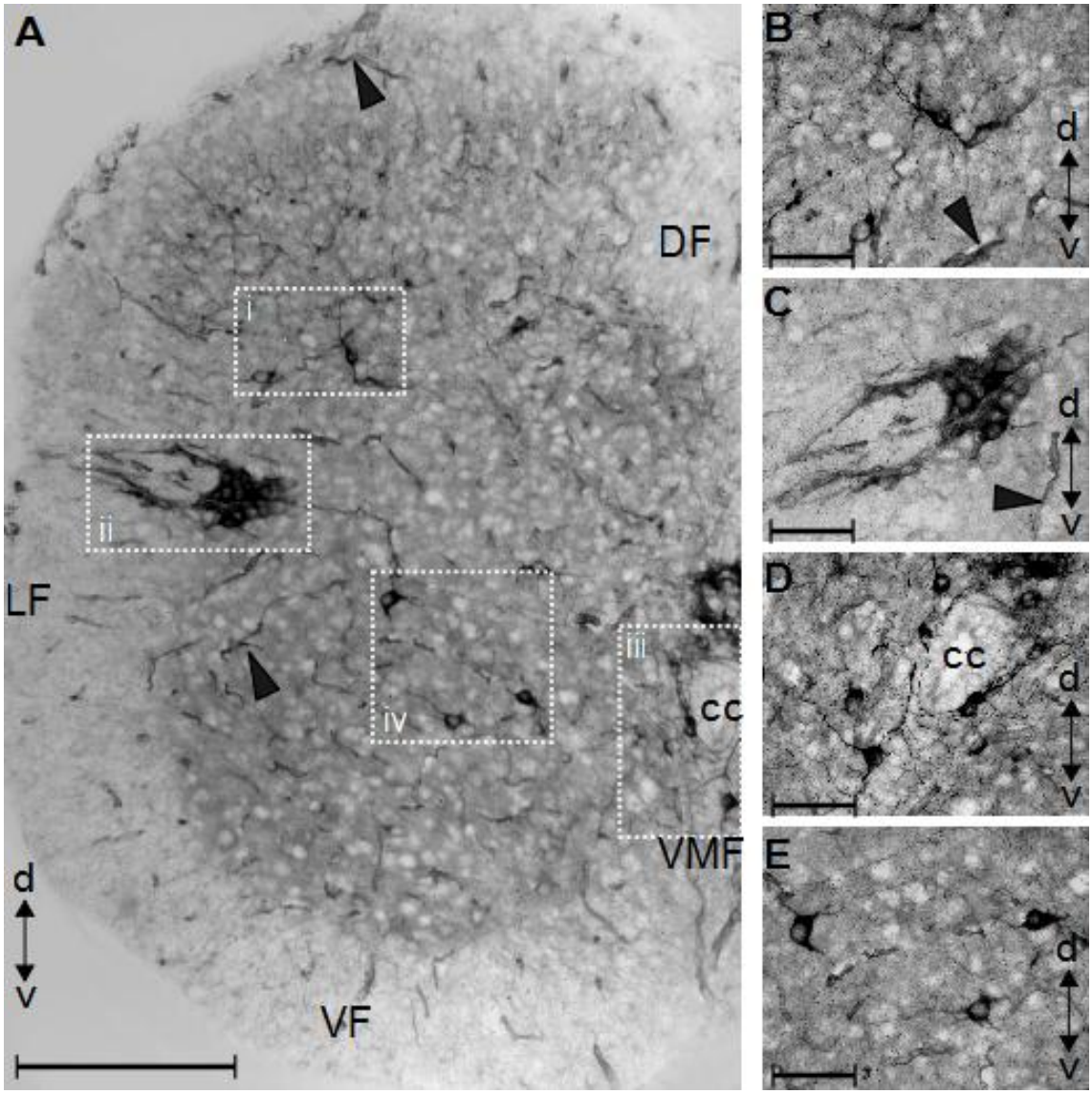

Figure 2.6. Transverse section taken at P7L1 demonstrates NADPH diaphorase reactivity in lumbar spinal cord. **A.** Discrete populations of neurons stain throughout the spinal cord section, stained neurons are visible in the dorsal **Ai,** intermediolateral layer **Aii** lamina X (LX) **Aiii** and lamina VII **Aiv.** High magnification (x40) brightfield images of typical neurons in the dorsal horn with dorsoventral projections **B, Ai**., sympathetic preganglionic neurons in the intermediolateral layer project laterally and are closely associated with the vasculature **C, Aii** and neurons in LX with both dorsoventral and lateral projections. Neurons in lamina VII are loosely distributed throughout the layer **E, Aiv.** Staining appears to be restricted to the cytoplasm in all lamina expect those of the superficial dorsal horn which appear to stain in both nucleus and cytoplasm. **D, Aiii**., Vascular staining is visible, throughout the section (black arrowheads). Annotations: cc – central canal, d – dorsal, DF – dorsal funiculus, LF – lateral funiculus, v – ventral, VF – ventral funiculus, VMF – ventral median fissure. Scale bars = 200µm, A; 50µm, B, C and D.

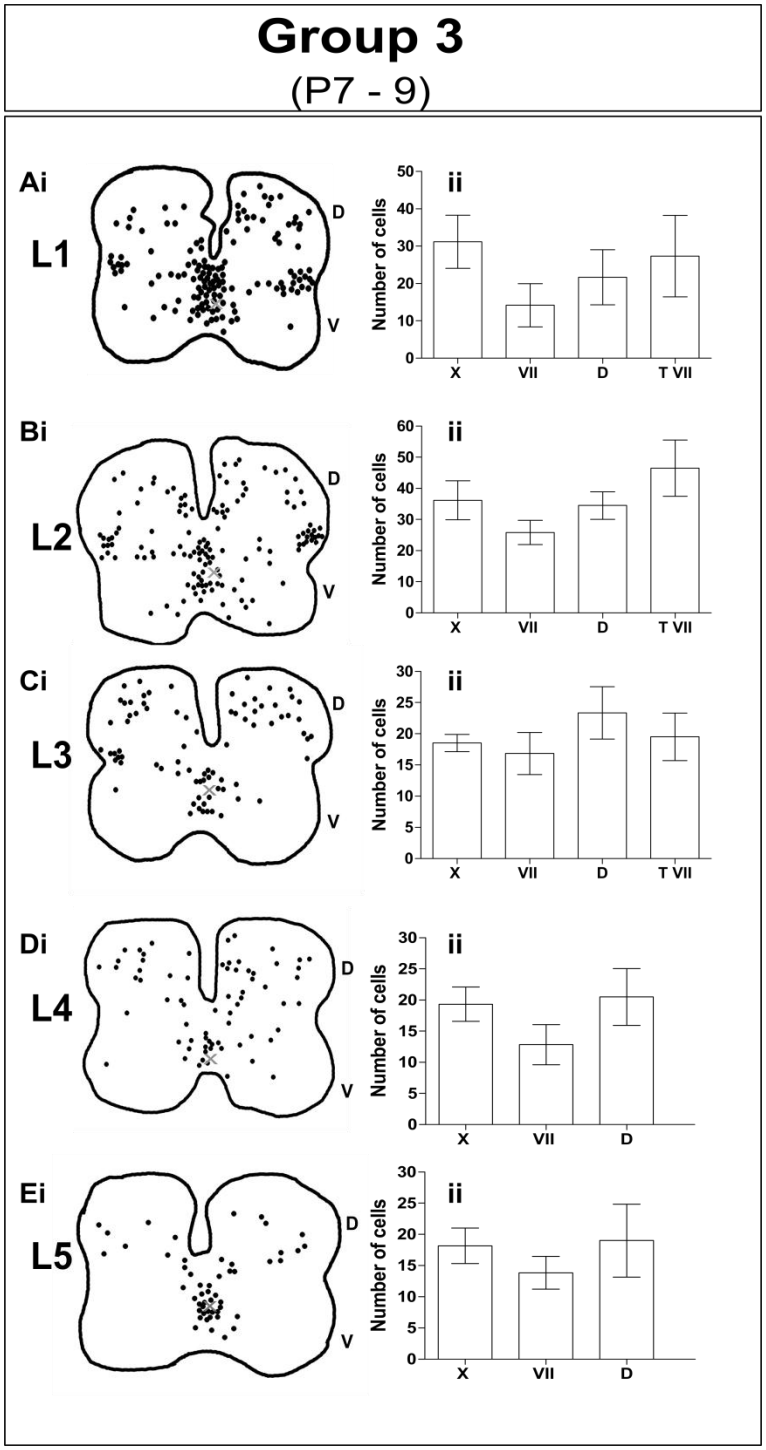

Figure 2.7. Schematic diagram of NADPH diaphorase activity in the mouse spinal cord at P7-9 taken from spinal segments lumbar (L)1-5. **Ai-Ei.** Approximate positions of positively stained neurons are indicated by black filled circles. Each lumbar segment represents 5 transverse segments from 1 mouse and each filled circle represents one neuron. d and v indicate dorsal and ventral orientation. Diagrams are not to scale. **Aii-Eii**. Graphs showing the total number of positively stained neurons in LX, LVII, D and the total in LVII which include the SPN cells of the IML (TVII for L1-3 only). Data are mean ±SEM, n=6.

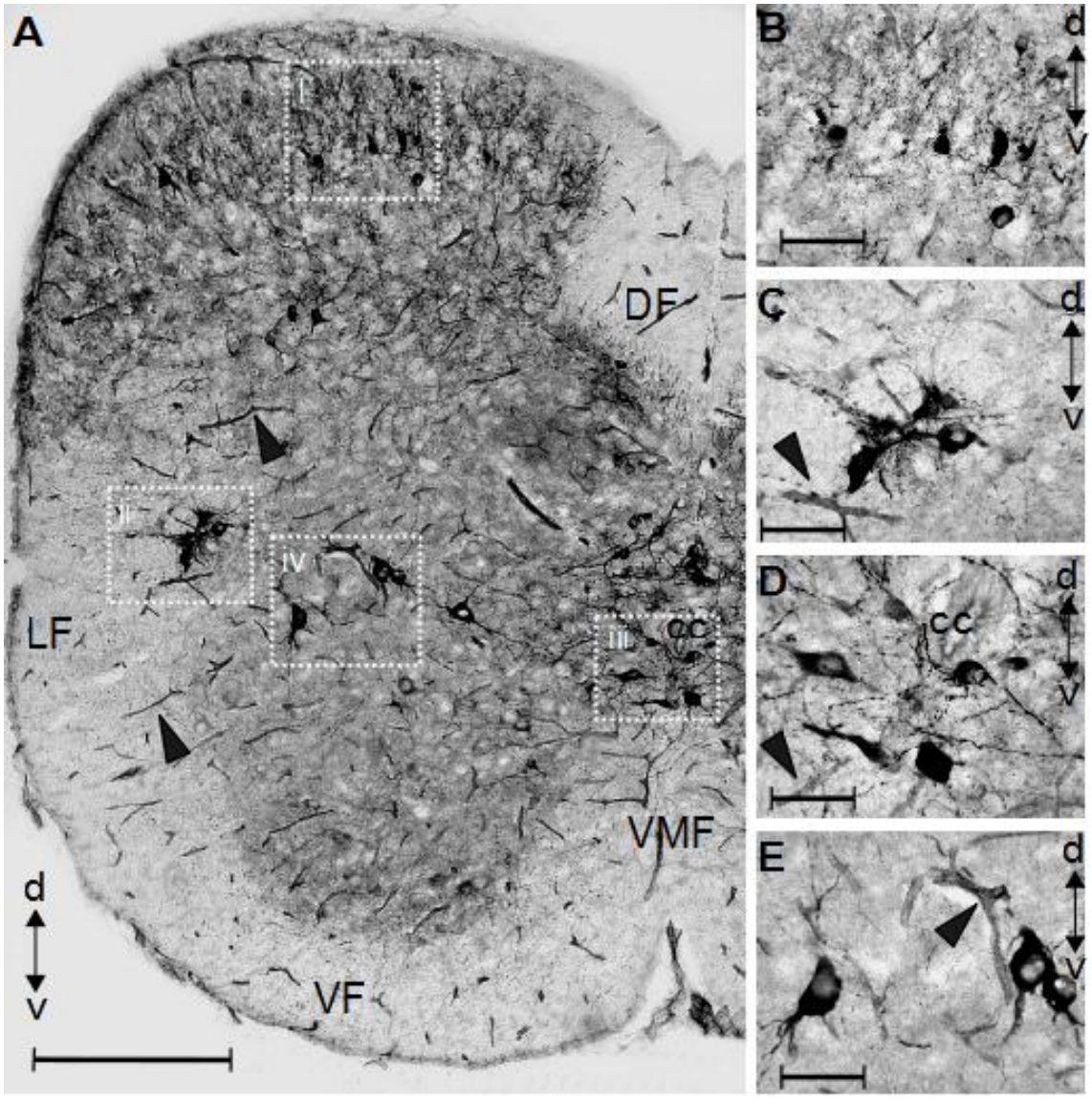

Figure 2.8. Transverse section taken at P12L1 demonstrates NADPH diaphorase reactivity in lumbar spinal cord. **A.** Discrete populations of neurons stain throughout the spinal cord section, stained neurons are visible in the dorsal **Ai,** intermediolateral layer **Aii** lamina X (LX) **Aiii** and lamina VII **Aiv.** High magnification (x40) brightfield images of typical neurons in the dorsal horn **B, Ai**., sympathetic preganglionic neurons in the intermediolateral layer project laterally **C, Aii**, neurons in LX **D, Aiii**, and lamina VII **E, Aiv**. Vascular staining is visible, throughout the section (black arrowheads). Annotations: cc – central canal, d – dorsal, DF – dorsal funiculus, LF – lateral funiculus, v – ventral, VF – ventral funiculus, VMF – ventral median fissure. Scale bars = 200µm, A; 50µm, B, C and D.

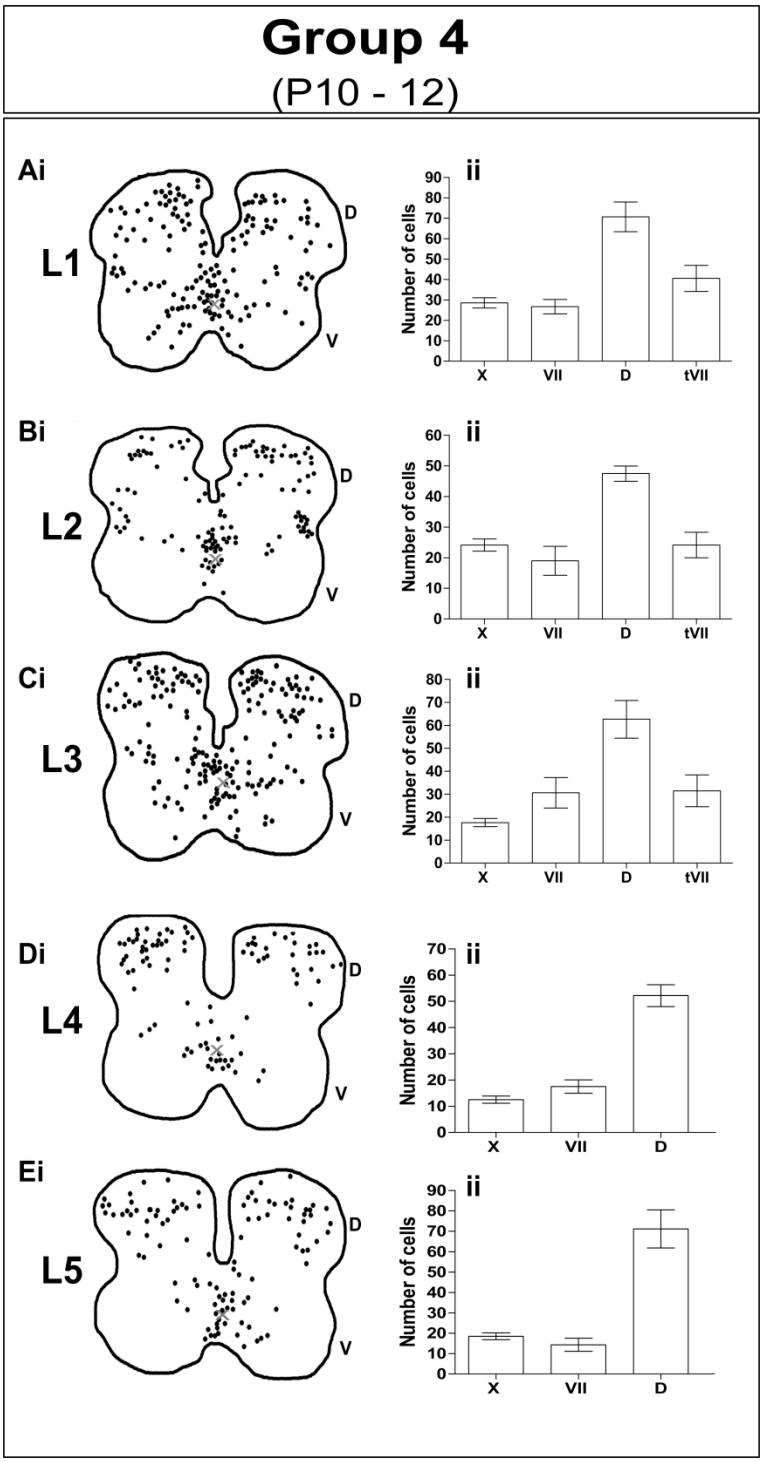

Figure 2.9. Schematic diagram of NADPH diaphorase activity in the mouse spinal cord at P10-12 taken from spinal segments lumbar (L)1-5. **Ai-Ei.** Approximate positions of positively stained neurons are indicated by black filled circles. Each lumbar segment represents 5 transverse segments from 1 mouse and each filled circle represents one neuron. d and v indicate dorsal and ventral orientation. Diagrams are not to scale. **Aii-Eii**. Graphs showing the total number of positively stained neurons in LX, LVII, D and the total in LVII which include the SPN cells of the IML (TVII for L1-3 only). Data are mean ±SEM, n=6.

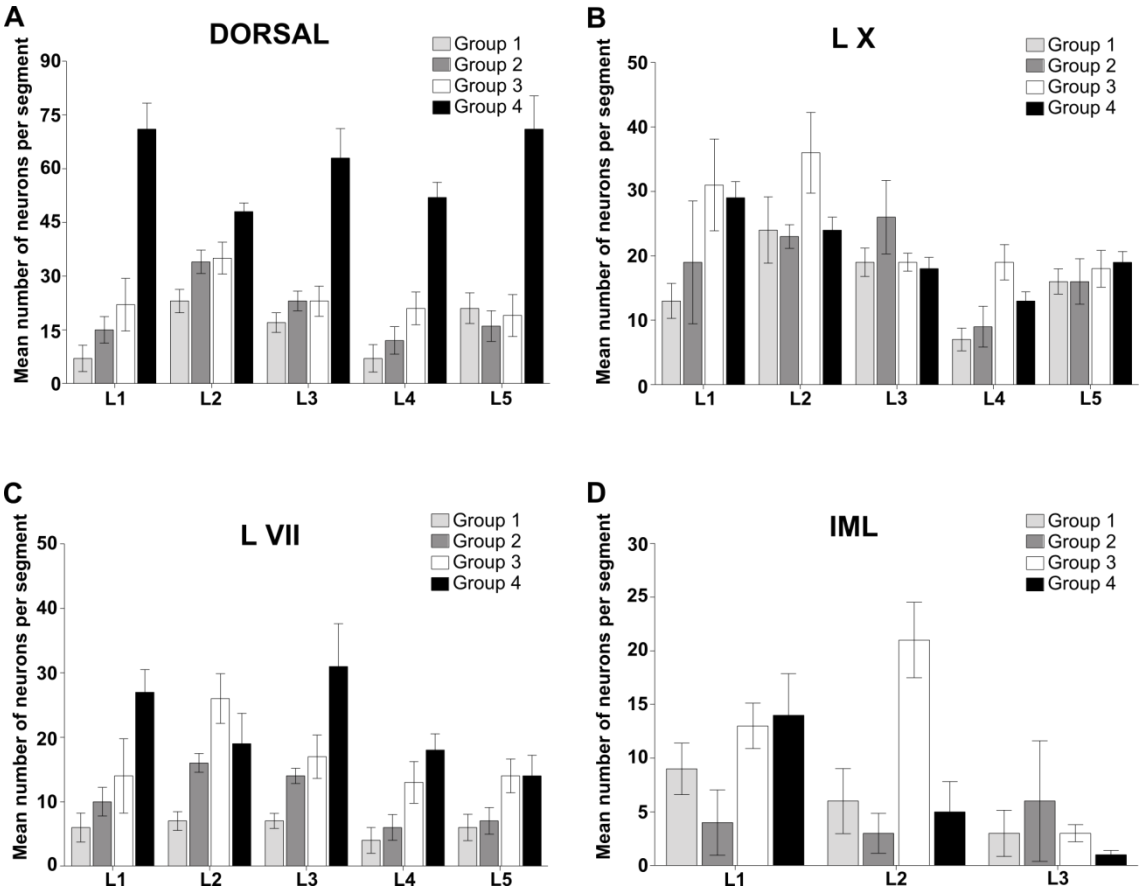

Figure 2.10. The spatiotemporal distribution of NADPH diaphorase reactive neurons in the lumbar spinal cord of the neonatal mouse from P1 – P12. The mean number of NADPH diaphorase reactive neurons in lumbar segments L1 to L5 of the **A** dorsal horn, **B** lamina X, **C** lamina VII and **D** IML of lamina VII (n=6 per group; see Table 2.3 and 2.4 for significance). Data are mean ± SEM.

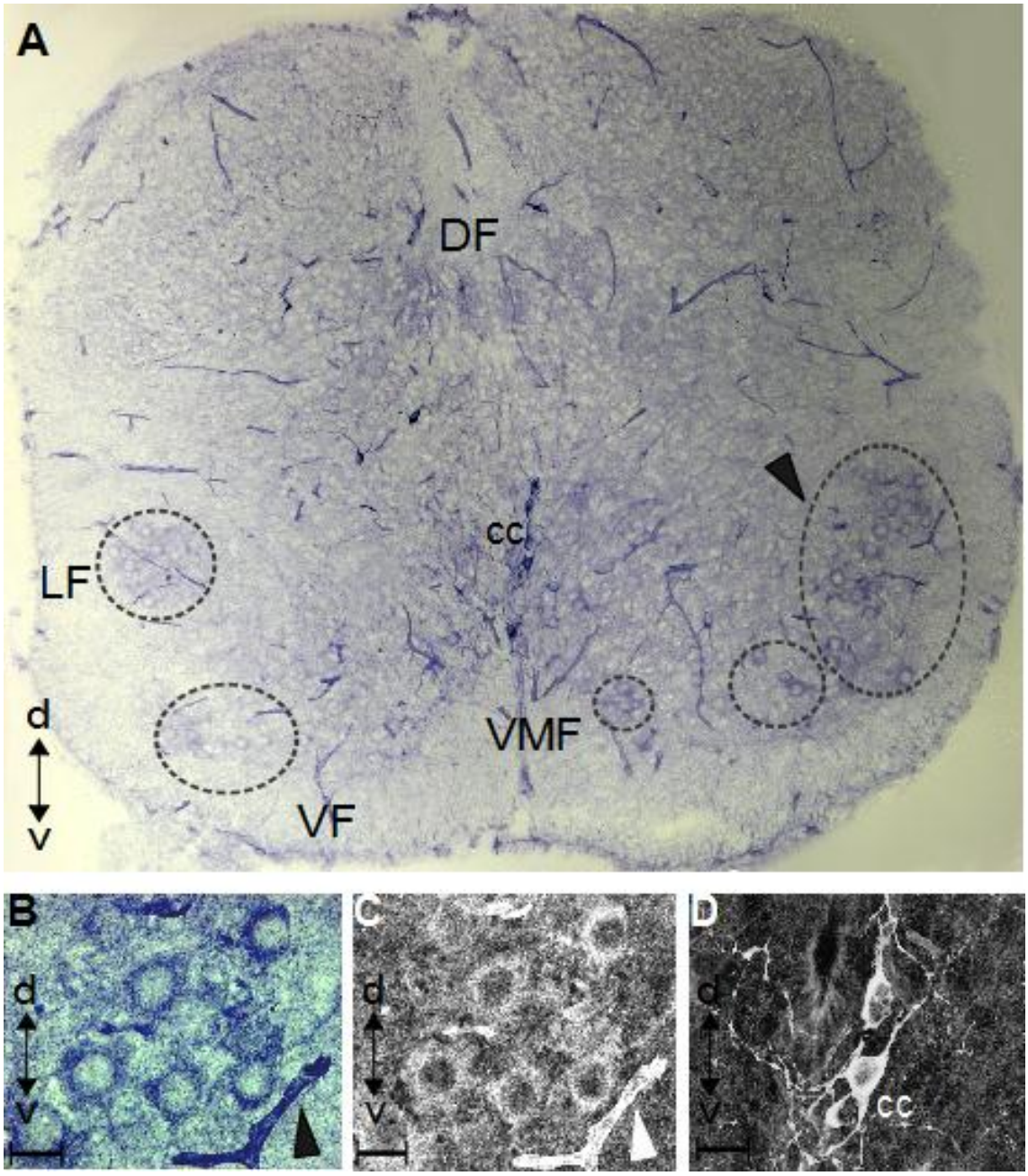

Figure 2.11. Transverse section taken at P3L5 demonstrates light NADPH diaphorase reactivity in lumbar spinal cord. **A.** Areas of light reactivity in the medial and lateral motor columns (lamina IX, position indicated by dashed circles). High magnification (x63) images show that this light reactivity is qualitatively different **B**, from typical somatic labelling as illustrated in **D**. Desaturated and inverted images highlight the qualitative difference in staining between soma/blood vessels and staining found around the soma **C, D**. Blood vessels are indicated by arrowheads. Annotations: cc – central canal, d – dorsal, DF – dorsal funiculus, LF – lateral funiculus, v – ventral, VF – ventral funiculus, VMF – ventral median fissure. Scale bars = 20μm, B, C and D. A not to scale.

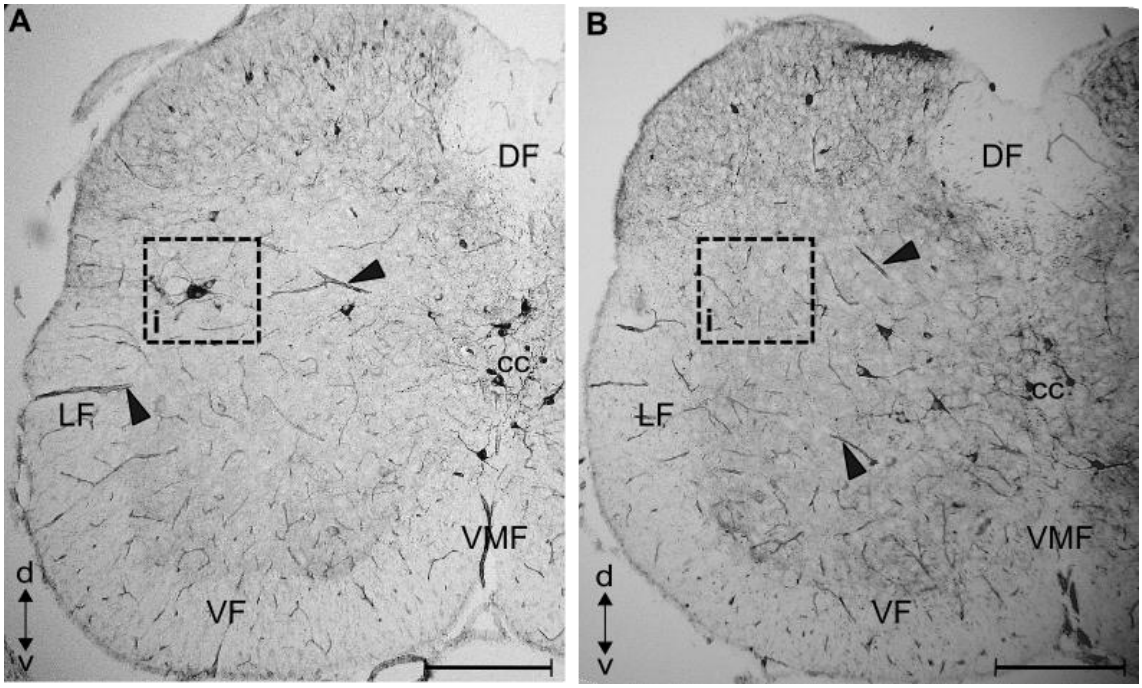

Figure 2.12. Transverse section taken at P12L2 demonstrates NADPH diaphorase reactivity in SOD^{WT} and SOD^{G93A} lamina VII intermediolateral layer. The pattern of reactivity in **A,** SOD^{WT} and **B**, SOD^{G93A} tissue closely resembles that demonstrated previously in CD1WT. Discrete populations of neurons stain throughout the spinal cord section, including the vasculature. Blood vessels are indicated by black arrowheads. The pattern of NADPH diaphorase reactivity of neurons in the IML of **Ai,** SOD^{WT} differs from the IML of **Bi**, SOD^{G93A} where fewer neurons or an absence of staining was observed. Annotations: cc – central canal, d – dorsal, DF – dorsal funiculus, LF – lateral funiculus, v – ventral, VF – ventral funiculus, VMF – ventral median fissure. Scale bars = 200μm, B, C and D.

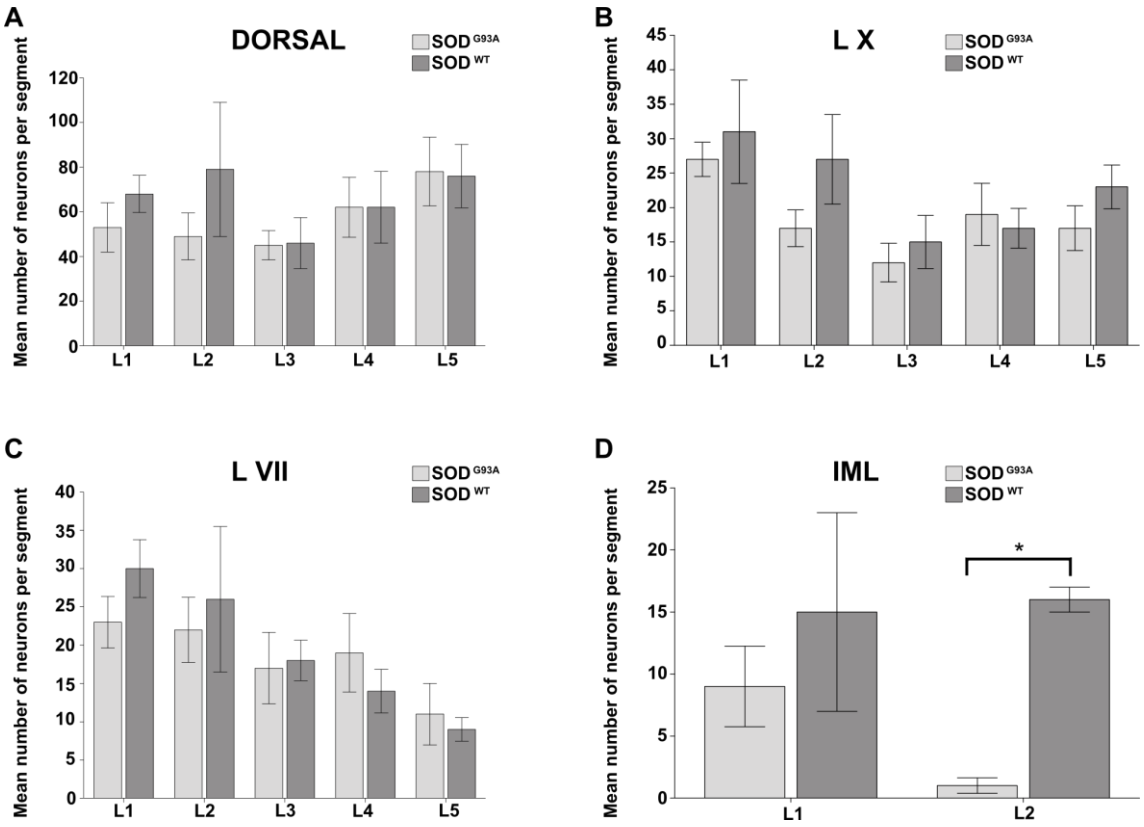

Figure 2.13. The spatiotemporal distribution of NADPH diaphorase reactive neurons in the lumbar spinal cord of the juvenile SOD^{WT} and SOD^{G93A} mouse at P12. The mean number of NADPH diaphorase reactive neurons in lumbar segments L1 to L5 of the **A** dorsal horn, **B** lamina X, **C** lamina VII and **D** IML of lamina VII (n=6 per group). The total number of NADPH diaphorase reactive neurons was significantly lower in SOD^{G93A} when compared to SOD^{WT} ($P<0.05$, 2-way ANOVA). The number of NADPH diaphorase reactive neurons was significantly lower in L2 IML SOD^{G93A} when compared to L2 IML SOD^{WT} ($P<0.05$, Mann-Whitney test). Data are mean ± SEM.

Table 2.1 Segmental and laminar distribution of NADPH diaphorase reactive neurons in each segment[1] of the developing neonatal mouse lumbar spinal cord.

Group	Segment	Total	±SEM	LVII	±SEM	LVIII	±SEM	LIX	±SEM	LX	±SEM	IML	±SEM	D	±SEM
1	L1	37.8	12.9	5.7	0.4	2.2	0.2	0.3	0.1	13.3	0.3	9.3	0.3	7.0	0.4
1	L2	60.7	16.0	7.0	0.2	0.3	0.1	0.5	0.1	24.3	0.5	5.7	0.4	22.8	0.4
1	L3	46.3	10.8	6.5	0.2	0.7	0.1	0.2	-	19.3	0.4	3.0	0.2	16.7	0.4
1	L4	18.5	8.5	3.8	0.2	0.7	0.1	-	-	7.0	0.3	-	-	7.0	0.4
1	L5	43.3	9.8	6.3	0.3	0.2	-	-	-	16.3	0.3	-	-	20.5	0.6
2	L1	49.7	21.3	9.7	0.5	1.5	0.2	1.0	0.1	18.8	0.7	3.5	0.4	15.2	0.8
2	L2	76.8	19.1	15.7	0.4	1.3	0.1	0.3	-	22.8	0.3	2.7	0.2	34.0	0.8
2	L3	58.5	13.3	10.8	0.3	1.0	0.1	-	-	20.8	0.4	6.0	0.5	19.8	0.4
2	L4	27.0	11.7	6.3	0.3	-	-	-	-	8.7	0.4	-	-	12.0	0.5
2	L5	39.2	10.5	7.2	0.3	-	-	-	-	16.3	0.4	-	-	15.7	0.5
3	L1	81.7	26.3	14.2	0.6	1.0	0.1	0.5	0.1	31.2	0.7	13.2	0.5	21.7	0.7
3	L2	117.8	29.3	25.8	0.5	0.7	0.1	-	-	36.2	0.7	20.7	0.6	34.5	0.6
3	L3	61.3	13.9	16.8	0.4	-	-	-	-	18.5	0.3	2.7	0.3	23.3	0.5
3	L4	52.7	12.6	12.8	0.5	-	-	-	-	19.3	0.4	-	-	20.5	0.5
3	L5	51.2	10.7	13.8	0.4	-	-	0.2	-	18.2	0.4	-	-	19.0	0.6
4	L1	144.5	29.6	26.7	0.5	4.2	0.2	0.7	0.1	28.5	0.5	13.8	0.4	70.7	1.0
4	L2	95.8	18.4	19.0	0.5	-	-	-	-	24.2	0.3	5.2	0.3	47.5	0.6
4	L3	112.5	26.0	30.7	0.7	0.5	0.1	0.2	-	17.7	0.3	0.8	0.1	62.7	1.1
4	L4	82.5	15.8	17.5	0.5	-	-	0.2	-	12.5	0.3	0.2	-	52.2	0.9
4	L5	104.0	24.0	14.3	0.5	-	-	-	-	18.5	0.4	-	-	71.2	1.1

1 Calculated as the average number of NADPH diaphorase reactive neurons in a lamina in 5 sections taken from one segment. Each segment is an average of 6 mice. Data mean ± SEM.

Table 2.2 Percentage[1] laminar distribution of NADPH diaphorase reactive neurons in each segment of the neonatal mouse lumbar spinal cord.

Group	Segment	LVII	±SEM	LVIII	±SEM	LIX	±SEM	LX	±SEM	IML	±SEM	D	±SEM
1	L1	15.0	3.1	5.7	1.6	0.9	0.8	35.2	2.3	24.7	2.3	18.5	3.1
1	L2	11.5	1.3	0.5	0.6	0.8	0.6	40.1	3.1	9.3	2.5	37.6	2.5
1	L3	14.0	1.9	1.4	0.9	0.4	-	41.7	3.7	6.5	1.9	36.0	3.7
1	L4	20.7	2.4	3.6	1.2	-	-	37.8	3.5	-	-	37.8	4.7
1	L5	14.6	3.1	0.4	-	-	-	37.7	3.1	-	-	47.3	6.1
2	L1	19.5	2.3	3.0	0.9	2.0	0.5	37.9	3.3	7.0	1.9	30.5	3.8
2	L2	20.4	2.1	1.7	0.5	0.4	-	29.7	1.6	3.5	1.0	44.3	4.2
2	L3	18.5	2.3	1.7	0.8	-	-	35.6	3.0	10.3	3.8	33.9	3.0
2	L4	23.5	2.6	-	-	-	-	32.1	3.4	-	-	44.4	4.3
2	L5	18.3	2.9	-	-	-	-	41.7	3.8	-	-	40.0	4.8
3	L1	17.3	2.1	1.2	0.4	0.6	0.4	38.2	2.5	16.1	1.8	26.5	2.5
3	L2	21.9	1.7	0.6	0.3	-	-	30.7	2.4	17.5	2.0	29.3	2.0
3	L3	27.4	2.9	-	-	-	-	30.2	2.2	4.3	2.2	38.0	3.6
3	L4	24.4	4.0	-	-	-	-	36.7	3.2	-	-	38.9	4.0
3	L5	27.0	3.7	-	-	0.3	-	35.5	3.7	-	-	37.1	5.6
4	L1	18.5	1.7	2.9	0.7	0.5	0.3	19.7	1.7	9.6	1.4	48.9	3.4
4	L2	19.8	2.7	-	-	-	-	25.2	1.6	5.4	1.6	49.6	3.3
4	L3	27.3	2.7	0.4	0.4	0.1	-	15.7	1.2	0.7	0.4	55.7	4.2
4	L4	21.2	3.2	-	-	0.2	-	15.2	1.9	0.2	-	63.2	5.7
4	L5	14	2	-	-	-	-	18	2	-	-	68	5

[1] Percentage distribution calculated as the average number of NADPH diaphorase reactive neurons in a lamina divided by the average total number of reactive neurons in that segment. Data mean ± SEM

Table 2.3 summary matrix for statistical comparison[1] of the main reactive lamina by segment.

Group	Segment	LVII vs. LX	LVII vs. D	LX vs. D
1	L1	****	ns	****
1	L2	****	****	ns
1	L3	****	****	****
1	L4	****	****	ns
1	L5	****	****	****
2	L1	****	****	****
2	L2	****	****	****
2	L3	****	****	ns
2	L4	*	****	***
2	L5	****	****	ns
3	L1	****	****	****
3	L2	****	****	ns
3	L3	ns	****	****
3	L4	****	****	ns
3	L5	****	****	ns
4	L1	ns	****	****
4	L2	****	****	****
4	L3	****	****	****
4	L4	****	****	****
4	L5	***	****	****

[1] Two-way ANOVA followed by Bonferroni Multiple comparison post-test

Table 2.4 Summary matrix for statistical comparison[1] of the main reactive lamina by group

Segment	Lamina	Gp1 vs. Gp2	Gp1 vs. Gp3	Gp1 vs. Gp4	Gp2 vs. Gp3	Gp2 vs. Gp4	Gp3 vs. Gp4
L1	X	****	****	****	****	****	ns
L1	VII	***	****	****	***	****	****
L1	IML	****	***	****	****	****	ns
L1	Dorsal	****	****	****	****	****	****
L2	X	ns	****	ns	****	ns	****
L2	VII	****	****	****	****	**	****
L2	IML	**	****	ns	****	ns	****
L2	Dorsal	****	****	****	ns	****	****
L3	X	****	ns	ns	****	****	ns
L3	VII	****	****	****	***	****	****
L3	IML	***	ns	*	***	****	*
L3	Dorsal	****	****	****	ns	****	****
L4	X	*	****	****	****	****	****
L4	VII	*	****	****	****	****	****
L4	IML	n/a	n/a	n/a	n/a	n/a	n/a
L4	Dorsal	****	****	****	****	****	****
L5	X	ns	*	****	*	****	ns
L5	VII	ns	****	****	****	****	ns
L5	IML	n/a	n/a	n/a	n/a	n/a	n/a
L5	Dorsal	****	*	****	****	****	****

[1] Two-way ANOVA followed by Bonferroni Multiple comparison post-test

Table 2.5. Segmental and laminar distribution of NADPH diaphorase reactive neurons in each segment[1] of the SOD1WT and SOD^{G93A} mouse lumbar spinal cord

Group	Segment	Total	±SEM	LVII	±SEM	LVIII	±SEM	LIX	±SEM	LX	±SEM	IML	±SEM	D	±SEM
SOD	L1	111	19.2	23	0.6	0	0.2	-	-	27	0.5	9	0.5	53	1.1
SOD	L2	88	14.9	22	0.5	-	-	-	-	17	0.3	1	0.0	49	1.0
SOD	L3	74	13.4	17	0.5	1	0.0	-	-	12	0.4	-	-	45	0.9
SOD	L4	100	20.5	19	0.7	-	-	-	-	19	0.5	-	-	62	1.4
SOD	L5	107	16.5	11	0.5	1	0.0	-	-	17	0.3	-	-	78	1.4
WT	L1	147	26.7	30	0.6	2	0.3	0	0.1	31	0.9	15	0.7	68	1.0
WT	L2	149	56.0	26	0.7	2	0.0	-	-	27	0.7	16	0.8	79	2.3
WT	L3	81	12.4	18	0.4	-	-	-	-	15	0.5	-	-	46	1.1
WT	L4	93	22.0	14	0.6	-	-	-	-	17	0.3	-	-	62	1.5
WT	L5	109	15.1	9	0.4	1	0.5	-	-	23	0.5	-	-	76	1.5

[1] Calculated as the average number of NADPH diaphorase reactive neurons in a lamina in 5 sections taken from one segment. Each segment is an average of 6 mice. Data mean ± SEM.

Table 2.6. Percentage[1] laminar distribution of NADPH diaphorase reactive neurons in each segment of the SOD1WT and SOD^{G93A} mouse lumbar spinal cord

Group	Segment	LVII	±SEM	LVIII	±SEM	LIX	±SEM	LX	±SEM	IML	±SEM	D	±SEM
SOD	L1	20.7	3.1	0.0	1.0	-	-	23.8	2.4	7.9	2.5	47.4	5.7
SOD	L2	24.9	3.4	-		-	-	18.7	2.0	1.4	0.0	55.0	6.8
SOD	L3	23.0	3.5	0.7	0.0	-	-	15.9	2.8	-	-	60.5	6.7
SOD	L4	19.0	3.2	-	-	-	-	18.8	2.4	-	-	62.2	7.0
SOD	L5	10.1	3.3	0.7	0.0	-	-	16.0	2.0	-	-	73.2	8.6
WT	L1	20.5	2.3	1.4	1.0	0.2	-	20.9	3.2	10.5	2.7	46.6	3.6
WT	L2	17.2	1.2	1.0	0.0	-	-	17.8	1.2	10.8	1.4	53.2	4.1
WT	L3	22.3	3.4	-	-	-	-	19.0	3.8	-	-	57.4	8.5
WT	L4	15.4	2.7	-	-	-	-	18.3	1.6	-	-	66.3	6.7
WT	L5	8.3	2.5	0.9	3.3	-	-	21.4	3.6	-	-	69.4	9.9

[1] Percentage distribution calculated as the average number of NADPH diaphorase reactive neurons in a lamina divided by the average total number of reactive neurons in that segment.

2.4 Discussion

NOS is a NADPH diaphorase enzyme, requiring NADPH to reduce L-arginine by a series of electron transfers to produce L-citrulline and NO (Hope et al., 1991). Diaphorase reactivity is formaldehyde-resistant and therefore ideal for post-fixation studies of spinal tissue. Substitution of L-arginine by a tetrazolium salt leads to the irreversible conversion of the substrate to a visible blue formazan. The reaction is non-specific, and thus all isoforms of the enzyme will exhibit reactivity, notably in the vasculature. In this chapter, the distribution of NO producing neurons is described in the CD1 wild-type mouse lumbar spinal cord over the postnatal period P1-P12 using the NADPH diaphorase histochemical reaction. The present study not only describes the distribution of NADPH diaphorase in the lumbar spinal cord of the neonatal mouse but also describes this distribution in higher temporal resolution than any of the aforementioned investigations. Additionally, in the present study, the distribution of NO producing (NADPH diaphorase reactive) neurons was described in the lumbar spinal cord of the $SOD1^{G93A}$ mouse model of human ALS at P12.

2.4.1 Spatiotemporal distribution of NADPH diaphorase reactivity in the CD1 WT

The distribution of NADPH diaphorase has been described previously in the spinal cord of the tadpole (McLean and Sillar, 2001, Ramanathan et al., 2006), mouse, cat, and squirrel monkey (Dun et al., 1993, Spike et al., 1993, Valtschanoff et al., 1992), rabbit (Schreiberová et al., 2006) and embryonic human (Foster and Phelps, 2000). Although NADPH diaphorase reactivity has been described in the hatchling tadpole, adult mammal and embryonic human, no such investigation has been conducted in the lumbar spinal cord of the neonatal mouse.

NADPH reactivity in the present study closely resembled that detailed in other studies with the majority of reactivity occurring in the dorsal horn, where NO signalling is involved in activity-dependent sensory processing in the dorsal horn (Maihofner et al.,

2000, Xu et al., 2006). However, the role of NADPH diaphorase reactive neurons in the ventral horn is less clear. The present study describes the distribution of NADPH diaphorase reactivity in the lumbar spinal cord to assess the possibility that NO may regulate, directly by autocrine or indirectly by paracrine mechanisms, the neurons in the locomotor network.

NADPH diaphorase reactivity was recorded in discrete areas of the ventral horn: lamina VII clustered in the IML and scattered across wider lamina VII; lamina X, around the central canal; and in very small numbers in laminae VIII and IX. Light staining was observed, predominantly in lamina IX, in the vicinity of the motor nuclei, but was not included in the tally of reactive neurons. Similarly, light staining has previously been observed in a preliminary investigation of NADPH diaphorase reactivity in L3-L5 (Collett, 2007).

Over the developmental period P1 to P12, the total number of NADPH diaphorase reactive neurons increased significantly in the lumbar spinal cord. Overall, the dorsal horn exhibited the largest population of reactive neurons, both by segment and by group. As the neuronal population in the dorsal horn is involved in sensory processing, and therefore outside the remit of the present study, the dorsal horn laminae were not individually described. However, the distribution of NADPH diaphorase in the present study was similar to that described in a previous study involving NADPH diaphorase producing neurons in the dorsal horn (Xu et al., 2006).

The NADPH diaphorase reactive neurons in lamina VII increased during development from P1 to P12, particularly in the rostral segments (L1 to L3). The number of NADPH diaphorase reactive neurons peaked in the rostral segments, particularly L2, of Group 3. The reason for this peak in the population in Group 3 is not clear from the anatomy alone. However, mice become functionally motor-mature around P8-P10 (Jiang et al., 1999) and it is possible that NOS expression and NO production are involved in maturation of the network in the days before the ability to bear weight and walk (anterior surface raised above ground) fully develops. NO is also expressed transiently during development but a definitive reason for transient expression is not always clear;

for instance, a small group of presumed somatic motor neurons in the cervical spinal cord, the location of the forelimb locomotor network, are transiently NADPH diaphorase positive in the embryonic rat (E15) spinal cord (Wetts et al., 1995). The peak in NOS expression in the present study, during a developmentally relevant period, warrants further investigation and would be an ideal time point at which to perform whole cell physiology to determine the effect of removal of endogenous NO on locomotor-related interneurons and the function of the whole locomotor circuit.

The rostral segments of the lumbar neonatal mouse spinal cord have greater rhythmogenic capacity compared to the more caudal segments (Bonnot et al., 2002b). The finding that expression of NOS is greater in the rostral segments, particularly prior to the most locomotor-relevant developmental stage, warrants further investigation to determine if NO is involved in locomotor network maturation and function. NADPH diaphorase reactive neurons in lamina X were more populous in the rostral segments (L1 to L3) as opposed to the caudal segments (L4 and L5). Lamina X neurons remained a consistent proportion of the total NADPH diaphorase reactive neurons in the lumbar spinal cord, except at P12 when the dorsal horn reactive population was highest. The consistent expression of NOS in neural populations within the sphere of influence of the locomotor-related interneurons increases the likelihood that NO may modulate the local CPG network.

Although it is not possible to visually identify locomotor-related interneurons in the present study, it is possible to speculate about which interneuron populations may produce (or at least are situated within the sphere of influence of) cells producing NO. Transcription factor-led identification of locomotor interneurons has provided a clearer connectivity pattern within the locomotor network by allowing the expression of fluorescent markers in selected neuronal subgroup and thus allowing selective and targeted study of their properties and connection patterns (Jessell, 2000, Goulding, 2009). A subset of interneurons, in laminae X, VII and VIII, are NOS positive but are not involved in cholinergic transmission to motor neurons (Miles et al., 2007). It is possible that Hb9 interneurons, involved in the maintenance of locomotor output, may themselves be modulated by NO or produce NO that modulates the output of motor

neurons (Brownstone and Wilson, 2008). Similarly, NO producing neurons in wider lamina VII, as well as those in the IML, could act as producers of paracrine NO, modulating neurons in the near vicinity.

Other neurons that could express NOS, or that could be affected by neurons in the vicinity which produce NO, include the V2b (Gata2/3) inhibitory interneurons that are located in lamina VII along with the V1 derived inhibitory Renshaw cells and Ia inhibitory interneurons (Alvarez and Fyffe, 2007). V0 (Dbx1) inhibitory interneurons are located in lamina VIII and are essential for normal alternating locomotion n (Lanuza et al., 2004). The scarcity of NADPH diaphorase reactive neurons in lamina VIII does not discount potential modulation of these interneurons by NO as they are located within the sphere of influence of NO-producing populations near the central canal and in lamina VII.

The sympathetic preganglionic autonomic neurons (SPN) are located in the IML and are known to integrate descending autonomic signals. Although these neurons are not directly involved in hind limb locomotor output, they are within signalling distance of the locomotor interneurons and, therefore, NO produced by the SPN could potentially affect locomotor output (Heise, 2004).

Although NADPH diaphorase histochemical reactivity in this study does not directly prove NO regulation of locomotor-related neurons, its presence implies that an active role in locomotion is possible, given the location of NOS positive neurons in the ventral horn amongst the locomotor-related interneurons and motor neuron nuclei. These data confirm the potential for NO to modulate a wide range of neurons involved in locomotor activity and further validate the aims of the present study to investigate the modulatory effects of NO on fictive locomotor output.

2.4.2 Distribution of NADPH diaphorase reactivity in the SOD1^{G93A}mouse model of human ALS

The distribution of NO-producing neurons was described in the lumbar spinal cord of the mouse model of human ALS SOD1^{G93A} and SOD1 wild-type littermates at P12. ALS is a fatal neurodegenerative disease leading to the loss of somatic motor neurons. Although mutations in the SOD1 gene are found consistently in FALS, the effect of SOD1 mutation on disease onset and progression is not known. The SOD1^{G93A} transgenic mouse expresses the human mutant form of the SOD1 gene and develops ALS-like symptoms, which are widely accepted to follow the course of human ALS (Van Den Bosch, 2011). It is thought that the SOD1 mutation leads to a toxic gain of function and that disease progression is multifactorial, including aberrant excitatory transmission, oxidative stress and mitochondrial malfunction (Barber and Shaw, 2007, Boillee et al., 2006). Electrophysiological data have provided direct evidence of intrinsic changes to motor neuron excitability in early SOD1^{G93A}development (Jiang et al., 2009, Kuo et al., 2004, Kuo et al., 2005, Pambo-Pambo et al., 2009, van Zundert et al., 2008). However, few anatomical studies have been carried out at early postnatal stages, as the focus remains on mostly pre -, early onset, late onset and end stage/post-mortem stages of the disease. Whether NO plays a role in ALS development is not known.

In the present study, the pattern of NADPH diaphorase reactivity in the SOD1^{G93A} and SOD1 wild-type lumbar spinal cord of littermates at P12 was similar to that shown in other species and closely resembled the distribution pattern in CD1 WT mice. Reactivity was recorded in the ventral horn; lamina VII in the IML and wider lamina VII; lamina X, around the central canal; and occasionally in laminae VIII and IX. Light staining was observed in lamina IX, in the vicinity of the motor nuclei, but again was not included in the tally of reactive neurons. The majority of reactive neurons were located in the dorsal horn, with bias towards the rostral segments. Similarly, the pattern and number of reactive neurons closely resembled that of the CD1 WT in both SOD1^{G93A} and SOD1 wild type, with the majority of reactive neurons in laminae VII and X located in the rostral segment. However, the reactive neuron population in the

IML of lamina VII was considerably diminished in the $SOD1^{G93A}$ compared to the SOD1 wild type.

During the symptomatic stage of ALS, the loss of integrity in blood vessel endothelium in the spinal cord has been detected in $SOD1^{G93A}$ mice, resulting in hemosiderin deposits near motor neurons and possibly contributing to their deaths (Zhong et al., 2008). Loss of neurons in the IML has been demonstrated in the thoracic segments (T2 to T9) in a study at the end-stage of the disease when some ALS patients require artificial ventilation (Iwanaga et al., 1997). Furthermore, aberrant sympathetic hyperactivity has been reported during symptomatic ALS (Oey et al., 2002). A reduction in nitrergic transmission resulting from the loss of NOS production could explain a reduction in resting vagal tone. However, the studies of the SPN and sympathetic outflow are largely centred on the thoracic spinal cord. In the absence of detailed information about changes to the NOS positive neurons in the lumbar IML during ALS, it is not clear what contribution to these effects is mediated by the loss or presence of NO.

The reason for this dramatic difference between NOS expression in the IML of $SOD1^{WT}$ and $SOD1^{G93A}$ mice is unprecedented. It is not clear whether NOS is no longer expressed or whether the absence of reactivity signals the loss of neurons altogether and this finding merits further study.

2.5 Conclusion

These results show that there are discrete sources of NO in the mammalian lumbar spinal cord. During the first twelve postnatal days, the number of NO-producing neurons increased and peaked between P7-P9, the period preceding hind limb network maturation. It is feasible that NO is involved in locomotor network activity, given the proximity of NADPH diaphorase neurons to the laminae in which locomotor related interneurons are located.

Defining the transcription factor and neurotransmitter phenotype of the NOS-positive neurons will give clearer indications of the nature of NO-mediated signalling; that is, whether it is involved in reciprocal or ipsilateral, excitation or inhibition. Additional studies in thick slice (~100μm) and/or longitudinal section will provide further detail of projection patterns not visible in the thin slices used in this study.

For the first time, a reduction in the number of sympathetic preganglionic neurons has been recorded at P12 in the mouse model of human ALS, $SOD1^{G93A}$, but not $SOD1^{WT}$ wild type littermates. It is not immediately clear whether this has any direct bearing on locomotor function or is related purely to autonomic transmission. Additional study and verification of this result by increasing the range and sample size will confirm the significance of the reduction observed in these experiments. Whole cord physiology in the $SOD1^{G93A}$ mice using inhibitors and donors of NO may also reveal the implications (if any) of a potential deficit in NO production.

In this chapter I have established the presence of NO-producing neurons in the mouse lumbar spinal cord. A logical extension to these results is to manipulate the levels of NO during fictive locomotion to define an active role for NO in the locomotor network. To this aim, the following chapter describes the results obtained from the manipulation of NO levels during lumbar locomotor network activity.

Chapter 3: Nitric oxide-mediated modulation of locomotor–rhythm generating networks in the isolated in vitro neonatal mouse spinal cord

3.1 Introduction

3.1.1 Background

The isolated spinal cord retains the capacity to generate a variety of spontaneous and/or rhythmic coordinated locomotor behaviours, such as swimming, scratching, and walking. These movements are modulated in a variety of natural environmental circumstances, for example, during the transition from a walk to a gallop or to generate escape swimming in response to stress.

In 1911, Thomas Graham Brown showed that the spinal cord contains sufficient circuitry to generate and maintain locomotion in the absence of supraspinal and sensory inputs. In this pivotal study, he postulated that proprioceptive inputs have a regulatory and not an intrinsic role in movement, that movement produced in the absence of afferents shared great similarity with movement when afferents remained intact, and that "The rhythmic sequence of the act of progression is consequently determined by phasic changes innate in the local centre" (Brown, 1914, Brown, 1911). Brown also proposed the half-centre model to describe the organisation of the 'innate local centres' within the spinal cord, now known as CPGs (Grillner, 2011), which control locomotion. In the half-centre model, each half-centre consists of excitatory interneurons that innervate motor neurons controlling flexor and extensor muscles, or muscles of the left and right sides of the body, which are innervated by roots originating from the same spinal segment e.g. L2 ipsilateral and contralateral roots. The excitatory interneurons within the two half-centres are prevented from synchronous activation by inhibitory interneurons (Renshaw, commissural or other ipsilateral inhibitory interneuron populations) in a process termed reciprocal inhibition. This synaptic organisation leads to an alternating pattern of output from motor neurons equivalent to that seen in the intact animal. However, this simple half-centre model does not account for the wide range of precisely controlled movements generated by the spinal cord, and thus, the

modified half-centre model, that accommodates increasing levels of excitatory and inhibitory sets of interneurons, currently dominates the theoretical debate on the control of locomotion (McCrea and Rybak, 2008). The two-layer half-centre model involves, firstly, the rhythm generator (RG) that is responsible for the timing of locomotor output, analogous to a pacemaker or clock. It is multiple orders above the last order interneurons that synapse directly onto motor neurons. The second layer of this model is the pattern generator (PG), consisting of last order interneurons, that synapse directly onto motor neurons, relaying intensity and temporal signals from the RG/rest of the network (McCrea and Rybak, 2008, Kiehn, 2011). The location and identity of the RG neurons remains a matter of great debate and research. In experiments where pharmacological or electrical stimulation perturbs the output from the *in vitro* locomotor network, effects on the output and thus the RG and PG can be inferred.

3.1.2 Modulation of rhythmic locomotor activity

In the absence of descending innervation, activation of the spinal locomotor network can be initiated by electrical stimulation, amines such as 5HT/DA (Christie and Whelan, 2005), combinations of N-Methyl-D-aspartic acid (NMDA), 5HT and dopamine (DA) (Beato et al., 1997, Bonnot et al., 2002a, Cazalets et al., 1992, Jiang et al., 1999, Whelan et al., 2000), as well as a wide range of endogenously produced peptides (Barriere et al., 2005). A rostrocaudal gradient exists in the hind-limb spinal cord circuitry, with greater rhythmogenic capacity located within the rostral (L1 – 3) than in the more caudal (L4 – 6) segments of the lumbar spinal cord (Chapter 1). Rhythmic locomotor activity is known to be modulated by activation of metabotropic G-protein-coupled receptors and biogenic amines (LeBeau et al., 2005). A relatively recent addition to this list of modulators is NO.

The role of NO as a neuromodulator of spinal locomotor networks has been established in vertebrate models of locomotion. In *Xenopus laevis* tadpoles, NO potentiates glycinergic mid-cycle inhibition and increases the frequency of GABAergic IPSPs (inhibitory postsynaptic potential), reducing swim episode duration and increasing cycle

period (McLean and Sillar, 2000, McLean and Sillar, 2002). In addition to this evidence of a direct inhibitory action, it has also been shown that NO modulation of noradrenaline release increases mid-cycle inhibition, slowing tadpole swimming frequency (McLean and Sillar, 2004). These inhibitory effects appear to be species specific as NO has the opposite, excitatory effect in *Rana temporaria* embryos (McLean et al., 2001) and in the lamprey (Kyriakatos et al., 2009).

In the adult lamprey *Lampetra fluviatilis/Petromyzon marinus*, mGluR1 activation during locomotion recruits both NO and endocannabinoid pathways (Kyriakatos and El Manira, 2007). An NO-dependent increase and long term potentiation of locomotor burst frequency occur as a result of a decrease in presynaptic release of glycine and, therefore, mid-cycle inhibition (Kyriakatos et al., 2009).

The distribution of neurons that express NOS in the locale of the locomotor circuitry, and therefore potentially represent the source of neuromodulatory NO, has been shown using immunohistochemistry and NADPH diaphorase activity in the tadpole and lamprey. In the tadpole, a population of reticulospinal neurons and their processes exhibit NADPH diaphorase reactivity and are potentially involved in modulation of descending locomotor commands (McLean and Sillar, 2001). Whilst NADPH diaphorase reactivity is largely absent from tadpole motor neurons, motor neurons in the lamprey express NOS, and both tadpole and lamprey motor neurons are modulated by NO (Kyriakatos et al., 2009, Ramanathan et al., 2006). In the present study, I have already described NADPH diaphorase reactivity in the ventral horn of the mouse spinal cord (Chapter 2) and shown that although NO reactivity is absent from the motor pools there are sources of NO within the sphere of influence of the motor pools. These NOS positive neurons increase in number during postnatal development and may be a source of NO involved in the modulation of locomotor activity.

3.1.3 Nitric oxide production and signalling pathways

Since the initial discovery that NO is endothelial-derived relaxating factor, the role of NO as a neurotransmitter and morphogen has been well established in a range of organs of both vertebrates and invertebrates. Three isoforms of the NO synthetic enzyme NOS are located throughout the CNS and both eNOS and nNOS are constitutively expressed (Knowles and Moncada, 1994). The primary cellular target for NO is the soluble form of guanylate cyclase (sGC), which catalyses the production of cyclic guanosine monophosphate (cGMP) from guanosine triphosphate (GTP) (Bellamy et al., 2002, Cary et al., 2006, Fernhoff et al., 2009, Zhao et al., 2000). cGMP then goes on to activate the protein kinase G signalling cascade (PKG) which is involved in a number of downstream effects, such as phosphorylation and protein synthesis (Wang and Robinson, 1997). cGMP can also directly activate cyclic nucleotide gated ion channels (CNGC) such as the HCN channels in the hippocampus (Wilson and Garthwaite, 2010, Neitz et al., 2011). In addition to signalling via cGMP-dependent pathways, NO signalling can also be mediated via highly reactive NO-derived radical products, such as peroxynitrite, which are formed by nitrosative and oxidative mechanisms and can react with lipids and proteins. Such reactions typically involve the addition of a nitroso (-NO) functional group to proteins, particularly thiols of cysteine residues (i.e. -SH) by a process termed s-nitrosation (Stamler et al., 1992{Jaffrey, 2001 #220)}. It has been theorized that direct effects of NO (such as sGC activation) occur at low, physiological concentrations, whilst indirect radical reactions (nitrosative/oxidative stress) occur at high pathophysiological concentrations of NO, particularly when iNOS is activated (Redford et al., 1997, Smith et al., 2001, Hofseth et al., 2003, Duncan and Heales, 2005)
.

3.1.4 Scope and importance of this study

Despite clear evidence of the importance of NO-mediated signalling in the control of the locomotor CPG in tadpole and lamprey swim circuits; the role of NO-mediated signalling in the mammalian locomotor CPG has yet to be investigated. Studies in the

mammalian respiratory network suggest NO is involved in activity-dependent modulation in concert with other neurotransmitters (Saywell et al., 2010). In light of this evidence, a role for NO in the control of mammalian hind limb lumbar spinal circuitry is likely. In the present study, sources of NO have been described in the developing mammalian lumbar spinal cord. The NO producing neurons are located in close proximity to the neurons involved in coordinating movement, around the central canal (lamina X) and the wider lamina VII, and thus, may potentially modulate locomotor output.

This chapter details the investigation of the role of NO in the mammalian locomotor circuit and the possible contribution of the NO/sGC/cGMP pathway to its effects, using pharmacologically induced fictive locomotion in the isolated spinal cord (Jiang et al., 1999) and the disinhibited isolated spinal cord preparation (Bracci et al., 1996). This involved manipulation of induced fictive locomotion by application of NO donors and the inhibition or removal of endogenous sources of NO, as well as modulators of the NO/sGC pathway.

These results represent the first investigation into the possibility that NO is involved in the modulation of mammalian locomotion. Identifying and clarifying a role for NO in mammalian locomotion will enhance our basic understanding of the functional circuitry involved in the generation and maintenance of movement, and consequently provide additional knowledge for consideration in dysfunctional and damaged circuits as a result of spinal cord trauma and neurodegenerative disease.

3.2 Materials and Methods

3.2.1 Tissue collection and preparation

All experiments were performed in accordance with the United Kingdom Animals (Scientific Procedures) Act 1986. C57BL6 wild-type mice were obtained from Charles River Laboratories (Scotland, UK). The mice were bred under conditions of a 12-h

light/dark cycle in individual ventilated cages at a constant temperature of 22°C and 56% humidity with free unrestricted access to food and water. Following cervical dislocation, decapitation, evisceration and vertebrectomy, spinal cord tissue from mid cervical to upper sacral region was isolated in a chamber containing artificial cerebral spinal fluid (aCSF; equilibrated with 95% oxygen, 5% carbon dioxide, ~4ºC). All procedures were carried out at room temperature (RT) (18-22°C). Neonatal mice aged postnatal day (P) 1-3 were used for the experiments detailed in this chapter.

Spinal cords were isolated from the mid-thoracic to mid-sacral regions and fixed with fine steel pins, ventral side up, to a sylgard-lined dissection chamber containing artificial cerebral spinal fluid (aCSF) equilibrated with 95% O_2/5% CO_2 (Jiang et al., 1999, Miles et al., 2007, Iwagaki and Miles, 2011). The pia mater was removed and the dorsal roots trimmed before the cord was moved to the recording chamber; a sylgard-lined custom-built Perspex chamber perfused with aCSF (equilibrated with 95% O_2/5% CO_2) at a rate of between 5-8 mL min^{-1}. The spinal cord was again fixed ventral surface up with fine steel pins.

3.2.2 Induction and recording of fictive rhythmic locomotion

Fictive rhythmic locomotion is characterised by rhythmic bursts of locomotor-related output which alternate between pairs of ventral roots originating from the same lumbar segment i.e. left-hand side/right-hand side (L/R) L2 (Fig. 3.2A, B rL2/lL2 and r∫L2/ l∫L2). Bursts of locomotor-related output also alternate between ipsilateral ventral roots which predominantly innervate flexor and extensor roots i.e. RHS L2/L5 (Fig.3.2A, B rL2/rL5 and r∫L2/r∫L5). The ventral root activity recorded at L2 is consistent with hind-limb flexor activity and activity recorded at L5 is consistent with hind-limb extensor activity as previously described (Kjaerulff and Kiehn, 1996, Bonnot et al., 2002b).

L/R ventral root activity was recorded by placing glass suction electrodes over L1, L2 or L3 roots (see Fig.3.2A, solid blue electrode). In experiments where flexor/extensor ventral root activity was compared, a third glass suction electrode was placed over an

ipsilateral L5 root (see Fig.3.2A, dotted blue electrode). Signals were amplified, filtered (30-3000Hz) and raw signals rectified and integrated (Qjin Design, ON, Canada). Raw and integrated signals were acquired at 1kHz using a Digidata 1440A A/D board and AxoScope software (version 7.0, Molecular Devices, Sunnyvale, CA).

Locomotor output (see Fig. 3.2B) was induced by bath application via the perfusate of 5μM *N*-methyl-d-aspartate (NMDA) and 10μM 5-hydroxytryptamine hydrochloride (5HT) and the pattern of alternating rhythmic output was allowed to develop for between 50-60 minutes on average before the addition of pharmacological agents used to investigate the roles of NO-mediated signalling in the control of locomotor output. Pharmacological agents affecting NO-mediated signalling were applied for 30 or 45 minutes after which time they were removed by gradual elimination from the perfusate. Pharmacologically induced fictive locomotion (5HT and NMDA) varied in frequency between 0.22 and 0.39Hz across different preparations (Fig. 3.1). Disinhibited fictive locomotion was induced by applying 10μM 5HT and 5μM NMDA in combination with 1μM strychnine and 10μM bicuculline. Disinhibited fictive locomotor activity was characterised by synchronous bursts of activity across all ventral roots. The disinhibited rhythm was much slower than the rhythm observed when inhibition remained intact, with frequencies varying between 0.09 and 0.07Hz (Fig. 3.1).

Recordings were defined as control condition when fictive rhythmic output was induced using 5HT and NMDA only (see Fig. 3.2A and B, Fig. 3.3A and B, control), except in the disinhibited preparation (see Fig. 3.6A and B, control) where the control solution contained strychnine and bicuculline in addition to 5HT and NMDA. Drug condition designates rhythmic output during the addition of pharmacological agents to the perfusate (for example see Fig. 3.3A and B, DEA NO) for a period of 30 or 45 minutes. Drug condition perfusate was systematically replaced by control solution containing 5HT and NMDA only, except in the disinhibited preparation (see Fig. 3.6A and B, washout) where the control solution also contained strychnine and bicuculline, and this was designated as wash or washout.

3.2.3 Analysis

Data (raw for amplitude, and integrated and smoothed for temporal) were analysed offline using Dataview software (version 6.3.2. courtesy of Dr W J Heitler, University of St Andrews).
The *in vitro* rhythmic preparation provides several quantitative parameters for analysis (see Fig. 3.1D). Those relevant to this study are:

Frequency – the onset-to-onset frequency of burst output from nerve roots, interpreted as the temporal signal received by motor neurons from the locomotor network CPG and/or its components (see Fig. 3.2Di);

Amplitude – the peak-to-peak burst amplitude from nerve roots, interpreted as the output from motor neurons transmitted via the nerve root to the effector muscle (see Fig. 3.2D ii);

Inter-burst amplitude – the mean inter-burst amplitude from nerve roots, interpreted as tonic, non-synchronous motor neuron activity (see Fig.3.2D iii);

Left/right and extensor/flexor alternation – the timing (phase) of burst onset between left/right ventral roots originating from the same segment (e.g. LHS/RHS L2) and between ipsilateral, flexor/extensor roots (e.g. RHS L2/L5; Fig.3.2D iv and v respectively; Section 3.2.2).

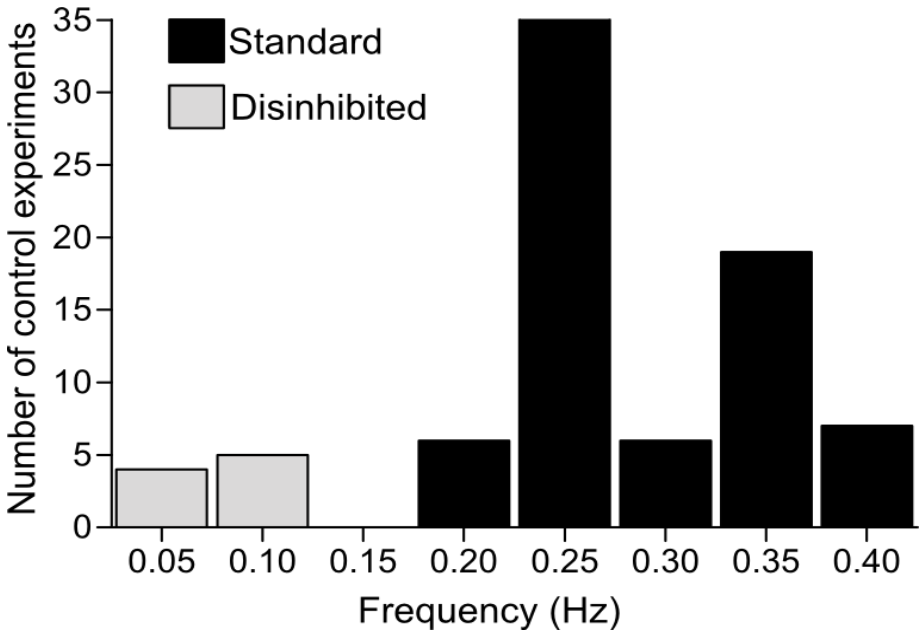

Figure 3.1. Frequency distribution of the frequency of pharmacologically induced fictive locomotion. Fictive locomotion was induced using 5µM NMDA and 10µM 5HT. Alternating rhythmic output was established over 50 – 60 minutes before recording output. Fictive locomotor output varied in frequency between 0.22 and 0.39Hz across different preparations. Disinhibited fictive locomotion was induced using 10µM 5HT and 5µM NMDA in combination with 1µM strychnine and 10µM bicuculline. Disinhibited locomotor-related output varied in frequency between 0.09 and 0.07Hz.

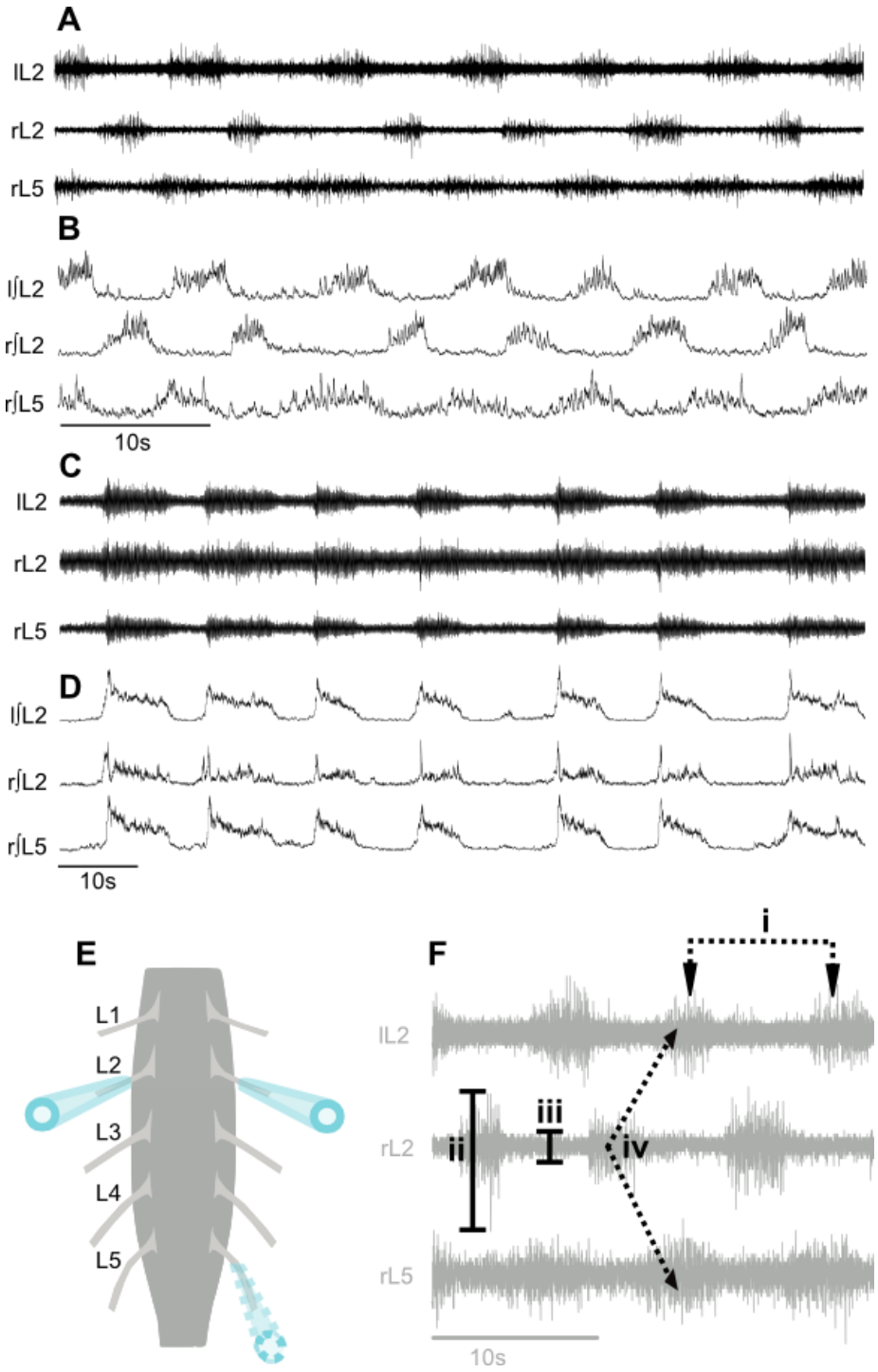

Figure 3.2. Experimental setup used to investigate pharmacologically induced fictive rhythmic locomotor output from the isolated mouse spinal cord. **A, C** Raw and **B, D** rectified/integrated traces of 5μM NMDA and 10μM 5HT induced fictive locomotion recorded from L2/flexor and L5/extensor ventral roots. **C** Raw and **D,** rectified/integrated traces of disinhibited synchronous fictive output induced by addition of 1μM strychnine and 10μM glycine to perfusate containing 5μM NMDA and 10μM 5HT. **E** Illustration of isolated lumbar spinal cord preparation showing suction electrodes attached to L2 ventral roots (solid outline) and one L5 root (dotted outline). Diagram adapted from original courtesy of Dr G.B Miles. **F** Measurement parameters of alternating fictive locomotion include; **i** burst frequency, **ii** burst amplitude, **iii** inter-burst amplitude, and **iv** left/right and extensor flexor alternation.

Data were averaged in 1-minute bins, and normalised by dividing with mean control values (10 minutes). Graphs and time plots were constructed using GraphPad Prism software (Graphpad, La Jolla, CA). Images of raw and integrated traces were imported into GNU Image Manipulation Program (Free Software Foundation Inc., Boston, MA) from Dataview for formatting, and figure assembly was performed in the Inkscape graphics package (Free Software Foundation Inc., Boston, MA).

The integrity of the phase relationship between left/right and flexor/extensor ventral root bursting during control and DEA NO application (n=3) were described using circular statistics (Kjaerulff and Kiehn, 1996, Bonnot et al., 2002a). Burst events (15-20) in both control conditions and during application of DEA NO were analysed and phase data calculated using Dataview. These phase data were used to compute circular descriptive statistics and circular plots in StatistiXL (version 1.8, 2007). The mean phase coordinate was calculated as previously described (Kjaerulff and Kiehn, 1996).

Coordinates plotted on the circular plot represent the burst phase, defined as the onset of ventral root activity on the left versus the right side of the spinal cord, as a number between 0 and 1 (on the graph the coordinate 0 represents both 0 and 1). Phase values clustered around 0 indicate synchronous burst output between compared roots and clustering around 0.5 indicates alternation of burst output between compared roots. Individual data points plotted around the circle comparing segmentally aligned, contralateral, flexor-related roots represent the onset of individual locomotor bursts recorded from L2 ventral roots on the right hand side. Data points plotted around the circle comparing L2- versus L5-related ipsilateral roots represent the onset of individual locomotor bursts recorded from L5 ventral roots.

The phase values for a single representative experiment were plotted with vectors originating from the centre of the circle indicating the mean phase for all experiments in which activity was recorded from both L2 and L5 ventral roots. The vector length indicates the concentration of data points around the mean.

3.2.4 Statistics

Statistical significance between control versus drug condition and wash or multiple drug conditions was tested using either the one way analysis of variance, with Dunnett post test or repeated measures analysis of variance, with Bonferroni post test (ANOVA; GraphPad Prism software, Graphpad, La Jolla, CA). Statistical significance is indicated by asterisk as follows; * = P<0.05, ** = P<0.01, *** = P<0.001, **** = P<0.0001. The strength of phase coupling was tested by Rayleigh's test for uniformity using StatistiXL (version 1.8, 2007). Changes are expressed as a percentage of control. Significance was defined as $P < 0.05$. All values are expressed as mean ± SEM.

3.2.5 Solutions and reagents

3.2.5.1 Solutions

Artificial cerebral spinal fluid (aCSF)

The aCSF composition: 127mM NaCl; 3mM KCl; 2mM $CaCl_2$; 1mM $MgCl_2$; 26mM $NaHCO_3$; 1.25mM NaH_2PO_4; and 10mM glucose.

3.2.5.2 Reagents

Reagents used in the present study have been summarised in Table 3.1.

Reagents obtained from Sigma-Aldrich Company Ltd., Dorset, UK were:
N-methyl-d-aspartate (NMDA) – agonist of NMDA-type ionotropic glutamate receptors which are activated during fictive locomotion (Schmidt et al., 1998, Cowley et al., 2005);

5-hydroxytryptamine hydrochloride (5HT) – monoamine neurotransmitter. 5HT2 and 5HT7 receptors have been shown to be involved in the initiation of fictive locomotion (Smith and Feldman, 1987, Kudo and Yamada, 1987, Liu and Jordan, 2005, Ung et al., 2008);

2-Phenyl-4, 4, 5, 5-tetramethylimidazoline-1-oxyl 3-oxide (PTIO) – imidazoline scavenger shown to ablate NO mediated vasodilatory effects observed in rabbit aorta between 75-95% at 100-300μM, within the range of concentrations used in the present study (Akaike et al., 1993, Pfeiffer et al., 1997);

(5*S*)-5-[(6*R*)-6,8-dihydro-8-oxofuro[3,4-*e*]-1,3-benzodioxol-6-yl]-5,6,7,8-tetrahydro-6,6-dimethyl-1,3-dioxolo[4,5-*g*]isoquinolinium iodide (bicuculline) – $GABA_A$ receptor antagonist;

(−)-Strychnine – alkaloid glycine receptor antagonist;

N5-(nitroamidino)-L-2,5-diaminopentanoic acid (L-NNA) – an inhibitor of the NOS isozymes with a specificity for nNOS > eNOS > iNOS (Ki = 15nM, bovine; 39nM, human; 4.4μM, murine) (Griffith and Kilbourn, 1996);

8-bromoguanosine 3′, 5′-cyclic monophosphate sodium salt (8BrcGMP) – membrane permeable PKG agonist.

Reagents obtained from Ascent Scientific Ltd., Bristol, UK were:
1H-[1, 2, 4] oxadiazolo [4, 3-a] quinoxalin-1-one (ODQ) – sGC inhibitor (Boulton et al., 1995);
N-nitro-L-arginine methyl ester hydrochloride (L-NAME) – a methyl ester of L-NNA which requires a hydrolysis step to produce L-NNA with similar kinetics (Griffith and Kilbourn, 1996).

Reagents obtained from Fluorochem Ltd., Derbyshire, UK were:
2-(N,N-diethyl amino)-diazenolate-2-oxide diethyl ammonium salt (DEA NO) – a NO donor, with a half-life of approximately 16 minutes at 22^{o}C (Keefer et al., 1996);

2-(4-carboxyphenyl)-4,4,5,5-tetramethylimidazoline-1-oxyl-3-oxide potassium salt (cPTIO) – a lipophobic imidazoline scavenger of NO shown to ablate NO mediated vasodilatory effects observed in rabbit aorta between 75-95% at 100-300μM, within the

range of concentrations used in the present study (Akaike et al., 1993, Pfeiffer et al., 1997).

Table 3.1 Reference summary of pharmacological agents used to manipulate NO concentration in the in vitro isolated spinal cord preparation.

Abbreviation	Synonym	CAS	MW	Mode of action	Selectivity	References
DEA NO	2-(N,N-Diethylamino)-diazenolate-2-oxide.Diethylammonium salt	56329-27-2	206.2	NO donor	1.5 moles of NO produced at RT; half-life 16 minutes	(Keefer et al., 1996)
PTIO	2-Phenyl-4,4,5,5-tetramethylimidazoline-1-oxyl 3-oxide	18390-00-6	233.3	NO scavenger	selective, reversible; IC50 of 0.11±0.03 mM	(Akaike et al., 1993, Pfeiffer et al., 1997)
cPTIO	2-(4-Carboxyphenyl)-4,4,5,5-tetramethylimidazoline-1-oxyl-3-oxide potassium salt 2-(4-Carboxyphenyl)-4,5-dihydro-4,4,5,5-tetramethyl-1H-imidazol-1-yloxy-3-oxide potassium salt	148819-94-7	315.4	NO scavenger	selective, reversible; 19.71±- 4.23pM	(Pfeiffer et al., 1997, Wanikiat et al., 1997, Akaike et al., 1993)
ODQ	1H-[1,2,4]oxadiazolo[4,3-a]quinoxalin-1-one	41443-28-1	187.2	sGC inhibitor	selective irreversible; IC_{50} ~20nM	(Garthwaite et al., 1995)
8BrcGMP	8-Bromoguanosine 3′,5′-cyclic monophosphate sodium salt	51116-01-9	423.2	PKGI agonist	selective, reversible; IC_{50}=8±0.03 nM	(Choi and Farley, 1998, Lee et al., 1997, Francis et al., 2010)
L-NNA	N^5-(Nitroamidino)-L-2,5-diaminopentanoic acid	2149-70-4	219.2	NOS inhibitor	non- specific; eNOS IC_{50}=3.1±0.4μM	(Griffith and Kilbourn, 1996)
L-NAME	N_ω-Nitro-L-arginine methyl ester hydrochloride	51298-62-5	269.7	NOS inhibitor	non- specific; eNOS IC50=3.1±0.4μM	(Griffith and Kilbourn, 1996, Rees et al., 1990)

3.3 Results

3.3.1 Modulation of fictive locomotion by exogenous nitric oxide

To investigate the potential role of NO-mediated signalling in the control of the spinal locomotor circuitry, the NO donor DEA NO, which will increase exogenous levels of NO, was applied to isolated spinal cord preparations in which fictive locomotion had been pharmacologically induced. Fictive locomotion was induced and maintained by activation of the spinal cord locomotor network using a combination of 10μM 5HT and 5μM NMDA by bath application via the circulating, oxygenated perfusate (Materials and Methods, Section 3.2.2.). Once output had stabilised (qualitative evaluation), approximately 60 minutes after application of 5HT and NMDA, 50μM (Fig. 3.3A and B), 100μM, 200μM or 400μM DEA NO was added to the perfusate for a period of 45 minutes. Rhythmic locomotor-related output was recorded from ventral roots via suction electrodes and the effects of DEA NO measured with any changes expressed as a percentage of control.

The frequency of bursts of locomotor-related activity recorded from ventral roots consistently and significantly decreased (Fig.3.3A, B, C and E), compared to control during the application DEA NO at concentrations of 50μM ($P<0.05$; -15±4%, n=7), 100μM ($P<0.05$; -5±3%, n=6), 200μM ($P<0.05$; -17±5%, n=13) and 400μM ($P<0.05$; -38±10%, n=10). Typically at the low concentrations (50/100μM), the decrease in frequency reached a maximum 5-10 minutes after DEA NO was added to the perfusate and gradually recovered to near control levels approximately 5-10 minutes before washout. Burst frequency then remained at control levels for the duration of the drug washout period (Fig 3.3C).

At higher concentrations (200/400μM), the peak decrease in frequency occurred 15-20 minutes after the addition of DEA NO to the perfusate and gradually recovered to near control levels approximately 5 minutes before washout. During washout, frequency remained near control levels for approximately 15 minutes and then appeared to increase for the remaining 30 minutes of wash. After approximately 25 minutes of

wash, the frequency increased at 400μM and at 200μM the frequency of output remained elevated above control levels.

The effects of DEA NO on the amplitude of bursts of locomotor-related output recorded from ventral roots were more complicated in comparison to frequency. The effect of DEA NO on burst amplitude varied between concentrations and within different preparations such that increases, decreases and biphasic responses, involving transient increases followed by longer lasting decreases, were observed.

During application of 50μM DEA NO, the amplitude increased and reached a peak in the first 10 minutes and remained elevated above control levels during washout ($P<0.05$; 50μM, control, +9±4%; Fig. 3.3F). The higher concentration of 200μM DEA NO caused an increase, when compared to control, in the amplitude of locomotor-related bursts in a subset of preparations ($P<0.05$; 200μM, +16±7%, n=7/13 and 400μM, +19±8%, n=6/10 Fig. 3.3F), additionally, a decrease in amplitude was recorded during the DEA NO applications of 200μM ($P<0.05$; -15±5%, n=8/13) and 400μM ($P<0.05$; -24±8%, n=7/10). Significant NO effects on both frequency and amplitude were observed at 50, 200 and 400μM but not at 100μM DEA NO, with peak frequency effects observed at 400μM, the highest concentration used, and a concentration dependent change in amplitude across the concentration range. These DEA NO-mediated effects indicate that exogenous sources of NO modulate burst output from the spinal locomotor circuitry.

Burst coordination was then examined to determine whether or not NO-mediated signalling is involved in regulating the pattern of locomotor output, specifically left/right and flexor/extensor alternation. Strong L2/L2 and L2/L5 alternation (Section 3.2.2. for definitions) was observed in control conditions (n=3). The fidelity of L/R alternation was maintained after the addition of 100μM DEA NO ($P<0.05$; Fig. 3.4Ai). However, mean vector values for L2/L2 alternation appeared to less uniform around the mean between control and drug conditions but the uniformity remained significant ($P<0.05$; Fig. 3.4Aii). This is most likely due to the longer L5 burst duration as opposed to a fundamental difference in control bursting between these roots or a DEA NO-

mediated effect. However, a larger sample of experiments will need to be conducted to clarify the possibility of a DEA NO-mediated effect.

Next, the effects of DEA NO on inter-burst activity were assessed to determine whether DEA NO modulates general excitation of the entire spinal circuitry or if its modulatory effects are specific to locomotor activity (Fig.3.5A and B). The amplitude of inter-burst activity recorded from ventral roots was not significantly affected by DEA NO application in these experiments, though a small increase in variability of inter-burst amplitude was noted. These data indicate that the NO-mediated effects observed on burst frequency and amplitude are specific to locomotor-related activity.

Previously, it has been shown that NO acts via potentiation of inhibitory transmission (glycinergic and GABAergic transmission) to reduce the duration and increase the cycle period of tadpole swimming (McLean and Sillar, 2004). To investigate whether NO-mediated effects on fictive mammalian locomotion occur via the modulation of excitatory or inhibitory transmission, DEA NO was applied to preparations in which disinhibited, synchronous activity was induced using bicuculline (10μM) and strychnine (1μM) in addition to 5HT (5μM) and NMDA (10μM). During pharmacological block of inhibition, the application of 50μM or 400μM DEA NO (Fig. 3.6A-F) were consistent with the effects seen in the presence of inhibitory transmission during the application of 50μM or 400μM DEA NO. DEA NO significantly decreased the frequency of disinhibited rhythms at concentrations of both 50μM ($P<0.05$; -34±4%, n=5) and 400μM ($P<0.05$; -59±12%, n=4; Fig. 3.6C and E). The decrease in frequency reached a maximum 15-20 minutes after the addition of 50μM and 400μM DEA NO to the perfusate and recovered, returning to near control levels after approximately 15 minutes of washout.

The application of a low concentration of DEA NO caused an increase in the amplitude of locomotor-related bursts recorded in disinhibited preparations ($P<0.05$; 50μM, +18±15%, n=5). Amplitude continued to increase for the duration of DEA NO application and remained elevated above control levels but did not appear to increase

further during washout (Fig. 3.6D and F). In contrast, high concentrations of DEA NO (400μM) did not significantly affect locomotor burst amplitude

Given that the application of DEA NO to disinhibited spinal cord preparations resulted in changes to both frequency and amplitude, consistent with those that were observed in the presence of inhibition at low donor concentrations, the main effects of NO-mediated signalling on the mammalian locomotor circuit are likely to involve the modulation of excitatory interneurons and/or excitatory synaptic transmission. A role for NO in the modulation of inhibitory transmission is still feasible considering that DEA NO has no effect on disinhibited rhythmic spinal activity.

3.3.2 Endogenously produced nitric oxide modulates fictive locomotion

To investigate the potential role of endogenous NO-mediated signalling on the spinal locomotor circuitry, scavengers and inhibitors of NO were applied to isolated spinal cord preparations in which fictive locomotion was induced pharmacologically (5HT, 10μM; NMDA, 5μM).

Removal of both extracellular and intracellular endogenous NO by the membrane permeable NO scavenger, PTIO, significantly increased burst frequency and decreased burst amplitude ($P<0.05$; 400μM; +12±5% and -6±3%, respectively; n=8; Fig.3.7A-F). The increase in burst frequency was reversed on washout but amplitude during washout and appeared to remain lower than control levels. Experiments were also conducted using the extracellular NO scavenger, carboxy-PTIO (cPTIO). cPTIO caused a significant increase in frequency at a concentration of 400μM ($P<0.05$; +12±5%, n=8) but not at 200μM and frequency returned to near control levels during washout. Amplitude was significantly increased at 200μM ($P<0.05$; +10±5%, n=10) but not during application of 400μM DEA NO. Burst amplitude values returned to near control levels during washout after application of both 200μM and 400μM DEA NO (Fig.3.7E and F). During carboxy-PTIO application greater variability in the frequency and amplitude of locomotor burst output was noted within and between preparations.

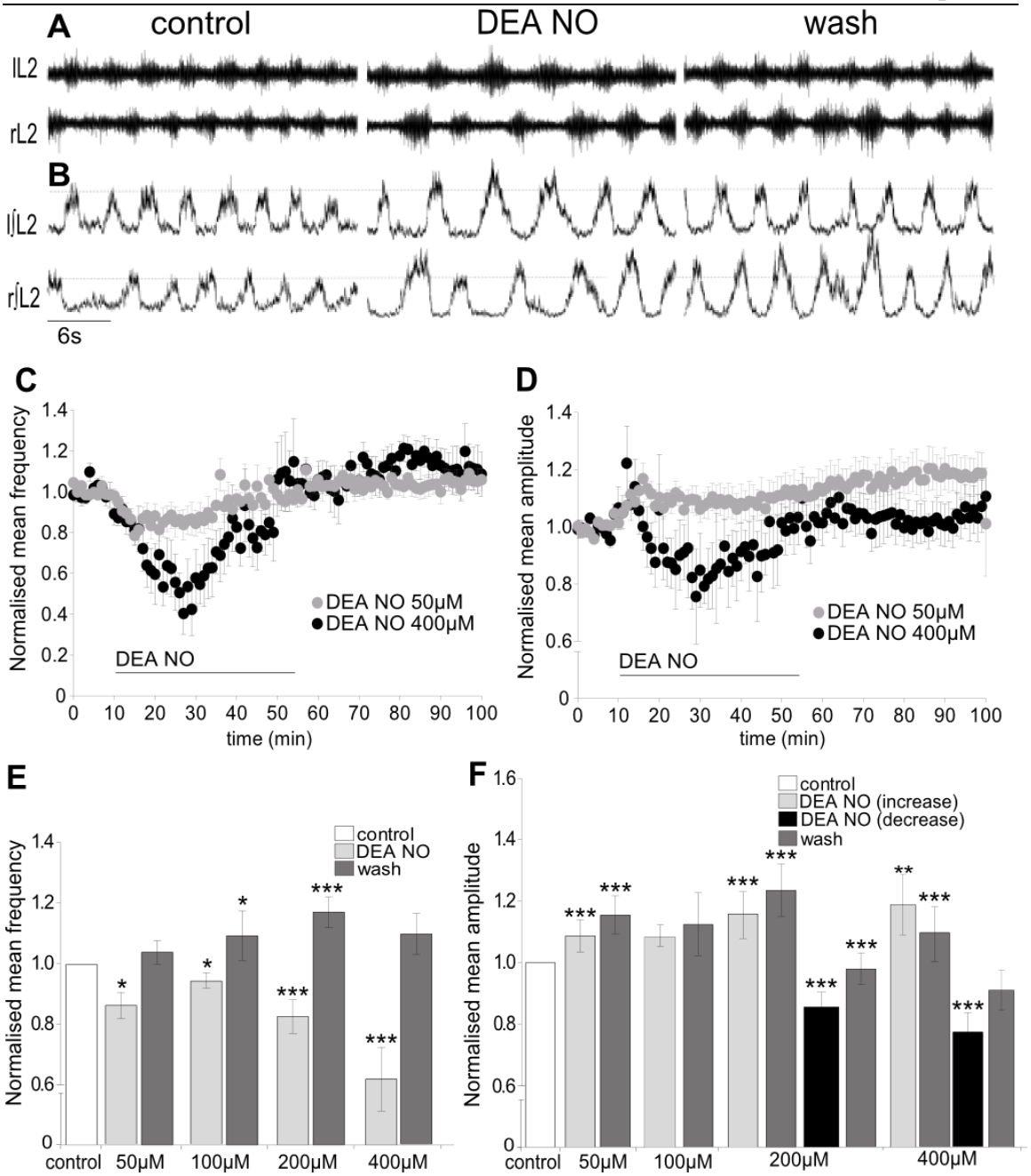

Figure 3.3. Exogenous NO modulates pharmacologically-induced fictive locomotion. Raw **A** and rectified/integrated **B** locomotor bursts induced by 5µM NMDA and 10µM 5HT recorded from the left and right ventral roots (L2 segment, lL2/rL2 and l∫L2/ r∫L2 respectively) before (control), during (DEA NO) and after (wash) application of the NO donor DEA NO (grey, 50µM; black, 400µM). Time course plots (data averaged in 1 minute bins) showing the effects DEA NO (grey, 50µM, n=7; black, 400µM, n=10) on, **C** frequency and **D** amplitude of locomotor bursts relative to control. **E**, DEA NO significantly decreased frequency during application at concentrations of 50, 100, 200 and 400µM (10min, $P<0.05$, respectively: n=7; n=6; n=13; n=10). **F**, DEA NO significantly increased amplitude at a concentration of 50µM (10min, $P<0.05$, n=7), 200µM (n=7/13) and 400µM (n=6/10) DEA NO caused a transient but significant increase (10min, $P<0.05$) followed by a significant decrease in amplitude at 200µM (n=8/13) and 400µM (n=7/10) DEA NO (10min, $P<0.05$). At the highest concentrations of 200µM and 400µM, an initial transient increase followed by a decrease in amplitude was observed (n=2/13 and n=3/10, respectively). Locomotor burst amplitude was not affected at concentrations of 200µM DEA NO. Data mean ±SEM.

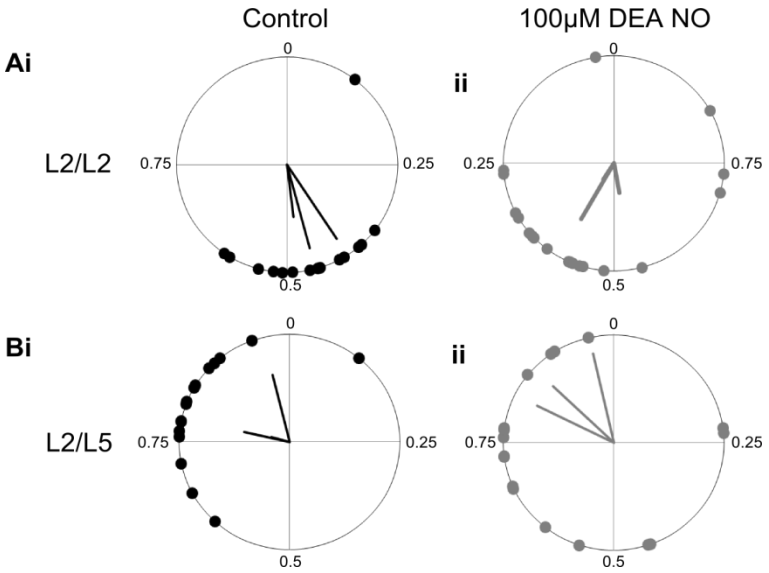

Figure 3.4. DEA NO does not affect left-right or flexor-extensor alternation during fictive locomotion. Circular phase-diagram depicting the phase onset of locomotor bursts recorded from the **Ai** right L2 root in relation to the onset of activity recorded from the left L2 root (flexor/flexor) and **Bi** right L2 root in relation to the onset of activity recorded from the right L5 root (flexor/extensor) in control conditions and **Aii, Bii** during 100µM DEA NO application. The mean phase value is indicated by vectors emanating from the centre of the circular plot. The length of the vector indicates the concentration of events around the mean. Events clustered around 0.5 suggest that bursting alternates between the left and right flexor roots **Ai** and was not affected **Aii** by application of 100µM DEA NO. **Bi** clustering around 0.75 for plots of flexor vs. extensor activity was most likely due to the longer L5 burst duration.

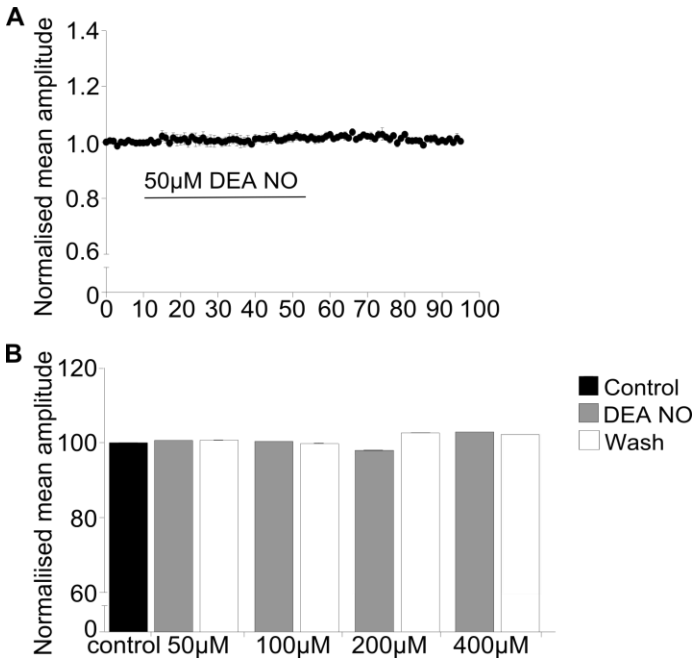

Figure 3.5. Inter-burst amplitude is not affected by DEA NO during fictive locomotion. **A** Time course plot (data averaged in 1 minute bins) demonstrating no effect on inter-burst amplitude during application of 50µM DEA NO. **B** DEA NO does not affect inter-burst amplitude at 50, 100, 200 and 400µM concentrations (n=7; n=5; n=10; n=8, respectively). Bar in **A** indicates duration of application, and error bars are SEM.

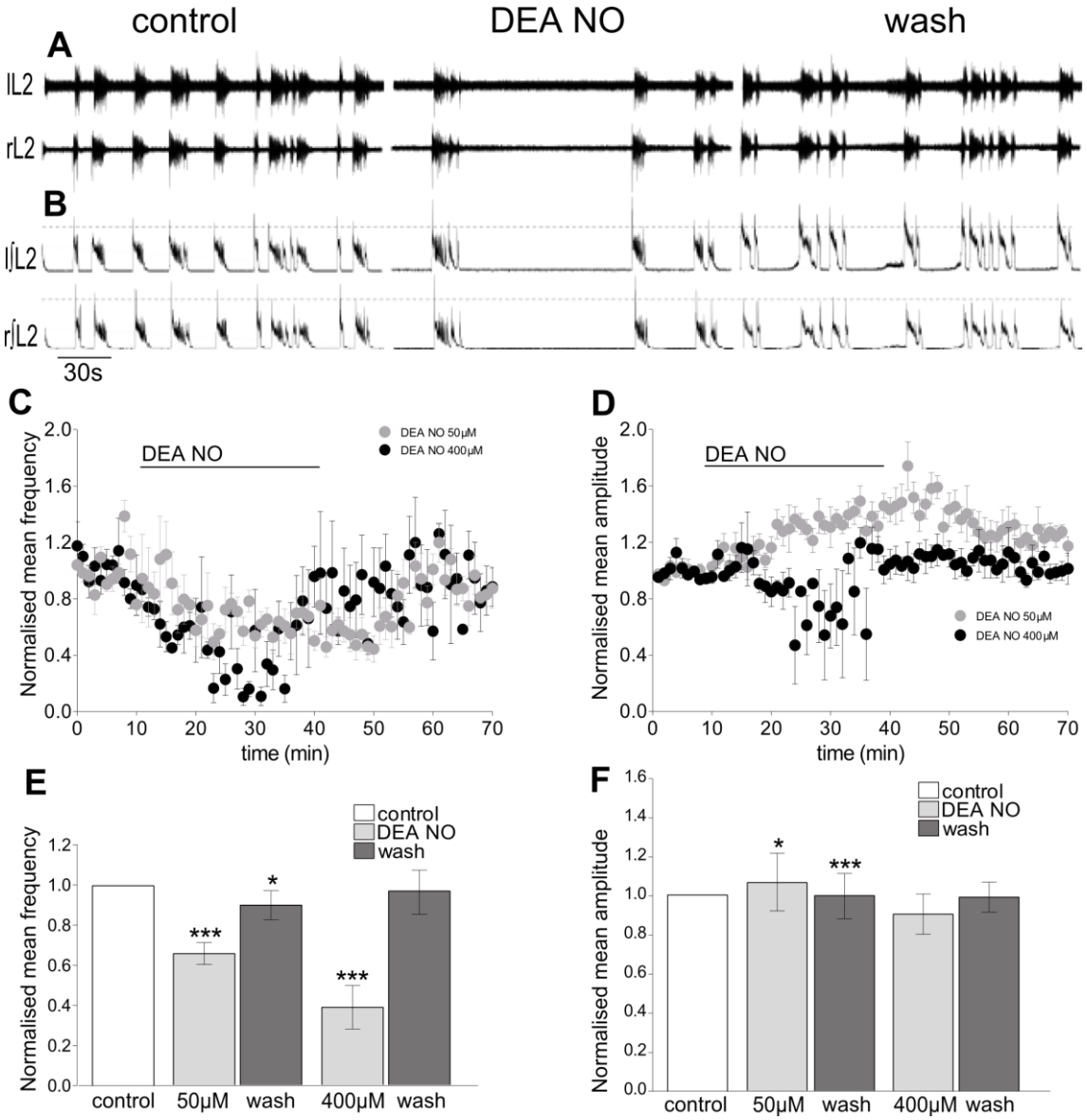

Figure 3.6. DEA NO modulates disinhibited rhythmic activity. Raw **A** and rectified/integrated **B** locomotor bursts induced by 5µM NMDA and 10µM 5HT in the presence of 1µM strychnine and 10µM bicuculline recorded from the left and right ventral roots (L2 segment, lL2/rL2 and l∫L2/ r∫L2) before (control), during (DEA NO) and after (wash) application of the NO donor DEA NO (grey, 50µM; black, 400µM). Time course plots (data averaged in 1 minute bins) showing the effects DEA NO (grey, 50µM, n=5; black, 400µM, n=4) on, **C** amplitude and **D** frequency of locomotor bursts relative to control. **E** DEA NO significantly decreased frequency at concentrations of 50 and 400µM (10min, $P<0.05$, n=5 and n=4, respectively). **F**, DEA NO significantly increased amplitude at a concentration of 50µM (10min, $P<0.05$, n=5) but did not significantly decrease amplitude at a concentration of 400µM. Bar in **C** and **D**, indicates duration of application, asterisk denotes significance relative to control and error bars are SEM.

These data confirm that NO produced within or in close proximity to the locomotor network has an inhibitory effect on frequency (PTIO and cPTIO). The variation observed in experiments where cPTIO was used may be due to effects resulting from the production, by side reaction, of peroxynitrite (ONOO-) and possibly due to the inability of cPTIO to traverse cell membranes to effectively neutralise NO.

Next, the NOS inhibitors L-NNA and L-NAME were used to prevent endogenous production of NO to clarify further the effect of endogenous NO on locomotor output. Both L-NNA and L-NAME were used in these experiments, as it has been previously shown that both compounds have the opposite effect to NO donors when applied to the tadpole during swimming (McLean and Sillar, 2000).

L-NNA significantly increased the frequency of burst output during application of 200μM or 400μM ($P<0.05$; +8±4%, n=6 and +7±4%, n=10; Fig. 3.7G and H). L-NNA caused a significant decrease in amplitude during application of both 200μM and 400μM L-NNA ($P<0.05$; -9±3%, n=6 and -6±3%, n=10, respectively). The NOS inhibitor L-NAME is a methyl ester of L-NNA and has previously been shown to be an effective inhibitor of NOS involved in tadpole swimming (McLean and Sillar, 2002). 200μM L-NAME significantly increased frequency and decreased amplitude of burst output (+24±9% and -10±4%, respectively; n=6; Fig.3.7G and H).

Consistent with the exogenous application of DEA NO, the inter-burst amplitude was not significantly affected by L-NAME, PTIO, or cPTIO application, confirming that the NO-mediated effects observed in these experiments are specific to locomotor-related activity.

In summary, inhibitors of NOS enzymes increase the frequency and decrease the amplitude of locomotor burst output, both effects being opposite to those observed with the application of exogenous NO at low concentrations. Scavengers of NO increase the frequency of locomotor burst output but either increase (cPTIO) or decrease (PTIO) the locomotor burst amplitude. These data suggest that a tone of endogenously produced

NO is involved in the control of the frequency and intensity of burst output generated by spinal locomotor circuitry.

3.3.3 Involvement of the NO/sGC/cGMP pathway in NO-mediated modulation of the locomotor network

NO exerts its biological effects by both direct and indirect mechanisms, involving biochemical reactions (nitrosative and oxidative stress, predominantly resulting in s-nitrosation) and via second messenger signalling (NO/sGC/cGMP). The contribution of sGC-mediated signalling mechanisms to NO-mediated modulation of spinal locomotor networks was tested.

The widely utilised membrane permeable partial PKG agonist, 8BrcGMP, was used to investigate the contribution of NO/sGC/cGMP mediated signalling towards changes in locomotor output that occur as a result of addition or removal of NO. Application of 200μM 8BrcGMP caused a significant decrease in the frequency of locomotor-related activity ($P<0.05$, -10±5%; n=6; Fig. 3.8E). A significant decrease in locomotor burst amplitude was observed during application of 8BrcGMP ($P<0.05$, -9±3%; n=6; Fig. 3.8F). These results suggest the NO-dependent activation of sGC contributes to the modulation of both CPG and motor neuron output in the lumbar locomotor system.

The soluble guanylate cyclase (sGC) inhibitor, ODQ, was used to investigate further the sGC-mediated effects of NO. Application of 200μM ODQ caused a transient increase followed by a significant decrease in frequency and a significant decrease in amplitude of burst output ($P<0.05$; -8±4% and -11±4%, respectively; n=6; Fig. 3.8E and F). During washout the frequency of burst output remained significantly reduced. Burst amplitude remained reduced over the course of ODQ application and during washout. ODQ is an inhibitor of sGC, reducing the sGC haem site. Inhibition of sGC using 200μM ODQ caused an unrecoverable inhibition of frequency and amplitude; therefore, in an attempt to inhibit sGC without an immediate and immeasurable reduction in output, a low concentration of ODQ was used to inhibit sGC with the subsequent

addition of DEA NO to ascertain the sGC-dependent effect of NO. A lower concentration of 50μM ODQ was applied for 15 minutes before co-application of 50μM DEA NO to ascertain whether inhibition of sGC can ablate the effects of DEA NO (Fig. 3.8A and B). ODQ caused a significant decrease in frequency ($P<0.05$, -6±2%; Fig.3.8C). During washout of both ODQ and DEA NO, the burst frequency increased significantly compared to control ($P<0.05$, +5±2 %). Greater variability in amplitude was noted in ODQ when compared to control, but at this lower concentration ODQ did not significantly change burst amplitude.

The DEA NO effect on frequency but not on burst amplitude in the presence of ODQ suggests that the NO/sGC/cGMP pathway predominantly mediates the effects of NO on the intensity of locomotor-related motor neuron output. The DEA NO effect on frequency in the presence of ODQ suggests that a component of NO modulation of locomotor activity is mediated by a non NO/sGC/cGMP pathway, possibly s-nitrosation.

3.4 Discussion

3.4.1 Nitric oxide modulates spinal neurons during rhythmic locomotor-related activity

Prior to the present study, the role of NO in the mammalian hind limb locomotor network had not been investigated, though previous studies have shown a modulatory role for NO in the locomotor network of non-mammalian vertebrates such as the lamprey and the *Xenopus* tadpole. The results presented in this chapter demonstrate that NO modulates locomotor output generated by the mammalian spinal locomotor network.

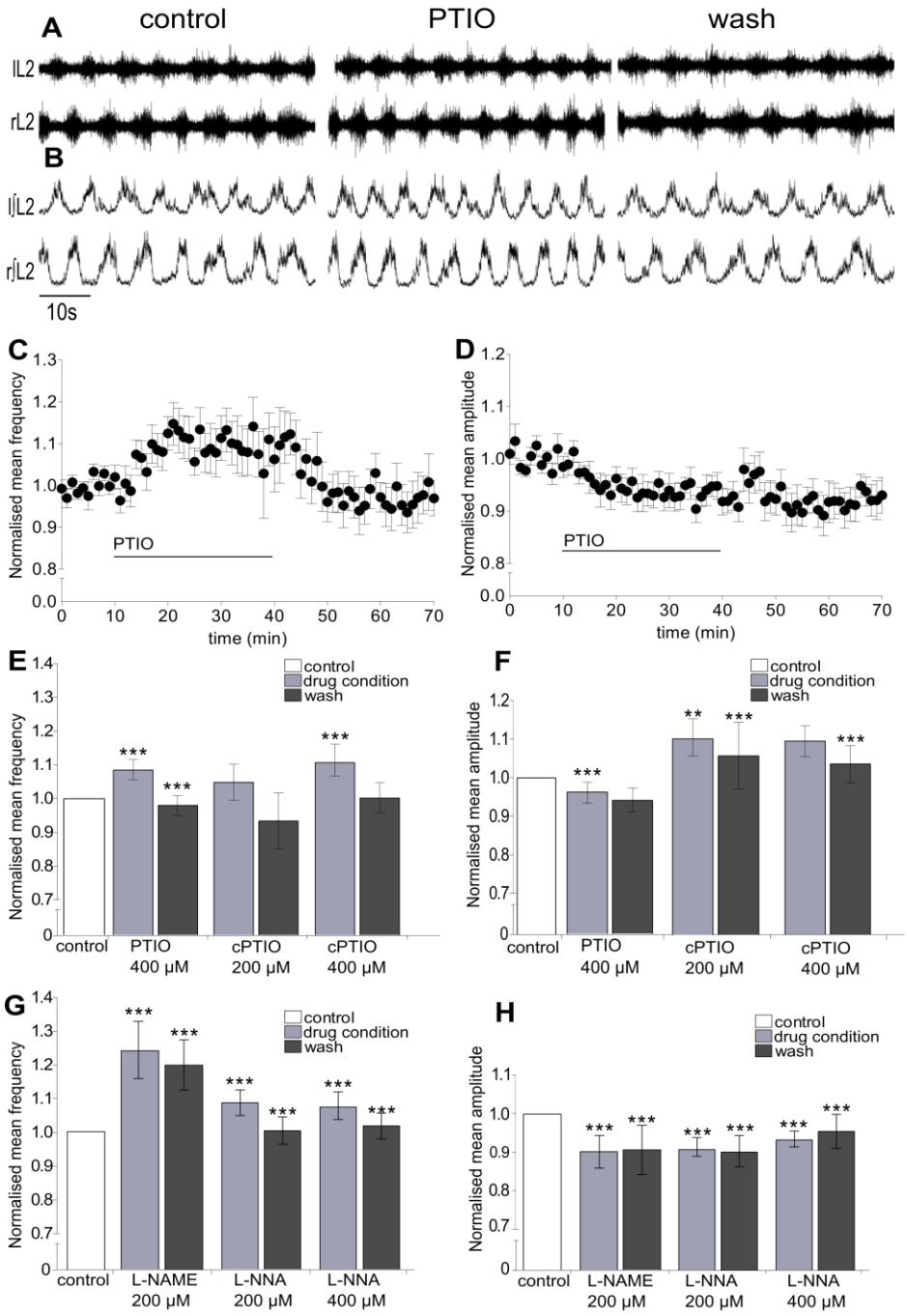

Figure 3.7. Endogenous sources of NO modulate locomotor activity. Raw **A** and rectified/integrated **B** locomotor bursts induced by 5µM NMDA and 10µM 5HT recorded from the left and right ventral roots (L2 segment) before (control), during (PTIO) and after (wash) the application of the membrane permeable NO scavenger PTIO. Time course plots (data averaged in 1 minute bins) showing the effects PTIO (400µM, n=8) on the **C** frequency and **D** amplitude of locomotor bursts relative to control. **E** removal of NO by scavengers PTIO and cPTIO significantly increased the frequency of locomotor output (400µM, n=8; 200µM, n=10; and 400µM, n=8 respectively. 10min, $P<0.05$). **F** cPTIO significantly increased burst amplitude (400µM, n=8; 200µM, n=10) while the membrane permeable scavenger PTIO significantly decreased burst amplitude (400µM, n=8; 10min, $P<0.05$). **G** The NOS inhibitors L-NAME and L-NNA, significantly increased the frequency of locomotor output (200µM, n=6, 10min, $P<0.05$; 200µM, n=6 and 400µM, n=10, respectively) **H** The NOS inhibitors L-NAME and L-NNA significantly reduced locomotor burst amplitude ($P<0.05$; 10min, 200µM, n=6, 200µM, n=6; and 400µM, n=10, respectively). Bar in **A** and **B**, indicates duration of application, asterisk denotes significance relative to control and error bars are SEM.

In both the lamprey and tadpole, NO affects the output of locomotor networks primarily by modulating synaptic transmission. However, the effects on synaptic transmission and the overall effects on locomotor output are different in the two species. In the tadpole, NO facilitates glycinergic transmission, via effects on another modulator NA, to reduce swim episode duration (McLean and Sillar, 2004). In addition to this, NO decreases motor neuron membrane conductance, enhancing the inhibitory effect of GABA release, and thus increasing cycle period (McLean and Sillar, 2002). In the lamprey, in contrast to the potentiation and facilitation of inhibition seen in the tadpole, NO increases the frequency of locomotor activity by facilitating post-synaptic on-cycle excitation and reducing mid-cycle inhibition by a presynaptic mechanism (Kyriakatos et al., 2009).

In the present study, NO-mediated modulation of hind limb fictive locomotion is described. Fictive locomotion was induced using 5HT and NMDA, raising the general level of excitation in neuronal circuits, leading to the development and maintenance of rhythmic alternating output (Jiang et al., 1999, Miles et al., 2007). The NO donor, DEA NO, was used to increase the level of NO in the locomotor circuitry during pharmacologically induced fictive locomotion. DEA NO was utilised at concentrations in the micromolar range because although research has shown that *in vivo* levels of NO are in the nanomolar range, to achieve similar levels of NO *in vitro*, concentrations of NO in the micromolar range are needed (Boulton et al., 1995, Thomas et al., 2008). This is due to the reduction in NO concentration at any point in the solution due to diffusion and the natural scavenging properties of the cellular environment; that is, scavenging by endogenous antioxidants, haemoglobin and superoxide (Thomas et al., 2001, Thomas et al., 2008, Kuzkaya et al., 2005).

DEA NO, and thus NO, caused a significant decrease in the frequency of rhythmic locomotor output produced by the locomotor CPG across the range of concentrations used. To investigate the potential involvement of modulation of inhibitory transmission, as described in the tadpole and lamprey, strychnine and bicuculline were used to inhibit glycinergic and GABAergic transmission (Bracci et al., 1996).

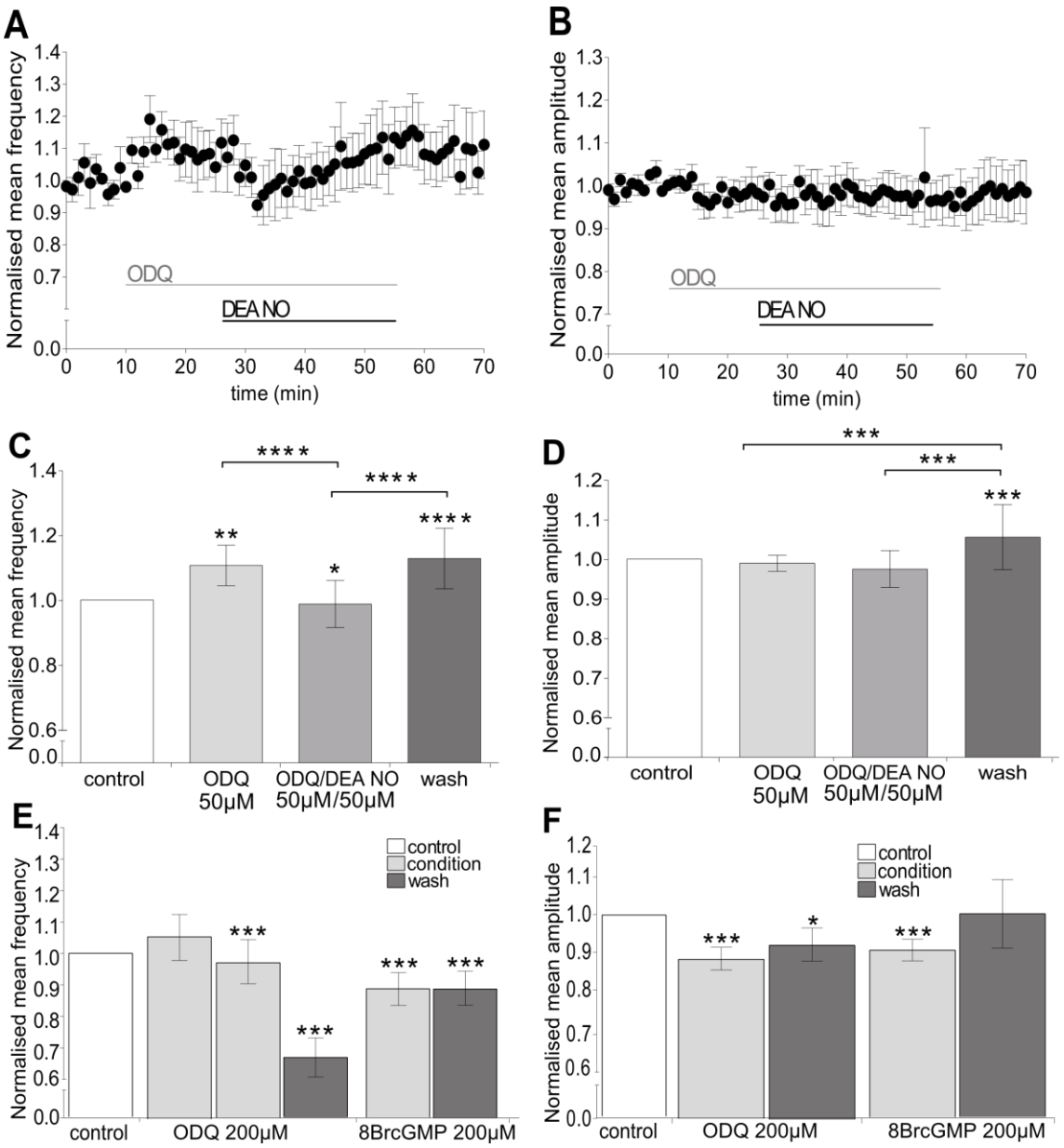

Figure 3.8. NO modulates fictive locomotor output by both cGMP-dependent and cGMP-independent pathways. Time course plots (data averaged in 1 minute bins) showing the effects of the sGC inhibitor ODQ (50μM) and the co-application of the NO donor DEA NO (50μM) in the presence of ODQ on locomotor burst **A** frequency and **B** amplitude. **C** ODQ significantly increased burst frequency while subsequent application of DEA NO, reversed this frequency-related effect. **D,** ODQ ablated the effects of DEA NO on burst amplitude. **E** ODQ significantly increased locomotor burst frequency (200μM; n=6, 10min $P<0.05$). Inhibition of sGC by ODQ led to a long-term unrecoverable reduction in output while the partial agonist of PKG, a downstream signaling pathway of sGC, 8BrcGMP significantly decreased burst frequency ($P<0.05$; 200μM; n=6, 10min). **F** Both ODQ and 8BrcGMP significantly decreased locomotor burst amplitude. Bar in **A** and **B**, indicates duration of application, asterisk denotes significance relative to control and error bars are SEM.

Although the motor circuitry generates disinhibited burst activity as result of pharmacological block, it is not known whether the same network and population of neurons are involved in generating fictive locomotion as in the standard *in vitro* preparation. In the absence of inhibition, the DEA NO-mediated decrease in frequency at the lowest concentration used in this study indicates that the effects of NO on frequency reflect a change in the properties of excitatory interneurons or synaptic transmission between excitatory interneurons within the central pattern-generating network. Modulation of excitatory components of the locomotor CPG by NO is consistent with findings in the lamprey locomotor network where NO facilitates on-cycle excitation (Kyriakatos et al., 2009). In addition, in the mammalian respiratory system, NO enhances excitatory transmission during the transition to the inspiratory phase controlled by neurons in the brainstem (Pierrefiche et al., 2007) and in concert with phenylephrine, enhances long-term facilitation of XII motor neuron output (Saywell et al., 2010). Precedents for NO-mediated modulation of excitation have also been provided by studies in other regions of the mammalian CNS, including the trigeminal motor nucleus (Pose et al., 2011) and the Calyx of Held (Steinert et al., 2008), where NO specifically modulates glutamatergic neurons. At the higher concentration of donor used in these experiments, a reduction in frequency analogous to that seen in the presence of inhibition suggests that either these effects are mediated primarily by inhibitory mechanisms or more likely by an alternative pathway such as s-nitrosation, as NO is known to act as a thiol modifying agent at high concentrations (Thomas et al., 2008).

The present study suggests that NO effects in the mouse occur predominantly via modulation of excitatory transmission as opposed to the tadpole where NO modulates inhibitory transmission. Interestingly, scavenging or blocking the production of NO in both systems increases locomotor burst frequency (McLean and Sillar, 2000). However, this is unsurprising given that an increase in burst frequency can occur by either a decrease in inhibition or an increase in excitatory transmission.

In the absence of inhibition, the DEA NO-mediated decrease in frequency was reversed to near control levels during washout. In contrast, in experiments conducted in the

presence of inhibition, locomotor frequency increased above control levels following the washout of DEA NO. This difference, after the removal of DEA NO in the present study, suggests that NO could also modulate an inhibitory component of the locomotor network which may have longer-term effects on network output. NO has previously been shown to mediate long-term changes in the output of motor systems. In rodent hypoglassal (XII) motor neurons, NO enhances phenylephrine induced long-term facilitation of XII nerve activity (Saywell et al., 2010). In the lamprey, mGluR1 activation leads to long-term increases in locomotor output frequency. This long-term potentiation involves endocannabinoid and NO signalling (Kyriakatos and El Manira, 2007). The present study may have uncovered a similar long-term effect of NO in the mammalian locomotor CPG, though additional evidence will need to be gathered to prove this definitively. A modification to the protocols detailed in this chapter, to specifically address the long-term effects of NO, is needed.

Fictive locomotion induced by addition of 5HT and NMDA to the circulating aCSF raises the level of excitation in an indiscriminate manner in all areas of the spinal cord. As a result of this, there is the possibility that NO applied in the same manner could affect non-locomotor-related activity. In light of this, the recordings made from ventral roots were scrutinised for evidence of non-locomotor-related changes in activity as a result of NO. Neuronal activity during the inter-burst interval was used to help assess the level of general activity, or biological noise, produced from the spinal neural network. The inter-burst amplitude, measured before and during application of all the NO-related pharmacological agents tested, was not significantly altered, suggesting that the modulatory effects of NO are directly related to locomotor activity.

DEA NO, and therefore NO, caused a significant increase in the amplitude of locomotor-related output from motor neurons at all concentrations used. However, at high concentrations, a mixed response was observed with just over half of the total number of experiments showing an overall decrease in amplitude, a little under half showing an increase in amplitude, and a small number of preparations exhibiting a transient increase followed by a significant decrease in burst amplitude. The concentration-dependent effects of NO on locomotor burst amplitude suggest that, at the

level of motor neurons, NO-mediated signalling may be complicated by the existence of multiple signalling pathways with opposing actions or that tonically active signalling pathways might be desensitised in the presence of high concentrations of NO. NO-mediated signalling might involve a balance between excitatory transmission and desensitisation or auto inhibition. For instance, initial activation of sGC with subsequent production of cGMP and initiation of PKG signalling may lead to increases in motor neuron output followed by desensitisation of the sGC haem causing cessation in cGMP production and reduction in PKG activity resulting in a reduction in motor neuron output (Fernhoff et al., 2009, Halvey et al., 2009). In addition, a cGMP-independent mechanism, such as s-nitrosation, might account for the broadly inhibitory action of NO at high concentrations. High levels of NO could result in the s-nitrosation of sGC, inhibiting cGMP production (Sayed et al., 2007) or potentially the s-nitrosation of NMDA receptors or other ion channels involved in excitatory transmission. Alternatively, the mixed, or biphasic, effect of NO on motor neuron output could reflect excessive excitation at the higher concentrations used, leading to a depolarising block or axonal conduction-block. Previous studies have shown that NO facilitates axonal conduction block (Redford et al., 1997, Smith et al., 2001) which has not been shown in the rodent locomotor preparation and would ideally be investigated in future studies of NO modulation of locomotion.

Scavengers of NO and blockers of NOS were used to investigate the role of endogenous NO production in the modulation of the spinal locomotor CPG. Experiments utilising the membrane soluble and, therefore, both extra- and intracellular scavenger of NO, PTIO, or NOS inhibitors, revealed an increase in locomotor burst frequency when endogenous NO was reduced or removed. An increase in locomotor burst frequency was also replicated using the less lipophilic and thus, less membrane permeable scavenger, cPTIO. However, it should be noted that cPTIO is involved in generating peroxynitrite radicals and other reactive nitrogen species, which may have effects on a wide range of cellular targets (Thomas et al., 2008). The production and effects of peroxynitrite may account for the increase in variability of output frequency during cPTIO application. The variable cPTIO results may be due to a mixture of NO and NO radical reactions as opposed to changes as a result of NO alone. Nevertheless, data using

a range of NO scavengers and NOS inhibitors demonstrate that endogenous NO, from sources within the mammalian spinal cord, acts to regulate the frequency of the output from the locomotor CPG.

Removal of NO by the membrane impermeable scavenger, cPTIO, potentiated motor neuron output as evidenced by an increase in the amplitude of locomotor bursts, whereas the membrane permeable scavenger, PTIO, decreased motor neuron output. The reason for this discrepancy is not clear, though it may be due to the relative membrane permeability of the two compounds or the propensity of cPTIO to generate peroxynitrite radicals. Non-specific NOS inhibitors reduced the amplitude of locomotor bursts consistent with the increase in amplitude during application of low levels of exogenous NO. The differences in effect on locomotor output by NO scavengers and NOS inhibitors might reflect the biochemical interaction of NO produced endogenously. Scavenging of NO and the breakdown and metabolism of NO involve the production of NO metabolites: peroxynitrite, nitrate and nitrite molecules, which are themselves biologically active and can also regenerate NO (Giovannoni, 1998, Lundberg et al., 2008). It is plausible that increased production of nitrates and subsequent formation of NO may cause the increase in amplitude of locomotor bursts observed in the presence of NO scavengers, whilst inhibition of the synthetic enzyme completely prevents NO or NO metabolite signalling-induced effects leading to a decrease in the intensity of locomotor output.

Support for peroxynitrite-mediated signalling as the cause of increased locomotor burst amplitude comes from the respiratory system. In inspiratory neurons of the ventral respiratory column, NO-mediated increases in excitation occur by both cGMP-dependent and independent mechanisms and exogenous application of uric acid, an endogenous antioxidant which neutralises peroxynitrite, indicates that the cGMP-independent increases observed are a result of peroxynitrite (Pierrefiche et al., 2007).

These results show that in the mammalian locomotor network, both exogenous and endogenous sources of NO modulate locomotor network activity. Effects on locomotor

burst frequency involve NO-modulation of excitatory interneurons whilst the effects on amplitude appear to be more complex.

3.4.2 Cyclic nucleotide dependent effects of nitric oxide on the locomotor network

NO is known to exert its effects primarily via sGC, catalysing the production of cGMP which then initiates the PKG pathway. NO can also modulate cellular properties by s-nitrosation, a reaction involving the production of reactive nitrogen species that modify thiol functional groups on proteins by addition of –NO (Thomas et al., 2008). As the main regulatory pathway for NO is via sGC, the present study assessed involvement of this pathway in NO-mediated changes in locomotor output.

The PKG partial agonist 8BrcGMP was first used to assess involvement of the cGMP-dependent signalling pathway in NO-mediated effects on the mammalian locomotor CPG. 8BrcGMP significantly affected both the frequency and amplitude of locomotor burst output. These data suggest that cGMP-dependent signalling is involved in the effects of NO on both locomotor burst amplitude and frequency. Further work is needed to ascertain whether or not the 8BrcGMP effect on amplitude observed in these experiments is concentration dependent compared to that of DEA NO.

To investigate further the likely contribution of the NO/sGC/cGMP/PKG pathway to motor network function, the pathway was inhibited using ODQ, an inhibitor of sGC (Zhao et al., 2000). ODQ reduces the ferrous binding site of sGC. On binding to the haem, sGC still exhibits a basal level of activity, although stimulation of cGMP production by addition of exogenous NO is ablated (Zhao et al., 2000). Locomotor burst frequency increased significantly during high concentration ODQ application (200μM) before declining to below control levels; burst frequency did not recover during washout. Burst amplitude significantly decreased in the presence of high concentrations of ODQ, an effect that again could not be reversed by washout of the inhibitor. Although these data suggest involvement of activation of the sGC signalling pathways

by endogenous NO, the non-reversible, inhibitory effects of high concentrations of ODQ on both locomotor burst amplitude and frequency suggest that the block of sGC has a profound and detrimental effect on the ability of the network to function.

To mitigate the detrimental effects of high concentrations of the sGC inhibitor and to investigate further the link between NO-mediated modulation of the locomotor network and the sGC pathway, a lower concentration (50μM) of ODQ was applied in combination with DEA NO. Burst frequency again increased during low concentration ODQ application and this increase was reversed by application of DEA NO. The initial increase in frequency as a result of sGC block indicates that a basal sGC activity is involved in maintaining locomotor frequency; whether this is due to endogenous NO production or some other mechanism is not clear. The subsequent reduction in frequency on addition of DEA NO suggests that NO modulates the frequency of locomotor output by cGMP-independent mechanisms or by further stimulation of sGC, though these mechanisms, again, have not been shown in the present study. In the respiratory system, NO modulates inspiratory drive by a cGMP-dependent mechanism and by a cGMP-independent mechanism, possibly peroxynitrite formation (Pierrefiche et al., 2007). To clarify this mechanism, additional experiments would need to be performed; for instance, extending the current protocol to include washout of DEA NO but not ODQ to determine whether burst frequency increases, or using antioxidant application to neutralise peroxynitrite.

The ODQ-mediated block of sGC prevented all DEA NO-mediated effects on locomotor burst amplitude, indicating the involvement of the NO/sGC/cGMP pathway in modulation of motor neuron output. It is not clear why ODQ at lower concentration does not alter locomotor burst amplitude; perhaps this is a result of the complex concentration-dependent relationship between NO production and locomotor output. Despite this, these results confirm for the first time that the NO stimulation of sGC and the subsequent activation of the PKG pathway by cGMP directly modulates motor neuron output.

It is also possible that NO inactivates nNOS via a Fe^{2+}-NO intermediate. NO is produced in pulses according to the turnover rate of the reaction to convert L-arginine to NO and L-citrulline (one pulse/140ms) and at high concentrations of NO (during high turnover), the inhibiting Fe^{2+}-NO intermediate stabilises and inactivates the enzyme (Salerno and Ghosh, 2009, Fernhoff et al., 2009). This turnover-dependent inhibition of nNOS (auto-inhibition) can be compared to the high levels of NO used in the present study, taking into consideration that exogenous increases in the concentration of NO will add to the endogenous tone that exists during locomotor activity. This mechanism could explain the changes in locomotor burst frequency and concentration-dependent changes in amplitude observed on addition of DEA NO.

Evidence for a NO-mediated positive feedback mechanism for the control of locomotor frequency has been put forward in the lamprey spinal cord where NO is produced in an activity-dependent manner and facilitates excitation via a presynaptic mechanism (Kyriakatos and El Manira, 2007). Data from the present study might support a negative feedback role for NO in the mammalian locomotor network. It is possible that by retrograde signalling NO could cause the amplification of presynaptic cGMP modulating neurotransmitter release. cGMP-independent inhibition by s-nitrosation of sGC, NMDA receptors or VDCC channels and auto-inhibition of nNOS might also effect a self-regulating negative feedback loop.

3.5 Conclusion

Future investigation into the effects of NO described here must be taken forward in the context of neuromodulation of the network. NO is known to exert its effects by directly activating secondary messenger pathways (sGC/cGMP/PKG; (Denninger and Marletta, 1999, Garthwaite, 2010), modifying protein residues (s-nitrosation) (Choi et al., 2000), and metamodulating the actions of other neurotransmitters such as glycine and GABA (McLean and Sillar, 2002, McLean and Sillar, 2004, Wexler et al., 1998). Subsequent studies in the locomotor preparation must take into account the nature of neuromodulatory interactions to assign definitively a role for NO in the locomotor CPG,

as it is not known whether NO is involved in meta-modulation in the mammalian locomotor network.

The divergent activity-dependent effects of NO in the present study may be a result of state-dependent modulation, and theoretically, a mechanism for state-dependent modulation *in vivo*. The endogenous availability of NO in combination with other neurotransmitters could be the cause of or exacerbate differing effects on the modulation of rhythmic output. For instance, NO enhances the postsynaptic effects of 5HT release at the synapse between *Lymnaea* cerebellar giant cells (CGC) and B4 motor neurons involved in feeding (Straub et al., 2007). In addition, in a behavioural study, NO inhibits the food intake stimulated by $5HT1_A$ agonists injected into the rat midbrain raphe (Currie et al., 2011). In spinal motor neurons, $5HT1_A$ receptors have a postulated role in inhibitory modulation at the motor neuron initial segment while $5HT_2$ and $5HT_7$ are involved in initiating locomotion (Heckman et al., 2009). Also in the rat spinal cord, low concentrations of 5HT facilitate locomotion in the presence of the mGluR1 agonist DHPG, while at high concentrations of 5HT, DHPG disrupts locomotor output (Taccola et al., 2003). The complexity increases with the evidence that endocannabinoids and NO facilitate long-term depression in the lamprey spinal cord via mGluR activation (Kyriakatos and El Manira, 2007). Therefore, a potential modulatory relationship between NO and 5HT is theoretically possible, given that NO interacts with 5HT at invertebrate motor synapses and neuromodulation by metabotropic mechanisms involving pathways modulated by 5HT and NO occurs in both mammalian and non-mammalian vertebrates.

The experiments reported by McLean and colleagues rely on the manipulation of fictive locomotion induced by electrical stimulation, whereas Kyriakatos and colleagues induced fictive locomotion with NMDA alone in their studies in the lamprey. Both NMDA and 5HT are used in the present study to induce locomotion before assessing the role of NO on the resulting locomotor output. If NO-mediated effects depend on the state, level or nature of excitation that initiates and maintains locomotion then modulation in these three systems must be calibrated to accommodate for the state-dependent differences resulting from different methods of inducing locomotor output.

In the isolated mouse spinal cord preparation, stimulation of the cauda equina and subsequent generation of locomotion would provide an endogenous-activity model for the study of endogenous NO effects. Likewise, fictive locomotion induced by 5HT or by NMDA alone would enable better comparison with the findings in the lamprey and reveal neurotransmitter specific interactions which have not been reported in the context of NO and spinal locomotor CPG activity.

If a state- or frequency-dependent interaction or action of NO exists in the lumbar spinal cord network, it could be revealed by further experiments manipulating the starting frequency; for example, by altering the concentrations of the neurotransmitters used to induce fictive locomotion.

The data in this chapter show that NO from both exogenous and endogenous sources modulates mammalian spinal locomotor output. Exogenous NO inhibits locomotor burst frequency and this was corroborated by evidence that endogenous NO, as revealed by both inhibitors and scavengers, increased locomotor output consistent with NO having an inhibitory modulatory role modulating excitatory transmission. NO appears to modulate locomotor burst output by mechanisms both dependent and independent of the classical NO/sGC/cGMP pathway.

Exogenous NO modulates locomotor burst amplitude in a concentration-dependent manner, potentiating burst amplitude at low concentrations and predominantly reducing burst amplitude at high concentrations. However, clarification of this concentration-dependent relationship by scavengers of endogenous NO was less clear, complicated by possible side reactions to produce reactive NO derivatives. Care should be taken in future to account for or avoid possible side reactions when designing experiments of this kind. Inhibition of NOS suggests that NO modulates excitatory transmission in the spinal locomotor network. NO appears to modulate locomotor burst amplitude by a cGMP-dependent mechanism, though further work is required to clarify the results detailed here.

Chapter 4: Nitric oxide-mediated modulation of the intrinsic properties of spinal neurons

4.1 Introduction

4.1.1 Background

The spinal cord is populated by a cornucopia of neurons, the full cellular and behavioural function of which is not yet fully known. Motor neurons, identifiable by their size, transmitter phenotype, and firing properties, have been studied in detail and the resulting knowledge of how motor neurons function and integrate central commands has led to a greater understanding of other neurons and circuits in the CNS. Motor neurons are known generally as the effectors of muscle contraction and more definitively as single neurons characterised by transcription factor expression (hind limb motor neurons, Lim3, Isl1 and Hb9) and cellular architecture (ion channels, signalling pathways) ((Section 1.1.2; (Jessell, 2000, Brownstone, 2006)). Motor neuron activity is critical for normal behavioural function and consequently, has been the subject of intense research for over a century, with motor neurons representing the first mammalian neurons in the CNS in which intracellular recordings were performed (Brock et al., 1952).

4.1.2 Properties of motor neurons

Motor neurons innervating the hind limb muscles are located in the ventrolateral column from lower thoracic to sacral spinal cord. Motor neurons innervating the axial and hind limb muscles are located, respectively, in the medial and lateral motor pools (lamina IX) of the ventral horn of the lumbar spinal cord. Motor neurons have large somas and extensive dendritic branches that integrate synaptic inputs and influence the excitability of the soma. However, research into the properties of motor neurons usually involves recordings from the soma using microelectrodes. This technique has revealed

and continues to reveal most of what we know about the properties of neurons, how they behave and how their activity is influenced by other synaptic inputs.

The intrinsic excitability of motor neurons is determined by the expression of ion channels at the cell membrane. Researchers have meticulously defined the stereotypical ion channel characteristics that determine motor neuron firing properties. At rest, the membrane potential is the result of inwardly rectifying (K_{ir}) and leak K^+ channels (outward), and external chloride levels. Synaptic input of large enough magnitude initiates the activation of K^+ and Na^+ channels (I_{Na}, I_{KNa}) and VDCC, the result of this activation of cation conductances is that an action potential (AP) is fired. Spike frequency adaptation (SFA) during repetitive firing is a hallmark characteristic of motor neurons, mediated by the slow-inactivation of Na^+ channels. After an action potential has been fired, the membrane repolarizes, which involves inactivation of depolarizing currents and activation of I_{KCa} and transient K+ conductance through I_A channels. A refractory period follows, during which no further action potentials can be generated. During this action potential AHP, the hyperpolarization activated Na^+/K^+ conductance (I_h) generates the post-inhibitory rebound (PIR) that can result in rebound firing of action potentials (Brownstone, 2006, Heckman et al., 2009, Miles et al., 2005, Rekling et al., 2000).

Motor neurons release the neurotransmitter acetylcholine (ACh) and as such can be identified by the presence of the enzymes that synthesize ACh, Choline acetyltransferase (ChAT), and degrades ACh, acetyl cholinesterase (AChE) (Ferguson and Blakely, 2004). Motor neurons receive extrinsic modulation (from outside the spinal motor networks) in the form of neurotransmitter release and subsequent signalling which alters their intrinsic properties. These include 5HT and NA from supraspinal fibres as well as a large number of other both excitatory and inhibitory neurotransmitters, i.e. adenosine, Substance P and Thyrotropin (Section 1.1.3).

The excitability of motor neurons determines the timing and intensity of action potential firing and subsequent contraction of muscles, such that an increase in excitability renders a neuron more likely to fire as a result of a given excitatory input. The

excitability of motor neurons, as a result of intrinsic properties or extrinsic modulation, heavily influences research into understanding motor neuron function and pathophysiology; for instance in ALS, where one of the current hypotheses to explain disease pathogenesis involves aberrant excitatory input to motor neurons leading to excitotoxicity and cell death (Boillee et al., 2006).

NO has been identified as a putative neurotransmitter in the mammalian locomotor circuit, having already been identified as a facilitator of inhibitory transmission in the *Xenopus* spinal locomotor network and an excitatory neuromodulator in the spinal cord of the lamprey (McLean and Sillar, 2004, Kyriakatos et al., 2009, McLean and Sillar, 2002, Kyriakatos and El Manira, 2007). The role of NO in mammalian motor control is not fully understood, providing the impetus for the present study.

4.1.3 Nitric oxide transmission

NO gas is produced on catalysis of L-arginine to L-citrulline and NO by NOS. There are three isoforms of the enzyme: neuronal (nNOS or NOS-1); endothelial (eNOS or NOS-3); and inducible (iNOS or NOS-2). The n/eNOS isoforms are constitutively expressed and require calcium for normal function whilst iNOS is produced on immune stimulation and is calcium independent. NOS is a NADPH diaphorase enzyme requiring calcium and several other cofactors for activity: **(**CaM (nNOS/eNOS only), FAD, FMN, haem, NADPH and BH_4. The enzyme is associated at the cell membrane with the NMDA receptor subunit NR2B linked by PSD95 and a PDZ domain (Brenman et al., 1996). NO acts via two main pathways, predominantly through secondary messenger cascades, such as protein kinase G (PKG), and direct modification of proteins by s-nitrosation (Section 1.2.2.1 to 1.2.2.4).

In Chapter 2, NADPH diaphorase reactive neurons were shown to be distributed in discrete populations in the mouse lumbar spinal cord. NADPH diaphorase reactive neurons were identified in the dorsal horn (laminae I-VI), the intermediolateral layer of lamina VII, dispersed throughout lamina VII, around the central canal (lamina X) and

very rarely in laminae VIII and IX. Over the developmental period P1-12, these neurons increased in number in all laminae, except laminae VIII and IX where intermittent staining was noted. Though NADPH diaphorase reactivity was largely absent from the motor pools, some light staining, not quantified in the present study. The spatial distribution of NO producing neurons in the ventral horn indicates that neurons potentially involved in or in close proximity to the locomotor circuitry produce or are influenced by the production of NO. Indeed, NO is free to diffuse from the site of production, unrestricted by lipid membranes, and is known to act as both an autocrine and paracrine agent.

As a reactive, radical gas, NO is involved in a range of physiological processes including long term potentiation (LTP) in the hippocampus (Yanagihara and Kondo, 1996), long term depression (LTD) in the cerebellum, modulation of inhibitory transmission in the hypothalamic paraventricular nucleus (Li et al., 2004), modulation of ion channel properties in the mammalian auditory complex (Steinert et al., 2011, Steinert et al., 2008), and excitability of cholinergic basal forebrain neurons (Kang et al., 2007, Toyoda et al., 2008). Evidence from invertebrates and non-mammalian vertebrates has shown that NO is involved in the regulation of locomotor output. However, until the present study, the role of NO in mammalian hind limb locomotor activity and its influences on neurons within mammalian motor networks has not been determined.

4.1.4 Nitric oxide in locomotor activity

In studies of locomotor activity, NO is known to reduce swim episode duration and increase cycle period in *Xenopus* tadpoles (McLean and Sillar, 2000, McLean and Sillar, 2002)and in combination with endocannabinoid signalling, induce long-term potentiation of locomotor burst frequency in the adult lamprey *Lampetra* (Kyriakatos and El Manira, 2007). In the present study, NO has been shown to modulate mouse locomotor output by reducing locomotor burst frequency and either increasing or reducing locomotor burst amplitude in a concentration-dependent manner (Chapter 3).

The actions of NO have been studied in a number of model organisms at the level of the limb motor neurons. The reported effects on cellular properties in invertebrates suggest that NO is involved in excitatory transmission at the level of the locomotor network. In the sea angel *Clione limacina*, NO depolarises and activates both motor neurons and interneurons (Moroz et al., 2000). NO depolarises the membrane potential and increases firing rates of buccal ganglion B5 neurons leading to a depolarising block in *Helisoma trivolvis* (Artinian et al., 2010).

In non-mammalian vertebrates, NO decreases membrane conductance and increases the amplitude of glycinergic mid-cycle and GABAergic terminating inhibitory postsynaptic potentials (IPSP) in the tadpole (McLean and Sillar, 2002). While in lamprey motor neurons, NO reduces the frequency but not the amplitude of mid-cycle miniature inhibitory postsynaptic currents (mIPSC) and increases the frequency and amplitude of the on-cycle miniature excitatory postsynaptic currents (mEPSC). This results in an increase in the frequency of locomotor output (Kyriakatos et al., 2009). NO modulates the synaptic activity of mammalian neurons. For example, in the rat auditory complex NO reduces the amplitude of AMPA and NMDA EPSCs in the Calyx of Held (Steinert et al., 2008) . While in the rat hypoglossal nuclei, motor neurons involved in the control of inspiration, the PKG agonist 8BrcGMP, also decreased the amplitude of AMPA mediated transmission **(Saywell et al., 2010).** Also in the hypoglossal nucleus, the use of the NOS inhibitor L-NAME has revealed NO-mediated facilitation of inhibitory inspiratory hypoglossal motor neuron activity (Montero et al., 2008). These studies suggest that NO in the mammalian CNS is involved in excitatory transmission. However, in terms of NO mediated transmission, it is highly likely that network and motor neuron pool specific roles will emerge as more research is conducted. For instance, in rat trigeminal motor neurons involved in control of oral motor tasks, NO decreased the frequency but not the amplitude of mEPSCs, suggesting that NO acts by a presynaptic mechanism only in these neurons (Pose et al., 2011). In mammals, specifically rodents, the role of NO has yet to be described at the level of the spinal motor neuron.

4.1.5 Scope and importance of this study

The modulation of spinal locomotor networks by NO has been demonstrated, previously in the tadpole and lamprey and in the mouse, in Chapter 3 of the present study. Despite the research characterising NO effects on synaptic transmission, little is known about the NO-mediated modulation of intrinsic motor neuron properties.

This chapter details the investigation of NO-mediated effects on the intrinsic properties of lumbar spinal motor neurons. The passive and active properties of motor neurons in lumbar spinal cord slices were recorded in response to the bath application of NO donor, DEA NO, and the membrane permeable scavenger of NO, PTIO. Identifying and clarifying a mechanism for the actions of NO observed on ventral root output during fictive locomotion will enhance our basic understanding of motor neuron physiology. Describing a mechanism for NO mediated effects in the context of the locomotor circuitry will also provide additional knowledge for consideration in dysfunctional and damaged circuits as a result of injury and illness.

The aim of the present study was therefore to investigate potential NO modulation of lumbar spinal neuron intrinsic properties.

4.2 Materials and Methods

4.2.1 Tissue collection and preparation

All experiments were performed in accordance with the United Kingdom Animals (Scientific Procedures) Act 1986.

C57BL6 wild-type mice (P1-9) were obtained from Charles River Laboratories (Scotland, UK). The mice were bred under conditions of a 12-h light/dark cycle in individual ventilated cages at a constant temperature of 22°C and 56% humidity and had free unrestricted access to food and water. All procedures were carried out at room

temperature (RT) (20-22°C). Following cervical dislocation, decapitation and evisceration, a segment of the spinal cord extending from the mid-thoracic to mid-sacral region was isolated in a sylgard-lined dissection chamber containing oxygenated (95% O_2/5% CO_2) dissecting solution on ice. The pia mater was removed and the nerve roots trimmed before the cord was mounted in an agar block and attached to a magnetic specimen plate using cyanoacrylate adhesive. The specimen plate was then moved to a buffer chamber containing oxygenated dissecting solution on ice. Transverse slices of lumbar spinal cord, 300μm thick, were cut from the immobilised block of spinal cord using a Leica VT1200 microtome with vibrating blade (Leica Biosystems, GmbH). Slices were transferred to oxygenated recovery solution and placed in a water bath set at 35°C for 30-40 minutes before transferral to oxygenated recording solution at room temperature. For composition of solutions, see Section 4.2.6.

4.2.2 Identification of neurons

Neurons were classified as either motor neurons (MN) or interneurons (IN) based on location and size. In a subset of experiments, the fluorescent retrograde marker, Fluoro Gold (Fig. 4.1A-D), was used to confirm validity of the criteria used to select presumed motor neurons (Miles et al., 2005, Miles et al., 2007).

Location

Presumed motor neurons were selected from the lateral and medial motor pools (lamina IX) in the ventral horn of the lumbar spinal cord. Neurons located outside the motor pools and within the ventral region of the ventral horn, at the level of or below the central canal, were termed interneurons (Fig.4.2B, Fig.4.6C and Fig.4.10A).

Size

Cells were further identified by whole cell capacitance (C_m) calculated by pClamp 10 software (Axon Instruments); cells were considered IN if the Cm values ranged from 17-49pF and MN if the Cm values ranged from 50-139pF.

Retrograde labelling of motor neurons

In a small subset of animals (n=2), the neuronal tracer Fluoro Gold was used as a retrograde marker for presumed motor neurons (herein the terms motor neuron, MN, and presumed motor neuron, pMN, are used interchangeably). As previously described, one to two days before experimentation intraperitoneal *(*i.p.) injections of FluoroGold (0.04 mg/g; Fluorochrome Inc., Denver, CO) were administered to mice in order to retrograde label MNs (Miles et al., 2007). Spinal cord slices were prepared as described (Section 4.2.1). FluoroGold-positive MNs were visualized with epifluorescence and infrared differential interference contrast (DIC) microscopy (Fig. 4.1A-D).

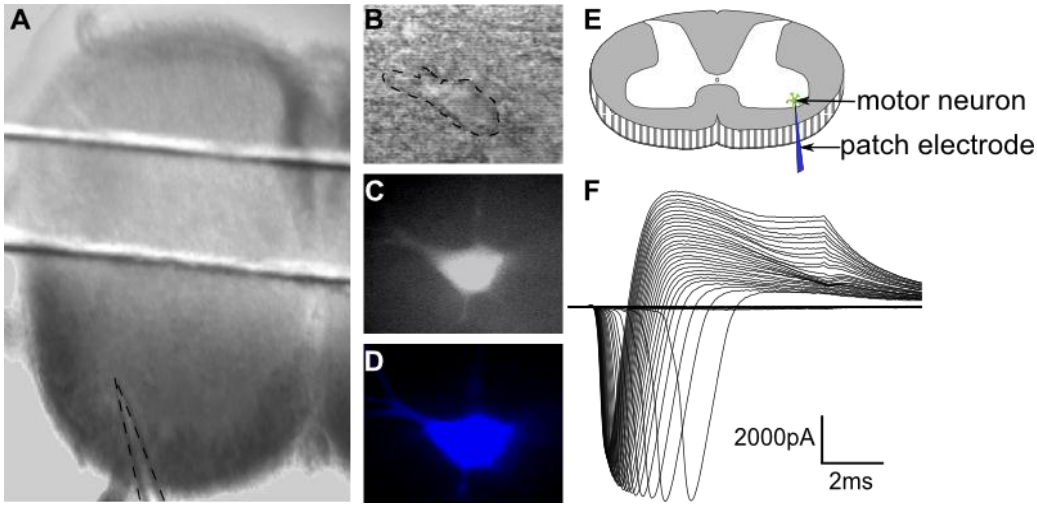

Figure 4.1. Intracellular recordings were made from identified lumbar spinal motor neurons. **A** Recordings from motor neurons were made in 300µm slices of lumbar spinal cord (glass electrode indicated by dotted lines). **B** DIC image of motor neuron (dotted line indicates perimeter). **C** I.p. injection of retrograde neuronal tracer Fluorogold was used to confirm motor neurons location. **D** Fluorescent dye, Alexa 594 was added to the intracellular electrode solution to visualise neuron after successful recording**. E** Illustration of the lumbar spinal cord slice with approximate location of motor neuron and patch electrode. Image adapted from the original (Courtesy Dr Gareth Miles). **F** Sodium channels were activated using brief depolarizing voltage steps to confirm intracellular configuration and cell viability.

4.2.3 Data collection

Patch-clamp signals were amplified and filtered (4-kHz low-pass Bessel filter) with a MultiClamp 700B amplifier (Molecular Devices) and acquired at ≥10 kHz using a Digidata 1440A A/D board and pClamp 10 software (Molecular Devices).
Whole cell patch-clamp recordings were analysed using Clampfit software (Molecular Devices) and series resistance (R_s), whole-cell capacitance (C_m), and input resistance (R_n) values were calculated by pClamp 10 software.

4.2.4 Whole-cell patch-clamp recording protocols and data analyses

Experiments were performed on lumbar spinal cord slices obtained from neonatal mice aged P1-9. Experiments were performed in a recording chamber that was perfused at room temperature with oxygenated recording solution. Patch electrodes (3-4MΩ) were pulled on a horizontal puller (Sutter Instrument, Novato, CA) from borosilicate glass (World Precision Instruments, Sarasota, FL).

Whole-cell patch-clamp recordings were made from neurons located throughout the ventral horn of the spinal cord (see Fig. 4.2B, Fig. 4.6C and Fig. 4. 10A). Neurons were visualized under infrared differential interference contrast (DIC) and fluorescent microscopy in experiments where the fluorescent compound, Alexa Fluor 594, was added to the intracellular electrode solution.

As sodium currents drive action potential firing, Na^+ current activation protocols were run in voltage-clamp mode to confirm whole-cell configuration and cell viability. Na+ currents were activated using a series of voltage steps (-70 to +20 mV, 2.5-mV increments, and 10-ms duration) from a holding potential of -60 mV in voltage-clamp mode (Fig. 4.1F).

During current-clamp protocols, sub-threshold changes in the resting membrane potential were offset by direct current injection to maintain the resting membrane

potential at -60mV, except where resting membrane potential remained steady at rest (V_m = -63 to -58mV). Current-clamp protocols were run in control recording solution and in recording solution containing pharmacological agents that manipulate NO-mediated signalling. Protocols were run in the period immediately before addition of pharmacological agents to the perfusate (Control), and then repeated three to five minutes (unless otherwise noted) after addition of pharmacological agents to the perfusate (Drug condition). Where possible, current-clamp protocols were then repeated after the circulating solution had been gradually replaced by fresh recording solution (Wash).

Current-clamp protocols were performed to investigate the passive (rest, sub-threshold) and active (firing, supra-threshold) properties of neurons in Control, Drug condition, and Wash as previously described.

Sub-threshold properties

The input resistance (R_n) of neurons was determined by measuring the membrane potential changes in response to the input of incremental, depolarising steps of square current (1s) (between 5 and 20 steps) applied in the sub-threshold range. Steady-state input resistance was measured from the slope of the linear regression of the mean membrane potential response to the sub-threshold range of depolarising steps of square current (Fig. 4.2A-C).

Supra-threshold properties

Repetitive firing of action potentials was evoked in neurons by the injection of square depolarizing current pulses (1-s duration). Where the V_m was affected by sub-threshold changes in potential, these were offset by direct current injection. This ensured that any changes induced by the pharmacological agent on membrane potential were isolated from other potential modulatory effects specifically affecting firing properties. The steady-state frequency-current (*f–I*) relationship was measured using the slope (Hz/nA) of the linear regression of the average steady state frequency. Spike frequency adaptation (the time-dependent decrease in action potential discharge rate) is an intrinsic property of mammalian motor neurons (Miles et al., 2005). To avoid adaptation that

occurs during the initial phase of repetitive firing, only the firing evoked during the second half (between 500 and 1000ms of 1s pulse) of depolarising current steps was used to produce steady-state f-I relationships (Fig. 4.3A-C).

The rheobase current, defined as the minimum current needed to elicit a single action potential (or the first current step to elicit action potentials), and the maximum firing frequency were also calculated using the *f–I* data (Fig. 4.3D and E).

Depolarising current-ramps (1s) ranging from between 500 to 2000pA were used to investigate the voltage threshold (mV), maximum rate of rise (V/s), and amplitude (mV) of the first action potential generated. Differentiation of the voltage traces recorded in response to current ramps (arithmetic calculation performed in Clampfit 10 software) was used to calculate the onset of action potentials (defined as the voltage at which dV/dT reached 10mV ms^{-1}) and hence their voltage threshold (mV), and the maximum rate of rise (V/s) of action potentials. The amplitude (mV) of the first action potential elicited by ramp protocols was measured from raw data (Fig. 4.4A-D).

Single action potentials were elicited by brief (10-ms) current pulses of increasing magnitude in order to allow measurement of the AHP. AHP amplitudes were measured as the difference between the resting membrane potential (from holding membrane potential -60mV) or rest, where rest was -60mV) and peak AHP (Fig. 4.5A-C).

4.2.5 Statistics

All data are reported as mean ± SEM. Differences in means were compared using either the one way analysis of variance or repeated measures analysis of variance, with Bonferroni post test (ANOVA; GraphPad Prism software, Graphpad, La Jolla, CA). Values of $P < 0.05$ were considered significant and data are presented as mean ±SEM. Statistical significance is indicated by asterisk as follows; * = P<0.05, ** = P<0.01, *** = P<0.001, **** = P<0.0001.

4.2.6 Solutions and Reagents

4.2.6.1 Solutions

Solutions were made according to previously published protocols (Miles et al., 2005, Iwagaki and Miles, 2011). The spinal cord is fragile and neurons are very sensitive to mechanical and ischemic/excitotoxic damage. The modified dissecting solution is used to reduce excitotoxicity ischemia by reducing the circulating Na concentration by substituting NaCl with charge neutral sucrose and adding a non-selective glutamate receptor antagonist (Aghajanian and Rasmussen, 1989). The ionic balance of aCSF and intracellular solution were consistent with maintaining a resting membrane potential of -60mV according to the Goldman-Hodgkin-Katz voltage equation.

Dissecting solution

The sucrose substituted, dissecting aCSF composition: 25mM NaCl; 188mM sucrose; 1.9mM KCl; 1.2mM NaH_2PO_4; 10mM $MgSO_4$; 1mM $CaCl_2$;; 26mM $NaHCO_3$; 25mM glucose; and 1.5mM kynurenic acid.

Recovery solution

The recovery aCSF composition: 119mM NaCl; 1.9mM KCl; 1.2mM NaH_2PO_4; 10mM $MgSO_4$; 1mM $CaCl_2$; 26mM $NaHCO_3$; 20mM glucose;1.5mM kynurenic acid; and 3% dextran.

Recording solution

The recording aCSF composition: 127mM NaCl; 3mM KCl; 2mM $CaCl_2$; 1mM $MgCl_2$; 26mM $NaHCO_3$; 1.25mM NaH_2PO_4; and 10mM glucose.

Intracellular solution

The intracellular aCSF composition: 134mM potassium methane sulfonate, 10mM NaCl, 1mM $CaCl_2$, 10mM HEPES, 1mM EGTA, 3mM Mg-ATP, and 0.4mM GTP-Na_2 (pH 7.2–7.3, adjusted with KOH).

4.2.6.2 Reagents

Reagents obtained from Sigma-Aldrich Company Ltd., Dorset, UK were:
2-Phenyl-4, 4, 5, 5-tetramethylimidazoline-1-oxyl 3-oxide (PTIO); and 8-Bromoguanosine 3′, 5′-cyclic monophosphate sodium salt (8BrcGMP). Described previously in Section 3.2.5.2

Reagents obtained from Fluorochem Ltd., Derbyshire, UK were:
2-(N, N-Diethyl amino)-diazenolate-2-oxide.Diethylammonium salt (DEA NO). Described previously in Section 3.2.5.2

Reagents obtained from Invitrogen, Paisley, UK were:
Alexa Fluor 594 hydrazide sodium salt, a fluorophore with excitation/emission maxima of ~590/617 nm (Molecular Probes).

Reagents obtained from Fluorochrome, Colorodo, USA were:
Fluoro-Gold (Hydroxystilbamidine), a fluorescent, retrograde neuronal tracer, incapable of trans-synaptic transport. Visualised using fluorescent microscopy, excitation/emission maxima of ~323/408 nm (Fluorochrome, LLC).

4.3 Results

4.3.1 Modulation of motor neuron properties by DEA NO

DEA NO is used widely in bioscience research to increase experimental levels of NO. In the previous chapter, a concentration-dependent response to DEA NO was established in pharmacologically induced fictive locomotion (Chapter 3, Section 3.3.1). Recordings from ventral roots showed that increased concentrations of exogenous NO, delivered using DEA NO, caused a reduction in the frequency of fictive locomotion suggesting an inhibitory role for exogenous NO in the hind limb locomotor central

pattern generating network. DEA NO also caused an increase in the burst amplitude of fictive locomotor output at low concentrations (50µM), and a transient increase followed by a decrease in burst amplitude at higher concentrations (200 and 400µM). These effects on burst amplitude suggest direct modulation of motor neurons and/or last order interneurons by NO.

These results clearly show that NO-mediated modulation occurs during locomotor network activity but do not indicate whether NO is produced as a result of network activity nor the mechanisms by which it exerts its effects. To ascertain whether or not NO modulates the properties of neurons in the locomotor network in the absence of induced activity, the whole-cell patch-clamp technique was used to investigate potential modulation, by DEA NO, of the intrinsic properties of spinal motor neurons. Motor neurons are a relatively homogenous population of neurons; identifiable by their size, location in the spinal cord and firing properties, additionally they are the final common pathways for central control of muscles in the periphery. These properties make motor neurons ideal for the characterisation of modulatory effects exerted by neurotransmitters such as NO, as their immediate and end organ effects can be observed. In the present study, the effects of NO were studied at the level of the motor neuron in the *in vitro* slice preparation.

Whole cell recordings were made from forty-two presumed motor neurons, identified by size (capacitance) and location in the ventral horn (lamina IX) (Fig. 4.1A). From this collection of recordings, neurons with a resting membrane potential greater than -50mV and those that did not fire repetitively (a hallmark of motor neurons) during control or pharmacological manipulation were discarded from the following analysis (total neurons analysed: 10µM, n= 7; 50µM, n=7; 200µM, n=6).

Protocols investigating the modulation of the firing properties of motor neurons before, during, and after exposure to DEA NO were run in current-clamp mode. During the current-clamp protocol, the resting membrane potential was maintained at -60mV, by offsetting sub-threshold changes in potential using direct current injection. DEA NO was bath applied at concentrations of 10µM, 50µM, 200µM and 400µM (n= 7, n=7,

n=1 and n=5 respectively) and the results for the 200-400µM experiments pooled and described as >200µM. These results describe the effects of the NO donor DEA NO at 10µM, 50µM and >200µM on twenty motor neurons. The passive properties of the twenty neurons from which recordings were made are listed in Table 2.1.

Table 4.1. Spinal motor neuron passive properties

Drug	Cell type	n	Cm, pF	Vm, mV	Rn, MΩ
DEA NO	MN	20	86±4	-57±1	58±4
DEA NO	IN	5	31±5	-49±4	/
PTIO	MN	7	71±4	-57±2	94±11

The results of DEA NO application to presumed motor neurons were collated by concentration: 10, 50µM and >200µM DEA NO. The effects of DEA NO on the following intrinsic neuronal properties were analysed: input resistance (MΩ); frequency-current **(*f–I*)** relationship (slope – Hz/nA); relative excitability; rheobase current; maximum firing frequency (Hz); action potential voltage threshold (mV); maximum rate of rise of action potential (V/s); fast AHP and slow AHP; and action potential amplitude (mV). For clear comparison between concentrations of DEA NO and motor neurons of different sizes (C_m range from 50-103pF), effects on these parameters are expressed as a percentage of the control value, unless stated otherwise.

Sub-threshold properties

Overall the resting membrane potential did not significantly change in the presence of 10 and 50µM DEA NO. A small depolarisation was noted at >200µM DEA NO. However, the response of individual neurons to DEA NO varied at each concentration. The resting membrane potential hyperpolarised (ns; n=4/7) and depolarised (ns; n=3/7) in each group during application of 10µM and 50µM DEA NO, while during application of >200µM DEA NO, the resting membrane appeared to depolarise (ns, Δ3.5±2mV n=5/6).

The input resistance (R_n) of motor neurons was determined before and after the addition of DEA NO by measuring the membrane potential changes in response to the input of incremental, depolarising steps of square current applied in the sub-threshold range

(Fig. 4.2B). The mean membrane potential response to each current step was plotted to give the voltage-current (V-*I*) relationship (Fig.4.2C). Overall input resistance was not significantly affected by application of DEA NO (Fig.4.2D).

DEA NO does not significantly affect the sub-threshold properties of motor neurons; there was no significant change in input resistance and resting membrane potential. Further confirmation that NO does not modulate sub-threshold properties would be gained by increasing the experimental sample size.

Supra-threshold properties

To investigate the effect of exogenous NO on supra-threshold motor neuron properties, DEA NO was bath-applied to lumbar spinal cord slices while recording from presumed motor neurons. The mean firing frequency was recorded during a series of incremental steps of depolarising current and the resulting firing frequency was plotted against the injected current (Fig. 4.3A and B). The frequency versus injected current, or frequency-current (*f–I*) relationship, was determined in control conditions and during the application of DEA NO at concentrations of 10µM, 50µM and >200µM.

At 10µM DEA NO, neurons appeared marginally more excitable compared to control and at the concentrations of 50µM and greater than 200µM, DEA NO did not cause a shift in frequency-current relationship or a change in the slope of the relationship (all concentrations, Fig. 4.3C).

During repetitive firing protocols, the additional measures of excitability - rheobase and maximum firing frequency, were measured. This measure of rheobase should be taken as an approximation as the depolarising steps injected to elicit repetitive firing and used for this calculation are relatively large (100pA). DEA NO did not affect rheobase at 10µM, 50µM and >200µM DEA NO (Fig. 4.2D). The maximum firing frequency was significantly increased at 10µM DEA NO ($P<0.05$; +48±14%, n=6) but no change was observed at 50µM and >200µM DEA NO (Fig. 4.3E).

A depolarising current-ramp, analogous to synaptic input, was used to elicit an action potential to determine the change in action potential parameters during control and drug condition. The voltage response to a depolarising current-ramp was used to measure the action potential amplitude and the voltage response to a depolarising current-ramp differentiated to calculate the maximum rate of rise, firing threshold of the first action potential fired (Fig. 4.4A).

The voltage threshold for the firing of an action potential was significantly reduced/hyperpolarized after the removal of 10µM DEA NO ($P<0.05$; -14±5%, n=6) and >200µM DEA ($P<0.05$; -34±10%, n=5) but no change was observed at 50µM (Fig. 4.4C). The maximum rate of rise and action potential amplitude were not significantly changed during 10µM, 50µM or >200µM DEA NO application (Fig. 4.4B and D, respectively).

The amplitude of the fast and slow AHP (fAHP and sAHP, respectively) was measured in control and during DEA NO application (Fig. 4.5A). The amplitude of the fAHP was not affected by application of 10µM, 50µM and 200µM DEA NO, furthermore, application of 10µM, 50µM and 200µM DEA NO did not significantly affect sAHP amplitude (Fig. 4.4C and D, respectively). However, during the washout of 50µM DEA NO the fAHP decreased in amplitude ($P<0.05$; -38±10%, n=4; Fig. 4.5C).

These experiments suggest that, DEA NO, may have an excitatory effect on motor neurons. Application of DEA NO increased the maximum firing frequency at10µM and depolarised the resting membrane potential at higher concentrations (>200µM). The mechanism by which NO modulates spinal motor neurons is currently unknown, thus limiting the interpretation of this relatively small sample size, in the absence of further mechanistic information. These data are indicative of a potential role for NO-dependent modulation of the excitability of spinal motor neurons. However, as the effects of NO were relatively small and varied between cells, within and between the concentrations used in the present study, further experiments are necessary to clarify the trends and effects identified in the present study and the statistical significance thereof.

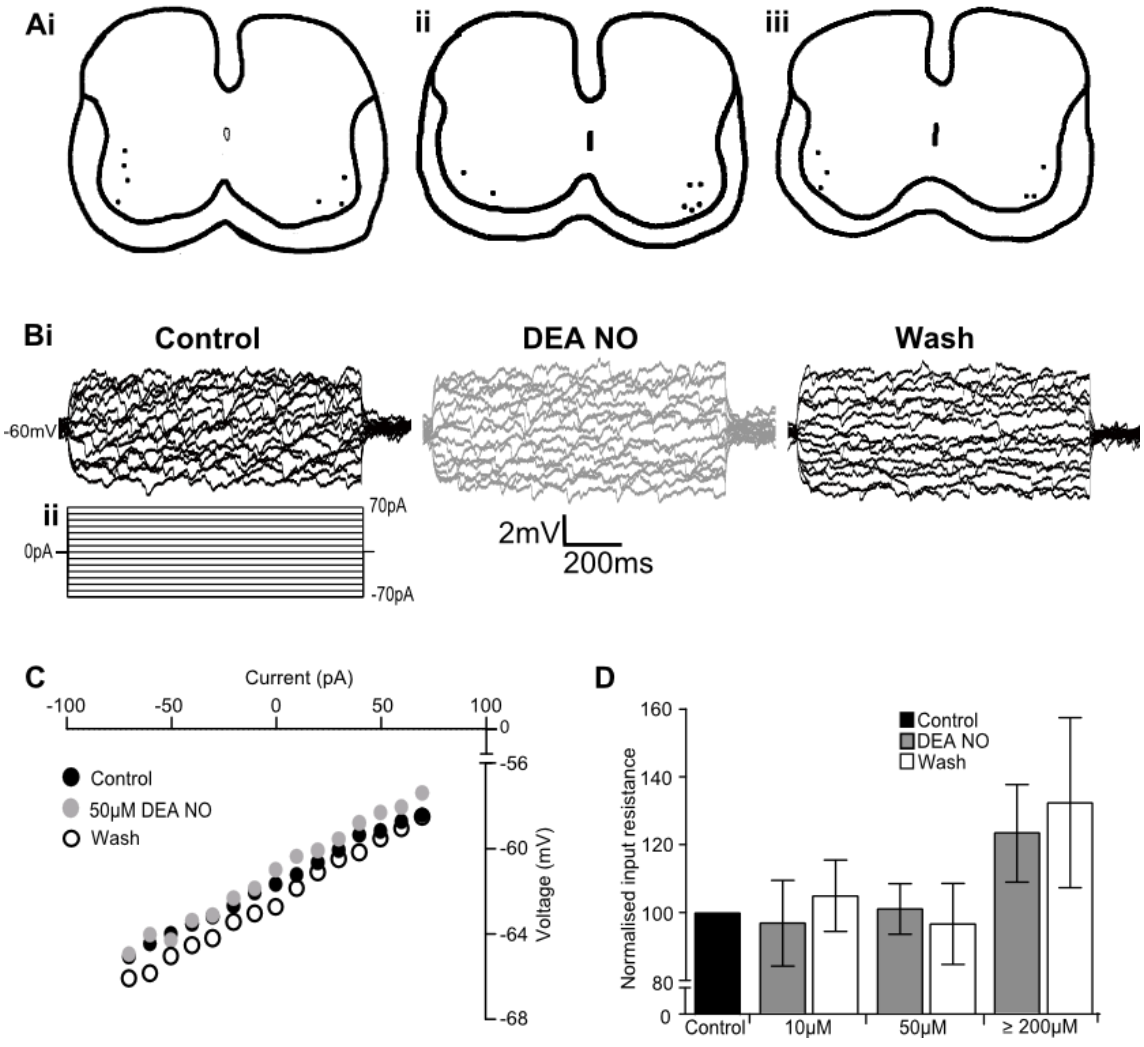

Figure 4.2. DEA NO does not affect the sub-threshold properties of spinal motor neurons. Cell plots indicating location of motor neurons exposed to **Ai** 10µM, **Aii 5**0µM and **Aiii >20**0µM. The change in membrane potential was recorded during **Bi** Control (aCSF alone), DEA NO (50µM) and Wash (aCSF alone) in response to **Bii** sub-threshold depolarising current steps. **C** Plot of the V-I relationship of a motor neuron obtained from the sub-threshold current step protocol in A. **D** Input resistance was not significantly affected by DEA NO application. Normalised input resistance of motor neurons in the presence of DEA NO (10µM, control and DEA NO n=7 and wash n=2; 50µM, control and DEA NO n=7 and wash n=7; >200µM, control and DEA NO n=6 and wash n=5).

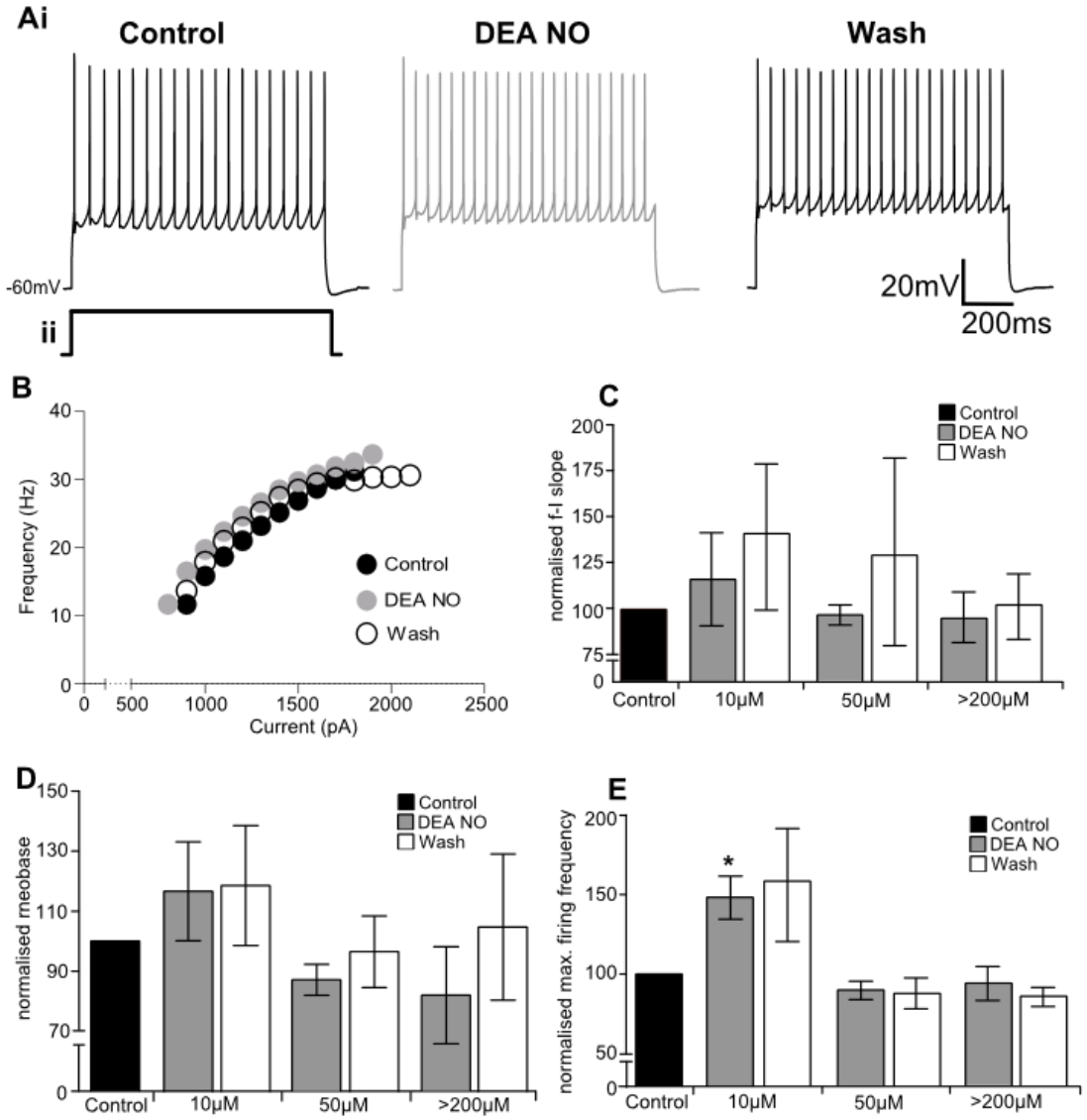

Figure 4.3. NO has a limited effect on the firing properties of spinal motor neurons. **Ai** Repetitive firing was recorded in Control (aCSF alone), DEA NO (50µM) and Wash (aCSF alone) in response to **Aii** incremental 1s square depolarising current steps (1100pA illustrated). **B** Firing frequency versus injected current (*f-I*) relationship shows no change during application of DEA NO (50µM). **C** The slope of the *f*-I relationship was not significantly affected by DEA NO at all concentrations (10µM, control and DEA NO n=7 and wash n=3; 50µM, control and DEA NO n=7 and wash n=6; >200µM, control and DEA NO n=6 and wash n=5). **D** the current required to elicit a single action potential, rheobase, was significantly decreased at 50µM DEA NO ($P<0.05$; control and DEA NO n=7 and wash n=6). Rheobase was not significantly affected by application of 10µM DEA NO, (control and DEA NO n=7 and wash n=4) or >200µM DEA NO (control and DEA NO n=6 and wash n=5). **E** Maximum firing frequency was significantly increased during application of 10µM DEA NO (control and DEA NO n=7 and wash n=3) but no effect was observed at 50µM DEA NO (control and DEA NO n=7 and wash n=6) or >200µM DEA NO (control and DEA NO n=6 and wash n=5). Asterisk denotes significance.

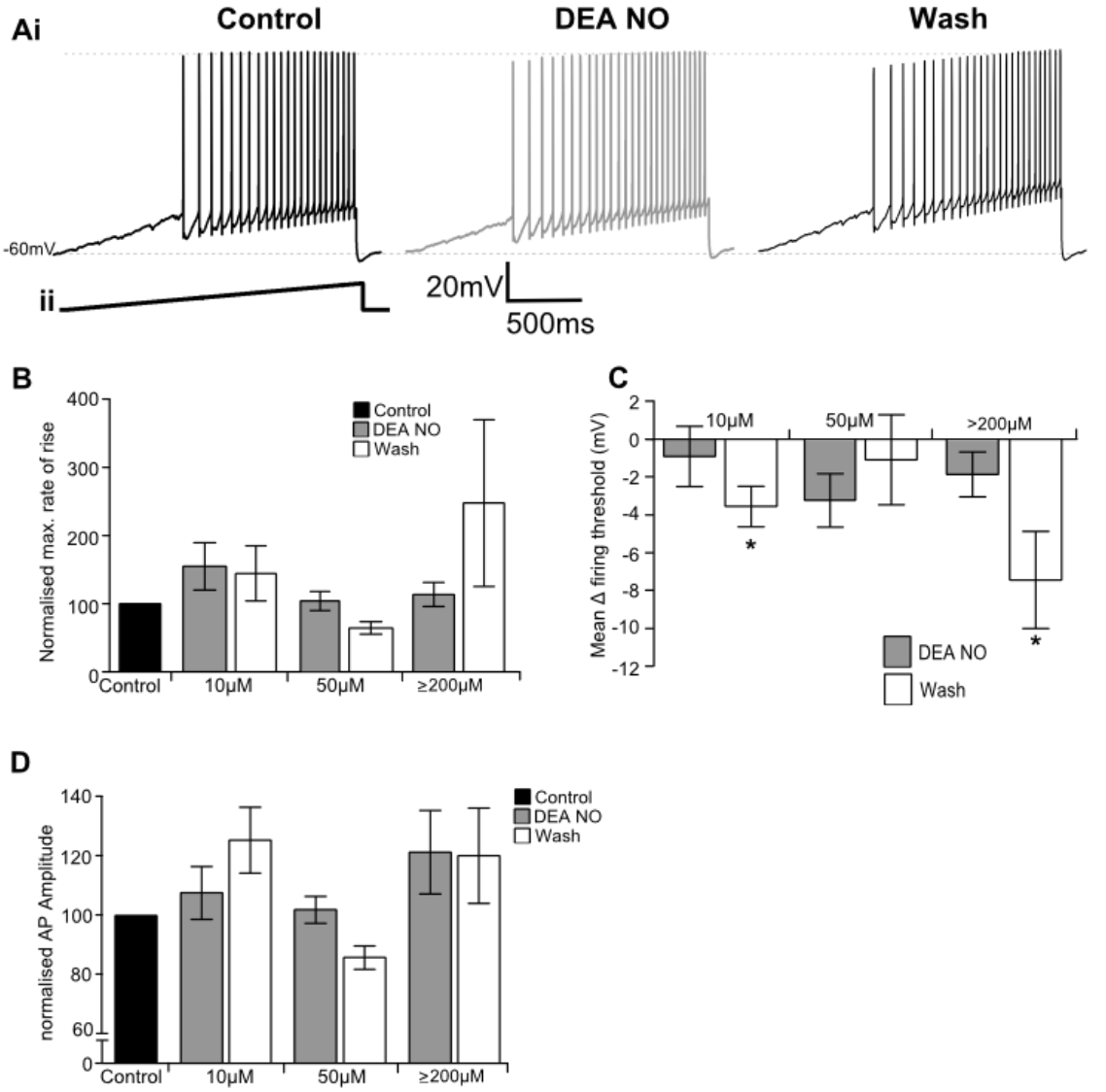

Figure 4.4. NO has subtle effects on action potential parameters. **Ai** Action potentials were recorded in Control (aCSF alone), DEA NO (50µM) and Wash (aCSF alone) in response to **Aii** a depolarising ramp of current (2000pA illustrated). **B** The maximum rate of rise (MRR) of the first action potential elicited by the ramp was not affected by the application of DEA NO but the MRR was significantly reduced after washout of 50µM DEA NO (10µM, control and DEA NO n=7 and wash n=4; 50µM, control and DEA NO n=6 and wash, P<0.05, n=5; >200µM, control and DEA NO n=6 and wash n=5). **C** The voltage threshold for action potential generation was significantly reduced during application of 50µM DEA NO and after washout of 10µM and >200µM DEA NO (10µM, control and DEA NO n=7 and wash, P<0.05, n=4; P<0.05, 50µM, control and DEA NO n=6 and wash n=5; >200µM, control and DEA NO n=6 and P<0.05, wash n=5). **D** The action potential amplitude was not significantly affected by DEA NO but was significantly reduced after washout of 50µM DEA NO (10µM, control and DEA NO n=7 and wash n=4; 50µM, control and DEA NO n=6 and wash, P<0.05, n=5; >200µM, control and DEA NO n=6 and wash n=5). Asterisk denotes significance.

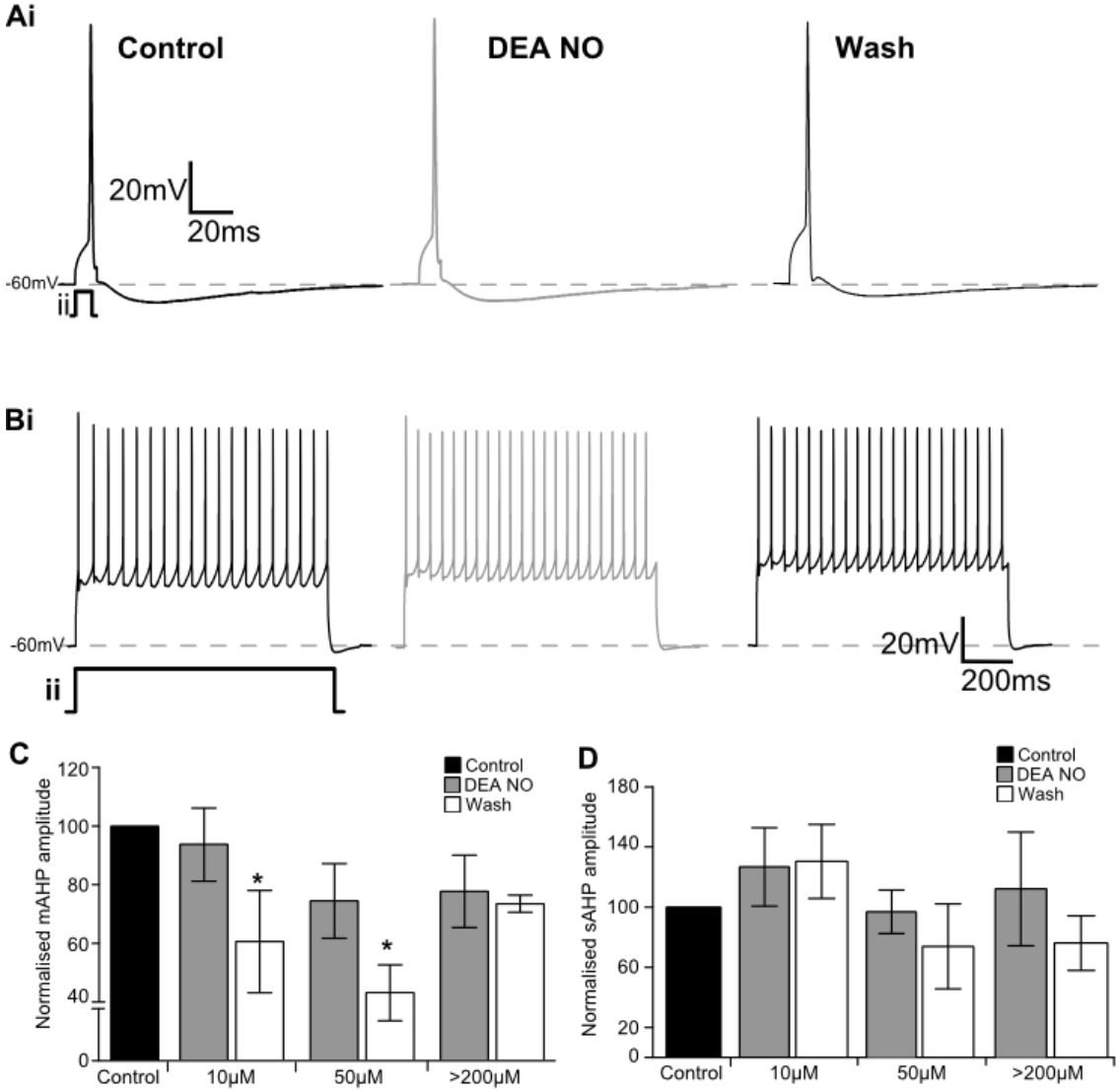

Figure 4.5. NO modulates the action potential AHP. **Ai, Bi** Action potentials were recorded in Control (aCSF alone), DEA NO (50µM) and Wash (aCSF alone) in response to **Aii** an incremental depolarising square current pulse (300pA illustrated and **Bii** incremental 1s square depolarising current steps (1100pA illustrated). **C** The fast AHP was decreased by the application of 50µM DEA NO (10µM, control and DEA NO n=7 and wash n=5; P<0.05, 50µM, control and DEA NO n=7 and wash n=6; >200µM, control and DEA NO n=3 and wash n=2). **D** The slow AHP was not significantly affected by the application of DEA NO (10µM, control and DEA NO n=7 and wash n=3; P<0.05, 50µM, control and DEA NO n=7 and wash n=6; >200µM, control and DEA NO n=6 and wash n=3).

4.3.2 Endogenous modulation of motor neuron properties by nitric oxide

In order to investigate the potential role of endogenously produced NO in the modulation of the intrinsic properties of spinal motor neurons, the nitronyl nitroxide NO scavenger, PTIO, was bath-applied to the lumbar spinal cord slices while recording from presumed motor neurons.

PTIO is a NO scavenger, referred to as membrane permeable as it is considerably more lipophilic than the carboxy analogue (cPTIO) and therefore will scavenge NO in both extra- and intra-cellular environments. Recordings from ventral roots showed that removal of endogenous NO during fictive locomotion by PTIO caused an increase in locomotor frequency, possibly by inhibition of excitatory output from the CPG, and an increase in locomotor amplitude, by scavenging NO and preventing activation of sGC at the level of the last order interneurons or directly at the motor neuron (Chapter 3, Section 3.3.2). These experiments suggest that NO has an endogenous modulatory role in the locomotor network; thus, PTIO was used to investigate changes to the intrinsic properties of presumed motor neurons.

Whole cell recordings were made from twelve presumed motor neurons, identified by size (capacitance) and location (Fig. 4.6C) in the ventral horn (lateral motor pools). From this collection of recordings, neurons with a resting membrane potential greater than -50mV were discarded. To maintain the resting membrane potential at -60mV, sub-threshold changes in potential induced by drug applications were offset by direct current injection. The passive neuron properties of the eight neurons from which recordings were made are listed in Table 2.1. These results describe the collated effects of the NO scavenger PTIO on the eight motor neurons.

The effect of PTIO on the following sub-threshold and supra-threshold intrinsic neuronal properties is reported: input resistance (MΩ); frequency-current **(*f*–*I*)** relationship (slope – Hz/nA); rheobase current; maximum firing frequency (Hz); firing threshold (mV); maximum rate of rise (V/s); fast AHP and slow AHP; and action potential amplitude (mV).

Sub-threshold properties

Overall the resting membrane potential did not appear to change with the application of PTIO (50µM); the resting membrane did not change in four cells, though it was marginally hyperpolarised in three cells and slightly depolarised in one cell during application of PTIO (ns; mean ΔR_m =3±3mV; n=8).

The input resistance (R_n) of motor neurons was determined before and after addition of 50µM PTIO by measuring the membrane potential change from -60mV in response to the input of incremental, depolarising steps of square current (1s) applied in the sub-threshold range. The mean membrane potential response to each current step was plotted to give the voltage-current (*V-I*) relationship (Fig.4.6A and B). PTIO caused an increase in the slope of the voltage-current relationship (n=6/8; Fig. 4.6A and B) and did not significantly alter the input resistance of motor neurons.

Supra-threshold properties

Next, the effects of the removal of endogenously produced NO on the frequency versus injected current or *f–I* relationships of motor neurons was investigated. The mean firing frequency was recorded during a series of incremental steps of depolarising current and the resulting firing frequency was plotted against the injected current.

In four of the eight cells from which recordings were made, an increase in excitability, indicated by the shift of the steady-state frequency-current relationship in an upward direction and to the left hand side, was noted in half of the neurons from which recordings were made (no change, n=4/8 and increase, n=4/8; Fig.4.7A and B). However, PTIO did not significantly change the excitability of motor neurons during repetitive firing as indicated by the slope of the relationship.

During repetitive firing protocols, the additional measures of excitability, rheobase current, and maximum firing frequency were measured in the group of eight neurons. PTIO did not significantly affect rheobase current (the minimum current required to

elicit an action potential) and from the frequency-current relationship data no change in maximum firing frequency was noted (Fig.4.7D).

A depolarising current-ramp, analogous to synaptic input, was used to elicit an action potential to determine the change in action potential parameters during control and drug condition. The voltage response to a depolarising current-ramp was used to measure the action potential amplitude and the voltage response to a depolarising current-ramp differentiated to calculate the maximum rate of rise, firing threshold of the first action potential fired (Fig. 4.8A). The maximum rate of rise and action potential amplitude were not significantly affected during PTIO application (Fig.4.8B and D, respectively). The voltage threshold for the firing of an action potential remained unchanged (Fig. 4.8C).

The amplitude of the fast and slow action potential AHP (fAHP and sAHP, respectively) was measured in control and during PTIO application (Fig. 4.9A and B, respectively). Overall, during the application of PTIO, the amplitude of the fAHP and the sAHP were not significantly affected (Fig.4.8A to D, respectively). However, both the fAHP and sAHP decreased in amplitude after PTIO was removed from the perfusate ($P<0.05$; -43±23%, n=6 and -58±22%, n= 6; Fig.4.9C and D, respectively).

From these data obtained from experiments using the NO scavenger PTIO to remove endogenous NO, it is likely that NO has an excitatory role in the modulation of motor neuron intrinsic properties as demonstrated by the decrease in both fAHP and sAHP, after removal of the NO scavenging agent, PTIO. These data suggest that endogenous NO is involved in the subtle modulation of the intrinsic properties of spinal motor neurons while the locomotor network is quiescent.

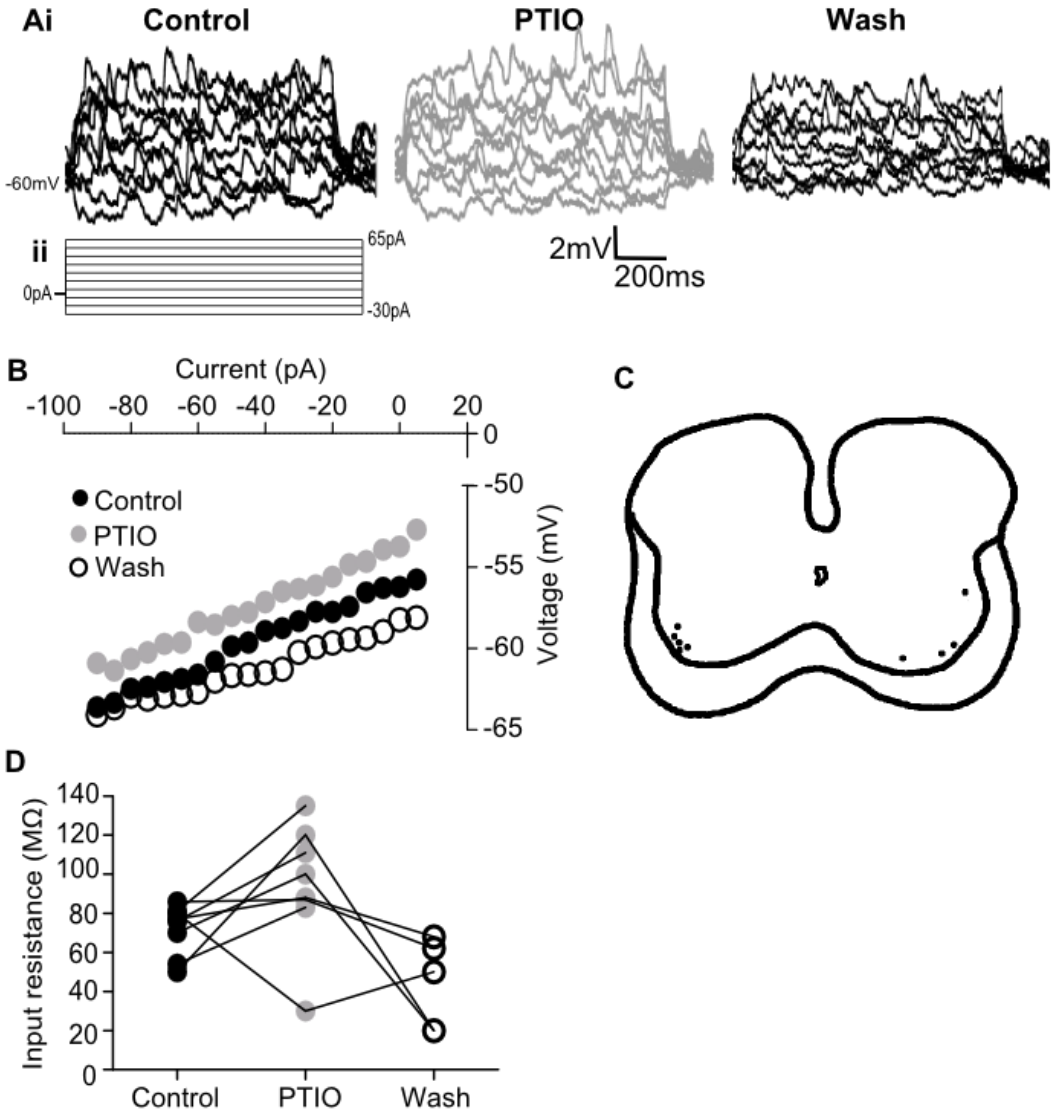

Figure 4.6. The NO scavenger PTIO does not alter the sub-threshold properties of spinal motor neurons. The change in membrane potential was recorded during **Ai** Control (aCSF alone), PTIO (50µM added to perfusate) and Wash (aCSF alone) in response to **Aii** sub-threshold depolarising current steps. **B** Plot of the V-I relationship of a motor neuron in control, PTIO and wash. **C** Cell plot indicating location of motor neurons exposed PTIO. **D** Input resistance was not significantly affected during PTIO application but was significantly reduced during wash (control and PTIO n=8 and wash n=5; $P<0.05$; asterisk indicates significance).

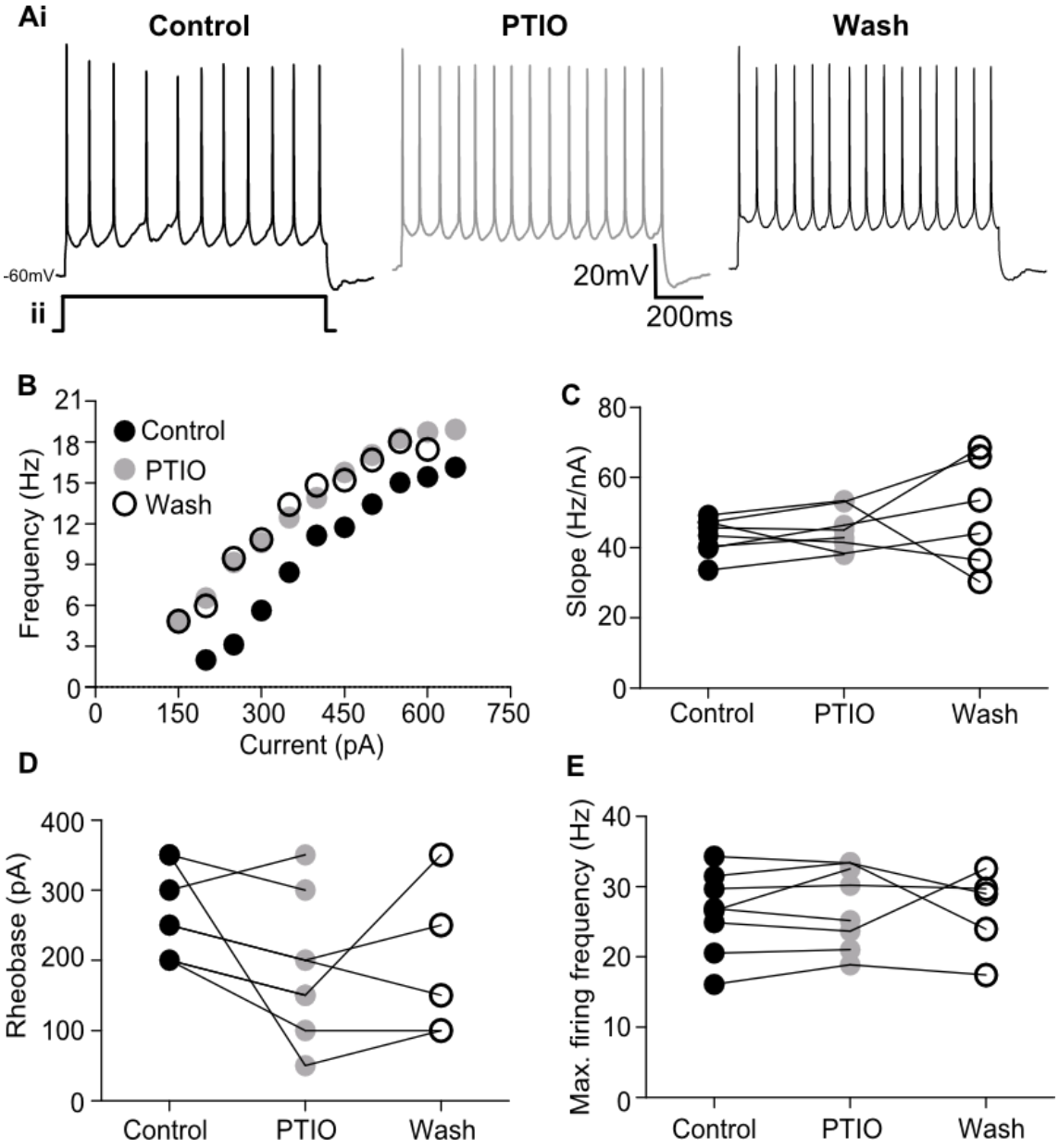

Figure 4.7. Endogenous sources of NO do not alter the firing properties of quiescent motor neurons. **Ai** Repetitive firing was recorded in Control (aCSF alone), PTIO (50µM added to perfusate) and Wash (aCSF alone) in response to **Aii** incremental 1s square depolarising current steps (900pA illustrated). **B** Firing frequency versus injected current (*f-I*) relationship exhibits a shift to the left-hand side indicating an increase in excitability during application of PTIO (50µM). **C** The slope of the *f*-I relationship was not significantly affected by PTIO at all concentrations (control and DEA NO n=8 and wash n=6). **D** the current required to elicit a single action potential, rheobase, was not significantly altered during PTIO application (control and PTIO n=8 and wash n=5). **E** The maximum firing frequency was not significantly affected by application of 50µM PTIO (control and PTIO n=8 and wash n=5).

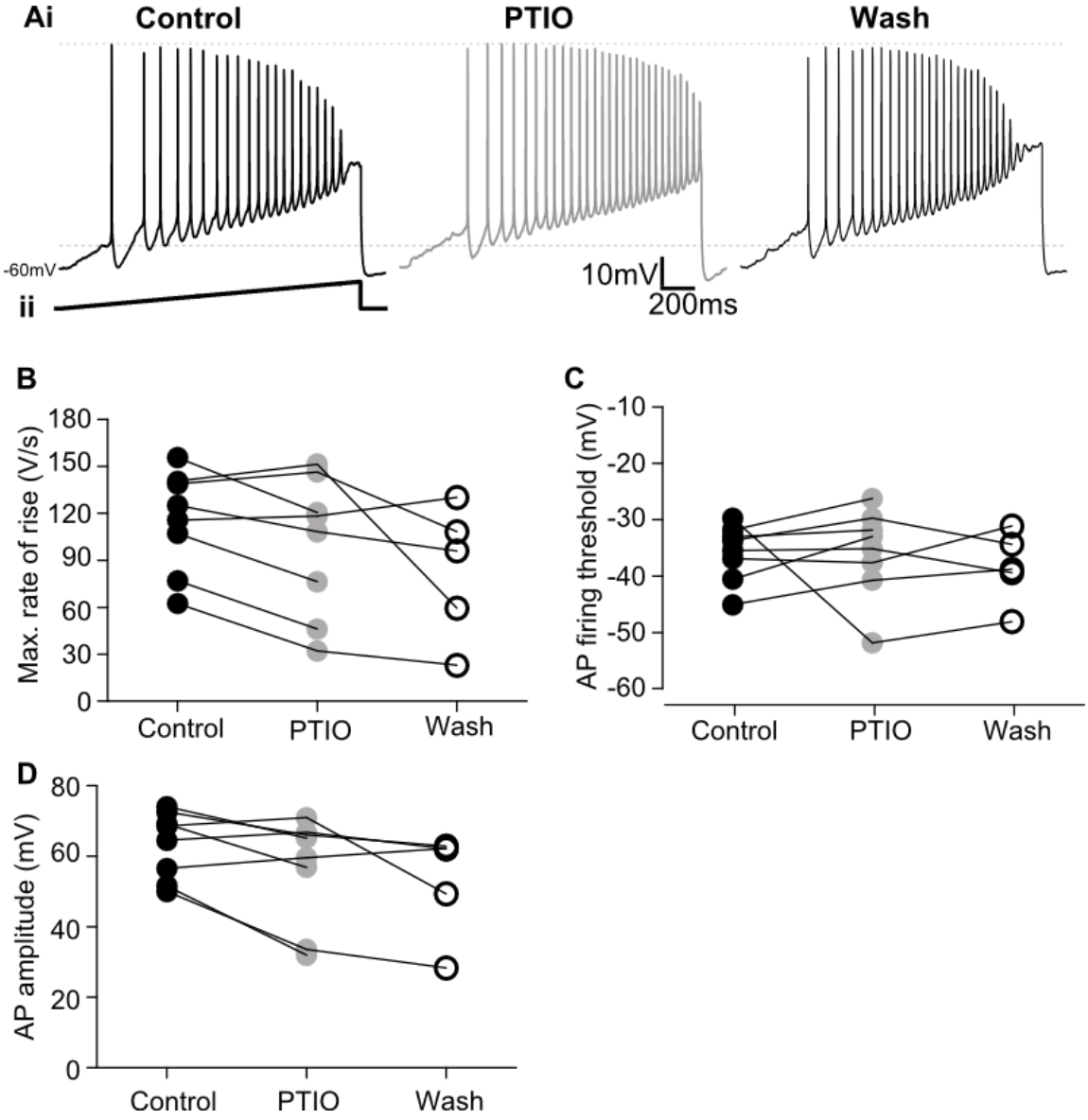

Figure 4.8. Removal of endogenous NO does not alter action potential parameters. **Ai** Action potentials were recorded in Control (aCSF alone), PTIO (50µM added to perfusate) and Wash (aCSF alone) in response to **Aii** a depolarising ramp of current (1500pA illustrated). **B** The maximum rate of rise (MRR), **C** voltage threshold for action potential generation and **D** action potential amplitude were not significantly affected by the application of PTIO (control and PTIO n=8 and wash n=5). However, both the MRR and AP amplitude showed trends towards a decrease. A larger sample of neurons is needed to determine whether this trend is significant.

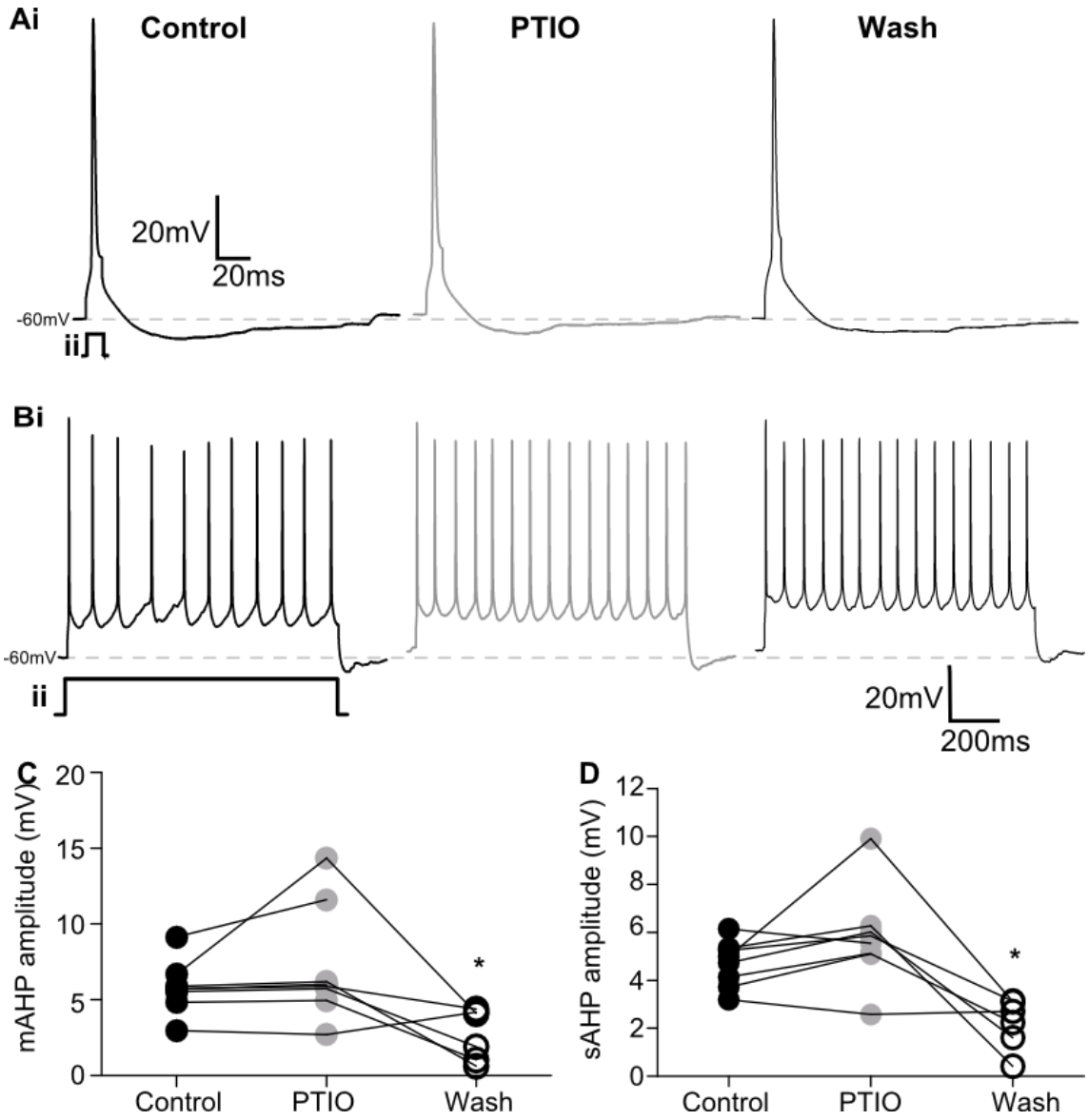

Figure 4.9. Endogenous NO modulates the action potential AHP. **Ai, Bi** Action potentials were recorded in Control (aCSF alone), PTIO (50µM added to perfusate) and Wash (aCSF alone) in response to **Aii** an incremental depolarising square current pulse (320pA illustrated and **Bii** incremental 1s square depolarising current steps (900pA illustrated). **C** The fast AHP was not affected by the application of 50µM PTIO but was significantly reduced during washout (control and PTIO n=8 and $P<0.05$, wash n=6). **D** The slow AHP was not affected by the application of PTIO but was significantly reduced during washout (control and PTIO n=8 and $P<0.05$, wash n=6).

4.3.3 Modulation of interneuron properties by DEA NO

The laminae of the ventral horn are populated by a heterogeneous population of interneurons. Developmental genetic studies combined with electrophysiological analyses have identified four heterogeneous classes of ventral interneurons (V0-V3) and at some level ascribed function to each class, as discussed in Section 1.1.2. These interneurons have been studied intensely to understand their role in the central pattern generating network and motor neuron output. In the present study, the effect of NO on a small group of unidentified, ventral interneurons was investigated.

Whole cell recordings were made in a small subset of eleven interneurons identified by size (capacitance) and location (Fig. 4.10A) in the ventral horn (lamina VII or X). From this collection of recordings, neurons with a resting membrane potential greater than -50mV, and those that did not fire repetitively during control or pharmacological manipulation, were discarded. To maintain the resting membrane potential at -60mV, sub-threshold changes in potential were offset by direct current injection. These results describe the effects of DEA NO (200/400μM) on the remaining 5 interneurons. The passive neuron properties of the 5 neurons from which recordings were made are listed in Table 2.1.

From this collection of recordings, neurons with a resting membrane potential greater than -50mV, and those that did not fire repetitively during control or pharmacological manipulation, were discarded. To maintain the resting membrane potential at -60mV, sub-threshold changes in potential were offset by direct current injection. These results describe the effects of DEA NO (200/400μM) on the remaining five interneurons. The passive neuron properties of the five neurons from which recordings were made are listed in Table 2.1.

During these experiments, data investigating the sub-threshold changes due to DEA NO in interneurons were not collected. It is therefore unclear, within this group of five neurons from which recordings were made, whether or not there was a passive increase or decrease in resting membrane potential as a result of the application of DEA NO.

Supra-threshold properties

The effect of >200µM DEA NO on the frequency versus injected current or frequency-current (*f–I*) relationship was investigated as previously described.

DEA NO caused a mixed response in excitability, indicated by the shift of the frequency-current relationship in an upward direction and to the left hand side in 2/5 neurons and a shift to a less excitable downward right hand side in 3/5 neurons. There was no correlation between the direction of shift of the frequency-current relationship and the magnitude of the slope. Overall, no effect on the slope of the frequency-current relationship was observed after DEA NO application, though the response of individual neurons was varied (Fig. 4.10B).

During repetitive firing protocols, the additional measures of excitability, rheobase current, and maximum firing frequency were noted. Neither the maximum firing frequency nor rheobase current, were affected by application of DEA NO (Fig. 4.10C and D, respectively).

As previously described, the voltage response to the current ramp was used to calculate the maximum rate of rise, firing threshold, and action potential amplitude. The maximum rate of rise was not significantly affected during DEA NO application and from the ramp protocol data, it was noted that the voltage threshold for the firing of an action potential did not significantly depolarise (n=4; mean Δ threshold= 2±1mV; min.Δ =0mV, max.Δ=6mV; Fig. 4.10F). Overall action potential amplitude was not affected by DEA NO (Fig. 4.10G).

The fast and slow action potential AHP amplitude was measured using the protocol described previously. The amplitude of both the fast and slow action potential AHP was not significantly affected by the application of DEA NO (Fig. 4.10H and I, respectively).

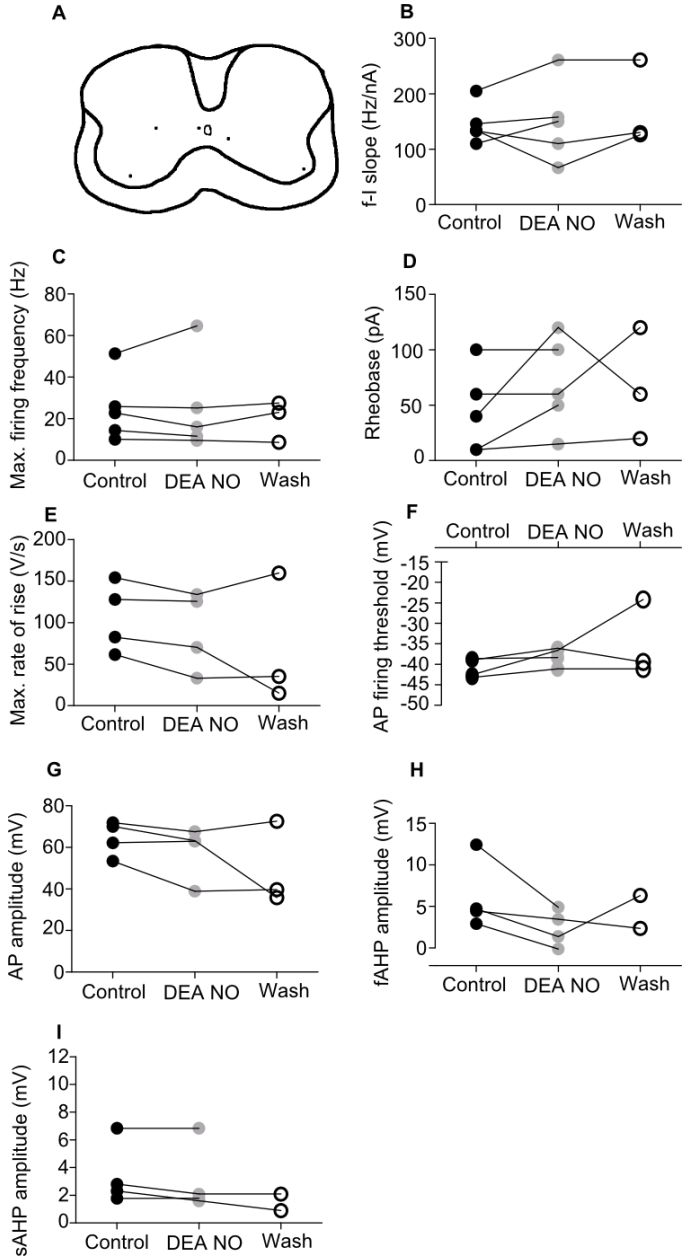

Figure 4.10. The effect of DEA NO the intrinsic properties of unidentified interneurons. **A** Cell plot indicating location of interneurons recorded from during DEA NO application. **B** The slope of the *f*-I relationship was not significantly affected by DEA NO (200µM, control and DEA NO n=5 and wash n=3). **C** The maximum firing frequency was not significantly affected by DEA NO (200µM, control and DEA NO n=5 and wash n=3). **D** Rheobase was not significantly affected by DEA NO (200µM, control and DEA NO n=5 and wash n=3). **E** The maximum rate of rise was not significantly affected by DEA NO (200µM, control and DEA NO n=4 and wash n=3). **F** The voltage threshold for the generation of an action potential was not significantly affected by DEA NO (200µM, control and DEA NO n=4 and wash n=3). **G** The action potential amplitude was not significantly affected by DEA NO (200µM, control and DEA NO n=4 and wash n=3). **H, I** Both the fast and slow AHP were not affected by application of DEA NO (200µM, control and DEA NO n=4 and wash n=2).

Though the effects of DEA NO on AHP were not significant, recordings from a larger sample of neurons, or identified subtypes of interneurons may reveal provide clarification of potential DEA NO-mediated reduction in the AHP of interneurons.

These data are not conclusive but do suggest that NO may reduce interneuron excitability (trends towards depolarised firing threshold and reduced maximum rate of rise). Due to the heterogeneous nature of the interneuron population and the absence of any phenotypic markers in this study, these data are indicative of the possibility that NO modulates the intrinsic properties of interneurons. A larger sample of recordings, preferably in identified interneurons, is needed to confirm and clarify these findings.

4.4 Discussion

In the present study, recordings were made from lumbar spinal motor neurons during application of DEA NO and the membrane permeable NO scavenger PTIO. The results in this chapter provide evidence for NO-mediated modulation of the intrinsic properties of spinal neurons.

4.4.1 DEA NO modulates the intrinsic properties of motor neurons

Despite the mixed effect on motor neurons of DEA NO, the major finding in this chapter is that NO appears to directly excite lumbar spinal motor neurons. The mechanism of this excitatory action is as yet undefined and will require further investigation, particularly the hyperpolarisation of the action potential firing threshold and reduction in action potential AHP.

DEA NO did not appear to modulate the sub-threshold properties of motor neurons. This is in agreement with the finding that NO does not change the resting properties of trigeminal motor neurons in the neonatal rat (Pose et al., 2011).

DEA NO appeared to increase the excitability of motor neurons by increasing the ability of motor neurons to fire repetitively at a higher frequency indicated by an increase in the maximum firing frequency was significantly increased during application of 10µM DEA NO. This subtle modulation of motor neuron properties, suggests that the role of NO in the quiescent network is excitatory and gives some suggestion as to the response to NO observed in Chapter 3. The mixed and, apparently, concentration-dependent actions of NO obtained in Chapter 3 – where DEA NO either increased or decreased burst amplitude during fictive locomotion – have not been definitively corroborated between the data in this chapter and the whole cord data. Comparison between the actions of NO during locomotion (whole nerve) and at the single cell level (whole cell) will require a larger sample population and the direct investigation of changes in the intrinsic properties of motor neurons in response to DEA NO during pharmacologically-induced locomotion.

It is possible to speculate on the likely mechanisms by which NO may modulate the intrinsic properties of spinal neurons. The main signalling pathway involved in NO-mediated effects is by the activation of sGC and downstream PKG. At high concentrations of NO in these slice preparations, sGC may become desensitised, resulting in a drop in cGMP and therefore an inhibition of PKG-dependent targets.

HCN channels underlie the I_h current and are expressed in motor neurons and NO activates HCN channels in deep cerebellar nuclei (Milligan et al., 2006, Wilson and Garthwaite, 2010, Neitz et al., 2011), but it is not clear from these data whether NO activates I_h, and additional experiments with adjusted protocols will provide clarification. It is likely that NO is modulating a number of targets at any time point; for example, an increase in excitability caused by NO could lead to depolarising block, while simultaneously nitrosative stress may cause modification of NMDA receptors (Choi et al., 2000) and subsequently cause a drop in excitability. Therefore, further experiments exploring the contribution of specific mechanisms potentially mediated by NO will provide further evidence of the range of NO targets and effects.

NO may facilitate or diminish excitatory transmission, however in the absence of data revealing the exact targets of NO, it is not possible to define the precise mechanisms of NO on synaptic transmission to motor neurons. Following on from the discussion in Chapter 3 where I postulated that NO may modulate the locomotor network in a state and/or activity-dependent manner, logically this may also be the case in relation to the direct modulation of motor neurons. The modulatory nature of NO may be very different in the active whole-spinal cord preparation compared to that in a quiescent slice, in the absence of network activity, that is, induced by inputs from the CPG. It will therefore be important to progress the results obtained in the present study to encompass the effects of DEA NO on motor neurons during locomotor activity.

The apparent reduction in fAHP during DEA NO application and after removal of the NO scavenger PTIO, suggests a modulation of apamin-sensitive potassium channels. Apamin is a bee venom toxin (*Apis mellifera*) and highly selective of the Ca_{2+}-activated K^+-channel ($IK_{CA\ (SK)}$), which underlies the AHP (van der Staay et al., 2008). Further experiments applying DEA NO in the presence of apamin will reveal the significance of this finding.

The result of DEA NO application to a sample of interneurons does not rule out neuron-specific effects of NO. Although the results from this small cohort of heterogenous interneurons showed did not reach significance, further recordings from identified excitatory interneurons will result in a better understanding of NO effects in future.

It is difficult to draw further conclusions about the nature of NO-mediated effects on locomotor-related interneurons as they are a heterogeneous population and the present study does not incorporate a large experimental sample or identify or discriminate between classes of interneurons, which may be differentially modulated by NO (Goulding, 2009) .

4.4.2 Endogenous NO modulates the intrinsic properties of motor neurons

In the previous chapters, it was shown that NO is probably not produced by lumbar spinal motor neurons (Chapter 2) and that removal of endogenous NO by the membrane permeable scavenger PTIO increased the frequency and amplitude of fictive locomotion (Chapter 3). The results in this chapter show that endogenously produced NO is involved in the modulation of motor neuron properties in the quiescent slice preparation.

Endogenous NO modulates the firing properties of motor neurons; consistent with the excitatory effects observed on addition of DEA NO, PTIO increased both the fast and slow action potential AHP during removal of the NO scavenger PTIO. This indicates that NO directly modulates the membrane properties of motor neurons towards an increase in excitability.

4.5 Conclusion

The results discussed in this chapter suggest that NO may be a homeostatic regulator of motor neuron excitability. However, these results are preliminary and it is difficult to speculate on the mechanisms by which NO modulates motor neuron properties without further experiments as suggested in Section 4.4. For instance, blocking apamin-sensitive potassium channels to confirm the modulation of these channels by NO to decrease the AHP. Blocking action potential-evoked synaptic transmission and recording miniature post-synaptic currents in control and in response to NO donors will go further and reveal the pre-synaptic and post-synaptic element of NO transmission. Crucially, whether NO is acting via cGMP-dependent or independent mechanisms will require additional experiments using a PKG agonist (8BrcGMP) or agonists of sGC (YC-1). State-dependent modulation of motor neurons will be revealed using induced fictive locomotion in concert with all of the aforementioned pharmacologically manipulations.

NO is difficult to manipulate in experimental conditions, even when donors are used, as the gas is free to diffuse to any number of specific and non-specific targets, potentially masking direct and relevant effects from observation. A slightly less blunt and more sophisticated approach would involve the use of pathway- or protein-specific pharmacological agents downstream of NO production to assess the impact of ablating or enhancing NO-mediated signalling. For example, using PKG agonists or antagonists to manipulate PKG signalling pathways, using HCN channel blockers to determine if NO affects these channels, and using PDE agonists or antagonists to manipulate the endogenous levels of cGMP. It is also possible that a meta-modulatory hierarchy exists in the mammalian locomotor network as it does in the tadpole (McLean and Sillar, 2004) and pond snail (Straub et al., 2007) where NO may enhance or reduce an effect mediated by another neuromodulator. This role could of course only be assessed when the secondary modulatory system is engaged, again perhaps during locomotor activity.

In their spectral investigation of NO pulse-production and nNOS auto inhibition, Salerno and Ghosh (Salerno and Ghosh, 2009) summarise the findings of CE Shannon in The Mathematical Theory of Communication (Shannon, 1948) with the following statement: "By contrast, information transfer in the unmodulated steady-state is zero because information transfer depends on bandwidth." Likewise in this study, in the absence of locomotor output (i.e. bandwidth) the true nature of NO modulation (i.e. communication) is difficult to categorically define.

Nevertheless, despite the relatively small sample size and subtle modulation of neuronal properties, these data provide some evidence of potential concentration-dependent NO-mediated effects in lumbar spinal neurons.

Chapter 5: A general discussion of the distribution and physiological roles of nitric oxide in locomotor circuitry of the mammalian spinal cord

5.1 NO is an endogenous physiological signalling molecule

The free radical gas NO is now an established signalling molecule in the central as well as the peripheral nervous system. Since the initial discovery that the molecule known as EDRF responsible for the vasodilation of vascular smooth muscle was in fact NO, the presence of NO synthases and the effect of NO have been recorded in many organs in a vast array of species. Most pertinent to the present study is the role of NO in central transmission, particularly the role of NO in the mammalian locomotor network, which has been largely under-studied.

NO is produced after the activation of NOS, an NADPH diaphorase enzyme (Hope et al., 1991). The calcium dependent nNOS and eNOS are activated by an influx of Ca^{2+} via glutamate binding to NMDA receptors/voltage dependent calcium channels or release from internal stores (Sun et al., 2001). The isozymes then catalyse the conversion of L-arginine to L-citrulline and NO at which point the gas is free to participate in cellular reactions in either an autocrine or paracrine manner. The sequence of events leading to NO production and the subsequent reactions - in which is a key component - appear to be tightly regulated within the cellular environment. In order for NO to reach its target receptor it must avoid inactivation by plasma scavengers and intracellular scavengers such as uric acid and ascorbate (Sunico et al., 2011) and auto regulation by feedback inhibition .

NO is known to predominantly exert its effects via the NO/sGC/cGMP secondary messenger pathway as well as acting in some extent through the thiol modification of peptides. Although a plethora of cellular targets has been identified, putative targets for NO continue to be described and its action identified (Denninger and Marletta, 1999, Brown and Borutaite, 2007, Kang et al., 2007, Mironov and Langohr, 2007, Wilson and Garthwaite, 2010). The present study is an investigation of the role of NO in the

mammalian locomotor network and provides evidence that in keeping with the flexible and wide ranging signalling profile of NO in biological systems, NO is produced by and modulates the neuronal circuitry that initiates and maintains locomotion *in vitro*.

5.2 NO is produced by the mammalian locomotor circuitry

While it has previously been established that NOS is present in the mammalian nociceptive network located primarily in the dorsal horn of the spinal cord, there is now unequivocal evidence that NOS is present in discrete populations of neurons in close proximity to or directly involved in the maintenance and modulation of mammalian locomotor activity. In Chapter 2 of the present study, I have shown that NOS positive neurons, located in the ventral horn of the rodent spinal cord, increase during the first 12 days of postnatal development and appear to be most numerous in regions known to contain the circuitry involved in the integration of locomotor commands (laminae X and VII). The pattern of NOS reactivity reported in the present study is consistent with that reported at various stages of development in other species (Dun et al., 1993, McLean and Sillar, 2000, Foster and Phelps, 2000, McLean and Sillar, 2001, Schreiberová et al., 2006). Additionally, the present study reports the pattern of NOS reactivity with high temporal resolution over a developmentally relevant period –the first 12 postnatal days – during which the spinal locomotor networks have been shown to undergo a maturation process linked to the development of quadrupedal locomotion (Clarac et al., 1998, Jiang et al., 1999).

I have shown that NOS reactivity is present in regions associated with locomotor-related activity, though it is not clear if these neurons belong to which, if any, of the defined neuron subpopulations currently identified by lineage or transmitter phenotype (Spike et al., 1993, Miles et al., 2007, Goulding, 2009, Kiehn, 2011). Further anatomical studies (for instance, immunohistochemical characterisation) are needed to establish the transmitter phenotypes to identify the possible transmitter profile of NOS positive neurons.

Identification of NOS positive neurons using transgenic genetic tools (for example, expressing eGFP in selective neuronal cell types such as the Hb9 interneurons (Wilson et al., 2005) in combination with traditional immunohistochemistry techniques) will provide future investigations with definitive evidence of the involvement of NOS positive neurons in the locomotor circuitry. This would provide further evidence to consider in determining the role of NO in locomotion and whether it is produced by neurons integral to the locomotor circuitry or produced by neurons in close association with the network but not directly involved in locomotion (i.e. is NO a cell subtype specific paracrine or autocrine modulator of locomotor output).

Consistent with the findings of previous studies, the present study confirms that NOS is largely absent from lumbar motor neurons (Dun et al., 1993, Collett, 2007). However, using the *in vitro* isolated spinal cord preparation, I have shown that NO does in fact modulate locomotor output at the level of the CPG and directly at the level of the motor neuron indicating that while motor neurons do not appear to express NOS, the sGC machinery is expressed and is stimulated by both the removal of endogenous NO and the wholesale increase in exogenous NO levels.

5.3 NO modulates the physiological output of the mammalian locomotor circuitry

Utilising the NO donor, DEA NO, to increase the exogenous level of NO at a range of concentrations significantly reduced the frequency of rhythmic locomotor output produced by the locomotor CPG. Additionally, DEA NO affected the amplitude of motor neuron output in a concentration dependent manner. Low concentrations significantly increased or did not significantly affect motor neuron output (50μM and 100μM DEA NO respectively, Section 3.3.1), while high concentrations appeared to significantly increase and decrease motor neuron output (200μM and 400μM DEA NO respectively, Section 3.3.1). In a subset of these experiments where a high concentration of DEA NO was used to investigate the effects of NO, biphasic modulation of motor neuron output was observed.

Consistent with the effects observed as a result of the increase in exogenous NO concentrations, the removal of NO by high concentrations of the scavenger molecules cPTIO and PTIO increased the frequency of locomotor output suggesting that NO may facilitate inhibition in the CPG network. Furthermore, experiments inhibiting NOS using the competitive, irreversible inhibitors L-NAME and L-NNA suggest that NO provides tonic inhibitory influence in the active locomotor network. Utilising the disinhibited preparation, which records the excitatory output from the locomotor network in the absence of inhibition (i.e. pharmacological block of glycinergic and GABAergic signalling using strychnine and bicuculline), DEA NO released NO reduces the frequency of rhythmic bursting indicating that NO is involved in inhibition of excitatory-driven rhythmic bursting in the locomotor CPG network. However, future studies to characterise this inhibitory effect of NO would be best designed in the presence of inhibition to clarify that NO mediated network modulation changes are due to the actions of NO and not due to significant alteration of the network as a result of pharmacological blockade by strychnine and bicuculline.

High concentrations of the scavenger molecules PTIO and cPTIO reduce and augment motor neuron output, respectively (400μM PTIO and 200/4000μM cPTIO, Section 3.3.2). While it appears that the more membrane permeable compound PTIO decreases motor neuron output, the more hydrophilic scavenger cPTIO increases motor neuron output. Scavenging of NO by membrane permeable PTIO results in a decrease in motor neuron output, consistent with an excitatory role for NO at the level of the motor neuron at relatively low concentrations. Scavenging of NO by the less membrane permeable cPTIO results in an increase in motor neuron output, consistent with an inhibitory role for NO at the level of the motor neuron at relatively high concentrations of NO donor used in the present study. If the discrepancy in response is due to the relative membrane permeability of these compounds, it can be concluded that low concentrations of NO, presumably from neurons in close proximity to the motor neurons, facilitate excitatory motor output confirming that while motor neurons do not produce NO, they express the machinery to process the NO as a result of paracrine activity.

These seemingly conflicting actions at the level of the motor neuron may be rationalised as a result of scavenging NO at distinctly different sites of action (either intra- or extra-cellularly). The reactive chemistry of the imidazolineoxyl N-oxide compounds is such that nitrate and nitrites are produced as a result of NO metabolism, (Radi, 2004, Kuzkaya et al., 2005, Thomas et al., 2008) with the possibility of further NO mediated reactions taking place. However, it is unlikely that the discrepancy observed in motor neuron response to these compounds is due to differences in nitrate/nitrite production as both PTIO and cPTIO have been shown to react with NO in stoichiometric manner (Akaike et al., 1993). However, based on this pivotal characterisation study, it is not clear whether the additional carboxy side chain which confers the greater hydrophilic nature of cPTIO versus PTIO, is also involved in nitrate/nitrite production as these experiments monitored the production of the conversion of PTIO to PTI and not of nitrate/nitrite production. Furthermore, NO may react with itself and its metabolites to produce peroxynitrite directly, in the presence of high concentrations of NO as well as on addition of cPTIO, especially in this experimental paradigm where O_2 is in excess within the cellular environment.

It is not clear why scavenging NO using cPTIO should result in a reduction of motor neuron output, opposite in sign to the effect observed with higher concentrations of NO. It is possible that the discrepancy is linked to the apparent concentration dependent effects of NO but further work is needed to clarify whether this is truly a result of NO scavenging at different locales, NO involved in both excitatory and inhibitory signalling, or side reaction chemistry of the scavenging molecules and the resulting biological effect of these by products in addition to the true effects of NO. Future studies should include the use of known peroxynitrite generators such as SIN1 to clarify the possible contribution of NO metabolites and generated reactive species in the modulation of locomotor output and/or the use of endogenous antioxidants, uric and ascorbic acid. Further work involving NO signalling will need to rely on manipulation of downstream signalling pathways as the obvious experimental control - application of depleted pharmacological agent (i.e. DEA NO) – may not result in definitive results. DEA NO metabolites include both nitrates and nitrites and any depletion experiment using this agent will need to first ascertain the effect of nitrates and nitrites alone on the

locomotor network. The most obvious and ideal pathway for manipulation is the metabolism of cGMP by phosphodiesterases as readily available commercial drugs target this portion of the signalling pathway (e.g. sildenafil). These experiments should be carried out in concert with manipulation of the PKG portion of the signalling pathway to provide substantive evidence of the downstream role of NO without the possibility of desensitising sGC by excessive stimulation with cGMP.The NOS inhibitors L-NAME and L-NNA increase the frequency of locomotor output, reaffirming the inhibitory role for NO in the CPG network. Lending some weight to the possibility that NO scavenging may be complicated by by-product side reactions, inhibition of NOS consistently causes a reduction in motor neuron output. Though these effects are subtle they are statistically significant and could be interpreted to support the metabolism and regeneration of NO from nitrates/nitrites as previously discussed.

As NO is able to modulate synaptic function through coupling to G proteins and the initiation of signalling cascades as well as direct modification of proteins by s-nitrosation, the contribution of the NO/sGC/cGMP pathway was investigated using the partial PKG agonist 8BrcGMP as well as the irreversible sGC inhibitor ODQ. The results show that inhibition of sGC by a high concentration of ODQ results in unrecoverable diminution of lumbar nerve output (Section 3.3.3). Although ODQ is an irreversible inhibitor of sGC, its simultaneous application with the NO donor DEA NO is justifiable in the protocols of the present study as it has previously been reported that at some level, inhibition of sGC NO binding sites occurs preventing NO mediated signalling without disruption to normal cellular function (Fernhoff et al., 2009, Cary et al., 2006, Derbyshire et al., 2010). The inhibition of sGC by a low concentration of ODQ, resulted in an increase in frequency of locomotor output followed by a subsequent decrease in frequency on addition of NO donor, again suggesting that NO is involved in maintaining an endogenous inhibitory tone during locomotor activity.

The amplitude of motor neuron output is not significantly affected by a low concentration of ODQ or by the simultaneous application of ODQ and DEA NO suggesting that the predominant mechanism by which NO mediates its effects in lumbar motor neurons is through the NO/sGC/cGMP pathway. Surprisingly, the partial PKG

agonist reduces the amplitude of motor neuron output at the relatively high concentration used in the present study. To clarify whether this is a true conflict or a result consistent with results shown herein – that high concentrations of NO donor reduce the amplitude of motor neuron output – further experiments will need to be conducted using a similar range of concentrations of agonist as donor used in the present study.

Taking into consideration the results from whole nerve recordings in the present study, initially it was not obvious whether NO is involved in maintaining an endogenous inhibitory tone during fictive locomotion by increasing inhibition or by a decrease in excitation. Using the disinhibited preparation, where glycinergic and GABAergic transmission is blocked, I have shown that the NO donor DEA NO produces results consistent with NO causing a reduction in excitation in the CPG network.
Furthermore, donor released NO increases motor neuron output at low concentrations and but does not decrease motor neuron output at high concentrations. These results confirm that the concentration dependent effects observed in the presence of inhibition are mediated by similar mechanisms (i.e. by a reduction in excitation at low concentrations with an inhibitory component revealed at high concentrations). Although it is likely that the excitatory network activated in the absence of inhibition is not identical to that in the standard preparation, these results are still very strongly indicative of an actual role for NO in modulating excitatory transmission.

Whole cell patch clamp recordings made from lumbar motor neurons in the presence of the NO donor DEA NO suggest that NO does modulate the excitability of motor neurons. As a result of NO donor application the firing threshold for action potentials as well as the action potential AHP are significantly reduced. These data suggest that NO increases the excitability of motor neurons, enabling them to fire more readily for a given synaptic input and increasing the ability of motor neurons to regenerate action potentials. Data from the whole nerve recordings indicate that the NO donor increases and decreases the amplitude of motor neuron output at low and high concentrations respectively. Taking into consideration the results obtained from whole cell recordings, it is possible that this NO mediated intrinsic increase in excitability results in increased

amplitude of motor neuron output at low concentrations but at higher concentrations, over excitation and thus, excitatory block may account for the decrease in amplitude of motor neuron output. Further data collection using whole cell recordings and targeting NO downstream signalling processes such as sGC conversion of GMP to cGMP (using YC-1) or PKG agonist 8BrcGMP, will confirm these results without the gross and indiscriminate activation of signalling pathways by bath application of NO. Furthermore, selective use of pharmacological agents can be used to confirm the NO mediated effects on firing threshold and action potential AHP. It would be prudent for future investigations to take into consideration the recent demonstration that the Na^+K^+ATPase is intimately involved in short-term memory of motor performance as well as cardiac function by clarifying the possible involvement of NO (Gan et al., 2012, Zhang and Sillar, 2012)

Although NO clearly modulated both fictive locomotion and individual motor neurons, several questions remain unanswered and I have attempted to identify these in my summary of the results detailed in this thesis. The task of taking forward these findings is to not only clarify the detailed sequence and mechanism of NO mediated effect but also determine the possibility that NO modulates locomotor output within a modulatory hierarchy or by action in concert with other neurotransmitters, as has already been described in the tadpole and lamprey (McLean and Sillar, 2004, Kyriakatos and El Manira, 2007).

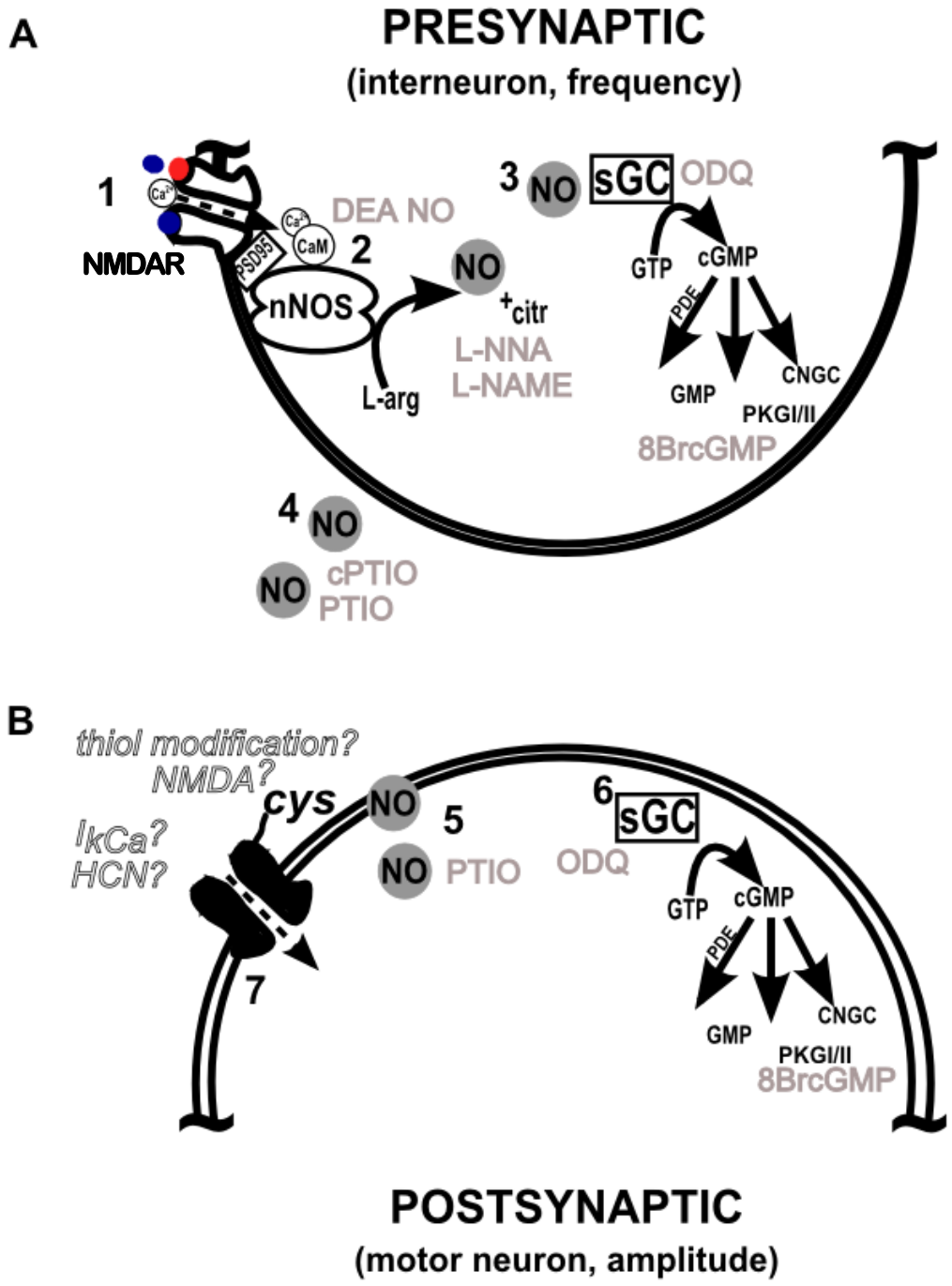

Figure 5.1. Schematic diagram summarizing the findings and possible sites of NO modulation in representative **A** pre and **B** postsynaptic neurons in the spinal locomotor circuitry. **1,** NMDA receptor activation triggers Ca^{2+} influx followed by the activation of NOS. **2**, Activated NOS catalyses the production of NO from L-arginine and **3**, NO binds to and activates sGC initiating the conversion of GMP to cGMP with the subsequent activation of secondary messenger pathways such as PKG. **4**, NO is free to diffuse to both intra and extracellular targets (auto and paracrine). **5**, NO diffuses across the synapse, **6** activating secondary messenger pathways in the postsynaptic neuron. **7,** NO targets not investigated in the present study but of relevance to future studies include direct and indirect activation ion channels as well as protein modifications such as s-nitrosation. Pharmacological agents used in the present study are indicated near their propose site of action in grey text.

5.4 A role for NO in neuropathophysiology

The involvement of NO in pathophysiological conditions has been studied in relation to Multiple Sclerosis (MS) and Alzheimer's Disease (AD) as well as Amyotrophic Lateral Sclerosis (Smith et al., 1997, Smith et al., 2001, Barber and Shaw, 2010). While NO does not appear to be a causative agent, the literature suggests that NO may be symptomatic or facilitative of disease progression. In Multiple Sclerosis research, NO primarily produced during the inflammatory response blocks axonal conduction and NO metabolites have been detected at high levels in the cerebrospinal fluid of MS patients (Giovannoni, 1998). Similarly, in Alzheimer's Disease, peroxynitrite produced by the reaction of nitric oxide with superoxide has been shown to nitrate neurons including those that contain neurofibrillary tangles (Smith et al., 1997). In AD, phosphodiesterase inhibitors have been shown to ameliorate the adverse effects of pathogenic NO (Pifarre et al., 2011).

As mentioned previously (Chapter 2, Section 2.1.4), in the mouse model of ALS, NO has been shown to facilitate axon retraction (C), synaptic stripping (C) and programmed cell death, by both cGMP dependent and independent mechanisms.
Although it is unlikely that NO is a causative agent of motor neuron loss, the aforementioned effects of NO in the mouse model of ALS, coupled with the absence of data investigating changes in NOS expression or any other changes occurring early in development before symptoms appear, provide the impetus to consider what developmental role NO may play in ALS. Indeed, recent studies have shown increased excitability linked to aberrant behaviour of both Na^{+} and Ca^{2+} channels early in development (Pambo-Pambo et al., 2009, Quinlan et al., 2011).

The present study has provided anatomical evidence that changes in protein expression are present in postnatal SOD^{G93A} mice. The NADPH diaphorase reactivity pattern in the $SOD1^{G93A}$ and SOD1 wild-type lumbar spinal cord of littermates at P12 is similar to the pattern documented in other species (Dun et al., 1993, Schreiberová et al., 2006) and closely resembled that of the CD1 inbred strain from the same species (Chapter 2, Section 2.3.1). However, NADPH diaphorase reactivity in the IML of lamina VII was

considerably lower in $SOD1^{G93A}$ mice compared to the SOD1 wild type (Chapter 2, Section 2.3.1). It is not possible to determine the relevance of this reduction in NADPH diaphorase reactivity based on anatomical evidence alone. It is also not possible to determine whether the reduction in NADPH diaphorase reactivity is a result of a reduction in NOS expression or a loss of NOS expressing neurons. It is known that neurons in the IML comprise of sympathetic preganglionic neurons and NO is known to facilitate vascular smooth muscle relaxation, but without further investigation it is not possible to give a putative role for NO in this cohort of neurons in this pathophysiological model. At this time, this is the first report and earliest developmental evidence that NOS reactivity is altered in the $SOD1^{G93A}$ mouse model of human ALS. NO is likely to be symptomatic and not the causative agent of ALS progression and thus a full investigation into the extent of and cause of NOS expression changes in the $SOD1^{G93A}$ mouse model of ALS is needed. The findings of the present study warrant further investigation, possibly using both whole nerve and single cell electrophysiology to determine the functional impact of this loss of NADPH diaphorase reactivity. Furthermore, additional anatomical studies are needed to determine the transmitter phenotype of the neurons that are not detected or are no longer NADPH diaphorase reactive.

5.5 Conclusion

In this thesis, I have shown that NO is produced by and acts as a potent modulator of locomotor related activity in the mammalian lumbar spinal cord. NO is produced by NOS which has long been established as an NADPH diaphorase enzyme. Utilising the NADPH diaphorase reaction, I have shown that in agreement with studies in other species, discrete populations of neurons express NOS in the developing spinal cord and that these neurons increase in number over the first 12 postnatal days. This thesis has reported the spatial and developmental distribution of NOS positive neurons in higher resolution than any other study at this time. The pattern of NOS reactivity in the SOD^{G93A} mouse model of human ALS was investigated at postnatal day 12 in both mutant and wild-type SOD mice. Consistent with the results of the inbred CD1 strain, SOD wild-type mice display similar number and identical distribution of NOS positive

neurons in the lumbar spinal cord. However, there is a marked reduction in NOS positive neurons in the IML lamina VII in SOD^{G93A} mice. This is the first report of a reduction in a distinct phenotype of neuron in the rodent ALS model at this postnatal stage of development and as such this result warrants further investigation and supports the investigation of NO mediated processes in neurodegenerative diseases.

I have shown for the first time that in the rodent, NO modulates pharmacologically induced fictive locomotion in the isolated spinal cord preparation. Using the NO donor DEA NO, the results here show that over a range of concentrations, sources of exogenous NO inhibit the frequency of locomotor related activity and that NO acts in a concentration dependent manner to increase (low concentrations) and decrease (high concentrations) the amplitude of motor neuron output. Scavengers of NO (cPTIO/PTIO) and inhibitors (L-NNA/L-NAME) of the NOS enzyme confirm that endogenous NO modulates the locomotor network in a similar manner to exogenous NO. However, due to the propensity for highly reactive NO to participate in numerous side reactions with oxidants (such as O_2 to form peroxynitrite), and with NO generated nitrates and nitrites, the results obtained using scavenger molecules such as cPTIO may conflate reactions of endogenous NO and therefore make interpretation of results obtained from experiments in which these agents are used difficult to interpret. Experiments utilising the disinhibited preparation, where inhibition is blocked using strychnine and bicuculline, suggest that NO predominantly exerts its effects through modulation of the excitatory neuronal locomotor network. I have also shown that NO alters the intrinsic properties of spinal motor neurons by reducing the threshold for action potential firing and reducing the action potential AHP.

It has been established that NO predominantly exerts its effects through sGC and the subsequent initiation by cGMP of the PKG pathway. In this thesis I have shown that the NO mediated modulation of locomotor output occurs predominantly by the NO/sGC/cGMP/PKG pathway using firstly the inhibitor of sGC, ODQ and the partial PKG agonist 8BrcGMP, as well as the coapplication of DEA NO and ODQ, to show that the cGMP pathway is the mechanism of modulation of motor neuron amplitude but that a component of the effects observed on frequency may be a result of thiol

modification. In future studies this will need to be clarified using pharmacological agents that either generate or ablate the effects of NO metabolites.

Taken as a whole, it can be concluded that NO modulates fictive locomotor output in the isolated mammalian spinal cord preparation by modulating the excitatory neuronal network although due to the complex reactivity of NO further research is needed to clarify and support the results herein.

References

AGGARWAL, S. & CUDKOWICZ, M. 2008. ALS drug development: Reflections from the past and a way forward. *Neurotherapeutics,* 5**,** 516-527.

AGHAJANIAN, G. K. & RASMUSSEN, K. 1989. Intracellular studies in the facial nucleus illustrating a simple new method for obtaining viable motor neurons in adult rat brain slices. *Synapse,* 3**,** 331-338.

AKAIKE, T., YOSHIDA, M., MIYAMOTO, Y., SATO, K., KOHNO, M., SASAMOTO, K., MIYAZAKI, K., UEDA, S. & MAEDA, H. 1993. Antagonistic action of imidazolineoxyl N-oxides against endothelium-derived relaxing factor/.bul.NO (nitric oxide) through a radical reaction. *Biochemistry,* 32**,** 827-832.

ALVAREZ, F. J. & FYFFE, R. E. W. 2007. The continuing case for the Renshaw cell. *The Journal of Physiology,* 584**,** 31-45.

ARTINIAN, L., TORNIERI, K., ZHONG, L., BARO, D. & REHDER, V. 2010. Nitric Oxide Acts as a Volume Transmitter to Modulate Electrical Properties of Spontaneously Firing Neurons via Apamin-Sensitive Potassium Channels. *The Journal of Neuroscience,* 30**,** 1699-1711.

BALLION, B., MORIN, D. & VIALA, D. 2001. Forelimb locomotor generators and quadrupedal locomotion in the neonatal rat. *European Journal of Neuroscience,* 14**,** 1727-1738.

BALTRONS, M., BORÁN, M., PIFARRÉ, P. & GARCÍA, A. 2008. Regulation and Function of Cyclic GMP-Mediated Pathways in Glial Cells. *Neurochemical Research,* 33**,** 2427-2435.

BARBER, S. C. & SHAW, P. J. 2007. Chapter 4 Molecular mechanisms of motor neuron degeneration in amyotrophic lateral sclerosis. *In:* ANDREW, A. E. & PAMELA, J. S. (eds.) *Handbook of Clinical Neurology.* Elsevier.

BARBER, S. N. C. & SHAW, P. J. 2010. Oxidative stress in ALS: Key role in motor neuron injury and therapeutic target. *Free Radical Biology and Medicine,* 48**,** 629-641.

BARRIERE, G., BERTRAND, S. & CAZALETS, J.-R. 2005. Peptidergic neuromodulation of the lumbar locomotor network in the neonatal rat spinal cord. *Peptides,* 26**,** 277-286.

BARROSO, A., OLIVEIRA, L., CAMPESATTO-MELLA, E., SILVA, C., TIMÓTEO, M. A., MAGALHÃES-CARDOSO, M. T., ALVES-DO-PRADO, W. & CORREIA-DE-SÁ, P. 2007. L-Citrulline inhibits [3H]acetylcholine release from rat motor nerve terminals by increasing adenosine outflow and activation of A1 receptors. *British Journal of Pharmacology,* 151**,** 541-550.

BEATO, M., BRACCI, E. & NISTRI, A. 1997. Contribution of NMDA and Non-NMDA Glutamate Receptors to Locomotor Pattern Generation in the Neonatal Rat Spinal Cord. *Proceedings: Biological Sciences,* 264**,** 877-884.

BELLAMY, T. C., WOOD, J. & GARTHWAITE, J. 2002. On the activation of soluble guanylyl cyclase by nitric oxide. *Proceedings of the National Academy of Sciences,* 99**,** 507-510.

BELLAMY, T. C., WOOD, J., GOODWIN, D. A. & GARTHWAITE, J. 2000. Rapid desensitization of the nitric oxide receptor, soluble guanylyl cyclase, underlies

diversity of cellular cGMP responses. *Proceedings of the National Academy of Sciences,* 97**,** 2928-2933.

BEN-ARI, Y., CHERUBINI, E., CORRADETTI, R. & GAIARSA, J. L. 1989. Giant synaptic potentials in immature rat CA3 hippocampal neurones. *The Journal of Physiology,* 416**,** 303-325.

BEN-ARI, Y. & SPITZER, N. C. 2010. Phenotypic checkpoints regulate neuronal development. *Trends in neurosciences,* 33**,** 485-492.

BENSIMON, G., LACOMBLEZ, L. & MEININGER, V. 1994. A Controlled Trial of Riluzole in Amyotrophic Lateral Sclerosis. *New England Journal of Medicine,* 330**,** 585-591.

BERTRAND, S. & CAZALETS, J.-R. 2002. The respective contribution of lumbar segments to the generation of locomotion in the isolated spinal cord of newborn rat. *European Journal of Neuroscience,* 16**,** 1741-1750.

BIEL, M., WAHL-SCHOTT, C., MICHALAKIS, S. & ZONG, X. 2009. Hyperpolarization-Activated Cation Channels: From Genes to Function. *Physiological Reviews,* 89**,** 847-885.

BOILLEE, S., VANDE VELDE, C. & CLEVELAND, D. 2006. ALS: A Disease of Motor Neurons and Their Nonneuronal Neighbors. *Neuron,* 52**,** 39-59.

BON, C. L. M. & GARTHWAITE, J. 2001. Exogenous nitric oxide causes potentiation of hippocampal synaptic transmission during low-frequency stimulation via the endogenous nitric oxide–cGMP pathway. *European Journal of Neuroscience,* 14**,** 585-594.

BONNOT, A., CHUB, N., PUJALA, A. & O'DONOVAN, M. J. 2009. Excitatory Actions of Ventral Root Stimulation During Network Activity Generated by the Disinhibited Neonatal Mouse Spinal Cord. *Journal of Neurophysiology,* 101**,** 2995-3011.

BONNOT, A., MORIN, D. & VIALA, D. 1998. Genesis of spontaneous rhythmic motor patterns in the lumbosacral spinal cord of neonate mouse. *Developmental Brain Research,* 108**,** 89-99.

BONNOT, A., WHELAN, P. J., MENTIS, G. Z. & O'DONOVAN, M. J. 2002a. Locomotor-like activity generated by the neonatal mouse spinal cord. *Brain Research Reviews,* 40**,** 141-151.

BONNOT, A., WHELAN, P. J., MENTIS, G. Z. & O'DONOVAN, M. J. 2002b. Spatiotemporal Pattern of Motoneuron Activation in the Rostral Lumbar and the Sacral Segments during Locomotor-Like Activity in the Neonatal Mouse Spinal Cord. *The Journal of Neuroscience,* 22**,** RC203.

BOSWELL-SMITH, V., SPINA, D. & PAGE, C. P. 2006. Phosphodiesterase inhibitors. *British Journal of Pharmacology,* 147**,** S252-S257.

BOULTON, C. L., SOUTHAM, E. & GARTHWAITE, J. 1995. Nitric oxide-dependent long-term potentiation is blocked by a specific inhibitor of soluble guanylyl cyclase. *Neuroscience,* 69**,** 699-703.

BRACCI, E., BALLERINI, L. & NISTRI, A. 1996. Localization of Rhythmogenic Networks Responsible for Spontaneous Bursts Induced by Strychnine and Bicuculline in the Rat Isolated Spinal Cord. *The Journal of Neuroscience,* 16**,** 7063-7076.

BRADLEY, S., TOSSELL, K., LOCKLEY, R. & MCDEARMID, J. R. 2010. Nitric Oxide Synthase Regulates Morphogenesis of Zebrafish Spinal Cord Motoneurons. *The Journal of Neuroscience,* 30**,** 16818-16831.

BRANCHEREAU, P., MORIN, D., BONNOT, A., BALLION, B., CHAPRON, J. & VIALA, D. 2000. Development of lumbar rhythmic networks: from embryonic to neonate locomotor-like patterns in the mouse. *Brain Research Bulletin,* 53**,** 711-718.

BREDT, D. S. & SNYDER, S. H. 1989. NITRIC-OXIDE MEDIATES GLUTAMATE-LINKED ENHANCEMENT OF CGMP LEVELS IN THE CEREBELLUM. *Proceedings of the National Academy of Sciences of the United States of America,* 86**,** 9030-9033.

BREDT, D. S. & SNYDER, S. H. 1992. NITRIC-OXIDE, A NOVEL NEURONAL MESSENGER. *Neuron,* 8**,** 3-11.

BRENMAN, J. E., CHAO, D. S., GEE, S. H., MCGEE, A. W., CRAVEN, S. E., SANTILLANO, D. R., WU, Z., HUANG, F., XIA, H., PETERS, M. F., FROEHNER, S. C. & BREDT, D. S. 1996. Interaction of Nitric Oxide Synthase with the Postsynaptic Density Protein PSD95 and Syntrophin Mediated by PDZ Domains. *Cell,* 84**,** 757-767.

BROCK, L. G., COOMBS, J. S. & ECCLES, J. C. 1952. The recording of potentials from motoneurones with an intracellular electrode. *The Journal of Physiology,* 117**,** 431-460.

BROWN, G. C. & BORUTAITE, V. 2007. Nitric oxide and mitochondrial respiration in the heart. *Cardiovascular Research,* 75**,** 283-290.

BROWN, G. C. & COOPER, C. E. 1994. Nanomolar concentrations of nitric oxide reversibly inhibit synaptosomal respiration by competing with oxygen at cytochrome oxidase. *FEBS Letters,* 356**,** 295-298.

BROWN, T. G. 1911. The Intrinsic Factors in the Act of Progression in the Mammal. *Proceedings of the Royal Society of London. Series B, Containing Papers of a Biological Character,* 84**,** 308-319.

BROWN, T. G. 1914. On the nature of the fundamental activity of the nervous centres; together with an analysis of the conditioning of rhythmic activity in progression, and a theory of the evolution of function in the nervous system. *The Journal of Physiology,* 48**,** 18-46.

BROWNSTONE, R. M. 2006. Beginning at the end: Repetitive firing properties in the final common pathway. *Progress in Neurobiology,* 78**,** 156-172.

BROWNSTONE, R. M. & BUI, T. V. 2010. Spinal interneurons providing input to the final common path during locomotion. *In:* GOSSARD, J. P. D. R. K. A. (ed.) *Breathe, Walk and Chew: The Neural Challenge: Part I.*

BROWNSTONE, R. M. & STUART, D. G. 2011. Whither motoneurons? . *Brain Research,* 1409**,** 93-103.

BROWNSTONE, R. M. & WILSON, J. M. 2008. Strategies for delineating spinal locomotor rhythm-generating networks and the possible role of Hb9 interneurones in rhythmogenesis. *Brain Research Reviews,* 57**,** 64-76.

BURKE, R. E., DEGTYARENKO, A. M. & SIMON, E. S. 2001. Patterns of Locomotor Drive to Motoneurons and Last-Order Interneurons: Clues to the Structure of the CPG. *Journal of Neurophysiology,* 86**,** 447-462.

BUTT, S. J. B., LUNDFALD, L. & KIEHN, O. 2005. EphA4 defines a class of excitatory locomotor-related interneurons. *Proceedings of the National Academy of Sciences of the United States of America,* 102**,** 14098-14103.

CADIOU, H., STUDER, M., JONES, N. G., SMITH, E. S. J., BALLARD, A., MCMAHON, S. B. & MCNAUGHTON, P. A. 2007. Modulation of Acid-

Sensing Ion Channel Activity by Nitric Oxide. *The Journal of Neuroscience,* 27**,** 13251-13260.

CARLIN, K. P., DAI, Y. & JORDAN, L. M. 2006. Cholinergic and Serotonergic Excitation of Ascending Commissural Neurons in the Thoraco-Lumbar Spinal Cord of the Neonatal Mouse. *Journal of Neurophysiology,* 95**,** 1278-1284.

CARY, S. P. L., WINGER, J. A., DERBYSHIRE, E. R. & MARLETTA, M. A. 2006. Nitric oxide signaling: no longer simply on or off. *Trends in biochemical sciences,* 31**,** 231-239.

CATTERALL, W. A. 2000. From Ionic Currents to Molecular Mechanisms: The Structure and Function of Voltage-Gated Sodium Channels. *Neuron,* 26**,** 13-25.

CAZALETS, J. R., SQALLI-HOUSSAINI, Y. & CLARAC, F. 1992. Activation of the central pattern generators for locomotion by serotonin and excitatory amino acids in neonatal rat. *The Journal of Physiology,* 455**,** 187-204.

CHOI, J. & FARLEY, J. M. 1998. Effects of 8-Bromo-Cyclic GMP on Membrane Potential of Single Swine Tracheal Smooth Muscle Cells. *Journal of Pharmacology and Experimental Therapeutics,* 285**,** 588-594.

CHOI, Y.-B., TENNETI, L., LE, D. A., ORTIZ, J., BAI, G., CHEN, H.-S. V. & LIPTON, S. A. 2000. Molecular basis of NMDA receptor-coupled ion channel modulation by S-nitrosylation. *Nat Neurosci,* 3**,** 15-21.

CHRISTIE, K. J. & WHELAN, P. J. 2005. Monoaminergic Establishment of Rostrocaudal Gradients of Rhythmicity in the Neonatal Mouse Spinal Cord. *Journal of Neurophysiology,* 94**,** 1554-1564.

CLARAC, F. O. 2008. Some historical reflections on the neural control of locomotion. *Brain Research Reviews,* 57**,** 13-21.

CLARAC, F. O., VINAY, L., CAZALETS, J.-R., FADY, J.-C. & JAMON, M. 1998. Role of gravity in the development of posture and locomotion in the neonatal rat. *Brain Research Reviews,* 28**,** 35-43.

CLEMENS, S., RYE, D. & HOCHMAN, S. 2006. Restless legs syndrome - Revisiting the dopamine hypothesis from the spinal cord perspective. *Neurology,* 67**,** 125-130.

COLLETT, E. 2007. *The developmental and activity-dependent distribution of nitric oxide synthase in the mouse spinal cord measured using NADPH-diaphorase histochemistry.* Bsc (Hons), University of St Andrews.

COWLEY, K. C., ZAPOROZHETS, E., MACLEAN, J. N. & SCHMIDT, B. J. 2005. Is NMDA Receptor Activation Essential for the Production of Locomotor-Like Activity in the Neonatal Rat Spinal Cord? *Journal of Neurophysiology,* 94**,** 3805-3814.

CRONE, S. A., QUINLAN, K. A., ZAGORAIOU, L., DROHO, S., RESTREPO, C. E., LUNDFALD, L., ENDO, T., SETLAK, J., JESSELL, T. M., KIEHN, O. & SHARMA, K. 2008. Genetic Ablation of V2a Ipsilateral Interneurons Disrupts Left-Right Locomotor Coordination in Mammalian Spinal Cord. *Neuron,* 60**,** 70-83.

CRONE, S. A., ZHONG, G., HARRIS-WARRICK, R. & SHARMA, K. 2009. In Mice Lacking V2a Interneurons, Gait Depends on Speed of Locomotion. *The Journal of Neuroscience,* 29**,** 7098-7109.

CURRIE, P. J., MIRZA, A., DONO, L. M., JOHN, C. S. & WALL, D. G. 2011. Anorexigenic action of nitric oxide synthase inhibition in the raphe nuclei. *NeuroReport,* 22**,** 696-699

CURY, Y., PICOLO, G., GUTIERREZ, V. P. & FERREIRA, S. H. 2011. Pain and analgesia: The dual effect of nitric oxide in the nociceptive system. *Nitric Oxide,* 25**,** 243-254.

DAFF, S. 2010. NO synthase: Structures and mechanisms. *Nitric Oxide,* 23**,** 1-11.

DAWSON, T. M., BREDT, D. S., FOTUHI, M., HWANG, P. M. & SNYDER, S. H. 1991. Nitric oxide synthase and neuronal NADPH diaphorase are identical in brain and peripheral tissues. *Proceedings of the National Academy of Sciences,* 88**,** 7797-7801.

DAWSON, T. M., SASAKI, M., GONZALEZ-ZULUETA, M. & DAWSON, V. L. 1998. Chapter 1 Regulation of neuronal nitric oxide synthase and identification of novel nitric oxide signaling pathways. *In:* R. RANNEY MIZE, T. M. D. V. L. D. & MICHAEL, J. F. (eds.) *Progress in Brain Research.* Elsevier.

DE VENTE, J., MARKERINK-VAN ITTERSUM, M. & VLES, J. S. H. 2006. The role of phosphodiesterase isoforms 2, 5, and 9 in the regulation of NO-dependent and NO-independent cGMP production in the rat cervical spinal cord. *Journal of Chemical Neuroanatomy,* 31**,** 275-303.

DENNINGER, J. W. & MARLETTA, M. A. 1999. Guanylate cyclase and the sGC/NO/cGMP signaling pathway. *Biochimica et Biophysica Acta (BBA) - Bioenergetics,* 1411**,** 334-350.

DERBYSHIRE, E. R., DENG, S. & MARLETTA, M. A. 2010. Incorporation of Tyrosine and Glutamine Residues into the Soluble Guanylate Cyclase Heme Distal Pocket Alters NO and O(2) Binding. *Journal of Biological Chemistry,* 285**,** 17471-17478.

DING, J.-D. & WEINBERG, R. J. 2006. Localization of soluble guanylyl cyclase in the superficial dorsal horn. *The Journal of Comparative Neurology,* 495**,** 668-678.

DOUGLAS, J., NOGA, B., DAI, X. & JORDAN, L. 1993. The effects of intrathecal administration of excitatory amino acid agonists and antagonists on the initiation of locomotion in the adult cat. *The Journal of Neuroscience,* 13**,** 990-1000.

DUN, N. J., DUN, S. L., WU, S. Y., FORSTERMANN, U., SCHMIDT, H. H. H. W. & TSENG, L. F. 1993. Nitric oxide synthase immunoreactivity in the rat, mouse, cat and squirrel monkey spinal cord. *Neuroscience,* 54**,** 845-857.

DUNBAR, M. J., TRAN, M. A. & WHELAN, P. J. 2010. Endogenous extracellular serotonin modulates the spinal locomotor network of the neonatal mouse. *The Journal of Physiology,* 588**,** 139-156.

DUNCAN, A. J. & HEALES, S. J. R. 2005. Nitric oxide and neurological disorders. *Molecular Aspects of Medicine,* 26**,** 67-96.

ELOFSSON, R., CARLBERG, M., MOROZ, L., NEZLIN, L. & SAKHAROV, D. 1993. Is nitric oxide (NO) produced by invertebrate neurones? *NeuroReport,* 4**,** 279-282.

FENG, C. & TOLLIN, G. 2009. Regulation of interdomain electron transfer in the NOS output state for NO production. *Dalton Transactions***,** 6692-6700.

FERGUSON, S. M. & BLAKELY, R. D. 2004. The choline transporter resurfaces: new roles for synaptic vesicles? *Molecular interventions,* 4**,** 22-37.

FERNHOFF, N. B., DERBYSHIRE, E. R. & MARLETTA, M. A. 2009. A nitric oxide/cysteine interaction mediates the activation of soluble guanylate cyclase. *Proceedings of the National Academy of Sciences,* 106**,** 21602-21607.

FOSTER, J. A. & PHELPS, P. E. 2000. Neurons expressing NADPH-diaphorase in the developing human spinal cord. *The Journal of Comparative Neurology,* 427**,** 417-427.

FRANCIS, S. H., BUSCH, J. L. & CORBIN, J. D. 2010. cGMP-Dependent Protein Kinases and cGMP Phosphodiesterases in Nitric Oxide and cGMP Action. *Pharmacological Reviews,* 62**,** 525-563.

FRIEBE, A. & KOESLING, D. 2003. Regulation of Nitric Oxide-Sensitive Guanylyl Cyclase. *Circulation Research,* 93**,** 96-105.

FRIEBE, A., MERGIA, E., DANGEL, O., LANGE, A. & KOESLING, D. 2007. Fatal gastrointestinal obstruction and hypertension in mice lacking nitric oxide-sensitive guanylyl cyclase. *Proceedings of the National Academy of Sciences,* 104**,** 7699-7704.

GABBAY, H. & LEV-TOV, A. 2004. Alpha-1 Adrenoceptor Agonists Generate a "Fast" NMDA Receptor-Independent Motor Rhythm in the Neonatal Rat Spinal Cord. *Journal of Neurophysiology,* 92**,** 997-1010.

GAN, X., HUNTER, J., HUANG, C., XUE, J., RAJAPUROHITAM, V., JAVADOV, S. & KARMAZYN, M. 2012. Ouabain increases iNOS-dependent nitric oxide generation which contributes to the hypertrophic effect of the glycoside: possible role of peroxynitrite formation. *Molecular and Cellular Biochemistry,* 363**,** 323-333.

GAO, S., CHENG, C., ZHAO, J., CHEN, M., LI, X., SHI, S., NIU, S., QIN, J., LU, M. & SHEN, A. 2008. Developmental regulation of PSD-95 and nNOS expression in lumbar spinal cord of rats. *Neurochemistry International,* 52**,** 495-501.

GARRAWAY, S. M. & HOCHMAN, S. 2001. Pharmacological characterization of serotonin receptor subtypes modulating primary afferent input to deep dorsal horn neurons in the neonatal rat. *British Journal of Pharmacology,* 132**,** 1789-1798.

GARTHWAITE, J. 2010. New insight into the functioning of nitric oxide-receptive guanylyl cyclase: physiological and pharmacological implications. *Molecular and Cellular Biochemistry,* 334**,** 221-232.

GARTHWAITE, J., SOUTHAM, E., BOULTON, C. L., NIELSEN, E. B., SCHMIDT, K. & MAYER, B. 1995. Potent and selective inhibition of nitric oxide sensitive guanyly cyclase by 1H- 1,2,4 Oxadiazolo 4,3-A quinoxalin-1-one. *Molecular Pharmacology,* 48**,** 184-188.

GIOVANNONI, G. 1998. Cerebrospinal fluid and serum nitric oxide metabolites in patients with multiple sclerosis. *Multiple Sclerosis,* 4**,** 27-30.

GOLDIN, A. L., BARCHI, R. L., CALDWELL, J. H., HOFMANN, F., HOWE, J. R., HUNTER, J. C., KALLEN, R. G., MANDEL, G., MEISLER, M. H., NETTER, Y. B., NODA, M., TAMKUN, M. M., WAXMAN, S. G., WOOD, J. N. & CATTERALL, W. A. 2000. Nomenclature of voltage-gated sodium channels. *Neuron,* 28**,** 365-368.

GONZALEZ-ISLAS, C., CHUB, N., GARCIA-BEREGUIAIN, M. A. & WENNER, P. 2010. GABAergic Synaptic Scaling in Embryonic Motoneurons Is Mediated by a Shift in the Chloride Reversal Potential. *The Journal of Neuroscience,* 30**,** 13016-13020.

GONZALEZ-ISLAS, C., CHUB, N. & WENNER, P. 2009. NKCC1 and AE3 Appear to Accumulate Chloride in Embryonic Motoneurons. *Journal of Neurophysiology,* 101**,** 507-518.

GORDON, I. T., DUNBAR, M. J., VANNESTE, K. J. & WHELAN, P. J. 2008. Interaction Between Developing Spinal Locomotor Networks in the Neonatal Mouse. *Journal of Neurophysiology,* 100**,** 117-128.

GORDON, I. T. & WHELAN, P. J. 2006a. Deciphering the organization and modulation of spinal locomotor central pattern generators. *Journal of Experimental Biology,* 209**,** 2007-2014.

GORDON, I. T. & WHELAN, P. J. 2006b. Monoaminergic Control of Cauda-Equina-Evoked Locomotion in the Neonatal Mouse Spinal Cord. *Journal of Neurophysiology,* 96**,** 3122-3129.

GOSGNACH, S., LANUZA, G. M., BUTT, S. J. B., SAUERESSIG, H., ZHANG, Y., VELASQUEZ, T., RIETHMACHER, D., CALLAWAY, E. M., KIEHN, O. & GOULDING, M. 2006. V1 spinal neurons regulate the speed of vertebrate locomotor outputs. *Nature,* 440**,** 215-219.

GOULDING, M. 2009. Circuits controlling vertebrate locomotion: moving in a new direction. *Nat Rev Neurosci,* 10**,** 507-518.

GRIFFITH, O. W. & KILBOURN, R. G. 1996. Nitric oxide synthase inhibitors: Amino acids. *In:* LESTER, P. (ed.) *Methods in Enzymology.* Academic Press.

GRIFFITHS, C., WYKES, V., BELLAMY, T. C. & GARTHWAITE, J. 2003. A New and Simple Method for Delivering Clamped Nitric Oxide Concentrations in the Physiological Range: Application to Activation of Guanylyl Cyclase-Coupled Nitric Oxide Receptors. *Molecular Pharmacology,* 64**,** 1349-1356.

GRILLNER, S. 2011. Control of Locomotion in Bipeds, Tetrapods, and Fish. *Comprehensive Physiology*.

GUTMAN, G. A., CHANDY, K. G., GRISSMER, S., LAZDUNSKI, M., MCKINNON, D., PARDO, L. A., ROBERTSON, G. A., RUDY, B., SANGUINETTI, M. C., STUHMER, W. & WANG, X. 2005. International Union of Pharmacology. LIII. Nomenclature and Molecular Relationships of Voltage-Gated Potassium Channels. *Pharmacological Reviews,* 57**,** 473-508.

HALVEY, E. J., VERNON, J., ROY, B. & GARTHWAITE, J. 2009. Mechanisms of Activity-dependent Plasticity in Cellular Nitric Oxide-cGMP Signaling. *Journal of Biological Chemistry,* 284**,** 25630-25641.

HAMMELMANN, V., ZONG, X., HOFMANN, F., MICHALAKIS, S. & BIEL, M. 2011. The cGMP-Dependent Protein Kinase II Is an Inhibitory Modulator of the Hyperpolarization-Activated HCN2 Channel. *PLoS ONE,* 6**,** e17078.

HAN, P., NAKANISHI, S. T., TRAN, M. A. & WHELAN, P. J. 2007. Dopaminergic Modulation of Spinal Neuronal Excitability. *The Journal of Neuroscience,* 27**,** 13192-13204.

HANSON, M. G. & LANDMESSER, L. T. 2003. Characterization of the Circuits That Generate Spontaneous Episodes of Activity in the Early Embryonic Mouse Spinal Cord. *The Journal of Neuroscience,* 23**,** 587-600.

HAYES, H. B., CHANG, Y.-H. & HOCHMAN, S. 2009. An In Vitro Spinal Cord‚ÄìHindlimb Preparation for Studying Behaviorally Relevant Rat Locomotor Function. *Journal of Neurophysiology,* 101**,** 1114-1122.

HECKMAN, C. J., MOTTRAM, C., QUINLAN, K., THEISS, R. & SCHUSTER, J. 2009. Motoneuron excitability: The importance of neuromodulatory inputs. *Clinical neurophysiology : official journal of the International Federation of Clinical Neurophysiology,* 120**,** 2040-2054.

HEISE, C. K., G. 2004. Cytoarchitecture of the Spinal Cord. *In:* WATSON, C., PAXINOS, G. & KAYALIOGLU, G. (ed.) *The Spinal Cord: A Christopher and Dana Reeve Foundation Text and Atlas* Elsevier Ltd.

HESS, D. T., PATTERSON, S. I., SMITH, D. S. & SKENE, J. H. P. 1993. Neuronal growth cone collapse and inhibition of protein fatty acylation by nitric oxide. *Nature,* 366**,** 562-565.

HILLE, B. 2001. *Ion channels of excitable membranes. Edition 3*.

HOFMANN, F., BERNHARD, D., LUKOWSKI, R. & WEINMEISTER, P. 2009. cGMP Regulated Protein Kinases (cGK) cGMP: Generators, Effectors and Therapeutic Implications. *In:* SCHMIDT, H. H. H. W., HOFMANN, F. & STASCH, J.-P. (eds.). Springer Berlin Heidelberg.

HOFSETH, L. J., SAITO, S., HUSSAIN, S. P., ESPEY, M. G., MIRANDA, K. M., ARAKI, Y., JHAPPAN, C., HIGASHIMOTO, Y., HE, P. J., LINKE, S. P., QUEZADO, M. M., ZURER, I., ROTTER, V., WINK, D. A., APPELLA, E. & HARRIS, C. C. 2003. Nitric oxide-induced cellular stress and p53 activation in chronic inflammation. *Proceedings of the National Academy of Sciences of the United States of America,* 100**,** 143-148.

HOPE, B. T., MICHAEL, G. J., KNIGGE, K. M. & VINCENT, S. R. 1991. Neuronal NADPH Diaphorase is a Nitric Oxide Synthase. *Proceedings of the National Academy of Sciences of the United States of America,* 88**,** 2811-2814.

IGNARRO, L. J., BUGA, G. M., WOOD, K. S., BYRNS, R. E. & CHAUDHURI, G. 1987. Endothelium-derived relaxing factor produced and released from artery and vein is nitric oxide. *Proceedings of the National Academy of Sciences,* 84**,** 9265-9269.

INGLIS, F. M., FURIA, F., ZUCKERMAN, K. E., STRITTMATTER, S. M. & KALB, R. G. 1998. The Role of Nitric Oxide and NMDA Receptors in the Development of Motor Neuron Dendrites. *The Journal of Neuroscience,* 18**,** 10493-10501.

IWAGAKI, N. 2011. *Modulation of mammalian spinal motor networks by group I metabotropic glutamate receptors: implications for locomotor control and the motor neuron disease Amyotrophic Lateral Sclerosis.* Doctor of Philosophy, Univeristy of St Andrews.

IWAGAKI, N. & MILES, G. B. 2011. Activation of group I metabotropic glutamate receptors modulates locomotor-related motoneuron output in mice. *Journal of Neurophysiology,* 105**,** 2108-2120.

IWANAGA, K., HAYASHI, S., OYAKE, M., HORIKAWA, Y., HAYASHI, T., WAKABAYASHI, M., KONDO, H., TSUJI, S. & TAKAHASHI, H. 1997. Neuropathology of sporadic amyotrophic lateral sclerosis of long duration. *Journal of the neurological sciences,* 146**,** 139-143.

JANKOWSKA, E. 2001. Spinal interneuronal systems: identification, multifunctional character and reconfigurations in mammals. *The Journal of Physiology,* 533**,** 31-40.

JANKOWSKA, E. 2008. Spinal interneuronal networks in the cat: Elementary components. *Brain Research Reviews,* 57**,** 46-55.

JEDLITSCHKY, G., BURCHELL, B. & KEPPLER, D. 2000. The Multidrug Resistance Protein 5 Functions as an ATP-dependent Export Pump for Cyclic Nucleotides. *Journal of Biological Chemistry,* 275**,** 30069-30074.

JENTSCH, T. J., STEIN, V., WEINREICH, F. & ZDEBIK, A. A. 2002. Molecular Structure and Physiological Function of Chloride Channels. *Physiological Reviews,* 82**,** 503-568.

JESSELL, T. M. 2000. Neuronal specification in the spinal cord: inductive signals and transcriptional codes. *Nat Rev Genet,* 1**,** 20-29.

JIANG, M., SCHUSTER, J. E., FU, R., SIDDIQUE, T. & HECKMAN, C. J. 2009. Progressive Changes in Synaptic Inputs to Motoneurons in Adult Sacral Spinal Cord of a Mouse Model of Amyotrophic Lateral Sclerosis. *The Journal of Neuroscience,* 29**,** 15031-15038.

JIANG, Z., CARLIN, K. P. & BROWNSTONE, R. M. 1999. An in vitro functionally mature mouse spinal cord preparation for the study of spinal motor networks. *Brain Research,* 816**,** 493-499.

JUVIN, L., SIMMERS, J. & MORIN, D. 2005. Propriospinal Circuitry Underlying Interlimb Coordination in Mammalian Quadrupedal Locomotion. *The Journal of Neuroscience,* 25**,** 6025-6035.

KANG, Y., DEMPO, Y., OHASHI, A., SAITO, M., TOYODA, H., SATO, H., KOSHINO, H., MAEDA, Y. & HIRAI, T. 2007. Nitric Oxide Activates Leak K+ Currents in the Presumed Cholinergic Neuron of Basal Forebrain. *Journal of Neurophysiology,* 98**,** 3397-3410.

KEEFER, L. K., NIMS, R. W., DAVIES, K. M. & WINK, D. A. 1996. NONOates, (1-substituted diazen-1-ium-1,2-diolates) as nitric oxide donors: Convenient nitric oxide dosage forms. *In:* LESTER, P. (ed.) *Methods in Enzymology.* Academic Press.

KIEHN, O. 2011. Development and functional organization of spinal locomotor circuits. *Current Opinion in Neurobiology,* 21**,** 100-109.

KIEHN, O. & EKEN, T. 1998. Functional role of plateau potentials in vertebrate motor neurons. *Current Opinion in Neurobiology,* 8**,** 746-752.

KIEHN, O. & KJAERULFF, O. 1996. Spatiotemporal characteristics of 5-HT and dopamine-induced rhythmic hindlimb activity in the in vitro neonatal rat. *Journal of Neurophysiology,* 75**,** 1472-1482.

KIEHN, O., SILLAR, K. T., KJAERULFF, O. & MCDEARMID, J. R. 1999. Effects of Noradrenaline on Locomotor Rhythm¸ÄìGenerating Networks in the Isolated Neonatal Rat Spinal Cord. *Journal of Neurophysiology,* 82**,** 741-746.

KIM, C. H., LEE, J., LEE, J.-Y. & ROCHE, K. W. 2008. Metabotropic glutamate receptors: Phosphorylation and receptor signaling. *Journal of Neuroscience Research,* 86**,** 1-10.

KJAERULFF, O. & KIEHN, O. 1996. Distribution of Networks Generating and Coordinating Locomotor Activity in the Neonatal Rat Spinal Cord In Vitro : A Lesion Study. *The Journal of Neuroscience,* 16**,** 5777-5794.

KNOWLES, R. G. & MONCADA, S. 1994. NITRIC-OXIDE SYNTHASES IN MAMMALS. *Biochemical Journal,* 298**,** 249-258.

KO, G. Y. & KELLY, P. T. 1999. Nitric Oxide Acts as a Postsynaptic Signaling Molecule in Calcium/Calmodulin-Induced Synaptic Potentiation in Hippocampal CA1 Pyramidal Neurons. *The Journal of Neuroscience,* 19**,** 6784-6794.

KOESLING, D., HERZ, J., GAUSEPOHL, H., NIROOMAND, F., HINSCH, K.-D., MULSCH, A., BOHME, E., SCHULTZ, G. & FRANK, R. 1988. The primary

structure of the 70 kDa subunit of bovine soluble guanylate cyclase. *FEBS Letters,* 239**,** 29-34.

KUDO, N. & YAMADA, T. 1987. N-Methyl-d,l-aspartate-induced locomotor activity in a spinal cord-indlimb muscles preparation of the newborn rat studied in vitro. *Neuroscience Letters,* 75**,** 43-48.

KUO, J. J., SCHONEWILLE, M., SIDDIQUE, T., SCHULTS, A. N. A., FU, R., BAR, P. R., ANELLI, R., HECKMAN, C. J. & KROESE, A. B. A. 2004. Hyperexcitability of Cultured Spinal Motoneurons From Presymptomatic ALS Mice. *Journal of Neurophysiology,* 91**,** 571-575.

KUO, J. J., SIDDIQUE, T., FU, R. & HECKMAN, C. J. 2005. Increased persistent Na+ current and its effect on excitability in motoneurones cultured from mutant SOD1 mice. *The Journal of Physiology,* 563**,** 843-854.

KUZKAYA, N., WEISSMANN, N., HARRISON, D. G. & DIKALOV, S. 2005. Interactions of peroxynitrite with uric acid in the presence of ascorbate and thiols: Implications for uncoupling endothelial nitric oxide synthase. *Biochemical Pharmacology,* 70**,** 343-354.

KWAN, A. C., DIETZ, S. B., WEBB, W. W. & HARRIS-WARRICK, R. M. 2009. Activity of Hb9 Interneurons during Fictive Locomotion in Mouse Spinal Cord. *The Journal of Neuroscience,* 29**,** 11601-11613.

KYRIAKATOS, A. & EL MANIRA, A. 2007. Long-Term Plasticity of the Spinal Locomotor Circuitry Mediated by Endocannabinoid and Nitric Oxide Signaling. *The Journal of Neuroscience,* 27**,** 12664-12674.

KYRIAKATOS, A., MOLINARI, M., MAHMOOD, R., GRILLNER, S., SILLAR, K. T. & EL MANIRA, A. 2009. Nitric Oxide Potentiation of Locomotor Activity in the Spinal Cord of the Lamprey. *The Journal of Neuroscience,* 29**,** 13283-13291.

LAMANAUSKAS, N. & NISTRI, A. 2008. Riluzole blocks persistent Na+ and Ca2+ currents and modulates release of glutamate via presynaptic NMDA receptors on neonatal rat hypoglossal motoneurons in vitro. *European Journal of Neuroscience,* 27**,** 2501-2514.

LANUZA, G. M., GOSGNACH, S., PIERANI, A., JESSELL, T. M. & GOULDING, M. 2004. Genetic Identification of Spinal Interneurons that Coordinate Left-Right Locomotor Activity Necessary for Walking Movements. *Neuron,* 42**,** 375-386.

LEBEAU, F. E. N., EL MANIRA, A. & GRILLER, S. 2005. Tuning the network: modulation of neuronal microcircuits in the spinal cord and hippocampus. *Trends in neurosciences,* 28**,** 552-561.

LEE, M. R., LI, L. & KITAZAWA, T. 1997. Cyclic GMP Causes Ca2+ Desensitization in Vascular Smooth Muscle by Activating the Myosin Light Chain Phosphatase. *Journal of Biological Chemistry,* 272**,** 5063-5068.

LI, D.-P., CHEN, S.-R., FINNEGAN, T. F. & PAN, H.-L. 2004. Signalling pathway of nitric oxide in synaptic GABA release in the rat paraventricular nucleus. *The Journal of Physiology,* 554**,** 100-110.

LI, W. C., PERRINS, R., SOFFE, S. R., YOSHIDA, M., WALFORD, A. & ROBERTS, A. 2001. Defining classes of spinal interneuron and their axonal projections in hatchling Xenopus laevis tadpoles. *The Journal of Comparative Neurology,* 441**,** 248-265.

LI, X. & BENNETT, D. J. 2007. Apamin-Sensitive Calcium-Activated Potassium Currents (SK) Are Activated by Persistent Calcium Currents in Rat Motoneurons. *Journal of Neurophysiology,* 97**,** 3314-3330.

LIPTON, S. A., CHOI, Y.-B., PAN, Z.-H., LEI, S. Z., CHEN, H.-S. V., SUCHER, N. J., LOSCALZO, J., SINGEL, D. J. & STAMLER, J. S. 1993. A redox-based mechanism for the neuroprotective and neurodestructive effects of nitric oxide and related nitroso-compounds. *Nature,* 364**,** 626-632.

LIU, J., AKAY, T., HEDLUND, P. B., PEARSON, K. G. & JORDAN, L. M. 2009. Spinal 5-HT7 Receptors Are Critical for Alternating Activity During Locomotion: In Vitro Neonatal and In Vivo Adult Studies Using 5-HT7 Receptor Knockout Mice. *Journal of Neurophysiology,* 102**,** 337-348.

LIU, J. & JORDAN, L. M. 2005. Stimulation of the Parapyramidal Region of the Neonatal Rat Brain Stem Produces Locomotor-Like Activity Involving Spinal 5-HT7 and 5-HT2A Receptors. *Journal of Neurophysiology,* 94**,** 1392-1404.

LOBE, C. G. & NAGY, A. 1998. Conditional genome alteration in mice. *BioEssays,* 20**,** 200-208.

LOCATELLI, F., CORTI, S., PAPADIMITRIOU, D., FORTUNATO, F., DEL BO, R., DONADONI, C., NIZZARDO, M., NARDINI, M., SALANI, S., GHEZZI, S., STRAZZER, S., BRESOLIN, N. & COMI, G. P. 2007. Fas small interfering RNA reduces motoneuron death in amyotrophic lateral sclerosis mice. *Annals of Neurology,* 62**,** 81-92.

LUNDBERG, J. O., WEITZBERG, E. & GLADWIN, M. T. 2008. The nitrate-nitrite-nitric oxide pathway in physiology and therapeutics. *Nat Rev Drug Discov,* 7**,** 156-167.

MADRIAGA, M. A., MCPHEE, L. C., CHERSA, T., CHRISTIE, K. J. & WHELAN, P. J. 2004. Modulation of Locomotor Activity by Multiple 5-HT and Dopaminergic Receptor Subtypes in the Neonatal Mouse Spinal Cord. *Journal of Neurophysiology,* 92**,** 1566-1576.

MAIHOFNER, C., EUCHENHOFER, C., TEGEDER, I., BECK, K. F., PFEILSCHIFTER, J. & GEISSLINGER, G. 2000. Regulation and immunhistochemical localization of nitric oxide synthases and soluble guanylyl cyclase in mouse spinal cord following nociceptive stimulation. *Neuroscience Letters,* 290**,** 71-75.

MARDER, E., BUCHER, D., SCHULZ, D. J. & TAYLOR, A. L. 2005. Invertebrate Central Pattern Generation Moves along. *Current Biology,* 15**,** R685-R699.

MARTIN, L. J., CHEN, K. & LIU, Z. 2005. Adult Motor Neuron Apoptosis Is Mediated by Nitric Oxide and Fas Death Receptor Linked by DNA Damage and p53 Activation. *The Journal of Neuroscience,* 25**,** 6449-6459.

MARTIN, L. J., LIU, Z., CHEN, K., PRICE, A. C., PAN, Y., SWABY, J. A. & GOLDEN, W. C. 2007. Motor neuron degeneration in amyotrophic lateral sclerosis mutant superoxide dismutase-1 transgenic mice: Mechanisms of mitochondriopathy and cell death. *The Journal of Comparative Neurology,* 500**,** 20-46.

MCCREA, D. A. & RYBAK, I. A. 2008. Organization of mammalian locomotor rhythm and pattern generation. *Brain Research Reviews,* 57**,** 134-146.

MCLEAN, D. L., MCDEARMID, J. R. & SILLAR, K. T. 2001. Induction of a non-rhythmic motor pattern by nitric oxide in hatchling Rana temporaria embryos. *Journal of Experimental Biology,* 204**,** 1307-1317.

MCLEAN, D. L. & SILLAR, K. T. 2000. The distribution of NADPH-diaphorase-labelled interneurons and the role of nitric oxide in the swimming system of Xenopus laevis larvae. *Journal of Experimental Biology,* 203**,** 705-713.

MCLEAN, D. L. & SILLAR, K. T. 2001. Spatiotemporal pattern of nicotinamide adenine dinucleotide phosphate-diaphorase reactivity in the developing central nervous system of premetamorphic Xenopus laevis tadpoles. *The Journal of Comparative Neurology,* 437**,** 350-362.

MCLEAN, D. L. & SILLAR, K. T. 2002. Nitric Oxide Selectively Tunes Inhibitory Synapses to Modulate Vertebrate Locomotion. *The Journal of Neuroscience,* 22**,** 4175-4184.

MCLEAN, D. L. & SILLAR, K. T. 2004. Metamodulation of a Spinal Locomotor Network by Nitric Oxide. *The Journal of Neuroscience,* 24**,** 9561-9571.

MENTIS, G. Z., ALVAREZ, F. J., BONNOT, A., RICHARDS, D. S., GONZALEZ-FORERO, D., ZERDA, R. & O'DONOVAN, M. J. 2005. Noncholinergic excitatory actions of motoneurons in the neonatal mammalian spinal cord. *Proceedings of the National Academy of Sciences of the United States of America,* 102**,** 7344-7349.

MILES, G. B., DAI, Y. & BROWNSTONE, R. M. 2005. Mechanisms underlying the early phase of spike frequency adaptation in mouse spinal motoneurones. *The Journal of Physiology,* 566**,** 519-532.

MILES, G. B., HARTLEY, R., TODD, A. J. & BROWNSTONE, R. M. 2007. Spinal cholinergic interneurons regulate the excitability of motoneurons during locomotion. *Proceedings of the National Academy of Sciences,* 104**,** 2448-2453.

MILES, G. B. & SILLAR, K. T. 2011. Neuromodulation of Vertebrate Locomotor Control Networks. *Physiology,* 26**,** 393-411.

MILLIGAN, C. J., EDWARDS, I. J. & DEUCHARS, J. 2006. HCN1 ion channel immunoreactivity in spinal cord and medulla oblongata. *Brain Research,* 1081**,** 79-91.

MIRONOV, S. L. & LANGOHR, K. 2007. Modulation of synaptic and channel activities in the respiratory network of the mice by NO/cGMP signalling pathways. *Brain Research,* 1130**,** 73-82.

MONCADA, S., PALMER, R. M. & HIGGS, E. A. 1991. Nitric oxide: physiology, pathophysiology, and pharmacology. *Pharmacological Reviews,* 43**,** 109-142.

MONTERO, F., PORTILLO, F., GONZÁLEZ-FORERO, D. & MORENO-LÓPEZ, B. 2008. The nitric oxide/cyclic guanosine monophosphate pathway modulates the inspiratory-related activity of hypoglossal motoneurons in the adult rat. *European Journal of Neuroscience,* 28**,** 107-116.

MORENO, H., DE MIERA, E. V.-S., NADAL, M. S., AMARILLO, Y. & RUDY, B. 2001. Modulation of Kv3 potassium channels expressed in CHO cells by a nitric oxide-activated phosphatase. *The Journal of Physiology,* 530**,** 345-358.

MORENO-LÓPEZ, B., SUNICO, C. & GONZÁLEZ-FORERO, D. 2011. NO Orchestrates the Loss of Synaptic Boutons from Adult "Sick" Motoneurons: Modeling a Molecular Mechanism. *Molecular Neurobiology,* 43**,** 41-66.

MORI, M. & GOTOH, T. 2000. Regulation of Nitric Oxide Production by Arginine Metabolic Enzymes. *Biochemical and Biophysical Research Communications,* 275**,** 715-719.

MOROZ, L. L., NOREKIAN, T. P., PIRTLE, T. J., ROBERTSON, K. J. & SATTERLIE, R. A. 2000. Distribution of NADPH-diaphorase reactivity and

effects of nitric oxide on feeding and locomotory circuitry in the pteropod mollusc, Clione limacina. *The Journal of Comparative Neurology,* 427**,** 274-284.

MOROZ, L. L., PARK, J.-H. & WINLOW, W. 1993. Nitric oxide activates buccal motor patterns in Lymnaea stagnalis. *NeuroReport,* 4**,** 643-646.

MURAD, F. 1986. Cyclic guanosine monophosphate as a mediator of vasodilation. *The Journal of Clinical Investigation,* 78**,** 1-5.

MURPHY, S. 2000. Production of nitric oxide by glial cells: Regulation and potential roles in the CNS. *Glia,* 29**,** 1-13.

MURRAY, A. J., PEACE, A. G. & SHEWAN, D. A. 2009. cGMP promotes neurite outgrowth and growth cone turning and improves axon regeneration on spinal cord tissue in combination with cAMP. *Brain Research,* 1294**,** 12-21.

NAKANE, M., MITCHELL, J., F√∂RSTERMANN, U. & MURAD, F. 1991. Phosphorylation by calcium calmodulin-dependent protein kinase II and protein kinase C modulates the activity of nitric oxide synthase. *Biochemical and Biophysical Research Communications,* 180**,** 1396-1402.

NAKANE, M., SAHEKI, S., KUNO, T., ISHII, K. & MURAD, F. 1988. Molecular cloning of a cDNA coding for 70 kilodalton subunit of soluble guanylate cyclase from rat lung. *Biochemical and Biophysical Research Communications,* 157**,** 1139-1147.

NEITZ, A., MERGIA, E., EYSEL, U. T., KOESLING, D. & MITTMANN, T. 2011. Presynaptic nitric oxide/cGMP facilitates glutamate release via hyperpolarization-activated cyclic nucleotide-gated channels in the hippocampus. *European Journal of Neuroscience,* 33**,** 1611-1621.

NISHIMARU, H., TAKIZAWA, H. & KUDO, N. 2000. 5-Hydroxytryptamine-induced locomotor rhythm in the neonatal mouse spinal cord in vitro. *Neuroscience Letters,* 280**,** 187-190.

NOGA, B. R., KRIELLAARS, D. J., BROWNSTONE, R. M. & JORDAN, L. M. 2003. Mechanism for Activation of Locomotor Centers in the Spinal Cord by Stimulation of the Mesencephalic Locomotor Region. *Journal of Neurophysiology,* 90**,** 1464-1478.

O'DONOVAN, M. J., CHUB, N. & WENNER, P. 1998. Mechanisms of spontaneous activity in developing spinal networks. *Journal of Neurobiology,* 37**,** 131-145.

OEY, P. L., VOS, P. E., WIENEKE, G. H., WOKKE, J. H. J., BLANKESTIJN, P. J. & KAREMAKER, J. M. 2002. Subtle involvement of the sympathetic nervous system in amyotrophic lateral sclerosis. *Muscle & Nerve,* 25**,** 402-408.

PALMER, R. M. J., ASHTON, D. S. & MONCADA, S. 1988. Vascular endothelial cells synthesize nitric oxide from L-arginine. *Nature,* 333**,** 664-666.

PALMER, R. M. J., FERRIGE, A. G. & MONCADA, S. 1987. Nitric oxide release accounts for the biological activity of endothelium-derived relaxing factor. *Nature,* 327**,** 524-526.

PALUMBO, A. 2005. Nitric oxide in marine invertebrates: A comparative perspective. *Comparative Biochemistry and Physiology - Part A: Molecular & Integrative Physiology,* 142**,** 241-248.

PAMBO-PAMBO, A., DURAND, J. & GUERITAUD, J.-P. 2009. Early Excitability Changes in Lumbar Motoneurons of Transgenic SOD1G85R and SOD1G93A-Low Mice. *Journal of Neurophysiology,* 102**,** 3627-3642.

PEARLSTEIN, E., BEN MABROUK, F., PFLIEGER, J. F. & VINAY, L. 2005. Serotonin refines the locomotor-related alternations in the in vitro neonatal rat spinal cord. *European Journal of Neuroscience,* 21**,** 1338-1346.

PFEIFER, A., ASZADI, A., SEIDLER, U., RUTH, P., HOFMANN, F. & FUSSLER, R. 1996. Intestinal Secretory Defects and Dwarfism in Mice Lacking cGMP-Dependent Protein Kinase II. *Science,* 274**,** 2082-2086.

PFEIFFER, S., LEOPOLD, E., HEMMENS, B., SCHMIDT, K., WERNER, E. R. & MAYER, B. 1997. Interference of Carboxy-PTIO with Nitric Oxide- and Peroxynitrite-Mediated Reactions. *Free Radical Biology and Medicine,* 22**,** 787-794.

PIERREFICHE, O., ABDALA, A. P. L. & PATON, J. F. R. 2007. Nitric oxide and respiratory rhythm in mammals: a new modulator of phase transition? *Biochemical Society Transactions,* 35**,** 1258-1263.

PIFARRE, P., PRADO, J., BALTRONS, M., GIRALT, M., GABARRO, P., FEINSTEIN, D., HIDALGO, J. & GARCIA, A. 2011. Sildenafil (Viagra) ameliorates clinical symptoms and neuropathology in a mouse model of multiple sclerosis. *Acta Neuropathologica,* 121**,** 499-508.

PLACHTA, N., TRAISTER, A. & WEIL, M. 2003. Nitric oxide is involved in establishing the balance between cell cycle progression and cell death in the developing neural tube. *Experimental Cell Research,* 288**,** 354-362.

POSE, I., FUNG, S., SAMPOGNA, S., CHASE, M. H. & MORALES, F. R. 2005. Nitrergic innervation of trigeminal and hypoglossal motoneurons in the cat. *Brain Research,* 1041**,** 29-37.

POSE, I., SILVEIRA, V. & MORALES, F. R. 2011. Inhibition of excitatory synaptic transmission in the trigeminal motor nucleus by the nitric oxide-cyclicGMP signaling pathway. *Brain Research,* 1393**,** 1-16.

QUINLAN, K. A., SCHUSTER, J. E., FU, R., SIDDIQUE, T. & HECKMAN, C. J. 2011. Altered postnatal maturation of electrical properties in spinal motoneurons in a mouse model of amyotrophic lateral sclerosis. *The Journal of Physiology,* 589**,** 2245-2260.

RADI, R. 2004. Nitric oxide, oxidants, and protein tyrosine nitration. *Proceedings of the National Academy of Sciences,* 101**,** 4003-4008.

RAMANATHAN, S., COMBES, D., MOLINARI, M., SIMMERS, J. & SILLAR, K. T. 2006. Developmental and regional expression of NADPH-diaphorase/nitric oxide synthase in spinal cord neurons correlates with the emergence of limb motor networks in metamorphosing Xenopus laevis. *European Journal of Neuroscience,* 24**,** 1907-1922.

RAOUL, C., BUHLER, E., SADEGHI, C., JACQUIER, A., AEBISCHER, P., PETTMANN, B., HENDERSON, C. E. & HAASE, G. 2006. Chronic activation in presymptomatic amyotrophic lateral sclerosis (ALS) mice of a feedback loop involving Fas, Daxx, and FasL. *Proceedings of the National Academy of Sciences,* 103**,** 6007-6012.

REDFORD, E. J., KAPOOR, R. & SMITH, K. J. 1997. Nitric oxide donors reversibly block axonal conduction: demyelinated axons are especially susceptible. *Brain,* 120**,** 2149-2157.

REES, D. D., PALMER, R. M., SCHULZ, R., HODSON, H. F. & MONCADA, S. 1990. Characterization of three inhibitors of endothelial nitric oxide synthase in vitro and in vivo. *Br J Pharmacol,* 101**,** 746-52.

REGEHR, W. G., CAREY, M. R. & BEST, A. R. 2009. Activity-Dependent Regulation of Synapses by Retrograde Messengers. *Neuron,* 63**,** 154-170.

REKLING, J. C., FUNK, G. D., BAYLISS, D. A., DONG, X.-W. & FELDMAN, J. L. 2000. Synaptic Control of Motoneuronal Excitability. *Physiological Reviews,* 80**,** 767-852.

REXED, B. 1954. A cytoarchitectonic atlas of the spinal coed in the cat. *The Journal of Comparative Neurology,* 100**,** 297-379.

ROBERTS, A., LI, W.-C. & SOFFE, S. R. 2010. How neurons generate behaviour in a hatchling amphibian tadpole: an outline. *Frontiers in Behavioral Neuroscience,* 4.

ROBERTSON, C. P., GIBBS, S. M. & ROELINK, H. 2001. cGMP Enhances the Sonic Hedgehog Response in Neural Plate Cells. *Developmental Biology,* 238**,** 157-167.

ROY, B., HALVEY, E. J. & GARTHWAITE, J. 2008. An Enzyme-linked Receptor Mechanism for Nitric Oxide-activated Guanylyl Cyclase. *Journal of Biological Chemistry,* 283**,** 18841-18851.

RUSSWURM, M., WITTAU, N. & KOESLING, D. 2001. Guanylyl Cyclase/PSD-95 Interaction. *Journal of Biological Chemistry,* 276**,** 44647-44652.

SALERNO, J. C. & GHOSH, D. K. 2009. Space, time and nitric oxide – neuronal nitric oxide synthase generates signal pulses. *FEBS Journal,* 276**,** 6677-6688.

SARDELLA, T. C. P., POLGAR, E., WATANABE, M. & TODD, A. J. 2011. A quantitative study of neuronal nitric oxide synthase expression in laminae I - III of the rat spinal dorsal horn. *Neuroscience,* 192**,** 708-720.

SASAKI, S., WARITA, H., ABE, K. & IWATA, M. 2002. Neuronal nitric oxide synthase (nNOS) immunoreactivity in the spinal cord of transgenic mice with G93A mutant SOD1 gene. *Acta Neuropathologica,* 103**,** 421-427.

SAYED, N., BASKARAN, P., MA, X., VAN DEN AKKER, F. & BEUVE, A. 2007. Desensitization of soluble guanylyl cyclase, the NO receptor, by S-nitrosylation. *Proceedings of the National Academy of Sciences,* 104**,** 12312-12317.

SAYWELL, S. A., BABIEC, W. E., NEVEROVA, N. V. & FELDMAN, J. L. 2010. Protein kinase G-dependent mechanisms modulate hypoglossal motoneuronal excitability and long-term facilitation. *The Journal of Physiology,* 588**,** 4431-4439.

SCHMIDT, B. J., HOCHMAN, S. & MACLEAN, J. N. 1998. NMDA Receptor-mediated Oscillatory Properties: Potential Role in Rhythm Generation in the Mammalian Spinal Cord. *Annals of the New York Academy of Sciences,* 860**,** 189-202.

SCHMIDT, H., WARNER, T. D. & MURAD, F. 1992. DOUBLE-EDGED ROLE OF ENDOGENOUS NITRIC-OXIDE. *Lancet,* 339**,** 986-986.

SCHMIDTKO, A., GAO, W., KOENIG, P., HEINE, S., MOTTERLINI, R., RUTH, P., SCHLOSSMANN, J., KOESLING, D., NIEDERBERGER, E., TEGEDER, I., FRIEBE, A. & GEISSLINGER, G. 2008. cGMP Produced by NO-Sensitive Guanylyl Cyclase Essentially Contributes to Inflammatory and Neuropathic Pain by Using Targets Different from cGMP-Dependent Protein Kinase I. *The Journal of Neuroscience,* 28**,** 8568-8576.

SCHMIDTKO, A., TEGEDER, I. & GEISSLINGER, G. 2009. No NO, no pain? The role of nitric oxide and cGMP in spinal pain processing. *Trends in neurosciences,* 32**,** 339-346.

SCHREIBEROVÁ, A., LACKOVÁ, M., KOLESÁR, D., LUKÁČOVÁ, N. & MARŠALA, J. 2006. Neuronal Nitric Oxide Synthase Immunopositivity in Motoneurons of the Rabbit's Spinal Cord After Transient Ischemia/Reperfusion Injury. *Cellular and Molecular Neurobiology,* 26**,** 1481-1492.

SHANNON, C. E. 1948. A MATHEMATICAL THEORY OF COMMUNICATION. *Bell System Technical Journal,* 27**,** 379-423.

SIEMBAB, V. C., SMITH, C. A., ZAGORAIOU, L., BERROCAL, M. C., MENTIS, G. Z. & ALVAREZ, F. J. 2010. Target selection of proprioceptive and motor axon synapses on neonatal V1-derived Ia inhibitory interneurons and Renshaw cells. *The Journal of Comparative Neurology,* 518**,** 4675-4701.

SILLAR, K. T., REITH, C. A. & MCDEARMID, J. R. 1998. Development and Aminergic Neuromodulation of a Spinal Locomotor Network Controlling Swimming in Xenopus Larvaea. *Annals of the New York Academy of Sciences,* 860**,** 318-332.

SILLAR, K. T., SWEDDERBURN, J. F. & SIMMERS, A. J. 1992. MODULATION OF SWIMMING RHYTHMICITY BY 5-HYDROXYTRYPTAMINE DURING POSTEMBRYONIC DEVELOPMENT IN XENOPUS-LAEVIS. *Proceedings of the Royal Society of London Series B-Biological Sciences,* 250**,** 107-114.

SILLAR, K. T., WOOLSTON, A.-M. & WEDDERBURN, J. F. S. 1995. Involvement of Brainstem Serotonergic Interneurons in the Development of a Vertebrate Spinal Locomotor Circuit. *Proceedings of the Royal Society of London. Series B: Biological Sciences,* 259**,** 65-70.

SIROIS, J. E., LYNCH, C. & BAYLISS, D. A. 2002. Convergent and reciprocal modulation of a leak K+ current and Ih by an inhalational anaesthetic and neurotransmitters in rat brainstem motoneurones. *The Journal of Physiology,* 541**,** 717-729.

SMITH, J. C. & FELDMAN, J. L. 1987. In vitro brainstem-spinal cord preparations for study of motor systems for mammalian respiration and locomotion. *Journal of Neuroscience Methods,* 21**,** 321-333.

SMITH, K. J., KAPOOR, R., HALL, S. M. & DAVIES, M. 2001. Electrically active axons degenerate when exposed to nitric oxide. *Annals of Neurology,* 49**,** 470-476.

SMITH, M. A., RICHEY HARRIS, P. L., SAYRE, L. M., BECKMAN, J. S. & PERRY, G. 1997. Widespread Peroxynitrite-Mediated Damage in Alzheimer's Disease. *The Journal of Neuroscience,* 17**,** 2653-2657.

SNYDER, S. H. & BREDT, D. S. 1992. BIOLOGICAL ROLES OF NITRIC-OXIDE. *Scientific American,* 266**,** 68-&.

SPIKE, R. C., TODD, A. J. & JOHNSTON, H. M. 1993. Coexistence of NADPH diaphorase with GABA, glycine, and acetylcholine in rat spinal cord. *The Journal of Comparative Neurology,* 335**,** 320-333.

SPITZER, N. C. 2010. How GABA generates depolarization. *The Journal of Physiology,* 588**,** 757-758.

STAMLER, J. S., SIMON, D. I., OSBORNE, J. A., MULLINS, M. E., JARAKI, O., MICHEL, T., SINGEL, D. J. & LOSCALZO, J. 1992. S-nitrosylation of proteins with nitric oxide: synthesis and characterization of biologically active compounds. *Proceedings of the National Academy of Sciences,* 89**,** 444-448.

STEINERT, J., ROBINSON, S., TONG, H., HAUSTEIN, M., KOPP-SCHEINPFLUG, C. & FORSYTHE, I. 2011. Nitric Oxide Is an Activity-Dependent Regulator of Target Neuron Intrinsic Excitability. *Neuron,* 71**,** 291-305.

STEINERT, J. R., KOPP-SCHEINPFLUG, C., BAKER, C., CHALLISS, R. A. J., MISTRY, R., HAUSTEIN, M. D., GRIFFIN, S. J., TONG, H., GRAHAM, B. P. & FORSYTHE, I. D. 2008. Nitric Oxide Is a Volume Transmitter Regulating Postsynaptic Excitability at a Glutamatergic Synapse. *Neuron,* 60**,** 642-656.

STRAUB, V. A., GRANT, J., O'SHEA, M. & BENJAMIN, P. R. 2007. Modulation of Serotonergic Neurotransmission by Nitric Oxide. *Journal of Neurophysiology,* 97**,** 1088-1099.

STROISSNIGG, H., TRANCIKOVA, A., DESCOVICH, L., FUHRMANN, J., KUTSCHERA, W., KOSTAN, J., MEIXNER, A., NOTHIAS, F. & PROPST, F. 2007. S-nitrosylation of microtubule-associated protein 1B mediates nitric-oxide-induced axon retraction. *Nat Cell Biol,* 9**,** 1035-1045.

SUN, J., XIN, C., EU, J. P., STAMLER, J. S. & MEISSNER, G. 2001. Cysteine-3635 is responsible for skeletal muscle ryanodine receptor modulation by NO. *Proceedings of the National Academy of Sciences,* 98**,** 11158-11162.

SUNICO, C. R., DOMÍNGUEZ, G., GARCÍA-VERDUGO, J. M., OSTA, R., MONTERO, F. & MORENO-LÓPEZ, B. 2011. Reduction in the Motoneuron Inhibitory/Excitatory Synaptic Ratio in an Early-Symptomatic Mouse Model of Amyotrophic Lateral Sclerosis. *Brain Pathology,* 21**,** 1-15.

SUNICO, C. R., GONZALEZ-FORERO, D., DOMINGUEZ, G., GARCIA-VERDUGO, J. M. & MORENO-LOPEZ, B. 2010. Nitric Oxide Induces Pathological Synapse Loss by a Protein Kinase G-, Rho Kinase-Dependent Mechanism Preceded by Myosin Light Chain Phosphorylation. *The Journal of Neuroscience,* 30**,** 973-984.

SUNICO, C. R., PORTILLO, F., GONZALEZ-FORERO, D. & MORENO-LOPEZ, B. 2005. Nitric Oxide-Directed Synaptic Remodeling in the Adult Mammal CNS. *The Journal of Neuroscience,* 25**,** 1448-1458.

TACCOLA, G., MARCHETTI, C. & NISTRI, A. 2003. Effect of metabotropic glutamate receptor activity on rhythmic discharges of the neonatal rat spinal cord in vitro. *Experimental Brain Research,* 153**,** 388-393.

TAKAHASHI, T. 1990. Membrane currents in visually identified motoneurones of neonatal rat spinal cord. *The Journal of Physiology,* 423**,** 27-46.

TAKAHASHI, T. & BERGER, A. J. 1990. Direct excitation of rat spinal motoneurones by serotonin. *The Journal of Physiology,* 423**,** 63-76.

TALPALAR, A., ENDO, T., LOW, P., BORGIUS, L., HUGGLUND, M., DOUGHERTY, K., RYGE, J., HNASKO, T. S. & KIEHN, O. 2011. Identification of Minimal Neuronal Networks Involved in Flexor-Extensor Alternation in the Mammalian Spinal Cord. *Neuron,* 71**,** 1071-1084.

THOMAS, D. D., LIU, X., KANTROW, S. P. & LANCASTER, J. R. 2001. The biological lifetime of nitric oxide: Implications for the perivascular dynamics of NO and O2. *Proceedings of the National Academy of Sciences,* 98**,** 355-360.

THOMAS, D. D., RIDNOUR, L. A., ISENBERG, J. S., FLORES-SANTANA, W., SWITZER, C. H., DONZELLI, S., HUSSAIN, P., VECOLI, C., PAOLOCCI, N., AMBS, S., COLTON, C. A., HARRIS, C. C., ROBERTS, D. D. & WINK, D. A. 2008. The chemical biology of nitric oxide: Implications in cellular signaling. *Free Radical Biology and Medicine,* 45**,** 18-31.

TIMOTEO, M. A., OLIVEIRA, L., CAMPESATTO-MELLA, E., BARROSO, A., SILVA, C., MAGALHAES-CARDOSO, M. T., ALVES-DO-PRADO, W. & CORREIA-DE-SA, P. 2008. Tuning adenosine A1 and A2A receptors activation mediates l-citrulline-induced inhibition of [3H]-acetylcholine release depending on nerve stimulation pattern. *Neurochemistry International,* 52**,** 834-845.

TODD, A. J. 2010. Neuronal circuitry for pain processing in the dorsal horn. *Nat Rev Neurosci,* 11**,** 823-836.

TOJIMA, T., ITOFUSA, R. & KAMIGUCHI, H. 2009. The Nitric Oxide,cGMP Pathway Controls the Directional Polarity of Growth Cone Guidance via Modulating Cytosolic Ca2+ Signals. *The Journal of Neuroscience,* 29**,** 7886-7897.

TOYODA, H., SAITO, M., SATO, H., DEMPO, Y., OHASHI, A., HIRAI, T., MAEDA, Y., KANEKO, T. & KANG, Y. 2008. cGMP Activates a pH-Sensitive Leak K+ Current in the Presumed Cholinergic Neuron of Basal Forebrain. *Journal of Neurophysiology,* 99**,** 2126-2133.

TRAISTER, A., ABASHIDZE, S., GOLD, V., YAIRI, R., MICHAEL, E., PLACHTA, N., MCKINNELL, I., PATEL, K., FAINSOD, A. & WEIL, M. 2004. BMP controls nitric oxide-mediated regulation of cell numbers in the developing neural tube. *Cell Death Differ,* 11**,** 832-841.

ULBRICHT, W. 2005. Sodium Channel Inactivation: Molecular Determinants and Modulation. *Physiological Reviews,* 85**,** 1271-1301.

UNG, R.-V., LANDRY, E. S., ROULEAU, P., LAPOINTE, N. P., ROUILLARD, C. & GUERTIN, P. A. 2008. Role of spinal 5-HT2 receptor subtypes in quipazine-induced hindlimb movements after a low-thoracic spinal cord transection. *European Journal of Neuroscience,* 28**,** 2231-2242.

VALTSCHANOFF, J. G., WEINBERG, R. J. & RUSTIONI, A. 1992. NADPH diaphorase in the spinal cord of rats. *The Journal of Comparative Neurology,* 321**,** 209-222.

VAN DEN BOSCH, L. 2011. Genetic Rodent Models of Amyotrophic Lateral Sclerosis. *Journal of Biomedicine and Biotechnology,* 2011.

VAN DER STAAY, F. J., RUTTEN, K., BARFACKER, L., DEVRY, J., ERB, C., HECKROTH, H., KARTHAUS, D., TERSTEEGEN, A., VAN KAMPEN, M., BLOKLAND, A., PRICKAERTS, J., REYMANN, K. G., SCHRODER, U. H. & HENDRIX, M. 2008. The novel selective PDE9 inhibitor BAY 73-6691 improves learning and memory in rodents. *Neuropharmacology,* 55**,** 908-918.

VAN ZUNDERT, B., PEUSCHER, M. H., HYNYNEN, M., CHEN, A., NEVE, R. L., BROWN, R. H., CONSTANTINE-PATON, M. & BELLINGHAM, M. C. 2008. Neonatal Neuronal Circuitry Shows Hyperexcitable Disturbance in a Mouse Model of the Adult-Onset Neurodegenerative Disease Amyotrophic Lateral Sclerosis. *The Journal of Neuroscience,* 28**,** 10864-10874.

VINAY, L., BROCARD, F., PFLIEGER, J.-F., SIMEONI-ALIAS, J. & CLARAC, F. 2000. Perinatal development of lumbar motoneurons and their inputs in the rat. *Brain Research Bulletin,* 53**,** 635-647.

VINAY, L. & JEAN-XAVIER, C. 2008. Plasticity of spinal cord locomotor networks and contribution of cation,Äìchloride cotransporters. *Brain Research Reviews,* 57**,** 103-110.

VLES, J. S. H., DE LOUW, A. J., STEINBUSCH, H., MARKERINK-VAN ITTERSUM, M., STEINBUSCH, H. W. M., BLANCO, C. E., AXER, H.,

TROOST, J. & DE VENTE, J. 2000. Localization and age-related changes of nitric oxide- and ANP-mediated cyclic-GMP synthesis in rat cervical spinal cord: an immunocytochemical study. *Brain Research,* 857**,** 219-234.

WANG, S. J., WANG, K. Y. & WANG, W. C. 2004. Mechanisms underlying the riluzole inhibition of glutamate release from rat cerebral cortex nerve terminals (synaptosomes). *Neuroscience,* 125**,** 191-201.

WANG, X. & ROBINSON, P. J. 1997. Cyclic GMP-Dependent Protein Kinase and Cellular Signaling in the Nervous System. *Journal of Neurochemistry,* 68**,** 443-456.

WANIKIAT, P., WOODWARD, D. F. & ARMSTRONG, R. A. 1997. Investigation of the role of nitric oxide and cyclic GMP in both the activation and inhibition of human neutrophils. *Br J Pharmacol,* 122**,** 1135-45.

WATSON, C., PAXINOS, G. & KAYALIOGLU, G. 2009. *The Spinal Cord: A Christopher and Dana Reeve Foundation Text and Atlas* Elsevier.

WEIL, M., ABELES, R., NACHMANY, A., GOLD, V. & MICHAEL, E. 2003. Folic acid rescues nitric oxide-induced neural tube closure defects. *Cell Death Differ,* 11**,** 361-363.

WERNER, C., RAIVICH, G., COWEN, M., STREKALOVA, T., SILLABER, I., BUTERS, J. T., SPANAGEL, R. & HOFMANN, F. 2004. Importance of NO/cGMP signalling via cGMP-dependent protein kinase II for controlling emotionality and neurobehavioural effects of alcohol. *European Journal of Neuroscience,* 20**,** 3498-3506.

WETTS, R., PHELPS, P. E. & VAUGHN, J. E. 1995. Transient and continuous expression of NADPH diaphorase in different neuronal populations of developing rat spinal cord. *Developmental Dynamics,* 202**,** 215-228.

WEXLER, E. M., STANTON, P. K. & NAWY, S. 1998. Nitric Oxide Depresses GABAA Receptor Function via Coactivation of cGMP-Dependent Kinase and Phosphodiesterase. *The Journal of Neuroscience,* 18**,** 2342-2349.

WHELAN, P., BONNOT, A. & O'DONOVAN, M. J. 2000. Properties of Rhythmic Activity Generated by the Isolated Spinal Cord of the Neonatal Mouse. *Journal of Neurophysiology,* 84**,** 2821-2833.

WIESINGER, H. 2001. Arginine metabolism and the synthesis of nitric oxide in the nervous system. *Progress in Neurobiology,* 64**,** 365-391.

WILSON, G. W. & GARTHWAITE, J. 2010. Hyperpolarization-activated ion channels as targets for nitric oxide signalling in deep cerebellar nuclei. *European Journal of Neuroscience,* 31**,** 1935-1945.

WILSON, J. M., BLAGOVECHTCHENSKI, E. & BROWNSTONE, R. M. 2010. Genetically Defined Inhibitory Neurons in the Mouse Spinal Cord Dorsal Horn: A Possible Source of Rhythmic Inhibition of Motoneurons during Fictive Locomotion. *The Journal of Neuroscience,* 30**,** 1137-1148.

WILSON, J. M., HARTLEY, R., MAXWELL, D. J., TODD, A. J., LIEBERAM, I., KALTSCHMIDT, J. A., YOSHIDA, Y., JESSELL, T. M. & BROWNSTONE, R. M. 2005. Conditional Rhythmicity of Ventral Spinal Interneurons Defined by Expression of the Hb9 Homeodomain Protein. *The Journal of Neuroscience,* 25**,** 5710-5719.

WINGER, J. A., DERBYSHIRE, E. R. & MARLETTA, M. A. 2007. Dissociation of Nitric Oxide from Soluble Guanylate Cyclase and Heme-Nitric Oxide/Oxygen Binding Domain Constructs. *Journal of Biological Chemistry,* 282**,** 897-907.

WINGLER, K., HERMANS, J. J. R., SCHIFFERS, P., MOENS, A. L., PAUL, M. & SCHMIDT, H. 2011. NOX1, 2, 4, 5: counting out oxidative stress. *British Journal of Pharmacology,* 164**,** 866-883.

WUNDER, F., TERSTEEGEN, A., REBMANN, A., ERB, C., FAHRIG, T. & HENDRIX, M. 2005. Characterization of the First Potent and Selective PDE9 Inhibitor Using a cGMP Reporter Cell Line. *Molecular Pharmacology,* 68**,** 1775-1781.

XIONG, G., MOJSILOVIC-PETROVIC, J., PÉREZ, C. A. & KALB, R. G. 2007. Embryonic motor neuron dendrite growth is stunted by inhibition of nitric oxide-dependent activation of soluble guanylyl cyclase and protein kinase G. *European Journal of Neuroscience,* 25**,** 1987-1997.

XU, L., MABUCHI, T., KATANO, T., MATSUMURA, S., OKUDA-ASHITAKA, E., SAKIMURA, K., MISHINA, M. & ITO, S. 2007. Nitric oxide (NO) serves as a retrograde messenger to activate neuronal NO synthase in the spinal cord via NMDA receptors. *Nitric Oxide,* 17**,** 18-24.

XU, L., MATSUMURA, S., MABUCHI, T., TAKAGI, K., ABE, T. & ITO, S. 2006. In situ measurement of neuronal nitric oxide synthase activity in the spinal cord by NADPH-diaphorase histochemistry. *Journal of Neuroscience Methods,* 150**,** 174-184.

YANAGIHARA, D. & KONDO, I. 1996. Nitric oxide plays a key role in adaptive control of locomotion in the cat. *Proceedings of the National Academy of Sciences,* 93**,** 13292-13297.

YVERT, B., BRANCHEREAU, P. & MEYRAND, P. 2004. Multiple Spontaneous Rhythmic Activity Patterns Generated by the Embryonic Mouse Spinal Cord Occur Within a Specific Developmental Time Window. *Journal of Neurophysiology,* 91**,** 2101-2109.

ZAGORAIOU, L., AKAY, T., MARTIN, J. F., BROWNSTONE, R. M., JESSELL, T. M. & MILES, G. B. 2009. A Cluster of Cholinergic Premotor Interneurons Modulates Mouse Locomotor Activity. *Neuron,* 64**,** 645-662.

ZAPOROZHETS, E., COWLEY, K. C. & SCHMIDT, B. J. 2006. Propriospinal neurons contribute to bulbospinal transmission of the locomotor command signal in the neonatal rat spinal cord. *The Journal of Physiology,* 572**,** 443-458.

ZAPOROZHETS, E., COWLEY, K. C. & SCHMIDT, B. J. 2011. Neurochemical excitation of propriospinal neurons facilitates locomotor command signal transmission in the lesioned spinal cord. *Journal of Neurophysiology,* 105**,** 2818-2829.

ZHANG, H.-Y. & SILLAR, K. T. 2012. Short-Term Memory of Motor Network Performance via Activity-Dependent Potentiation of Na+/K+ Pump Function. *Current biology : CB,* 22**,** 526-531.

ZHANG, Y., NARAYAN, S., GEIMAN, E., LANUZA, G. M., VELASQUEZ, T., SHANKS, B., AKAY, T., DYCK, J., PEARSON, K., GOSGNACH, S., FAN, C.-M. & GOULDING, M. 2008. V3 Spinal Neurons Establish a Robust and Balanced Locomotor Rhythm during Walking. *Neuron,* 60**,** 84-96.

ZHAO, Y., BRANDISH, P. E., DIVALENTIN, M., SCHELVIS, J. P. M., BABCOCK, G. T. & MARLETTA, M. A. 2000. Inhibition of Soluble Guanylate Cyclase by ODQ. *Biochemistry,* 39**,** 10848-10854.

ZHONG, G., DROHO, S., CRONE, S. A., DIETZ, S., KWAN, A. C., WEBB, W. W., SHARMA, K. & HARRIS-WARRICK, R. M. 2010. Electrophysiological

Characterization of V2a Interneurons and Their Locomotor-Related Activity in the Neonatal Mouse Spinal Cord. *The Journal of Neuroscience,* 30**,** 170-182.

ZHONG, Z., DEANE, R., ALI, Z., PARISI, M., SHAPOVALOV, Y., O'BANION, M. K., STOJANOVIC, K., SAGARE, A., BOILLEE, S., CLEVELAND, D. W. & ZLOKOVIC, B. V. 2008. ALS-causing SOD1 mutants generate vascular changes prior to motor neuron degeneration. *Nat Neurosci,* 11**,** 420-422.